Dental development and replacement in Lagomorpha

Ludivine Bertonnier-Brouty

Numéro National de Thèse : 2019LYSEN018

THESE de DOCTORAT DE L'UNIVERSITE DE LYON

opérée par

l'Ecole Normale Supérieure de Lyon

Ecole Doctorale N°340
Biologie Moléculaire, Intégrative et Cellulaire
Discipline : **Biologie**

Soutenue publiquement le 03/07/2019, par :

Ludivine BERTONNIER-BROUTY

Etude du développement et du remplacement dentaire chez les lagomorphes

---

Devant le jury composé de :

Pr. Buchtova, Marcela - Masaryk University	Rapporteure
Pr. Jernvall, Jukka - University of Helsinki	Rapporteur
Pr. Bleicher, Françoise - Université Claude Bernard	Examinatrice
Dr. Michon, Frédéric - Université de Montpellier	Examinateur
Pr. Tucker, Abigail - King's College London	Examinatrice
Dr. Charles, Cyril – ENS de Lyon	Directeur de thèse
Dr. Joly, Thierry – ISARA Lyon	Invité
Dr. Lazzari, Vincent - Université de Poitiers	Invité

ACKNOWLEDGMENTS

As the tradition, let's start this thesis manuscript with acknowledgments. I want to thank all the people that helped and supported me during this PhD. I would like to start by thanking my PhD supervisor, Cyril. You offered me the opportunity to do an internship at the end of my bachelor degree, and here I am 6 years later, finishing my PhD under your supervision. Thank you for having trusted me and having made me discover a research topic that I did not leave since. Thank you Laurent, even without being officially my supervisor during all these years, you always kept an eye on my research and gave relevant advice and valuable comments.

I want to thank my PhD committee, Pr. Françoise Bleicher, Dr. Vincent Lazzari and Dr. Thierry Joly who helped me to clarify my project over the years and gave me useful guidance and suggestions and who agreed to examine this thesis manuscript. I also thank the member of my jury, Pr. Marcela Buchtova, Pr. Jukka Jernvall, Dr. Frédéric Michon and Pr. Abigail Tucker who agreed to evaluate this thesis manuscript.

I also want to thank all the people that help me to obtain all the specimens used during my PhD. Thank you Thierry for providing us with the rabbit embryos. Thanks to Aline for providing us with irradiated samples. Thanks to all the museums and the people who gave me access to the collections: Eileen Westwig (AMNH), Cécile Callou (MNHN), François Vigouroux (Musée des Confluences) and Emmanuel Robert (Geological Collections, University Lyon 1).

I have been really happy to prepare my PhD at the IGFL. I have met and worked with great people these last years. Thanks to the administration team and more specifically Martine for its effectiveness in managing all administrative matters, always with the smile. Thank to Christian Lamy, responsible for the glassware, always benevolent. Thank you Pierre for the help in histology and microscopy. Thanks to all the other PhD of the institute for scientific

exchanges as well as the evening out of the lab. Finally, thanks to all the people from the institute for every interaction we had during these last years.

I want to warmly thank all the past and present members of the “Evolution of vertebrate dentition” team: Thank you Laurent and Beatrice for your infectious laughter that were as important as your scientific help during this thesis. Jérémie, we started at the same time and am very happy to be able to taunt you by finishing (a bit) before you. Thank you for making us laugh (but also exasperated) regularly. Thomas thank you for having experimented with me the joys and disappointments of molecular biology but also for your melodious whistles as background music. Thank you Pauline M. for teaching me so much during my first internship by always being in a good mood and caring. Finally, thank you Mathilde for your help with the lab work and the microtomography but also for all our lunch breaks together.

During my PhD, I moved in the “Biomodeling” team. Thank you Nicolas for welcoming us to your team. Thank you Louise, official roommate at each congress, for always having been there to discuss (or drink beers). Thank you Fidji to defend with me the real teeth with the help of Roland against the conodontologists surrounding us. Thanks to the conodontologists, Pauline G., Sam and Nick for promoting a good atmosphere in the office. Also, thank you Pauline J. for your help in statistics but especially for sing all your favorite Disney songs all the day and your great cakes.

I want to thank my parents and family. Thank you for having believed in me and having supported me, for doing everything to understand the strange world of research and to encourage me at every step. Thanks to my little brother to ask me at each family meeting "so, what's new about lagomorphs?”. Antonin, thank you for being here every day to support me and take the time to listen me speaking (or complain) too much about my thesis and my crazy holiday dreams. Finally, thanks to all my friends, and especially Cynthia and Elise for all the shared moments and the laughs. Thanks a lot!

TABLE OF CONTENTS

LIST OF THE TABLES AND FIGURES

ABBREVIATIONS

MUSEUMS

AMNH: American Museum of Natural History, New York City

Confluences: Musée des Confluences, Lyon

MNHN: Muséum national d'Histoire naturelle, Paris

UCBL-FSL: Geological Collections, University Lyon 1, Lyon

TOOTH NOMENCLATURE

I: Incisor

P: Premolar

M: Molar

d: deciduous

X^x: Upper tooth

X_x: Lower tooth

STAGES

dpf: Days post-fertilization

dpn: Days post-natal

DENTAL MORPHOLOGY DESCRIPTION

CL: cervical loops

HERS: Hertwig epithelial root sheath

IEE: Inner enamel epithelium

OEE: Outer enamel epithelium

RSDL: Rudimentary successional dental lamina

TECHNIQUES

CRISPR: Clustered Regularly Interspaced Short Palindromic Repeats

LIPUS: Low intensity pulsed ultrasound

ABSTRACT

Français

Le développement dentaire est essentiellement étudié chez la souris, modèle mammifère le plus commun en biologie. Cependant, contrairement à la majorité des mammifères, les souris ne remplacent pas leurs dents. Ainsi, les mécanismes impliqués dans le remplacement dentaire mammalien sont encore inconnus. Au cours de cette thèse, nous nous sommes intéressés au développement et remplacement dentaire mammalien en utilisant le lapin *Oryctolagus cuniculus* comme modèle d'étude. Le lapin étant déjà séquencé, utilisé en recherche biomédicale, avec une période de gestation courte et remplaçant ses dents, il semblait être un modèle pertinent en odontologie. Le lapin était un modèle méconnu du point de vue du développement dentaire, j'ai donc d'abord réalisé une étude histo-morphologique afin de caractériser la mise en place des dents déciduales et permanentes. Des reconstructions 3D des tissus mous ont été réalisés à différents stades embryonnaires afin d'obtenir une chronologie du développement et remplacement dentaire. Cette chronologie commence aux premières observations morphologiques de l'initiation du développement des premières dents jusqu'à la minéralisation des dernières dents à se développer. Puis, suite à l'identification dans la bibliographie de gènes candidats potentiellement impliqués dans le remplacement dentaire, j'ai étudié les profils d'expressions de ces gènes afin de mieux comprendre la régulation spatio-temporelle du remplacement dentaire chez le lapin. Nous avons ensuite replacé nos résultats sur le développement chez le lapin dans un contexte évolutif. Ainsi, j'ai réalisé une étude d'anatomie comparée chez les lagomorphes actuels et quelques fossiles afin d'identifier des variations morphologiques dentaires au cours de leur histoire évolutive. Nous nous sommes particulièrement intéressé à la mise en place des cuspides au cours de l'odontogénèse ainsi

qu'aux variations de la surface occlusale des dents supérieure tout au long de la vie des lapins et autres lagomorphes. En comparant les variations au cours de l'évolution avec celles observées lors de l'ontogénie dentaire chez le lapin nous avons identifié des processus d'hétérochronies du développement. Nous avons montré que la molaire actuelle du lapin suit un processus de péramorphose, donc de surdéveloppement, en comparaison aux lagomorphes fossiles. Le lapin est ainsi un modèle animal prometteur en biologie du développement et en évolution afin de mieux comprendre la mise en place du remplacement dentaire mammalien ainsi que les variations de forme dentaire au cours de l'évolution des mammifères.

English

Tooth development is essentially studied in mice, the favorite mammalian model in biology. However, mice do not replace their teeth on contrary to numerous mammals. So, the mechanisms involved in mammalian tooth replacement are still unknown. During this thesis, we focused on mammalian dental development and replacement using the European rabbit *Oryctolagus cuniculus* as animal model. The European rabbit is already sequenced, used in biomedical field, has a short gestation time and replaced its teeth, so rabbit seemed to be a relevant model in dental research. Rabbit dental development was not defined, so I first performed a histo-morphological study to characterize the development of deciduous and permanent teeth. 3D soft tissue reconstructions were performed at different embryonic stages to obtain a chronology of tooth development and replacement. This chronology begins with the first morphological observations of the initiation of the development of the first tooth until the mineralization of the last tooth to develop. Then, we identified in the bibliography candidate genes potentially involved in dental replacement. I studied the expression profiles of these genes in order to better understand the spatio-temporal regulation of tooth replacement in rabbits. We then returned our results to rabbit development in an evolutionary context. Thus, I performed a

comparative anatomy study in the current lagomorphs and some fossils in order to identify dental morphological variations during their evolutionary history. We were particularly interested in the setting of cusps during odontogenesis as well as in the variations of the occlusal surface of the upper cheek teeth throughout the life of rabbits and other lagomorphs. Comparing changes during evolution with those observed during dental ontogeny in rabbits allow us to identify heterochronous processes of development. We have shown that the current molar rabbit follows a process of peramorphosis, so an overdevelopment compared to fossil lagomorphs. The rabbit is thus a promising animal model in developmental and evolutionary biology to better understand the implementation of mammalian tooth replacement and tooth shape variations during mammalian evolution.

Key words

Tooth development, mammalian dental replacement, rabbit teeth, peramorphosis, heterochrony, odontongenesis, cusp

RESUME SUBSTANTIEL EN FRANÇAIS

Les dents, une innovation chez les vertébrés, se sont diversifiés en forme, en nombre et en capacité de remplacement. En paléontologie, les dents sont très étudiées car elles sont les tissus minéralisés les plus solides et donc les mieux conservés durant la fossilisation. L'étude d'anatomie comparée des dents fossiles donne de nombreuses informations en évolution et taxonomie. De plus, les dents sont sujettes à une forte pression de sélection puisque la forme des dents corrèle avec le régime alimentaire. Ainsi, les variations morphologiques dentaires entre les espèces sont étudiées pour comprendre les conséquences des modifications de formes en évolution et écologie (i.e Gómez Cano et al., 2013; Renvoisé et al., 2012). Les dents font aussi partie des organes ectodermaux les mieux conservés chez les vertébrés. La dentition est ainsi un modèle pertinent en biologie évolutive du développement chez les vertébrés (Evo-Devo). L'étude des dents dans un contexte d'Evo-Devo nécessite d'identifier les mécanismes moléculaires impliqués dans le développement et la morphogenèse dentaire afin de comprendre les variations morphologiques entre les espèces, éteintes ou actuelles. De même, l'étude des fossiles et les acquisitions morphologiques au cours de l'évolution aident à comprendre la morphogénèse dentaire. Le développement dentaire est étudié chez de nombreuses espèces comme les poissons cartilagineux (i.e. Rasch et al., 2016), les reptiles (i.e. Richman and Handrigan, 2011) et les mammifères (i.e. Renvoisé and Michon, 2014). Même si ces espèces sont phylogénétiquement séparés depuis approximativement 450 million d'années, les voies de signalisations impliqués dans le développement dentaire sont très conservés entre les vertébrés (Rasch et al., 2016). Les vertébrés ancestraux avaient la capacité de remplacer leurs dents de manière continue tout au long de leur vie, ils étaient polyphyodontes. La majorité des vertébrés actuels sont polyphyodontes, mais les mammifères ont perdu cette capacité de remplacement et la majorité d'entre eux possèdent deux générations dentaires au cours de leur vie

(diphyodontie), corrélé avec une augmentation de complexité de la morphologie dentaire. Chez les mammifères, la majorité des études d'odontogénèse utilisent la souris comme modèle. Cependant, la souris ne remplace pas ses dents donc les mécanismes du remplacement dentaire chez les mammifères sont mal connus. Nous avons donc décidé pour cette thèse d'utiliser le lapin (*Oryctolagus cuniculus*) comme modèle animal pour étudier (1) les mécanismes impliqués dans le développement et le remplacement dentaire chez les mammifères et (2) l'évolution des dents chez les lagomorphes.

Un bon animal modèle doit pouvoir être élevé en laboratoire, donner de nombreux embryons, avoir une période de gestation assez courte et être séquencé. Dans le cadre de notre thématique de recherche, le remplacement dentaire est aussi un critère essentiel. Le lapin respecte tous ces critères, de plus il est déjà utilisé comme modèle animal en recherche biomédicale et orthodontie (Abtahi et al., 2018). La littérature disponible sur le développement dentaire chez le lapin est assez ancienne et incomplète, obtenues grâce à des techniques désormais obsolètes et avec un manque de connaissances sur certaines dents et stades de développement (Horowitz et al., 1973; Navarro et al., 1976; Ooë, 1980). Nous avons donc décidé de mettre à jour les connaissances sur la morphogénèse dentaire du remplacement dentaire chez le lapin en utilisant les techniques actuelles. Nous avons étudié chaque dent du lapin depuis l'initiation de la dent déciduale à la minéralisation de la dent de remplacement, soit entre 12 jours post fertilisation et 4 jours post natal, représentant 23 jours de développement. Nous avons réalisé des reconstructions 3D des tissus dentaires épithéliaux pour chaque dent à chaque stage en utilisant la microtomographie à rayons X. En complément, une étude histologique a été réalisée afin d'obtenir une description complète de la chronologie de l'odontogénèse. Nous avons ainsi obtenu une chronologie complète de la morphogénèse dentaire chez le lapin *Oryctolagus cuniculus* afin de pouvoir cibler les stades de développement importants pour l'étude moléculaire du remplacement dentaire mammifère. Au cours de cette

étude, nous avons aussi identifié une caractéristique des incisives de lapin non décrite jusque-là. Ainsi, à la naissance, les incisives supérieures de lapin présentent des trous dans la dentine qui ouvrent la cavité pulpaire. Ces trous sont rapidement réparés par les odontoblastes préexistants qui continuent de secréter de la dentine malgré la perturbation.

Les voies de signalisations supposément impliqués dans le remplacement dentaire sont majoritairement étudiés chez les souris transgéniques (Ahn et al., 2010; Popa et al., 2019) ou chez les espèces polyphyodontes (Tucker and Fraser, 2014; Whitlock and Richman, 2013). Seulement quelques données ont été collectés chez des espèces mammifères diphyondontes comme le furet ou le cochon nain (Jussila et al., 2014; Wang et al., 2019). Mais pour le moment, aucune étude ne suit le pattern d'expression de gènes candidats à chaque étape du remplacement dentaire. Nous avons donc utilisé le lapin comme animal modèle pour étudier la régulation spatio-temporelle du développement et remplacement dentaire chez les mammifères. Nous avons identifié dans la littérature cinq gènes candidats qui pourraient être impliqués dans le remplacement dentaire : Shh, Sostdc1, Runx2, Lef1 et Sox2. Nous avons suivi leur profil d'expression par hybridation *in situ* et la localisation des protéines par immunohistochimie à chaque étape clé du remplacement dentaire. La localisation des proteines Runx2 et Sostdc1 correlent avec un mechanisme d'inhibition du remplacement. De plus, comme chez la souris, Shh et Sostdc1 sont localisés dans l'epithelium adamantin interne et pourraient réguler le pattern des cuspides. Le lapin semble ainsi être un modèle pertinent pour étudier le développement et le remplacement dentaire.

En Evo-Devo, l'étude du développement peut permettre de mieux comprendre les processus évolutifs. Par exemple, les changements dans la vitesse ou la durée des évènements développementaux induisent des changements de taille ou de forme des organes au cours de l'évolution, ce sont les hétérochronies du développement. Ces hétérochronies peuvent être identifiées en étudiant les dents fossiles ainsi que l'odontogénèse des espèces actuelles. Les

différentes espèces fossiles de lagomorphes sont principalement définies par leurs dents. Ainsi, il y a eu des variations nettes de morphologie dentaire au cours de l'évolution des lagomorphes. Les dents des lagomorphes au Paléocène étaient modérément hyposondontes avec des racines alors que les lagomorphes actuels ont des dents hyselondontes à croissance continue (Kraatz et al., 2010). Les relations phylogéniques entre les lagomorphes sont souvent basées sur la morphologie de la troisième prémolaire inférieure (Čermák et al., 2015a; Hibbard, 1963) mais les modifications de forme des autres dents sont peu étudiées. Habituellement, la première molaire supérieure est la dent utilisée en anatomie comparée chez les mammifères. Nous avons donc décidé de suivre les variations de forme de la première molaire supérieure au cours de l'évolution des lagomorphes et de l'ontogénie du lapin *Oryctolagus cuniculus*. Chez les lapins adultes, les faces occlusales des dents jugales sont complètement plates. Cependant nous avons montré que les dents de lapins possèdent transitoirement des cuspides sur leur face occlusale. Les cuspides sont un caractère essentiel pour étudier l'histoire évolutive à travers l'étude de l'homologie des cuspides chez les mammifères. Les terminologies utilisées pour définir les cuspides des lagomorphes dans la littérature sont nombreuses et il est difficile de trouver un consensus (Kraatz et al., 2010). Afin de mieux définir les cuspides chez les lagomorphes nous avons étudié leur mise en place au cours de l'odontogénèse chez le lapin. Nous avons suivi l'ordre d'apparition des cuspides et nous les avons nommées d'après la nomenclature définie par Butler (1956). Nous avons observé au cours de la cuspidogénèse chez le lapin des millions d'années d'évolution dentaire par homologie de forme. Ainsi, au cours du développement de la molaire supérieure du lapin nous avons clairement identifié des homologies de forme avec le pattern tribosphénique commun chez les mammifères ancestraux.

Les changements de formes dentaires continuent au cours de l'ontogénie chez les lapins. Nous avons donc étudié les changements de formes de la première molaire supérieure au cours de l'ontogénie du lapin et de l'évolution des lagomorphes. Afin de caractériser les changements

de la morphologie dentaire en relation avec l'âge nous avons étudiés la variabilité morphologique des molaires supérieures chez différentes espèces de la naissance à l'âge adulte. Puisque les dents de lagomorphes actuels sont à croissance continue, nous avons pu extrapoler la surface occlusale à différents stades d'usures en réalisant des sections virtuelles de reconstructions 3D de dents obtenues par microtomographie 3D. Nous avons observé que les changements de forme dentaire pendant l'évolution des lagomorphes et l'odontogénèse chez le lapin semblent corréler, indiquant possiblement un mécanisme d'hétérochronie du développement. Ainsi, il semblerait que les molaires supérieures de lapin ont évolué par péramorphose, avec une rétention des caractères ancestraux au début de l'odontogénèse ainsi que par l'apparition de nouveaux caractères, les crénulations. La mise en place des crénulations semble liée à la prolifération cellulaire à la base de la dent dans la zone de croissance. Ainsi, en perturbant la prolifération cellulaire par des irradiations, le pattern de crénulations est affecté. Toutefois, nous n'avons pas identifié la fonction de ces crénulations dans les dents de lapins.

Pour conclure, le lapin semble être un modèle pertinent en recherche dentaire. Nous avons montré dans cette thèse que les lapins pouvaient être un modèle utile pour étudier la morphogénèse dentaire. L'étude du développement et du remplacement dentaire chez les lapins pourraient permettre de comprendre les mécanismes de remplacement dentaires chez les mammifères. Nous avons montré que les protocoles de biologie moléculaires utilisés chez la souris pouvaient être facilement transposés aux tissus de lapin. De plus, le développement de la dentition du lapin semble suivre l'évolution des dents des mammifères, les dents de lapins pourraient donc être un modèle pertinent dans les thématiques d'Evo-Devo dentaires.

General Introduction & Literature Review

True teeth are an innovation in vertebrates and they then diversified in shape, number and replacement abilities among extant and extinct vertebrates. Teeth are highly studied in paleontology, first because teeth are the hardest mineralized tissues of the body and so are well preserved during fossilization. Using comparative anatomy, tooth fossils give information to study evolution and taxonomy. Then, teeth are subject to strong selective constraints due to the correlation between tooth shape and diet. So morphological variations of teeth between species are studied for understanding consequences of shape modifications in evolution and ecology (Gómez Cano et al., 2013; Renvoisé et al., 2012). Moreover, teeth are among the most conserved ectodermal organs throughout vertebrates. So, teeth are useful models to study vertebrate Evo-Devo. In tooth Evolutionary Developmental Biology, we need to identify the molecular mechanisms involved in tooth development and dental morphogenesis in order to understand the morphological variations of the teeth between extant and extinct vertebrates. Similarly, the study of fossils and morphological acquisitions during evolution helps to understand the dental morphogenesis. Tooth development is studied in numerous extant species as cartilaginous fishes (i.e. Rasch et al., 2016), reptiles (i.e. Richman and Handrigan, 2011) and mammals (i.e. Renvoisé and Michon, 2014). Even if these species are separated since approximately 450 million years, gene pathways involved in tooth development are highly conserved among vertebrates (Rasch et al., 2016). Basal vertebrates had the ability to replace their teeth during all their life span. Majority of the extant vertebrates still have a continuous tooth replacement system but mammals lost this ability and most of them possess two dental generations over their life, correlated with an increase in the dental shape complexity. In mammals, most of odontogenesis studies use the mouse as a model species. However, the mouse has no dental replacement. So, for now, the mechanisms of tooth replacement in mammals are poorly known. We thus decided in the present thesis to use the European rabbit

(*Oryctolagus cuniculus*) as a new model to study (1) mechanism underlying mammal tooth development and replacement and (2) Lagomorph tooth evolution. I here review in the scientific literature the actual knowledge about signaling events involved in tooth development and replacement in Amniota and summarize the knowledge available before this thesis about the rabbit tooth development and the evolutionary history of lagomorphs.

Tooth development in Amniota

Teeth are ectodermal organs: they are originating from two distinct layers of tissues, the epithelium and the mesenchyme. Teeth develop from the interaction of mesenchymal cells derived from the neural crest and oral epithelium cells (Chai et al., 2000). The signaling events involved in initiation of the tooth development are common with the other ectodermal organs as the hair or the salivary glands despite the diversity in form and function (Pispa and Thesleff, 2003). Tooth development is commonly divided into the following stages: the thickening, the bud, the cap, the bell, and finally the maturation. Numerous signaling pathways between the epithelial and the mesenchymal cells have been identified in mice to explain all the stage transitions (**Figure I. 1**, Balic and Thesleff, 2015; Sharir and Klein, 2016).

The first observation of tooth development initiation is a thickening of the oral epithelium, giving rise to the dental lamina. The surrounding mesenchyme condensates around the dental lamina, which forms a dental placode. During all the tooth morphogenesis, epithelial-mesenchymal interactions occur to regulate the development. In the placode, an early epithelial signaling center grouping five signaling families has been identified to give at the epithelium an odontogenic potential: the Wnt, Shh, BMP, FGF, and Edar signaling pathways (Balic & Thesleff, 2015). All these signals regulate the proliferation and the budding of the placode; the

tooth begins its morphogenesis. The epithelial bud is more invaginated in the mesenchyme that continues to condensate around it. The bud also possesses a signaling center at the tip that is not proliferating: the primary enamel knot (Vaahtokari et al., 1996). Signals coming from the enamel knot induce the formation by the dental epithelium of the cervical loops; it defines the bud to cap stages transition. Cervical loops contain epithelial dental stem cells. At the cap stage, the primary enamel knot matures and is morphologically identifiable. Cells begin to histo-differentiate; we can identify the different cell types that constitute the tooth germ. Then, at the bell stage, cells finish to differentiate, giving layers of functional ameloblasts and odontoblasts. For multicuspid teeth, secondary enamel knots appear and regulate the patterning of the tooth cusps. When cells begin to secrete mineralized tooth tissues, tooth finishes its morphogenesis and the maturation stage begins. The ameloblasts secrete enamel and the odontoblasts secrete dentin, the mineralized tissues of the tooth crown. Then, the cervical loops of the tooth close and differentiate in the Hertwig epithelial root sheath (HERS) cells to form roots (Zeichner-David et al., 2003). Roots are then covered with dentin followed by an apposition of cementum.

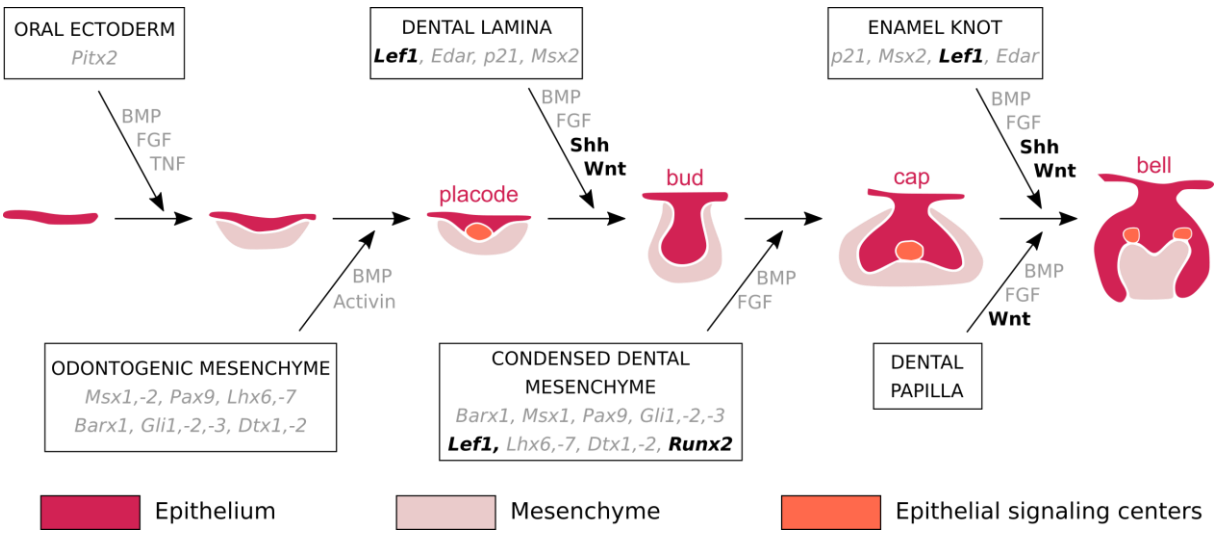

Figure I. 1. Histo-morphological stages and genetic control of tooth development in the mouse. *In color, the mouse tooth development stages. In the boxes and arrows, some of the epithelium-mesenchyme interactions during mouse tooth development from initiation to crown morphogenesis. The genes in black are studied in this thesis (from Thesleff, 2004, colors modified). The color code is the same for all the figures.*

In mammals, by comparing the height of the crown, rooted teeth are separated in two categories: Brachyodont teeth have a short crown whereas hypsodont teeth have a high crown. However, not all the teeth develop roots. Hypselodont teeth are defined by their ability to grow during all the life of the animal (**Figure I. 2**). In hypselodonts, the cervical loops at the basis of the tooth never close, inducing a dental stem cell maintenance and so a continuous renewal of the dental tissues (Renvoisé and Michon, 2014). Some epithelial stem cells markers have been identified in the cervical loops of the ever-growing teeth such as *Sox2* (Juuri et al., 2012), Bmi1 (Biehs et al., 2013) or Lgr5 (Sanz-Navarro et al., 2018, see Annex 1, **p187)**. Tooth ever-growing ability in some mammals could compensates for the loss of the capacity to continuously replacing their teeth (Jernvall and Thesleff, 2012).

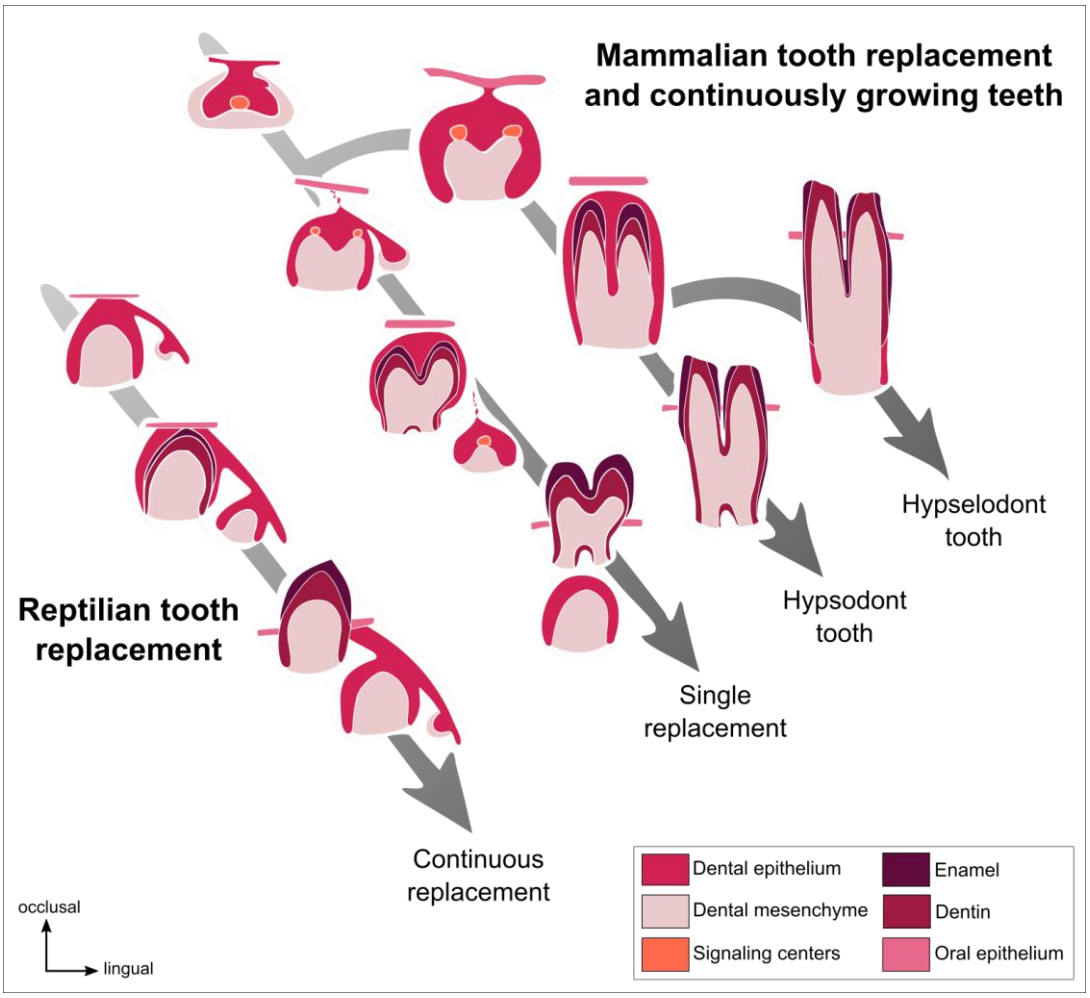

Figure I. 2. Tooth renewal capacity varies among species. *Reptiles have a continuous tooth replacement whereas majority of the mammals have a single tooth replacement and only some of the mammals have continuously growing teeth. (From Jernvall and Thesleff, 2012, colors modified).*

Tooth replacement in Amniota

Tooth replacement in Amniota is divided in categories in function of the number of tooth generations: the polyphyodonts continuously replace their teeth, the diphyodonts replace their teeth only once, and the monophyodonts do not replace their teeth (Bertin et al., 2018). The polyphyodonty is the ancestral condition of all vertebrate dentitions (Maisey et al., 2014; Rucklin et al., 2012).

State of the art regarding dental replacement in polyphyodont reptiles

Tooth replacement is mainly studied in polyphyodont species, which have the ability to replace their teeth during all their life span. Reptiles are polyphyodonts and some species can be raised in animal facilities. The ball python (*Python regius*) has a continuous tooth replacement throughout its life. The tooth replacement in the ball python begins by the formation of the replacement dental lamina (also named successional lamina) at the lingual extremity of the dental lamina (**Figure I. 3**). The replacement teeth bud from the vestibular side of this replacement dental lamina. The preservation of the replacement dental lamina is essential to maintain the continuous tooth replacement.

Handrigan and Richman (2010b) showed that Shh is necessary for tooth initiation and morphogenesis as described in mouse (Hardcastle et al., 1998) but is not involved in the successional dental lamina formation. These authors also studied the Wnt signaling activity and the BMP pathway in the dental tissues of the ball python in order to identify the signaling pathways involved in tooth replacement (Handrigan and Richman, 2010a). Using LEF1 staining, they showed that the canonical Wnt pathway is persistently active at the growing tip of the dental lamina and replacement dental lamina (**Figure I. 3**). They also showed that the *Shh*

expression domain and the canonical Wnt domain are complementary in the tooth tissues and that SHH may restricts Wnt activity. They suggest that canonical Wnt signaling could order tooth replacement by promoting proliferation of the replacement dental lamina tip in snakes.

Dental stem cells have been identified in the lingual side of the dental lamina of the leopard gecko (*Eublepharis macularius*) (Handrigan et al., 2010). These stem cells are *Lgr5*$^{+}$, *Dkk3*$^{+}$ and *IGfbp5*$^{+}$, genes already known as hair bulge stem cells (Jaks et al., 2008; Tumbar et al., 2004). These cells have low proliferation rates and are not directly involved in tooth morphogenesis. However, they may play a role in the maintenance of the replacement dental lamina.

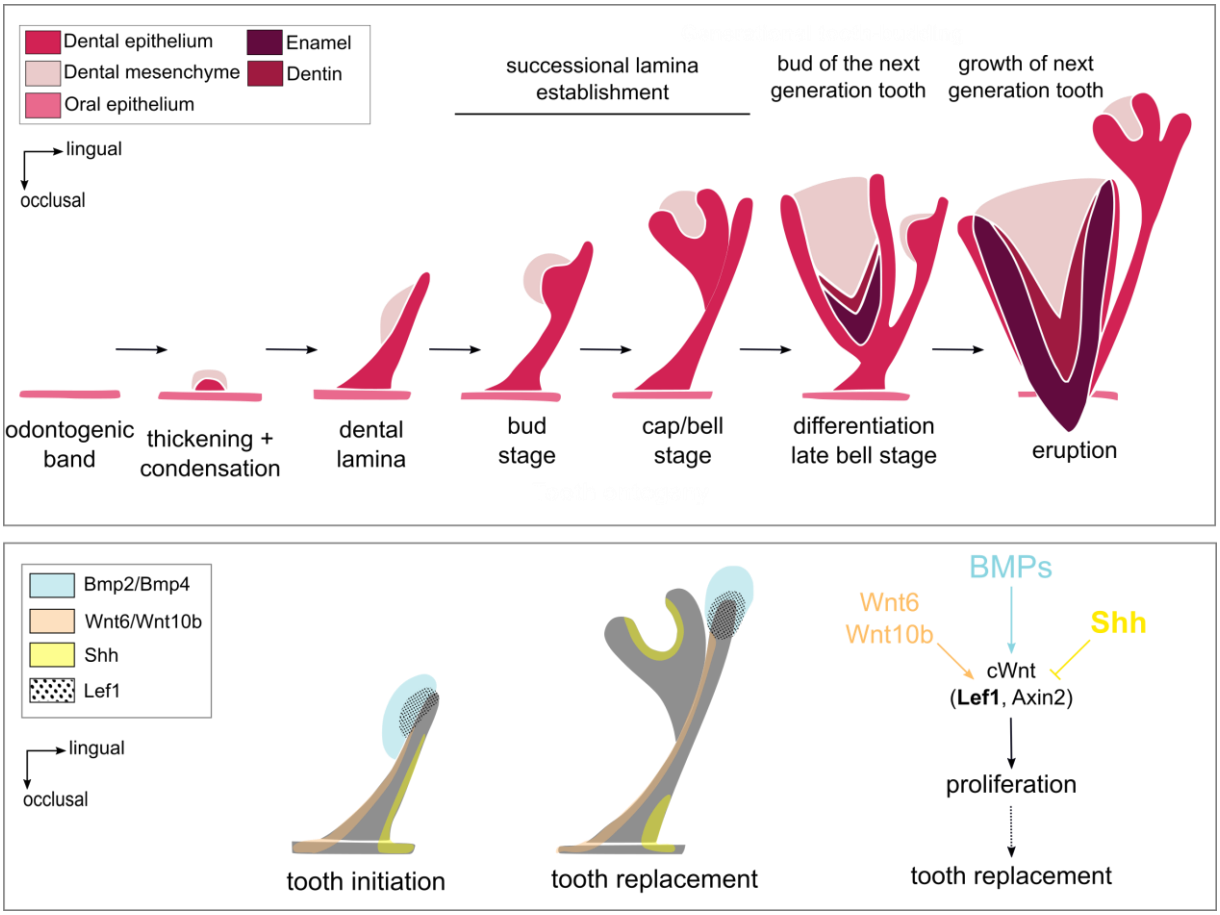

Figure I. 3. Tooth development and continuous dental replacement in Squamates. *At the top, the tooth development stages in Squamates (adapted from Richman and Handrigan, 2011). At the bottom, the signaling pathways involved in tooth initiation and continuous tooth replacement (adapted from Handrigan and Richman, 2010a). In bold, the genes that are studied in this thesis.*

Juuri et al. (2013) identified another dental stem cell population in reptile teeth, the *Sox2*$^{+}$ cells. They localized *Sox2*$^{+}$ cells in the replacement dental lamina of five reptile species: the American alligator (*Alligator mississippiensis*), the green iguana (*Iguana iguana*), the leopard gecko (*Eublepharis macularius*), the ball python (*Python regius*) and the corn snake (*Elaphe guttata*). They showed that *Sox2* is expressed in the replacement dental lamina excepted in the tip. So, dental stem cells involved in maintenance of ever-growing tooth ability are also present in the replacement dental lamina allowing continuous tooth replacement.

To sum up, in reptiles, the active canonical Wnt signaling in the replacement dental lamina and the presence of dental stem cells are involved in the maintenance of the dental renewal capacity.

State of the art regarding dental replacement in diphyodont mammals

Majority of the mammals are diphyodonts, their dentitions are limited to two dental generations. Diphyodonty is a character derived from the polyphyodonty, mammals shifted from numerous teeth with simple shape to more complex teeth with a limited replacement capacity (Luo et al., 2008). Studies done in tooth replacement in diphyodont mammals are reviewed below.

Dental replacement in the ferret

Ferrets (*Mustela putorius furo*) are diphyodonts, their genome is sequenced (MusPutFur1.0) and they are already used as model in biomedical field (Ball, 2006; Pillet et al., 2009). Due to these characteristics, the ferret can be a good model for tooth replacement studies. Järvinen et al. (2009) described the tooth replacement of the canine and the premolars from 34

days post fertilization (dpf) to 2 days post-natal (dpn). They showed that the tooth replacement begins at the lingual part of the deciduous tooth by a budding of the dental lamina, giving the replacement dental lamina (**Figure I. 4**A). Then this replacement dental lamina elongates. In the canine, the permanent tooth develops from the replacement dental lamina when it is still connected to the deciduous tooth. In premolars, the dental lamina first detaches from the deciduous tooth and then gives rise in the permanent premolars.

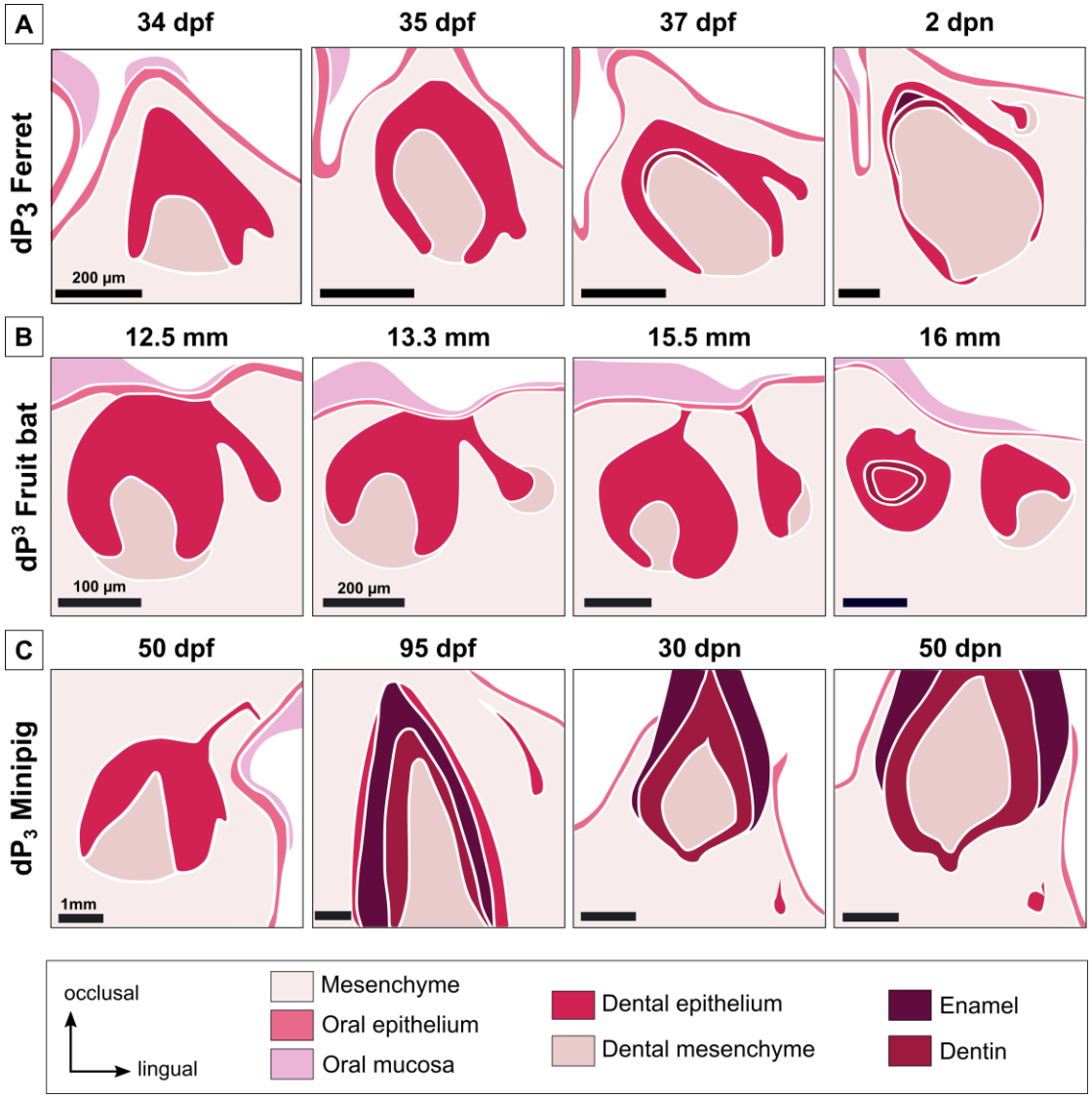

Figure I. 4. Initiation of tooth replacement in the ferret, the fruit bat and the minipig. *Initiation of the tooth replacement of the lower third premolar for the ferret (A) and the minipig (C) and the upper third premolar for the fruit bat (B). Timing of development is indicated in days post fertilization or post-natal for the ferret and the minipig and in embryo size for the fruit bat. Summary of the dental replacement*

has been obtained using the histological sections of ferret (Järvinen et al., 2009), fruit bat (Popa et al., 2016) and minipig (Wang et al., 2014a).

At the molecular level, Järvinen et al. (2009) showed that *Sostdc1*, a Wnt/BMP inhibitor, is expressed in the dental epithelium at the intersection between the deciduous tooth and the replacement dental lamina. They also showed that Shh has a similar expression pattern than in the mouse with an expression in the enamel knot and then in the inner enamel epithelium but no expression in the replacement region. *Sox2*$^{+}$ stem cells have been identified at the lingual part of the replacement dental lamina with a free area of *Sox2* in the tip of the replacement dental lamina (Juuri et al., 2013). Jussila et al. (2014) completed the study of tooth replacement in ferret by studying more developmental stages. By following Edar expression, they suggested that this signaling pathway is not involved in tooth replacement.

These results provided the first molecular observations of the mechanisms of tooth replacement in mammals. They identified the same signaling events than in the reptiles with a regulation of the Wnt pathway by SOSTDC1 and the presence of *Sox2*$^{+}$ cells, indicating the presence of epithelial dental stem cells. However, few developmental stages were studied in ferrets due to the difficulty to obtain embryos at the correct stage and the presence of seasonal estrus.

Dental replacement in the fruit bat

3D reconstructions and histological sections has been published to illustrate tooth replacement from the budding of the replacement dental lamina to the morphogenesis of the permanent tooth in the fruit bat embryos, *Eidolon helvum* (Popa et al., 2016). The authors showed that tooth replacement in the fruit bat always begins with a budding of the replacement dental lamina from the dental lamina at the lingual side of the deciduous tooth, as in the ferret

(**Figure I. 4**B). Then the separation of the replacement dental lamina from the deciduous tooth and the spatial arrangement between the deciduous and the permanent teeth can vary throughout the jaw (**Figure I. 5**). So, even if the tooth replacement always begins similarly, the spatial arrangement is variable and specific for each tooth. 3D reconstructions allow visualizing the spatial configuration of teeth during their development. This configuration is probably determined by specific signals according to the teeth. However, authors indicated that this species is no longer available for experimental purposes and that specimens studied were captured in 1972-73, so no molecular analyses can be realized.

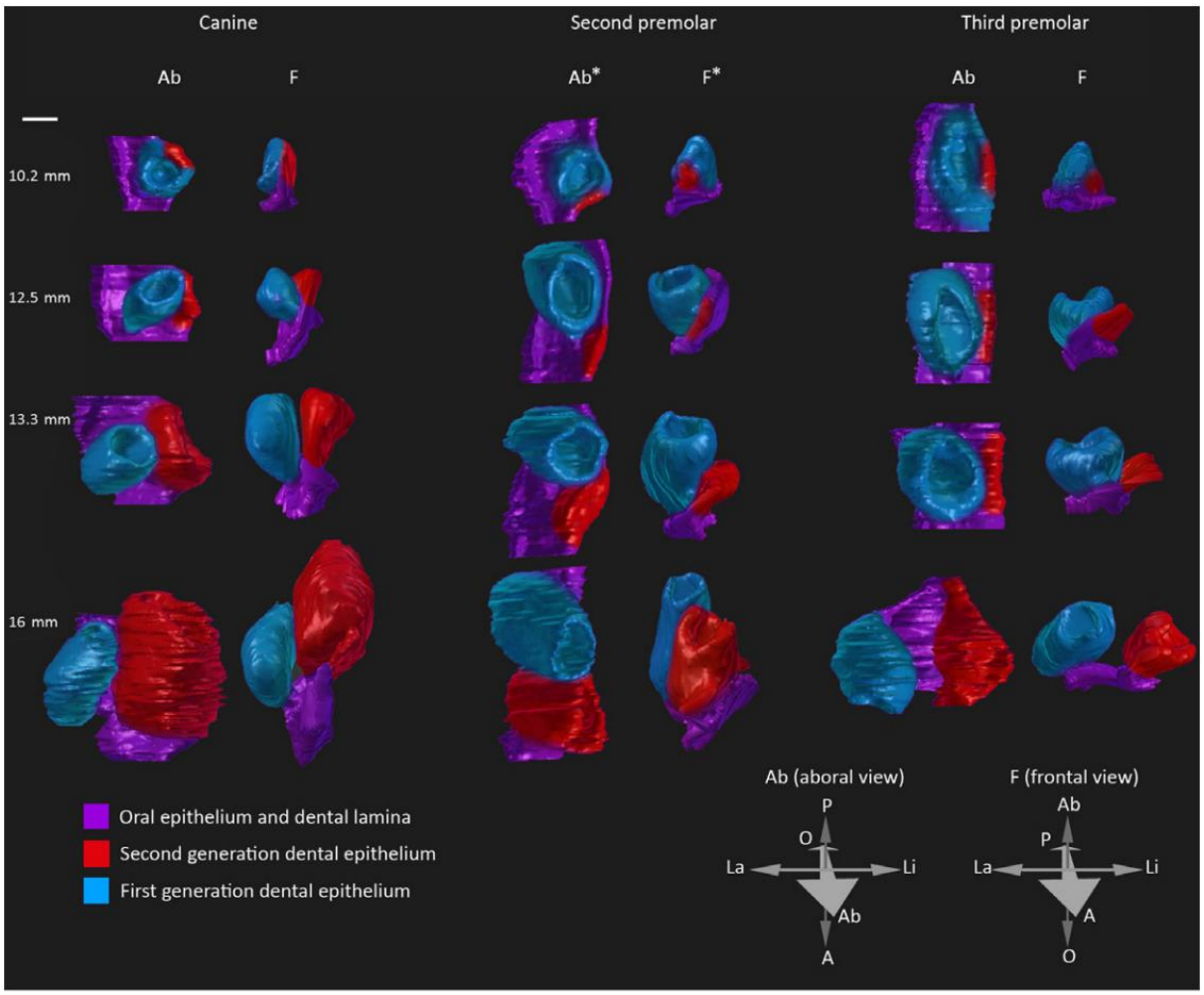

Figure I. 5. 3D-reconstructions of the dental replacement in the fruit bat. *3D-reconstructions of the canine, the second and the third premolar tooth replacement. In the fruit bat, variations of the spatial configuration of teeth during their development and replacement are observed. In function of the tooth, the replacement tooth develops in various position compared to their deciduous teeth: directly on the*

lingual side for the canine, directly posterior for the second premolar and completely separated from the third premolar before starting its morphogenesis (figure from Popa et al., 2016).

Dental replacement in the minipig

Wang et al. (2014a) described tooth development in the minipig *Sus scrofa* as a model for diphyodonty. By their size and morphology, the minipig deciduous teeth are pretty similar to humans. The authors studied the development from 40 dpf to 90 dpn, so for approximately 164 days (Wang et al., 2014a). The tooth replacement in the minipig begins as in the ferret by a budding of the dental lamina at the lingual part of the deciduous tooth. In the minipig, the replacement dental lamina is detected when the deciduous tooth is already at a late bell stage, later than for the ferret and the fruit bat. So, the timing of tooth replacement initiation varies from a species to another. In the minipig, the replacement lamina elongates, detaches from the deciduous tooth, and then starts its tooth morphogenesis (**Figure I. 4**C). At least 100 days are necessary from the appearance of the replacement dental lamina to the mineralization of the replacement tooth.

Some molecular studies have been done in the minipig. Ki67 staining showed that more cells are proliferating in the lingual part of the replacement dental lamina (Wang et al., 2014a). The authors correlate this asymmetry of proliferation with the inclined growth of the replacement dental lamina in the minipig. Global transcriptome has been obtained for various stages during early morphogenesis of teeth; this transcriptome could be very useful to identify signaling events correlated with tooth replacement (Wang et al., 2014b). The authors indicated in the supplementary files that Wnt10B expression is up regulated between 40 and 50 dpf, stage were the replacement dental lamina begins its development in the minipig, indicating a role of the Wnt signaling in tooth replacement. It has also been shown that *in vitro* studies of tooth

development are possible in the minipig by transplanting the tooth germ in the mouse subrenal capsule (Wang et al., 2019). However, the slow development, the size of the animal and ethical concerns are significant obstacles to study tooth development in the minipig.

Dental replacement in humans

Humans are diphyodonts: incisors, canines and premolars are replaced once. Tooth development and replacement timelines are well known in humans. Histological sections that illustrate tooth replacement in human show that the permanent tooth is developing at the lingual position of the deciduous tooth (Kumar, 2014). However, very few studies give information about molecular mechanisms involved in human tooth development.

Juuri & Balic (2017) reviewed the molecular processes involved in tooth number abnormalities in humans. Tooth agenesis, the absence of at least one tooth, can give information about tooth replacement when it affect only permanent teeth. Juuri & Balic summarize that 50% of the tooth agenesis are attributed to WNT10A mutations, and that mutations of the Wnt inhibitor AXIN2 affect the permanent tooth formation (**Figure I. 6**). Other genes have been identified in agenesis syndrome, as Pitx2, Msx1 or the EDA signaling pathway (Juuri & Balic, 2017). Humans can also have supernumerary tooth formation, named hyperdontia. Developmental causes of supernumerary tooth formation are still unclear (**Figure I. 6**). Juuri & Balic listed mutated genes associated with supernumerary teeth. They indicate that Sox2, Runx2, IL11RA and Wnt pathway mutations are correlated with supernumerary teeth (Juuri & Balic, 2017).

So, in humans numerous genes have been identified to be associated with tooth developmental failure. As in reptiles and ferret, the Wnt pathway seems to play an essential role

in the tooth replacement. However, molecular and cellular studies are not possible in humans. We need a model to clearly identify the role of these genes and how their mutations disrupt tooth development and replacement.

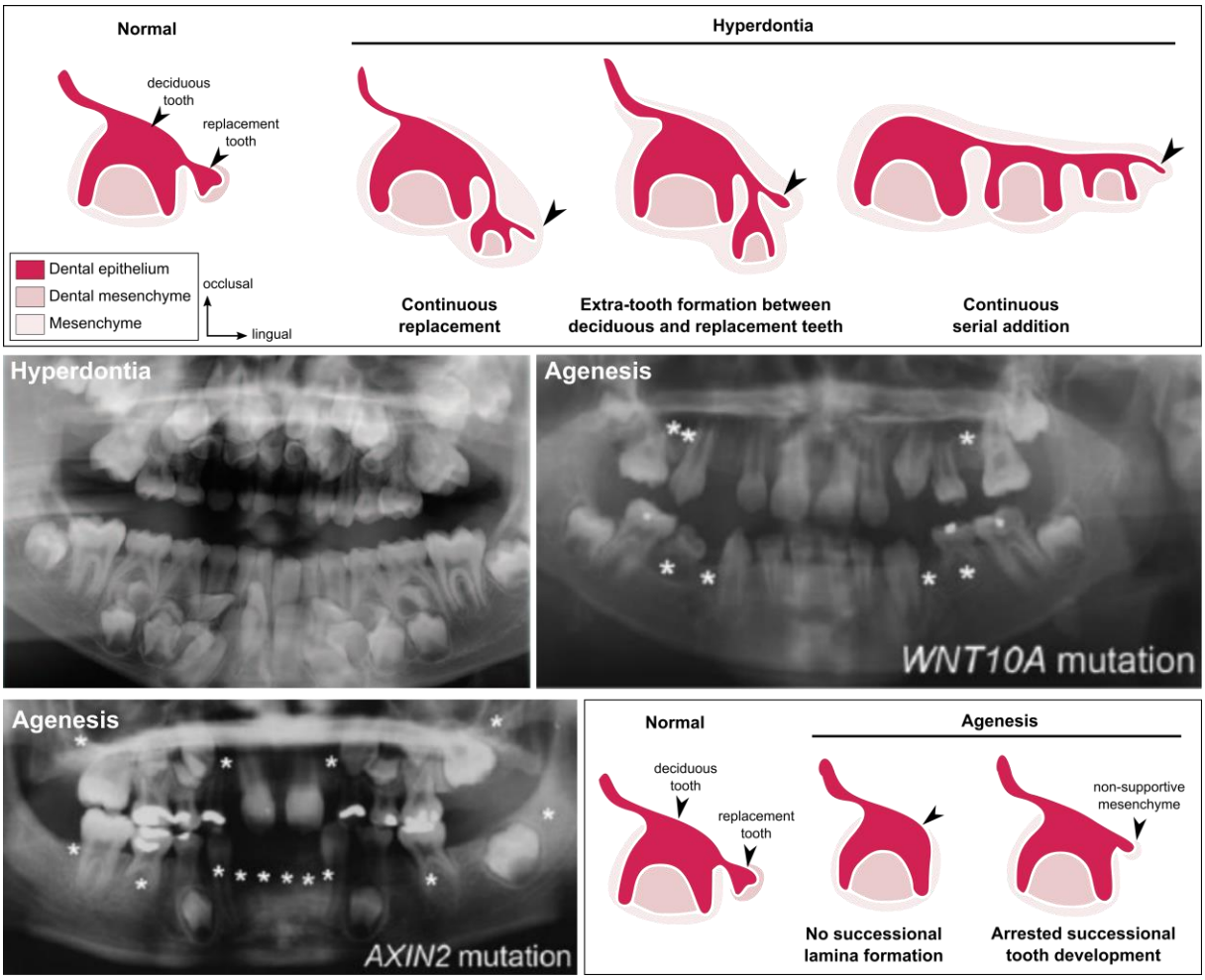

Figure I. 6. Tooth number abnormalities in humans: hyperdontia and agenesis. *At the top, schematics of possible mechanisms leading to tooth hyperdontia: continuous replacement, extra-tooth formation or continuous serial addition. Panoramic radiograph showing hyperdontia of a child (9 years old) with cleidocranial dysplasia. Panoramic radiographs of children (10 and 8 years old) showing agenesis with homozygous WNT10A mutation and AXIN2 mutation. At the bottom, schematics of possible mechanisms leading to tooth agenesis: no successional lamina formation or arrested successional tooth development. Missing teeth marked by asterisks (adapted from Juuri & Balic, 2017).*

From studies of various diphyodont species, we possess histological description of the tooth replacement and some candidate genes. However, studies are always limited by the constraints of the animal models. For now, no ideal diphyodont animal has been found to study the molecular basis of tooth development and replacement in mammals.

State of the art regarding dental replacement in monophyodont mammals

To better understand dental developmental processes, majority of the genes involved in human tooth disorders have been studied in transgenic mice. Mice are monophyodonts (only one set of teeth), but some transgenic mice have been used to study tooth replacement.

The mouse possesses one incisor and three molars per quadrant. The incisors have the ability to grow during the entire animal's life due to stem cells maintenance in the incisor growing area. The molars develop from a continuous dental lamina, have roots and are never replaced. However, during molar development in the mouse we can observe a rudimentary successional dental lamina (RSDL) in the lingual part of the tooth germ (Dosedělová et al., 2015). This RSDL structure is visible in the mouse molars from 16 dpf to 10 dpn and some *Sox2*$^{+}$ cells can be identify at the lingual part of the RSDL (**Figure I. 7**). The RSDL will then regress, correlated with a loss of Sox2 signal and a decrease of proliferation in the RSDL (Dosedělová et al., 2015).

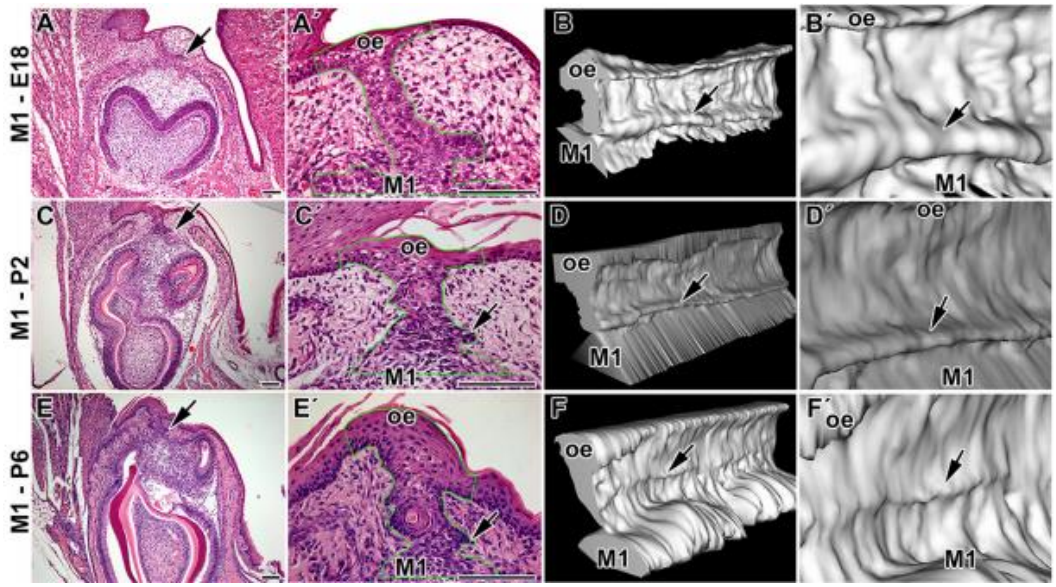

Figure I. 7. Rudimentary successional dental lamina in the developing mouse molar*. Hematoxylin-eosin staining and 3D-reconstructions of the dental lamina in the first lower molar. Arrow, rudimentary successional dental lamina; oe, oral epithelium; E, embryonic day; P, post-natal. Scale bars: 100 µm. (From Dosedělová et al., 2015).*

The RSDL in wild type mouse does not have odontogenic potential (Popa et al., 2019). However, some transgenic mice are able to develop a new tooth from the RSDL. Popa et al. (2019) showed that by stabilizing the Wnt/β-catenin signaling in the *Sox2*$^{+}$ cells during embryo development, so in the lingual RSDL, they were able to maintain the proliferation of the RSDL. By isolating the RSDL in culture, they were even able to obtain a mineralized tooth. They showed that the RSDL could continue its development in transgenic mice thanks to the presence of Wnt signaling at the tip of the lamina when the RSDL is isolated from the main tooth. So, the deciduous molar seems to have the capacity to inhibit the development of the RSDL. By stabilizing Wnt/ β-catenin signaling, they observed expression of odontogenic markers as *Shh*, *Fgf4*, *Fgf3*, *Bmp4* and *Sostdc1* in the RSDL that are not expressed in controls. So, activation of the Wnt/ β-catenin signaling induces the odontogenic potential of the RSDL.

Transgenic mice can also have variation in their tooth number without affecting directly the RSDL; some mutations induce the development of rudimentary teeth. Ahn et al. (2010) showed that inactivation of *Sostdc1* in mouse induce elevated Wnt and Spry2/4 signaling and

the formation of supernumerary teeth. Sprouty mutants also present supernumerary teeth (Klein et al., 2006, see Annex 2, **p213)**. On the contrary, the overexpression of *Sostdc1* induces a diminution of the tooth number. Munne et al. (2009) described the *Sostdc1* expression pattern during normal tooth development and indicated an intensive expression in the lingual side of the incisor, where a new incisor is developing in *Sostdc1* deficient mutants. They hypothesize that theses extra-incisors are replacement teeth. So, SOSTDC1 seems to inhibit the tooth development and replacement in wild type mice (**Figure I. 8**A). This gene is described as an inhibitor of the Wnt signaling (Itasaki et al., 2003). Inhibiting *Sostdc1* induces tooth formation, indicating that Wnt signaling plays a role as activator of tooth development.

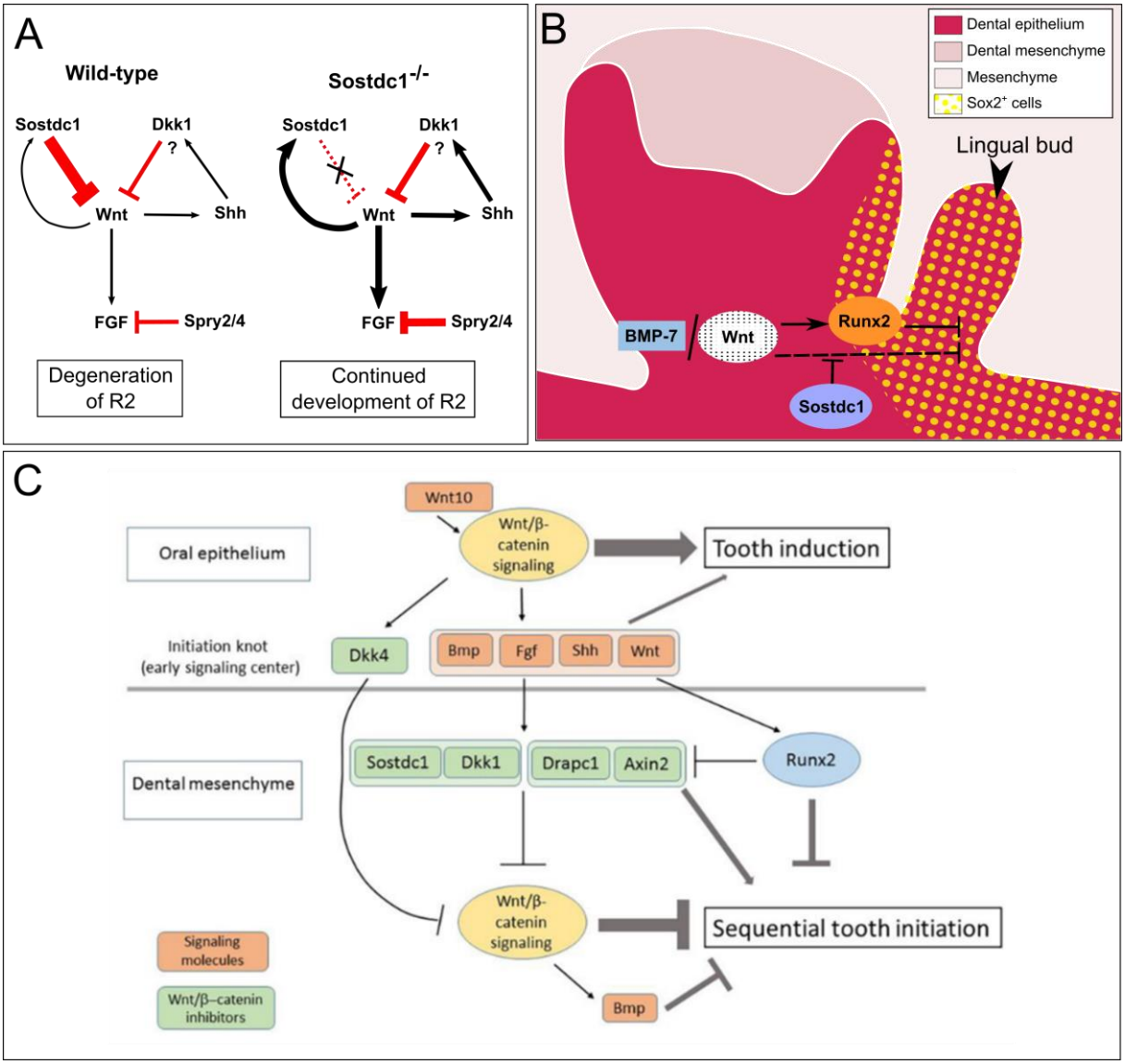

Figure I. 8. Signaling pathways involved in tooth number regulation in the mouse. *(A) Sostdc1 signaling identified in mouse (from Ahn et al., 2010). (B) Signaling pathways involved in the development of a lingual bud in the mouse (from Togo et al., 2016, colors modified). (C) Role of the Wnt signaling in tooth induction and initiation (from Järvinen et al., 2018).*

On the contrary, some mutants are unable to develop teeth, as *Runx2* null mice (Togo et al., 2016). At birth, the mutants do not have mineralized molars (they stopped their development during embryogenesis). However, during odontogenesis the *Runx2* null mice can present a lingual bud with *Sox2*$^{+}$ cells (**Figure I. 8**B). Interestingly, by inactivating both *Runx2* and *Sostdc1*, the dental phenotype is rescuing in 25% of the mice at birth and this double mutant present less supernumerary teeth than *Sostdc1* mutants. Togo et al. (2016) suggested that *Sostdc1* and *Runx2* have an antagonistic function in the tooth development. It has been

suggested that inhibition of *Runx2* could arrest primary tooth development but stimulates the formation of a secondary tooth (Wang et al., 2005).

Moreover, by expressing β-catenin in oral and dental epithelium, the tooth morphogenesis is disturbed. At the beginning of tooth development in mouse mutants, Järvinen et al. (2006) observed numerous small buds of teeth that possess each an enamel knot instead of a normal tooth bud with a unique enamel knot. In this mutant, the expression of Sostdc1 is not modified between mutants and wild type mice. By isolating the numerous buds in the mutant, they showed that all these buds had the capacity to give a mineralized tooth. These results suggest a direct role of the epithelial Wnt signaling in the formation of supernumerary teeth (**Figure I. 8**C). On the contrary, activation of Wnt signaling in the mesenchyme inhibits the sequential formation of the molars, indicating an opposite effect of increased epithelial and mesenchymal Wnt/ β-catenin signaling (Järvinen et al., 2018).

To conclude, these various mutants indicate that the Wnt signaling seems to be a key regulator of the tooth number in mouse as previously shown in other species. SOSTDC1 is identified as an inhibitor of the Wnt signaling (**Figure I. 8**A), *Runx2* plays a dual role in the tooth development and the presence of *Sox2*$^{+}$ cells seems necessary to induce a tooth replacement (**Figure I. 8**B). The suggested signaling pathways that could regulate the tooth numbers are summarized in **Figure I. 8**C. These signaling pathways include numerous candidate genes identified in ferret but also those related to human pathologies.

However, it is necessary to keep in mind that these results come from mutants with abnormal development of extra-teeth. This is why it is necessary to follow these candidate genes during the tooth development and replacement in a wild-type diphyodont mammal.

Rabbit as a model for tooth Evo-Devo studies

We thus decided to use the rabbit (*Oryctolagus cuniculus*) as a new model to study tooth development and replacement. The rabbit is already an important model for biomedical research (Bosze and Houdebine 2006) and the whole genome has been sequenced (OryCun2.0). On contrary to the ferret, the rabbit does not have seasonal estrus, gives numerous embryos per litter, and when the environmental conditions are stabilized (temperature, food) the gestation time does not vary (31 days of gestation only). Rabbit teeth are sufficiently small to perform all the conventional molecular studies primarily designed for mice. Moreover, more complex gene-targeting technology have been successfully applied in rabbit, as CRISPR/Cas9 system (Yan et al., 2014).

The rabbit dentition is diphyodont with a replacement of one incisor and all premolars (**Figure I. 9**, Horowitz et al., 1973, see annex 4 p256). Rabbits are heterodont: they possess on each side two uppers and one lower incisors, three upper and two lower premolars and three upper and lower molars.

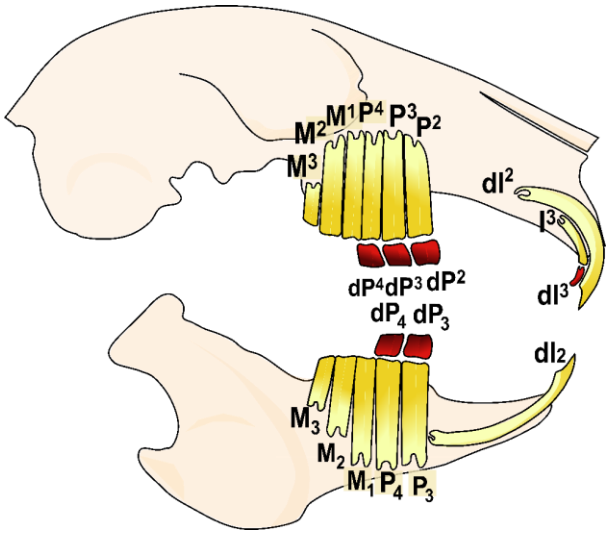

Figure I. 9. Schematic representation of the rabbit skull and its dental formula. *In red, the teeth that are replaced, in yellow the permanent teeth (replacement teeth and deciduous teeth not replaced). I, incisor; P, premolar; M, molar.*

In rabbit, the deciduous premolars have a limited growth with root formation whereas permanent teeth are continuously growing (Sych & Reade, 1987). Concerning the incisors, the dI2 and the permanent I^3 are ever-growing but the dI^3 has roots.

Rabbit tooth development

Rabbit tooth development has been studied during the 70-80's. Horowitz and collaborators did a complete chronology of deciduous tooth eruption using radiography, giving information on the mineralized part of the teeth (Horowitz et al., 1973). Navarro et al. did histological studies of the postnatal development in maxillary (1975) and mandibular cheek teeth (1976). However at birth the deciduous incisors and premolars are fully developed. In embryos, Ooë (1980) and Hirschfeld (1973) have studied the incisor development, but nothing has been reported for the cheek teeth development. All these studies give a composite chronology of the tooth development in rabbit and no molecular data has been acquired. The aim of this thesis is to characterize the precise chronology of the tooth morphogenesis in the rabbit and to follow the spatio-temporal regulation of the tooth replacement. By studying the tooth morphogenesis during ontogeny, we also point out possible links between rabbit tooth development and the evolution of the Lagomorpha cheek teeth.

Characteristics of extant Lagomorpha

The lagomorph order contains extant rabbits, hares and pikas. Lagomorpha is the sister group of Rodentia, named together the Glires. Lagomorphs are defined by their dentition: they possess two upper incisors one behind the other (Rose, 2006). In extant species, all the permanent teeth are hypselodont and adapted for feeding on grass and other vegetation. Lagomorphs are divided in two families, the Leporidae (rabbits and hares) and the Ochotonidae

(pikas). The Ochotonidae family contains only one living genus, Ochotona, which includes 30 species living in North America and Central Asia (Hoffmann and Smith 2005). Ochotonidae have only two upper molars instead of Leporidae. Leporidae includes 11 living genera and 61 species that have colonized Africa, Eurasia and North and South America. The European rabbit, *Oryctolagus cuniculus*, is the only extant species of the *Oryctolagus* genus. The common names hare and rabbit are used to designate different leporid genera (**Figure I. 10**).

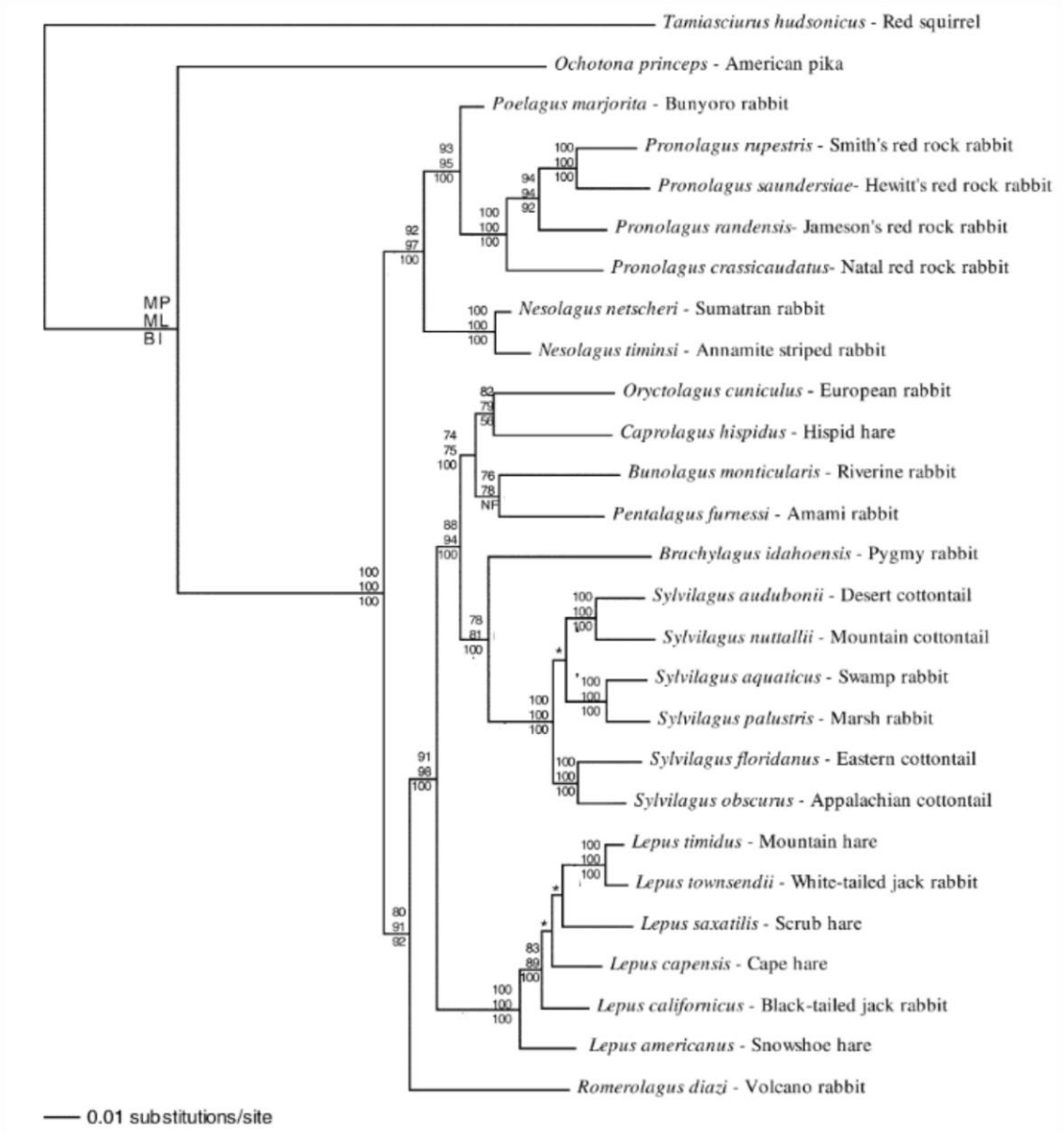

Figure I. 10. Molecular phylogeny of the extant Leporidae. *Phylogeny obtained using seven gene fragments. Values above and below nodes represent the nodal support (MP=maximum parsimony bootstrap; ML=maximum likelihood bootstrap; and BI=bayesian inference posterior proba-bility) for associations among the 25 ingroup taxa. An asterisk indicates that the node was not supported by>50% bootstrap support. (Simplified from* Matthee et al., 2004)

Evolutionary history of Lagomorpha

Duplicidentata mirorder contains the lagomorphs and their sister group, the mimotonids. Lagomorpha is a monophyletic group whereas recent analyses show that mimotonids are a paraphyletic group that contains the stem lagomrpha ancestor. Mimotonids, known from the late Paleocene to the middle Eocene, have two incisors in both upper and lower jaws and their cheek teeth are unilaterally hypsodont and rooted (Rose, 2006). As mimotonids, the stem lagomorphs group was originated from Asia, and they diversified then in different continents. Stem Lagomorpha, as *Dawsonolagus* from late early Eocene, had hypsodont rooted cheek teeth and are described as morphologically transitional between mimotonids and lagomorphs (Li et al. 2007). The Oligocene marks the separation of the Lagomorpha in two families, the Ochotonidae and the Leporidae. At the end of the Miocene, the Leporidae are represented by the genera *Alilepus*, and especially *Alilepus hibbardi*, a suggested ancestor of the extant genera of Leporids (Jin *et al*. 2010).

Lagomorpha teeth evolved from moderate hypsodont rooted cheek teeth in late Paleocene to hypselodont teeth. The shape variations of the P_3 is highly studied because this tooth bears informative characters about phylogenetic relationships among Lagomorpha (Hibbard 1963; Cermák 2015). We decided in the present thesis to study the variation of the M^1 morphology during European rabbit ontogeny and lagomorph evolution notably because this tooth shows the typical bilophodont pattern of the jugal dentition of modern lagomorph and because it is the mostly used tooth for comparative anatomy purposes in mammals (Hershkovitz 1971).

PART 1

TOOTH DEVELOPMENT AND REPLACEMENT IN *ORYCTOLAGUS CUNICULUS*

Since decades, tooth development mechanisms in mammals are highly studied using mouse as model (i.e. Balic and Thesleff, 2015; Chavez et al., 2012; Lan et al., 2014). However, the mouse does not replace its teeth. As a consequence, mammal tooth replacement is poorly known. As previously presented in introduction, various species have been studied in order to identify a good animal model for dental replacement studies (Järvinen et al., 2009; Popa et al., 2016; Wang et al., 2014a). However, for now, any model answer both morphological and molecular questions about mammal tooth replacement. A good mammal animal model has to replace its teeth, be easy to maintain, breed in large numbers in a laboratory facility, have the shorter generation time possible and be sequenced. If possible, it is even more interesting to have a model animal that has already been used for genetic manipulation techniques or *in vitro* studies.

In this thesis, we decided to study tooth development and replacement using the European rabbit, *Oryctolagus cuniculus* as model. The European rabbit is already used as model in biomedical research, is sequenced, has already be used for CRISPR-CAS9 genetic manipulation and in vitro organ culture (Bosze and Houdebine, 2006; Glasstone, 1938; Yan et al., 2014). The European rabbit is currently used in dentistry research to study orthodontic process (Abtahi et al., 2018). Studying rabbit dental development with modern techniques is necessary, the available studies in literature being rather old and incomplete (Horowitz et al., 1973; Navarro et al., 1976; Ooë, 1980). We show in this first part that the European rabbit is an efficient model to study both morphological and molecular mechanisms involved in tooth development and replacement.

Chapter 1.1 – Morphological characteristics of tooth development and replacement in *Oryctolagus cuniculus*

The review of publications about rabbit tooth development and replacement leads to a composite developmental chronology, with a lack of knowledge about some tooth types and developmental stages. Moreover, the studies already carried out are about 50 years old, some techniques used in these papers are now obsolete (Glasstone, 1938; Horowitz et al., 1973; Yardin, 1968). Most of the current studies on rabbit dentition are about orthodontic or veterinary cares, with few studies on rabbit embryos (Abtahi et al., 2018; Meredith, 2007).

In the following paper, we decided to update the knowledge on the dental morphogenesis in the European rabbit using modern techniques. We studied each rabbit tooth from the initiation of the development to the mineralization of the replacement teeth, so from 12 days post-fertilization to 4 days post-natal, representing 23 days of development. We performed 3D reconstructions of dental epithelial tissues for each tooth using X-ray microtomography associated with a histological study to follow the rabbit dental development. We obtained the complete description of the histo-morphological chronology of the tooth development and replacement in rabbit. During this study, we also observed an undescribed rabbit incisor characteristic: at birth, the growing upper incisors of the rabbit present holes in the dentin, opening the pulp cavity. These holes are quickly repaired with a new apposition of dentin from the pre-existing odontoblasts that continue to secrete despite the disruption.

The new dental morphogenesis chronology of the rabbit *Oryctolagus cuniculus* presented in the following paper will allow further molecular studies to better understand mammal tooth replacement. Moreover, the 3D epithelium surface reconstructions are available online in Morphomuseum for who is interested to re-use these surfaces for other scientific works.

Article 1: Morphological features of tooth development and replacement in the rabbit *Oryctolagus cuniculus*

Ludivine Bertonnier-Brouty[1*], Laurent Viriot[1], Thierry Joly[2, 3], Cyril Charles[1]

[1] Institut de Génomique Fonctionnelle de Lyon, Université de Lyon, CNRS UMR 5242, Ecole Normale Supérieure de Lyon, Université Claude Bernard Lyon 1, Lyon, France

[2] ISARA-Lyon, F-69007 Lyon, France

[3] VetAgroSup, UPSP ICE, F-69280 Marcy l'Etoile, France

[*] Corresponding author: Ludivine.bertonnierbrouty@ens-lyon.fr

Abstract

Dental development mechanisms in mammals are highly studied using the mouse as a biological model. However, the mouse has a single, unreplaced, set of teeth. Features of mammalian tooth replacement are thus poorly known. In this paper, we study mammalian tooth development and replacement using the European rabbit, *Oryctolagus cuniculus*, as a new model. Using 3D-reconstructions associated with histological sections, we obtained the complete description of the histo-morphological chronology of dental development and replacement in rabbit. We also describe the presence of holes in the dentin opening the pulpal cavity in newborns. These holes are quickly repaired with a new and fast apposition of dentin from the pre-existing odontoblasts. The detailed dental morphogenesis chronology presented allows us to propose the rabbit *Oryctolagus cuniculus* as a suitable model to study mammalian tooth replacement

Keywords

Tooth development, mammalian tooth replacement, 3D-reconstructions, rabbit teeth

Introduction

The signaling pathways involved in tooth development and morphogenesis are highly studied in mice (Balic and Thesleff, 2015), fishes (Rasch et al., 2016), or reptiles (Whitlock and Richman, 2013). Regarding tooth replacement (Bertin et al., 2018), a majority of fish and reptiles have the ability to replace their teeth continuously throughout their life (polyphyodonty) contrary to the majority of mammals that replace their teeth only once (diphyodonty). In mammals, most odontogenesis studies use the mouse as a model species and mouse tooth development is well described from its morphogenesis to the genetic mechanisms involved. Tooth development is commonly divided into five stages: the placode, the bud, the cap, the bell, and finally the maturation stages. At first, a dental placode appears from the oral epithelium by thickening. Next, at the bud stage, the dental epithelium invaginates, followed by a condensation of the dental mesenchyme. Then, the epithelium starts to fold, forming the cap stage; this stage marks the beginning of histo-differentiation. The tooth cuspidogenesis starts at the bell stage. Cells begin to secrete dentin and enamel layers at the late bell stage. In the maturation stage, the tooth gets fully mineralized. Because the mouse has no dental replacement, the mechanisms of tooth replacement in mammals are poorly known. Some studies have been done in the ferret (Järvinen et al., 2009; Jussila et al., 2014), the shrew (Järvinen et al., 2008), the fruit bat (Popa et al., 2016) and the minipig (Wang et al., 2014a, 2019). Altogether, these studies have characterized the morphological changes involved in tooth replacement: the initiation of tooth replacement begins by a budding of the replacement dental lamina at the lingual part of the tooth stalk. Then the replacement dental lamina plunges into the mesenchyme and the tooth morphogenesis begins. Moreover, the first molecular observations of tooth replacement mechanisms in mammals have been done in the ferret *Mustela putorius furo* (Järvinen et al., 2009; Jussila et al., 2014). However, few developmental stages were studied due to the difficulty to obtain ferret embryos at the correct stage and the

presence of seasonal estrus. The shrew *Sorex araneus* is limited as a model because their deciduous teeth never erupt. In the fruit bat *Eidolon helvum*, 3D reconstructions and histological sections are good illustrations of mammalian tooth replacement but authors indicated that this species is no longer available for experimental purposes (Popa et al. 2016). Tooth development and replacement has also been described in the minipig *Sus scrofa,* whose teeth size and morphology are pretty similar to human teeth (Wang et al. 2014). However, at least 100 days are necessary from the appearance of the replacement dental lamina to the mineralization of the replacement tooth in the minipig. So, the slow development, the size of the animal and ethical concerns are significant obstacles to study tooth development in the minipig. For now, any model can answer both morphological and molecular questions about mammalian tooth replacement, and previous studies are restricted to some parts of dental development. We thus decided to use the European rabbit (*Oryctolagus cuniculus*) as a new model to study tooth development and replacement. The rabbit is already an important model for biomedical research (Bosze and Houdebine, 2006) and the whole genome has been sequenced (OryCun2.0, 2009). The rabbit dentition is diphyodont with a replacement of some incisors and all premolars (Horowitz et al., 1973). They possess two upper and one lower incisors, three upper and two lower premolars and three upper and lower molars on each side. Deciduous premolars have a limited growth with root formation whereas permanent teeth are continuously growing (Sych and Reade, 1987). Associated with this continuous growth, each permanent tooth in the rabbit is supposed to possesses a pool of mesenchymal and epithelial stem cells in its growing part, as in all hypselodont species (Tummers & Thesleff, 2003). Rabbit dental development has been studied during the 70's and 80's, Horowitz and collaborators (1973) completing a chronology of deciduous tooth eruption using radiography, giving information on the mineralized part of the teeth. Navarro carried out histological studies of the postnatal development in maxillary (1975) and mandibular cheek teeth (1976). However, the deciduous incisors and premolars are

completely mineralized at birth and thus Navarro et al. do not document their development. Hirschfeld et al. (1973) and Ooë (1980) have studied the incisor development in embryos, but nothing has been reported for the cheek teeth development. Michaeli et al., (1980) gave a simplified chronology of rabbit cheek tooth development during embryogenesis without separating each tooth and with histological illustrations only for the post-natal stages. All these studies result in a composite and fragmental chronology of the tooth development in rabbit. The purpose of our work is to supply a complete report of the development of all deciduous and permanent teeth in the rabbit. We decided to study rabbits from 12 days post fertilization to 4 days post-natal in order to obtain a complete chronology of tooth development from the initiation of the deciduous tooth to the mineralization of the replacement teeth. Using histological studies and 3D-reconstruction of soft tissues, we present the developmental and morphological characteristics of rabbit teeth.

Material & Method

Samples

Embryos and newborn rabbit samples used for histology and X-Ray microtomography were obtained through collaboration with a standard production for feeding recorded at the Biology Departmental livestock establishment (EDE) n°38044102. We worked on common rabbit breeding regularly crossed with wild rabbits to ensure genetic mixing. The gestation period for a rabbit is about 31 days. We collected embryos at 12, 14, 16, 18, 20, 22, 24, 26 and 28 days post fertilization (dpf) and rabbits at 0, 1, 2, 3 and 4 days post-natal (dpn). 3 to 21 embryos were analyzed for each developmental stage. For juvenile and adult rabbits, observations were made on 230 specimens of *Oryctolagus cuniculus* from the Muséum National d'Histoire Naturelle (MNHN, Paris, France). Age of the specimens were not indicated so we used the skull size as proxy, our sampling contained skull size from 36.65 to 108.8mm. In the

230 specimens, only four still had their deciduous teeth. Each tooth is specifically named: we use ’I‘, ’P‘ and ’M‘ for incisor, premolar and molar respectively; the deciduous teeth are indicated with a ’d‘; the tooth number is in exponent for the upper teeth and in index for the lower teeth.

Histology

After dissection of the upper and lower jaws, samples were fixed overnight in 4% PFA. Samples were then rehydrated and fixed in Holland Bouin solution during 1 day. Jaws were demineralized for 1 to 7 days in Morse’s solution (10% sodium citrate + 22% formic acid) or in RNase-free 12.5% EDTA + 2.5% PFA during 6 weeks, according to the subsequent experiment to be performed. Then, jaws were embedded in paraffin and serially sectioned with a Leica microtome (7 µm thick slices). Sections were carried out in parasagittal or frontal plane. For histological purpose, samples were dewaxed in xylene, and then colored via an optimized Masson's trichrome protocol with aniline blue, hemalum and fuschin.

In situ hybridization

Specific probes for *Osteocalcin* and *K14* have been designed using the rabbit genome available online (OryCun2.0, 2009). Each probe has been sequenced before use, and then probes were synthesized with RNA-dig labeling nucleotides. Classical mouse *in situ* protocol has been optimized to be compatible with rabbit tissues. Tissues were treated with HCl 0.2M, with proteinase K 5µg/ml and then incubated with TEA-Acetic anhydride. Hybridization step were done at 62°C. Sections were whashed in a warm washing buffer (1X SSC and 50% formamide) and in MABT solution. After 2 hours in a blocking solution, slides were covered of anti-Dig-AP-antibody solution at 4°C overnight. Sections were washed with MABT and NTMT with teramisol. Sections were stained with BM purple solution and mounted in Aquatex.

X-ray microtomography and 3D reconstruction

Conventional X-ray microtomography allows reconstructing 3D models of mineralized tissues such as bony head and teeth, thus providing a non-invasive access to internal structures. Using phosphotungstic acid (PTA) staining, that binds heavily to various proteins and connective tissue (Metscher, 2009); we were able to detect soft tissues by X-Ray microtomography. After fixation, half-head samples were stained in a solution 0.3% PTA in 70% ethanol between 1 week and 8 months according to the size of the sample. Oldest specimens were demineralized to better detect the soft tissue staining. Once the PTA contrast staining was complete, samples were embedded in paraffin and radiographed using a Phoenix Nanotom S (GE Measurement and Control), which was set up with a tungsten source X-ray tube operating at 100 kV and 70 µA for the mineralized tissues and 60kV and 70µA for the soft tissues. The Phoenix datosx2CT software was applied to gather radiographies in a reconstructed 3D volume, in which the voxel size ranged from 1 to 12 µm depending on the size of the specimen. Post-treatment of 3D volumes, including virtual sectioning as well as sub-volume extractions, was performed using VG-studio max software. Surface smoothing was done with Meshlab software. Incisors hole positions were detected using VG-studio max software and frontal sections were done at each hole using a rotation section plane to respect the natural curvature plane of the incisors. We studied 59 holes from ten incisors (6 individuals), the two remaining insisors were used for histology purposes. The centroid of the incisor section was drawn using ImageJ software and mesio-distal and linguo-vestibular axes were positioned in the incisor section. An angle was calculated to determine the hole position, with the mesial position at 0° (and 360°), the vestibular at 90°, the distal at 180° and the lingual position at 270°. Plots were made using R software and the ggplot2 library.

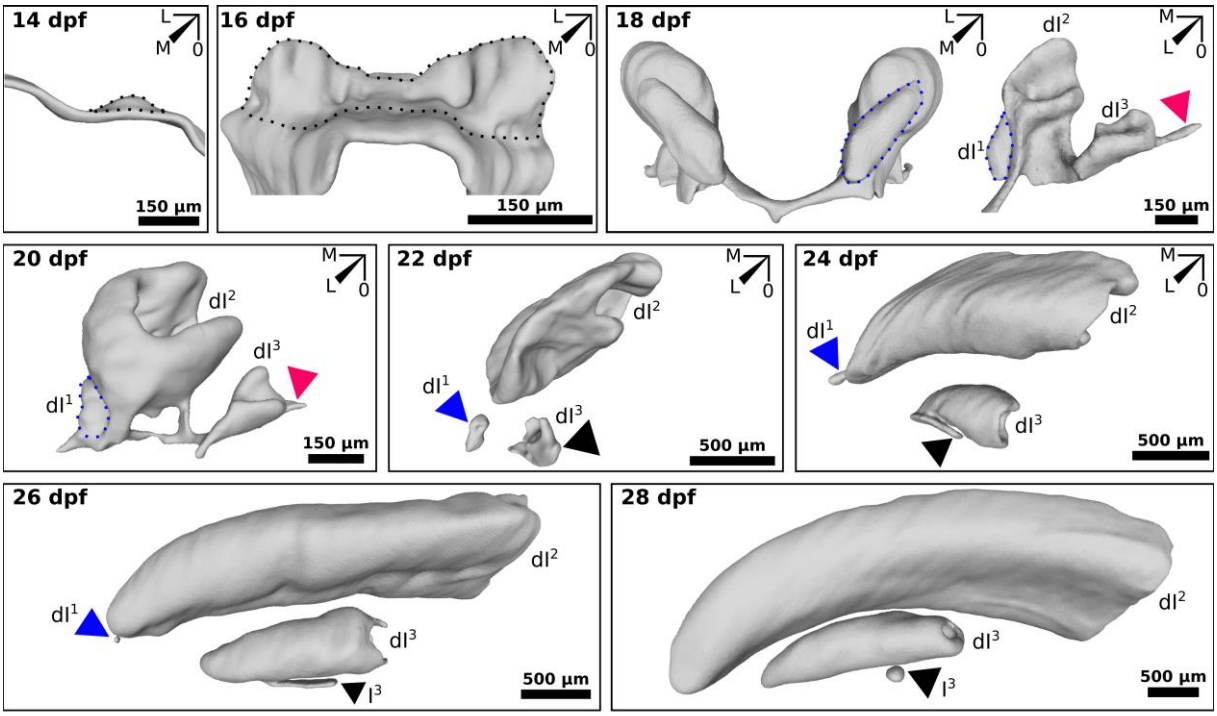

Figure 1. 1. 3D-reconstructions of the epithelial part of the upper incisors during development. *Development of the dI^1, dI^2, dI^3 and I^3 from 14 to 28 days post-fertilization (dpf). Indicated in blue, the vestigial incisor; in pink, the interdental lamina; in black (dotted line), the dental tissues; in black (arrow), the replacement tissues. M, mesial; L, lingual; O, occlusal.*

Results

Chronology of incisor development and replacement

We have observed the establishment of the incisors on the upper and lower jaws. The dI1 and the dI2 incisors in the upper and lower jaws appear synchronous in their development. Rabbits have another incisor in the maxillary, named the dI^3, which is replaced during ontogeny. We will focus here on the description of the upper incisors (**Figure 1. 1**), since we do not observe dental replacement in the lower ones. All our 3D reconstructions of the epithelial parts of the incisors are available in Morphomuseum (3D Dataset will remain locked until publication of the main article, Bertonnier-Brouty et al., 2019).

Vestigial incisor dI^1

At 18 dpf, the first upper incisor is already mineralized with dentin surrounded by dental soft tissues very close to the oral epithelium. This dI^1 is a vestigial tooth; it will not give rise to a functional incisor (**Figure 1. 2**, A). At 24 dpf, the dI^1 has passed through the oral epithelium and is now trapped in the oral mucosa (blue triangle in **Figure 1. 1**, **Supplementary 1. 1**). At 28 dpf, the dI^1 is shed.

dI^2

At 18 dpf, the dI^2 is at the cap stage, linked mesialy to the other dI^2 and in rotation. As in mouse (Mucchielli and Mitsiadis, 2000), the dI^2 rotates antero-posteriorly and become parallel to the long axis of the jaws, contrary to molars that stay perpendicular to the jaw axis (**Figure 1. 1**). At 20 dpf, the dental lamina that links the teeth together is completely disorganized and the two dI^2 are no longer linked. The dI^2 has already secreted a thin layer of dentin and the 3D reconstructions show that the vestibular and lingual cervical loops are well formed. These structures are supposed to contain the stem cells that will allow the continuous growth of the tooth during the animal's entire life. At 22 dpf, the teeth are completely separated. At 24 dpf, the dI^2 occlusal surface is very close to the oral epithelium and highly mineralized. The dI^2 presents enamel in its entire mineralized surface. We observed a big cervical loop at the vestibular side and a very small one at the lingual part and this incisor has a fold on its vestibular surface on the mesial side.

Figure 1. 2. 3D-reconstructions of the mineralized part of the rabbit teeth. *(A) Mineralized tissues of the upper incisors from embryo to adult. (B) Mineralized tissues of the upper cheek teeth from newborn to adult. (C) Mineralized tissues of the lower cheek teeth in newborn and adult. (D) Tooth nomenclature: "I", "P" and "M" for incisor, premolar and molar; the deciduous teeth are indicated with a "d"; the tooth number is in exponent for the upper teeth and in an index for the lower teeth. In blue the vestigial incisor, in red all the deciduous teeth that will be replaced.*

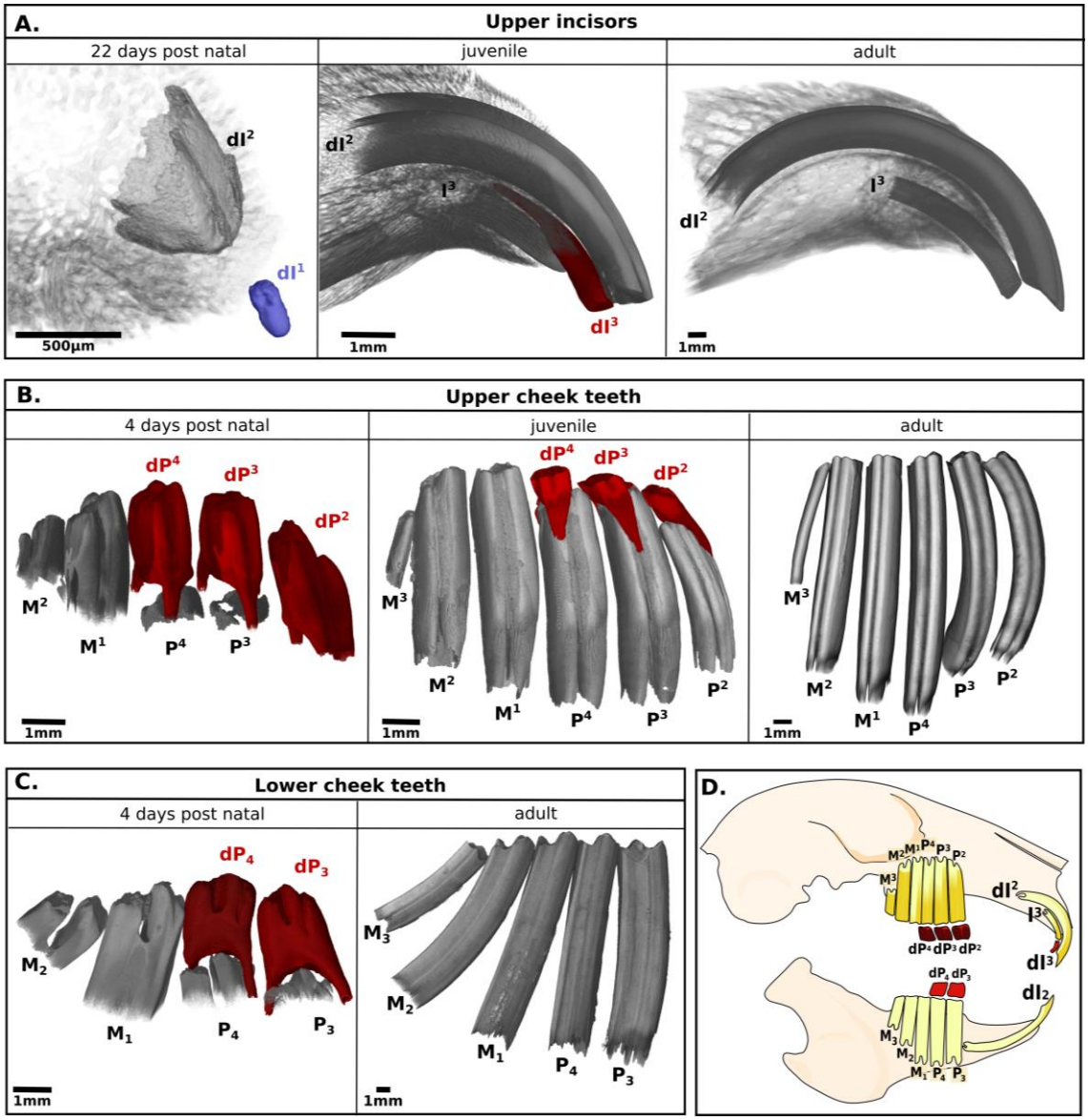

At 26 dpf, the dI^2 is close to erupt. The secretion of enamel at the vestibular and lingual part of the tooth continues. At 28 dpf, the dI^2 is erupting. At birth, the unworn dI^2 presents enamel in the entire erupted occlusal surface. In direction to the growth zone, we detect enamel in the vestibular and the lingual part, and then the enamel production in the lingual part stops and enamel is secreted only in the vestibular part of the tooth (**Supplementary 1. 2**). At 4 dpn, the dI^2 are worn in their occlusal surface, showing the dentin. In the juvenile, around 1 month post-natal, we observed that the dI^2 present enamel only in the vestibular surface, so the entire part with enamel in the lingual and vestibular position is already worn (**Figure 1. 2**, A). In adult, the dI^2 is ever-growing. We observed that the dI^2 and the I^3 do not have the same shape at the

occlusal surface, the dI^2 has a sharper beveled edge form compared to the I^3, linked to the gnaw ability of the dI^2.

dI^3

At 18 dpf, we observed the dI^3 in a transitional stage between bud and cap at the distal position of the dI^2. At the vestibular part of the dI^3, we observed an epithelium structure distally oriented that is probably a dental lamina rest (**Figure 1. 1**, pink triangle). At 20 dpf, the dI^3, still connected to the dI^2, is now in a cap stage and rotates antero-posteriorly. At 22 dpf, dI^3 is still linked to the oral epithelium but separated to the dI^2. We observed a lingual budding of the replacement dental lamina in the dI^3 (**Figure 1. 1**, black triangle). At 24 dpf, the dI^3 is already well mineralized and now perfectly orientated compared to the working position. The dI^3 presents small cervical loops at the vestibular and lingual part of the tooth. We detect the replacement dental lamina of the dI^3 attached to the antero-lingual part of the tooth, already parallel to the oral epithelium. At 26 dpf, the cervical loops of the dI^3 are reduced; we observed the start of the root formation. The replacement dental lamina has grown but is still linked to the dI^3. At 28 dpf, the dI^3 has erupted to the oral epithelium but still do not exit of the oral mucosa. The dI^3 is the only incisor that develops roots; the pulpal cavity seems to close. The I^3 is in a bud stage and no longer linked to the dI^3. At birth, the dI^3 present enamel in the entire occlusal surface. The I^3 continues its development in a cap stage. At 4 dpn, the permanent I^3 begins to mineralize, the roots of the dI^3 are still in mineralization. The dI^3 is worn in the occlusal surface, showing the dentin. In the juvenile, the roots of the dI^3 have finished mineralizing and we observed root resorption. The I^3 is now well mineralized and will soon replace the dI^3 (**Figure 1. 2**, A). Interestingly, the I^3 is entirely covered by enamel on the while the dI^2 have enamel only in the vestibular part of the tooth (**Supplementary 1. 2**). In adult, the I^3 is still entirely covered by enamel, only the worn occlusal surface shows dentin (**Figure 1. 2**, A).

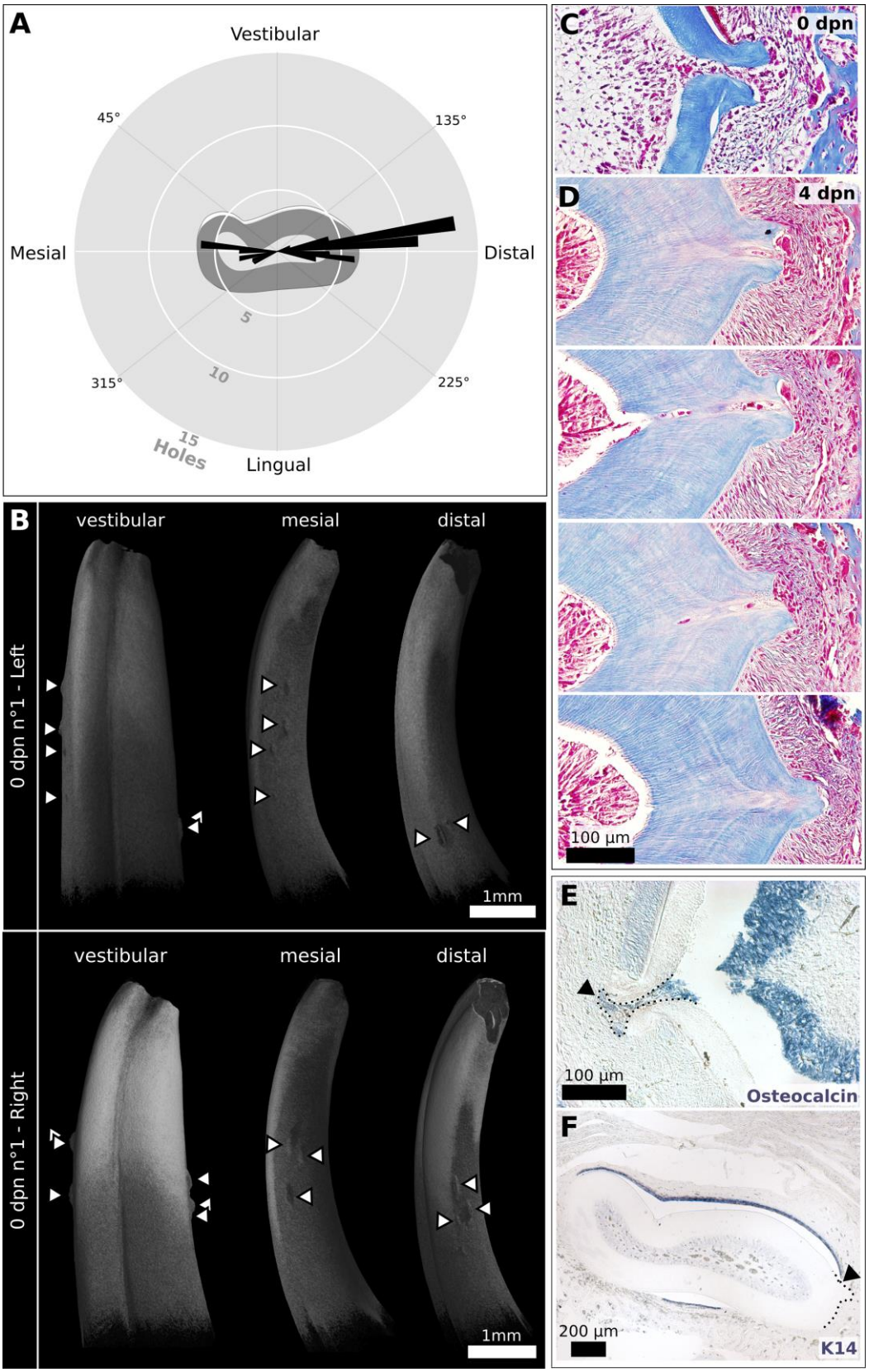

Figure 1. 3. Hole repartition in the upper incisor. *(A) Distribution of the holes in 10 upper incisors from 0 to 4 day post-natal (dpn). (B) Distribution of the holes in the two dI2 from a same individual. Each arrow indicates a fold. (C) Histological sections of a hole in a 0 and (D) 4 dpn individual. (E) Osteocalcin staining and (F) Keratin 14 staining in a 0 dpn incisor.*

Specificity of the rabbit incisors: dentin holes in the newborn incisors

The dI^2 incisor mineralizes at 24 dpf, a thin and continuous layer of dentin is secreted by the odontoblasts. Enamel is first secreted in all the surface of the dI^2, then restricted to the vestibular and lingual sides to finally be secreted only in the vestibular part of the tooth (Fig.S2). In samples from 24 dpf to 28 dpf, the dentin layer of the dI^2 is continuous; no uneven formation of dentin is detected. However, we observed dentin defects in newborn rabbits. In rabbits from 0 to 4 dpn, we detect the presence of holes in the dentin of the dI^2, opening the pulp cavity at specific locations, the lower incisors are not affected (**Figure 1. 3**, A-D). Older samples, from juveniles to adults, do not have holes in their incisors, indicating a mechanism of tooth repair.

To study the appearance and repair of the holes, we identified 59 holes in 10 dI^2 incisors from six individuals from 0 to 4 dpn. We precisely localized each hole in frontal section of the incisor by calculating an angle in function of the incisor centroid and the mesio-distal and linguo-vestibular planes (**Figure 1. 3**, A). We observed that the majority of the holes are at the distal side of the tooth (73%), and some in the mesial part (27%). No hole is observed in the vestibular or lingual part of the incisor.

By comparing the repartition of the holes in right and left incisors of a same individual, we conclude that holes are independently localized in the two incisors on the proximo-occlusal axis; we did not observe any symmetry (**Figure 1. 3**, B). Moreover, the number of holes is variable from one tooth to another, even in the same individual. Interestingly, on the 3 and 4 dpn rabbits, we observed a reparation system by the presence of dentin and cells inside the hole (**Figure 1. 3**, D). This reparation seems very efficient as the holes appear at birth and are repaired two days later.

We decided to use Osteocalcin *in situ* staining as a marker for the dentin formation process (**Figure 1. 3**, E). We observed that the cells in the holes are odontoblasts still expressing Osteocalcin, so still in a secretion stage. These secreting odontoblasts, coming from the pre-existing odontoblast layer, could explain the presence of new dentin in the holes. Keratin 14 staining indicates the epithelial cells (**Figure 1. 3**, F). We wanted to check if the holes could deform the layer of epithelial cells. We detect in the incisor a perfect layer of ameloblasts that is not disrupted by the presence of the hole that are formed at the mesial or distal edges of the enamel layer.

Therefore, these holes are present only in newborns at the mesial or distal limits of the enamel layer, are repaired by the pre-existing odontoblasts and no longer observed during adulthood. Holes seem thus to occur in a very short period of development around or just after the birth of the animal.

Chronology of cheek teeth development and replacement

We observed the establishment of the cheek teeth on the upper (**Figure 1. 4**) and lower (**Figure 1. 5**) jaws. We focus here our description on the mechanisms of tooth replacement. The steps of the tooth replacement are illustrated in the figure indicating all the tooth tissues (**Figure 1. 6**). All our 3D-reconstructions of the epithelial parts of the cheek teeth are available in Morphomuseum (Bertonnier-Brouty et al., 2019).

Figure 1. 4. 3D-reconstructions of the epithelial tissues and histology in rabbit upper cheek teeth from 14 dpf to 28 dpf. *3D-reconstruction of the epithelial tissues of the upper cheek teeth and frontal sections associated for each tooth. Indicated with the black arrow, the permanent premolars. M, mesial; L, lingual; O, occlusal; D, distal; V, vestibular.*

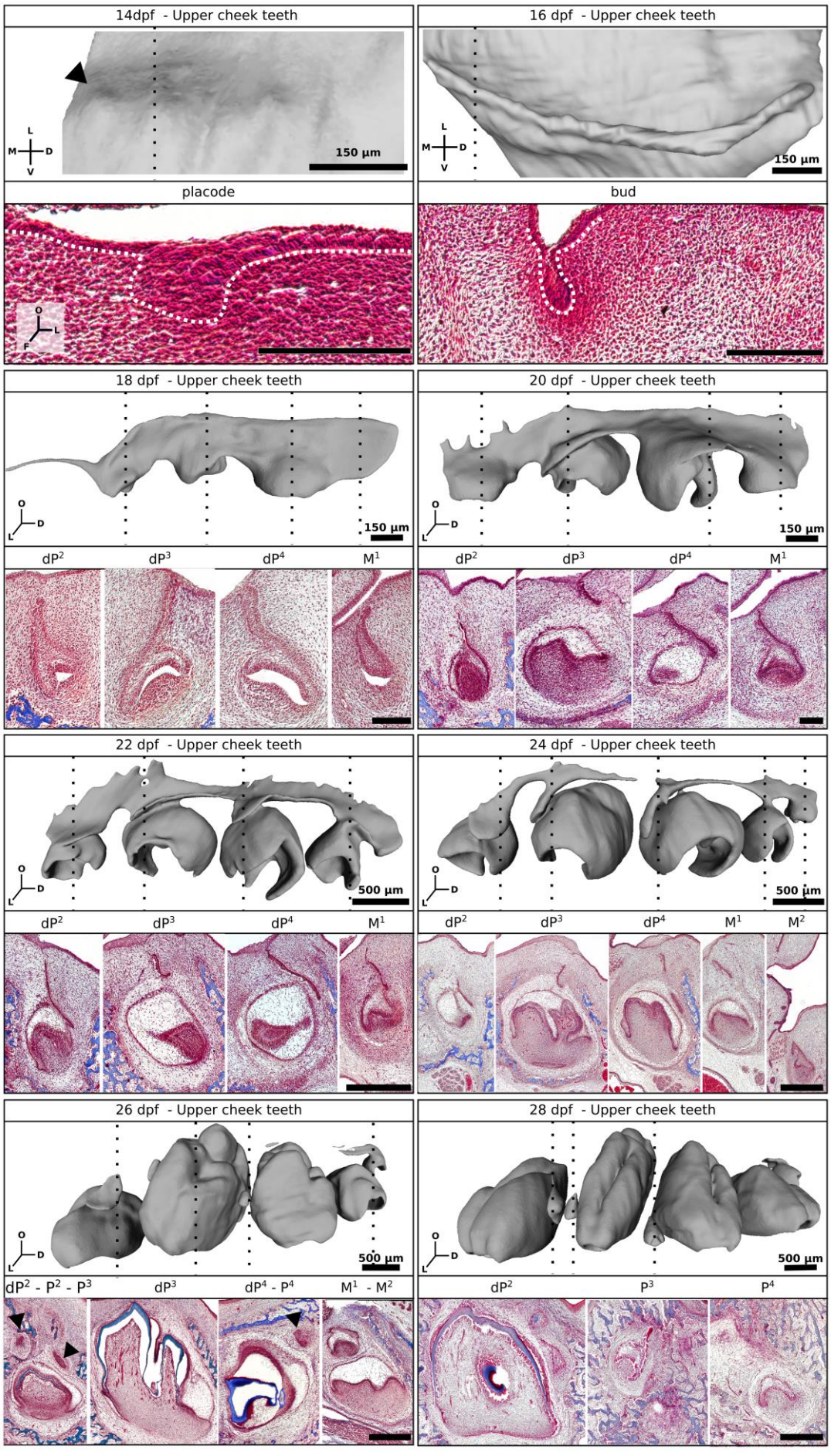
14dpf - Upper cheek teeth
150 µm
placode
16 dpf - Upper cheek teeth
150 µm
bud
18 dpf - Upper cheek teeth
150 µm
dP2 dP3 dP4 M1
20 dpf - Upper cheek teeth
150 µm
dP2 dP3 dP4 M1
22 dpf - Upper cheek teeth
500 µm
dP2 dP3 dP4 M1
24 dpf - Upper cheek teeth
500 µm
dP2 dP3 dP4 M1 M2
26 dpf - Upper cheek teeth
500 µm
dP2 - P2 - P3 dP3 dP4 - P4 M1 - M2
28 dpf - Upper cheek teeth
500 µm
dP2 P3 P4

At 12 dpf, the oral epithelium is regular in thickness; we detect no morphological trace of tooth development initiation. Two days later, the oral epithelium has thickened in the upper and lower jaws, forming the dental lamina (**Figure 1. 4**, **Figure 1. 5**). The dental lamina thickens continuously over a large part of each mouth quadrant and the mesenchyme seems condensed around it, forming the dental placode. In contrast to humans (Juuri and Balic, 2017), the rabbits do not have a unique continuous dental lamina around the jaw arch but distinct dental laminas for the right cheek teeth, the incisors and the left cheek teeth. At 16 dpf, we observed the budding of the dental lamina with a high condensation of mesenchyme around it. At this stage, it is still impossible to name the teeth, the epithelium being continuous in thickness and shape over the entire length of the bud. In the upper jaw, the budding tooth row is rounded, following the vestibular commissure, and measures 1.3mm long from the mesial to distal part of the bud (**Figure 1. 4**). In the lower jaw, the budding tooth row is straighter and smaller with only 0.8 mm long (**Figure 1. 5**). From 18 dpf on, we can identify the teeth and so we will now described the development of each tooth individually. Rabbit cheek teeth have a thin and long dental stalk compared to the mouse or the fruit bat (Dosedělová et al., 2015; Popa et al., 2016).

We observed that the development of the dP_4 is the fastest, followed by the dP_3, dP^3 and dP^4 that are synchronous and then by the dP^2 so we described tooth development following these categories. For the molars, the M1 is the first to develop and then the development timing follows the mesio-distal organization plan. The lower molar begins their development before the upper molar.

Figure 1. 5. 3D-reconstructions of the epithelial tissues and histology in rabbit lower cheek teeth from 14 dpf to 28 dpf. *3D-reconstruction of the epithelial tissues of the lower cheek teeth and frontal sections associated for each tooth.*

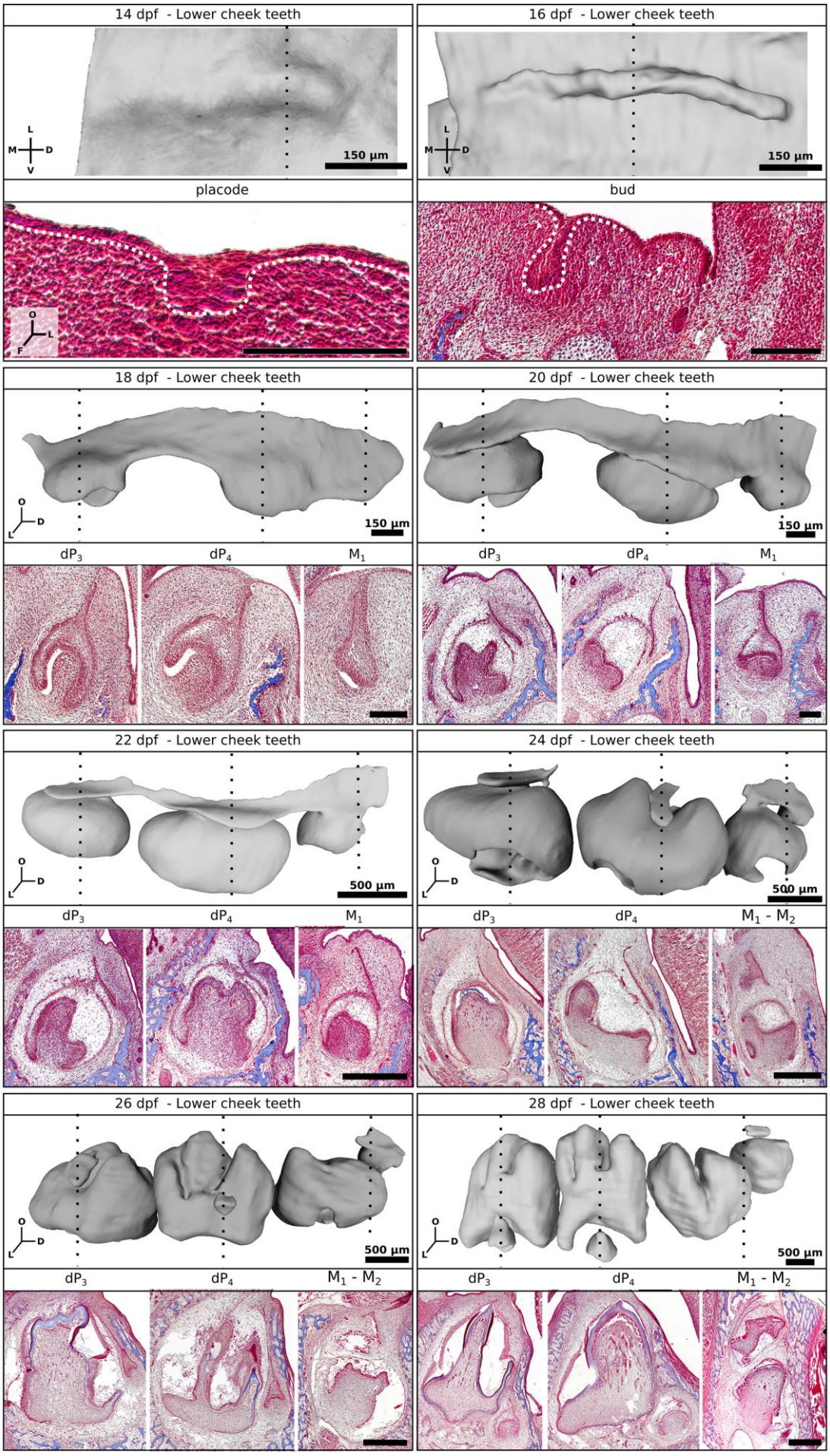
14 dpf - Lower cheek teeth
16 dpf - Lower cheek teeth
150 µm
placode
bud
18 dpf - Lower cheek teeth
20 dpf - Lower cheek teeth
dP3
dP4
M1
22 dpf - Lower cheek teeth
24 dpf - Lower cheek teeth
500 µm
M1 - M2
26 dpf - Lower cheek teeth
28 dpf - Lower cheek teeth

dP^2-P^2

At 18 dpf, the dP^2 is at a transition stage between bud and cap (**Figure 1. 4**). The tooth is connected to the oral epithelium and to the followed tooth by the interdental lamina. At the mesial part of the dP^2, the interdental lamina is present in almost all the diastema length with an oral epithelium link only in the mesial and distal extremities. At 20 dpf, the dP^2 is in a cap stage. The interdental lamina at the mesial part has disappeared but is still present in the distal part of the dP^2. The dental lamina stalk begin to detach from the oral epithelium. At 22 dpf, the dP^2 is in a bell stage. Initiation of the replacement begins with an epithelial bud from the dental lamina in the lingual part of the dP^2, called the replacement dental lamina (also named successional lamina). At 24 dpf, the dP^2 is completely detached from the oral epithelium. The replacement dental lamina, still connected to the dP^2, plunges into the mesenchyme by keeping a lingual orientation (**Figure 1. 4**). The interdental lamina is now very thin but still connects the replacement dental lamina of the dP^2 to the replacement dental lamina of the dP^3. At 26 dpf, the dP^2 begins its mineralization. The dental replacement lamina of the dP^2 is still growing in a lingual direction. At 28 dpf, the dP^2 have the crown completely mineralized and just begins to mineralize at the root level. The P^2 is in a cap stage and is localized in a disto-lingual plane compared to the dP^2. At birth, the dP^2 is completely mineralized from the occlusal surface to the roots and the P^2 is still in a cap stage. Four days later, the P^2 is now at the bell stage and begins to move from its lingual position to apical to the dP^2. Then, around 1 month old, the rooted dP^2 is pushed by the P^2 (**Figure 1. 2**, B). The dP^2 has a completely worn crown surface and the roots begin to reduce, the P^2 is ready to erupt. P^2 is hypselodont (with an unlimited growth) whereas the dP^2 was hypsodont. In adult, the P^2 display a complex shape with numerous folds filled with cementum at the mesial part of the tooth.

dP^3-P^3 / dP_3-P_3 / dP^4-P^4

At 18 dpf, the dP_3, dP^3 and dP^4 are at the cap stage. The teeth are linked to the oral epithelium and connected to each other with the interdental lamina. (**Figure 1. 4**). At 20 dpf, the dP_3, dP^3 and dP^4 are in a bell stage (**Figure 1. 4**, **Figure 1. 5**). Initiation of the replacement begins in the lingual part of the teeth; we detected the replacement dental laminas. The tooth replacement begins in the dP^4 and we observed a shift in the initiation of replacement with a gradient of development from the distal premolar towards the most mesial premolar. The interdental lamina continues to link all the teeth together but the dental lamina begins to be detached from the oral epithelium. At 22 dpf, the dP^3, dP_3 and dP^4 are at the bell stage. All the premolars display a replacement dental lamina in the lingual side, and in the dP^4, we can see that this dental lamina begins to dive in the mesio-lingual direction. Each upper and lower tooth is still connected to the others but dental lamina is completely detached from the oral epithelium. At 24 dpf, the premolars have finished their morphogenesis and now mineralize by secreting dentin and enamel. The replacement dental laminas are highly invaginated into the mesenchyme and are still attached to some elements of the interdental laminas. The replacement dental laminas from the dP^3 and dP^4 grow in a mesial orientation whereas the replacement dental lamina of the dP_3 grows towards the base of the deciduous tooth while maintaining its lingual orientation. The interdental lamina is resorbed around the dP_3, detached of the dP^3, broken between the dP^3 and the dP^4, and very thin between the other upper teeth. At 26 dpf, the deciduous premolars are now highly mineralized in their occlusal surface. The replacement dental laminas are budding to give the replacement teeth. The P_3 is developing at the lingual basis of the dP_3, the P^3 in a mesio-distal plane of the dP^3 and the P^4 in a mesio-lingual plane of the dP^4. At 28 dpf, the dP_3, dP^3 and dP^4 are mineralized to the roots. The permanent premolars are all in the cap stage, localized at the basis of the deciduous teeth in different positions: The P_3 is localized at the basis of the dP_3 in the lingual side, the P^3 is in a mesio-vestibular plane

compared to the dP^3 and the P^4 is in a mesio-lingual plane compared to the dP^4. At birth, the deciduous premolars are well mineralized with dentin, enamel and cementum. The P_3, P^3 and P^4 are in a bell stage. The P_3 begins to migrate from its lingual position to under the dP_3 whereas P^3 and P^4 are still in their developing position. At 2 dpn, the P^4 begins to mineralize followed two days later by the P_3 and P^3. These permanent premolars are now positioned under their deciduous teeth (**Figure 1. 2**, B, C). Then, around 1 month old, the rooted deciduous teeth dP_3, dP^3 and dP^4 are pushed by the permanent premolars (**Figure 1. 2**, B). The deciduous premolars have a completely worn crown surface and the roots begin to reduce, the permanent teeth are ready to erupt. All the permanent cheek teeth are hypselodont. In adult, the P^3 and P^4 have a molarized bilophodont shape with a lingual fold filled with cementum, whereas the P_3 has a complex shape with more folds at the mesial part of the tooth (**Figure 1. 2**, B, C).

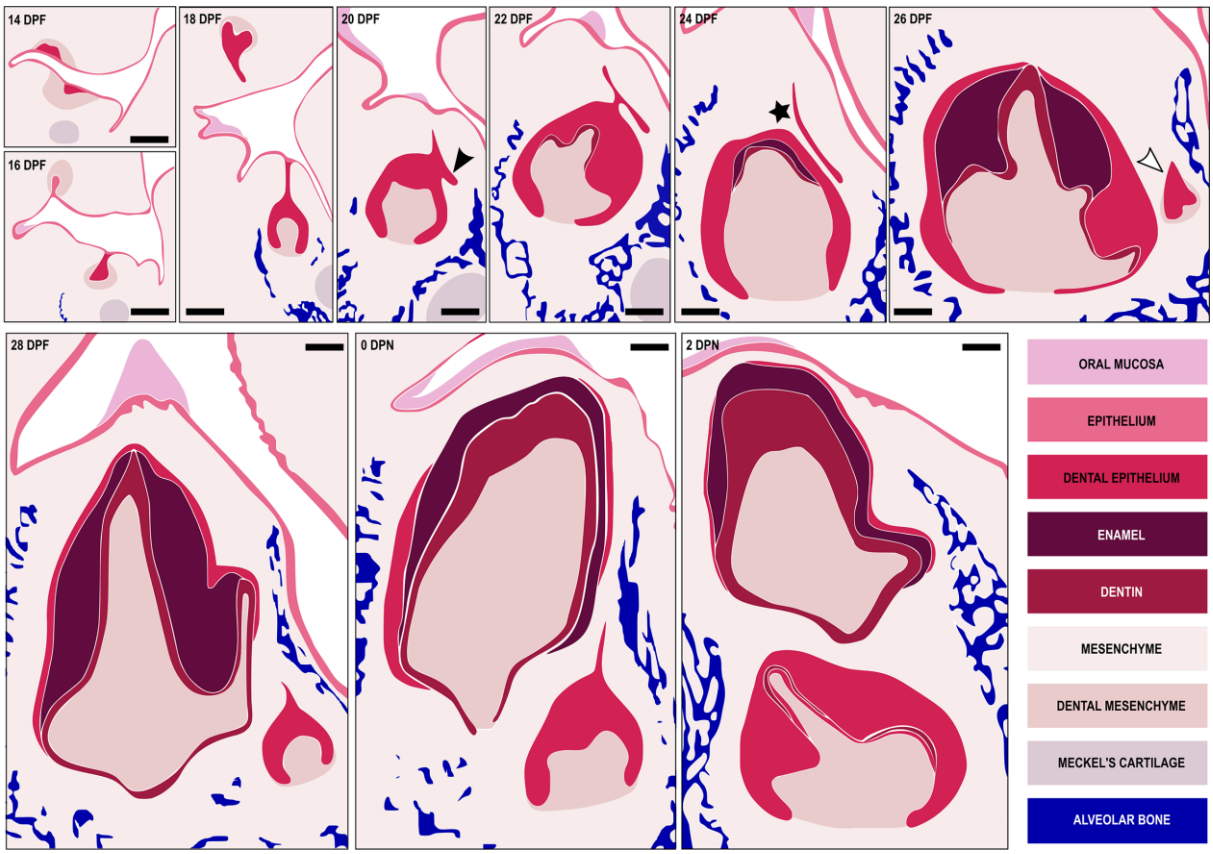

Figure 1. 6. Summary of the dental replacement progression in rabbit*. The black triangle shows the initiation of the replacement dental lamina, the black star the separation of the replacement dental lamina and the deciduous tooth and the white triangle the morphogenesis initiation of the permanent tooth. Scale bar: 200µm*

dP_4-P_4

At 18 dpf, the dP^4 is at the cap stage. The dP_4 is connected to the oral epithelium and to the other teeth of the row by the interdental lamina (**Figure 1. 5**). 2 days later, the dP_4 is at the bell stage and the initiation of the replacement has begun at the lingual part of the tooth, where we detect the replacement dental lamina. At 22 dpf, the dP_4 is the first cheek tooth to mineralize. The tooth is detached from the oral epithelium, but the replacement dental lamina is still connected to the deciduous tooth. At 24 dpf, the replacement dental lamina is detached from the dP_4 that is detached to the other teeth. The replacement dental lamina plunges into the mesenchyme keeping the lingual orientation. At 26 dpf, the P_4 is budding from the replacement dental lamina at the lingual basis of the dP_4 crown. At 28 dpf, the dP_4 is completely mineralized and the P_4 is at the cap stage, localized at the basis of the dP_4 in the lingual side. At birth, the P_4 is the first permanent cheek tooth to mineralize and begins to migrate from its lingual position to below the fully mineralized dP_4. Two days later the permanent tooth is well-localized bellow the dP_4. At 4 dpn, the dP_4 is the first cheek tooth to erupt (**Figure 1. 2**, C). Then, around 1 month old, the dP_4 has a completely worn crown surface and the roots begin to reduce, the P_4 is ready to erupt. P_4 is hypselodont with a continuous growth. In adult, the P_4 has a molarized bilophodont shape (**Figure 1. 2**, C).

M_1-M^1

At 18 dpf, the M_1 is in a bud to cap stage transition and the M^1 in a bud stage (**Figure 1. 4**, **Figure 1. 5**). At 20 dpf, the M_1 and M^1 are in a cap stage. At 22 dpf, the M_1 is at the early bell stage and the M^1 is in the cap stage. We observed an epithelial bud at the lingual part of the M_1 and M^1, indicating a transient rudimentary successional lamina. At 24 dpf, The M^1 and M_1 are in a bell stage and the lingual buds are no more visible. Molars are connected distally to the M^2 and M_2 but only the M^1 is still connected to a premolar mesialy. At 26 dpf, the M_1 begins its

mineralization and the M^1 finishes its morphogenesis. At 28 dpf, the M_1 and M^1 have the crown completely mineralized, with dentin, enamel and cementum. Then, in juveniles and adults, we observed that the molars are hypselodont with a bilophodont shape (**Figure 1. 2**, B, C).

M_2-M^2

At 22 dpf, we observed the budding of the continual lamina at the distal part of the tooth row that will give the M^2 and M_2 by serial addition of molars (**Figure 1. 4**, **Figure 1. 5**). At 24 dpf, the M_2 and M^2 are in a cap stage, and these teeth are still attached mesialy to the interdental dental lamina. At 26 dpf, the M_2 and M^2 are in the cap stage and are the only teeth connected with the remains of dental and interdental lamina. At 28 dpf, the M_2 is now detached from the dental lamina and is in a bell stage. The M^2, in cap stage, is still linked to the dental lamina. At birth, the M_2 begins to mineralize its occlusal surface whereas the M^2 is in bell stage. At 2 dpn, the M^2 and M_2 are mineralizing with dentin, enamel and cementum (**Figure 1. 2**, B, C). Then, in juveniles and adults, we observed that the molars are hypselodont with a bilophodont shape.

M_3-M^3

At 28 dpf, we observed a completely separated dental lamina that is budding in the distal part of the lower tooth row that will gives the M_3 (**Figure 1. 5**). In the upper row, we also detect the budding of the dental lamina in the distal part of the M^2 that will give the M^3 (**Figure 1. 4**). At 2 dpn, the M_3 is at the cap stage, followed two days later by the M^3. Then, in a juvenile around 1 month old, we observed that the M^3 is well mineralized but not erupted (**Figure 1. 2**, B). In adult, the M_3 and M^3 are highly reduced compared to other molars. Among 188 observed adult *Oryctolagus cuniculus* specimens, two lacked the upper third molars with no sign of loss, indicating that this tooth can sometimes not be fully developed.

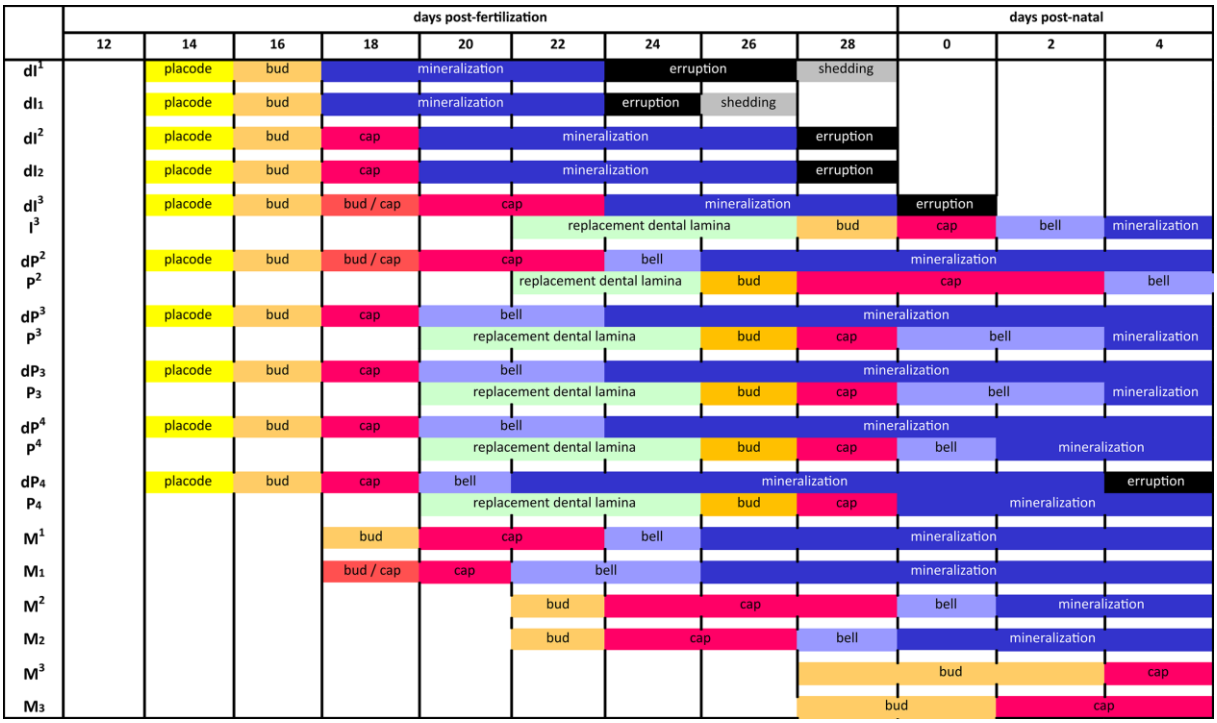

Figure 1. 7. Chronology of dental development and replacement for each rabbit tooth from 12 dpf to 4 dpn.

To summarize, the development of the maxillary teeth is late compared to the mandible counterparts and all the teeth of a same row are not synchronized. In the upper and lower rows, the dP4 is the first forming tooth, that will be followed by the dP3, and then, only in the maxillary, by the dP^2 (**Figure 1. 7**). The development of replacement teeth follows the same order. Regarding the molars, the M1 is the first to develop, followed by the M2 and finally the M3.

Discussion

We show here the morphology (**Figure 1. 6**) and the chronology of rabbit teeth development (**Figure 1. 7**). Using 3D reconstructions, we were able to clearly identify the different steps of tooth development and replacement. Our study contains more developmental stages and we separated the results for each tooth, allowing us to obtain a complete and more precise chronology than the ones available in the literature (Hirschfeld et al., 1973; Michaeli et

al., 1980; Navarro et al., 1975; Ooë, 1980). 3D-reconstructions from the placode stage lead to the conclusion that the canine and first premolars dP^1 and dP_{1-2} are never detected in rabbit embryos. These results suggest a complete loss of these teeth in rabbits, contrary to vestigial tooth rudiments in mice (homologous to the dP_3 and dP_4), detected in early tooth development (Sadier et al., 2019; Viriot et al., 2002). However, some observations still need to be clarified, as the epithelium link between the vestigial incisor dI^1 and the dI^2. This relationship was already problematic for Ooë (1980), who discussed the localization of the dI^2 compared to the dI^1. In mammals, replacement teeth begin their development at the lingual part the deciduous predecessor (Järvinen et al., 2009). Here the dI^1 and dI^2 incisors are in a mesio-distal plan and not in a vestibulo-lingual plan, so it seems more similar to serial development with an interdental lamina between deciduous incisors. However, the rabbit dI^2 has the specificity of being the only tooth to be deciduous and ever growing. For other teeth, the ever-growing ability appears only in permanent teeth. Hirschfeld et al. (1973) concluded that due to its ever-growing capacity the so-called dI^2 is the permanent tooth coming from the dI^1. More data on the precise dynamics of the tooth development between 16 and 18 dpf are needed to fully understand the nature of the so-called dI^2. Reconstructions of the concerned structures during the transition from bud to separated teeth in 3D should help to conclude on the links between these incisors.

One particularity of incisor development in rabbits is the appearance of holes that occur only in newborns. The cause of these holes is unknown. These tooth defects have been observed in all our samples, indicating a common phenomenon. We did not find in literature any description of systematic presence of tooth defects at one specific age in rabbits or other species. In this study, we worked on common rabbit breeding regularly crossed with wild rabbits to ensure genetic mixing, limiting the possibility that these dental abnormalities are specific to one genetic selection in a closed breeding. Some hypotheses can be considered to explain the hole

formation, as a possible mechanical compression due to the development of adjacent teeth or bone mineralization or the result of molecular signals. It could be interesting to identify which mechanical forces at birth could be responsible for tooth fractures without morphologically affecting the other tissues. These causes could be purely mechanical (development of the bones or the other upper incisors) or molecularly facilitated (involvement of signaling pathways involved in root resorption for example). The observed reparation system, which systematically takes place in the first days of an animal's life, indicates an ability of quick tooth repair, probably due to the high secretion capacity of the odontoblasts in the ever-growing incisor. This speed in tooth repair is incompatible with the classical reparative dentin that require differentiation and migration of new odontoblasts from a pulpal progenitor cell (Moses et al., 2006). So here, another type of tertiary dentin could close the hole, the reactionary dentin that is formed from a pre-existing odontoblast.

The 3D-reconstructions of the rabbit premolars indicate that the permanent upper premolar begins its morphogenesis in a mesio-vestibular plane compared to its deciduous tooth, so in the opposite side in contrast to the other teeth. Popa et al. (2016) presented in the fruit bat different modalities of tooth replacement throughout the jaw. They showed, using 3D-reconstructions, that the canine, the second and the third premolar do not have the same modalities of replacement due to the relative position of the deciduous and permanent teeth. In rabbit, the initiation of the tooth replacement always begins by a growth of the dental lamina at the lingual position of the tooth that will give the replacement dental lamina as in the ferret or fruit bat (Jussila et al., 2014, Popa et al., 2016). Then, the separation between the first generation of teeth, the oral epithelium and the replacement dental lamina can vary. First, the teeth lose their connection with the oral epithelium. Variations are then observed; the replacement dental lamina can first be separated from the tooth or from the interdental lamina. Concerning the tooth

position of the second generation compared to the first it also depends on the teeth as in the fruit bat. For the lower premolars and the upper incisor, the permanent teeth develop directly on the lingual side of the deciduous teeth. For the upper cheek teeth, the position of the second-generation development varies for each premolar. The tooth replacement begins at the lingual part of the deciduous tooth, but then the replacement dental lamina plunges and develops in different orientation depending on the tooth. The P^2 is localized in a disto-lingual plane compared to the dP^2, the P^3 is in a mesio-vestibular plane compared to the dP^3 and the P^4 is in a mesio-lingual plane compared to the dP^4. Indeed, the P^2 and P^3 develop on the same frontal plan, with one lingualy and the other vestibulary. Then, all the permanent teeth migrate under the associated deciduous teeth. Compared to the fruit bat or the ferret (Järvinen et al., 2009; Popa et al., 2016), the rabbit dental replacement lamina seems to plunge much deeper into the mesenchyme before it begins to initiate its permanent tooth morphogenesis, as observed in the minipig (Wang et al. 2014).

During rabbit molar development, we observed buddings at the lingual part of the first molars that quickly disappear. Same tooth shape has been observed in the mouse; a rudimentary successional dental lamina (RSDL) is visible in the lingual part of the M_1 tooth germ (Dosedělová et al., 2015). The RSDL in mouse as in the rabbit does not have odontogenic potential (Popa et al., 2019). However, by stabilizing the Wnt/ β-catenin signaling in the RSDL, it is possible to obtain a new tooth (Popa et al., 2019). The molars can be considered as deciduous teeth that are never replaced (Luckett, 1993); the study of this budding observed in the rabbit with the molecular information obtained in mutant mice could identify why these teeth are not replaced.

In this study, we have shown that the rabbit seem to be a good model in dental research. Rabbits are already used in odontological studies but we showed here that they are also useful for studying tooth morphogenesis. Studies of tooth development and replacement in rabbits could allow understanding the mechanisms of mammalian tooth replacement. We showed that common molecular experiments can be done in rabbit tissues as *in situ* hybridization and rabbits can also be a relevant model to use more advanced techniques as CRISPR/Cas9 technology (Yan et al., 2014). Compared to other species used to study tooth replacement (the ferret, the fruit bat, the shrew and the minipig), rabbit embryos are easy to get, with large litters of embryos and a pretty short gestation time (31 days). The main disadvantage to the study of the rabbit compared to the other models already proposed is an incomplete dentition with the lack of the canines. However, rabbits have also ever-growing permanent teeth, allowing study of other issues such as dental stem cells maintaining in addition to mammalian dental replacement.

Conclusion

We provided here the description of the complete histo-morphological chronology of the tooth development and replacement in rabbit. It can be considered as a new dataset that allows a better understanding of the dental replacement among mammals. The 3D-reconstructions gave useful information about the geometric organization of the dental replacement and the precise knowledge of the dental development and replacement chronology in this species is a starting point that will allow further studies of gene functions at specific time windows.

Acknowledgements

We thank Nicolas Goudemand and all the members of his team for their help and support. We thank all the members of the “Evolution of vertebrate dentition” for the helpful

advices and comments. We thank Joanne Burden for help in the final preparation of the manuscript. We thank Cécile Callou, who is responsible for the collection of the lagomorphs at the Museum National d'Histoire Naturelle (MNHN) of Paris, for giving us access to these collections and for her help during our visit. We are grateful to Mathilde Bouchet-Combe, from the SFR Biosciences (UMS3444/CNRS, US8/Inserm, ENSL, UCBL1), who helped for X-Ray microtomographic analyses. The authors declare no conflict of interest

Author contributions

L.B.B: contributed to design, to acquisition, analysis, and interpretation, drafted manuscript. L.V: contributed to conception, to analysis and interpretation, critically revised manuscript. T.J: contributed to interpretation, critically revised manuscript. C.C: contributed to conception and design, to analysis and interpretation, critically revised manuscript.

References

Balic A, Thesleff I (2015) Tissue Interactions Regulating Tooth Development and Renewal. *Curr Top Dev Biol* **115**, 157–186.

Bertin TJC, Thivichon-Prince B, LeBlanc ARH, et al. (2018) Current Perspectives on Tooth Implantation, Attachment, and Replacement in Amniota. *Front Physiol* **9**, 1630.

Bertonnier-Brouty L, Viriot L, Joly T, et al. (2019) 3D reconstructions of dental epithelium during Oryctolagus cuniculus embryonic development related to the publication "Morphological features of tooth development and replacement in the rabbit Oryctolagus cuniculus". *MorphoMuseuM,* 5:e90.

Bosze Z, Houdebine LM (2006) Application of rabbits in biomedical research: a review. *World Rabbit Sci* **14**, 01-14.

Dosedělová H, Dumková J, Lesot H, et al. (2015) Fate of the molar dental lamina in the

monophyodont mouse. *PLoS One* **10**, e0127543.

Hirschfeld Z, Weinreb MM, Michaeli Y (1973) Incisors of the Rabbit: Morphology, Histology, and Development. *J Dent Res* **52**, 377–384.

Horowitz SL, Weisbroth SH, Scher S (1973) Deciduous dentition in the rabbit (Oryctolagus cuniculus). A roentgenographic study. *Arch Oral Biol* **18**, 517–23.

Järvinen E, Tummers M, Thesleff I (2009) The role of the dental lamina in mammalian tooth replacement. *J Exp Zool Part B Mol Dev Evol* **312B**, 281–291.

Järvinen E, Välimäki K, Pummila M, et al. (2008) The taming of the shrew milk teeth. *Evol Dev* **10**, 477–486.

Jussila M, Crespo Yanez X, Thesleff I (2014) Initiation of teeth from the dental lamina in the ferret. *Differentiation* **87**, 32–43.

Juuri E, Balic A (2017) The Biology Underlying Abnormalities of Tooth Number in Humans. *J Dent Res* **96**, 1248–1256.

Luckett WP (1993) An Ontogenetic Assessment of Dental Homologies in Therian Mammals. In *Mammal Phylogeny*. New York, NY, 182–204.

Metscher BD (2009) MicroCT for comparative morphology: simple staining methods allow high-contrast 3D imaging of diverse non-mineralized animal tissues. *BMC Physiol* **9**, 11.

Michaeli Y, Hirschfeld Z, Weinreb MM (1980) The cheek teeth of the rabbit: morphology, histology and development. *Cells Tissues Organs* **106**, 223–239.

Moses KD, Butler WT, Qin C (2006) Immunohistochemical study of small integrin-binding ligand, N-linked glycoproteins in reactionary dentin of rat molars at different ages. *Eur J Oral Sci* **114**, 216–22.

Mucchielli ML, Mitsiadis TA (2000) Correlation of asymmetric Notch2 expression and mouse incisor rotation. *Mech Dev* **91**, 379–382.

Navarro JAC, Sottovia-Filho D, Leite-Ribeiro MC, et al. (1976) Histological study on the

postnatal development and sequence of eruption of the mandibular cheek-teeth of rabbits (Oryctolagus cuniculus). *Arch Histol Jpn Nippon soshikigaku kiroku* **39**, 23–32.

Navarro JAC, Sottovia-Filho D, Leite-Ribeiro MC, et al. (1975) Histological Study on the Postnatal Development and Sequence of Eruption of the Maxillary Cheek-Teeth of Rabbits (Oryctolagus cuniculus). *Arch Histol Jpn* **38**, 17–30.

Ooë T (1980) Développement embryonnaire des incisives chez le lapin (Oryctolagus cuniculus L.). Interpretation de la formule dentaire. *Mammalia* **44**, 259–270.

Popa EM, Anthwal N, Tucker AS (2016) Complex patterns of tooth replacement revealed in the fruit bat (*Eidolon helvum*). *J Anat* **229**, 847–856.

Popa EM, Buchtova M, Tucker AS (2019) Revitalising the rudimentary replacement dentition in the mouse. *Development* **146**, dev171363.

Rasch LJ, Martin KJ, Cooper RL, et al. (2016) An ancient dental gene set governs development and continuous regeneration of teeth in sharks.

Sadier A, Twarogowska M, Steklikova K, et al. (2019) Modeling Edar expression reveals the hidden dynamics of tooth signaling center patterning C. S. Hill, ed. *PLOS Biol* **17**, e3000064.

Sych LS, Reade PC (1987) Heterochrony in the development of vestigial and functional deciduous incisors in rabbits (Oryctolagus cuniculus L.). *J Craniofac Genet Dev Biol* **7**, 81–94.

Supplementary files

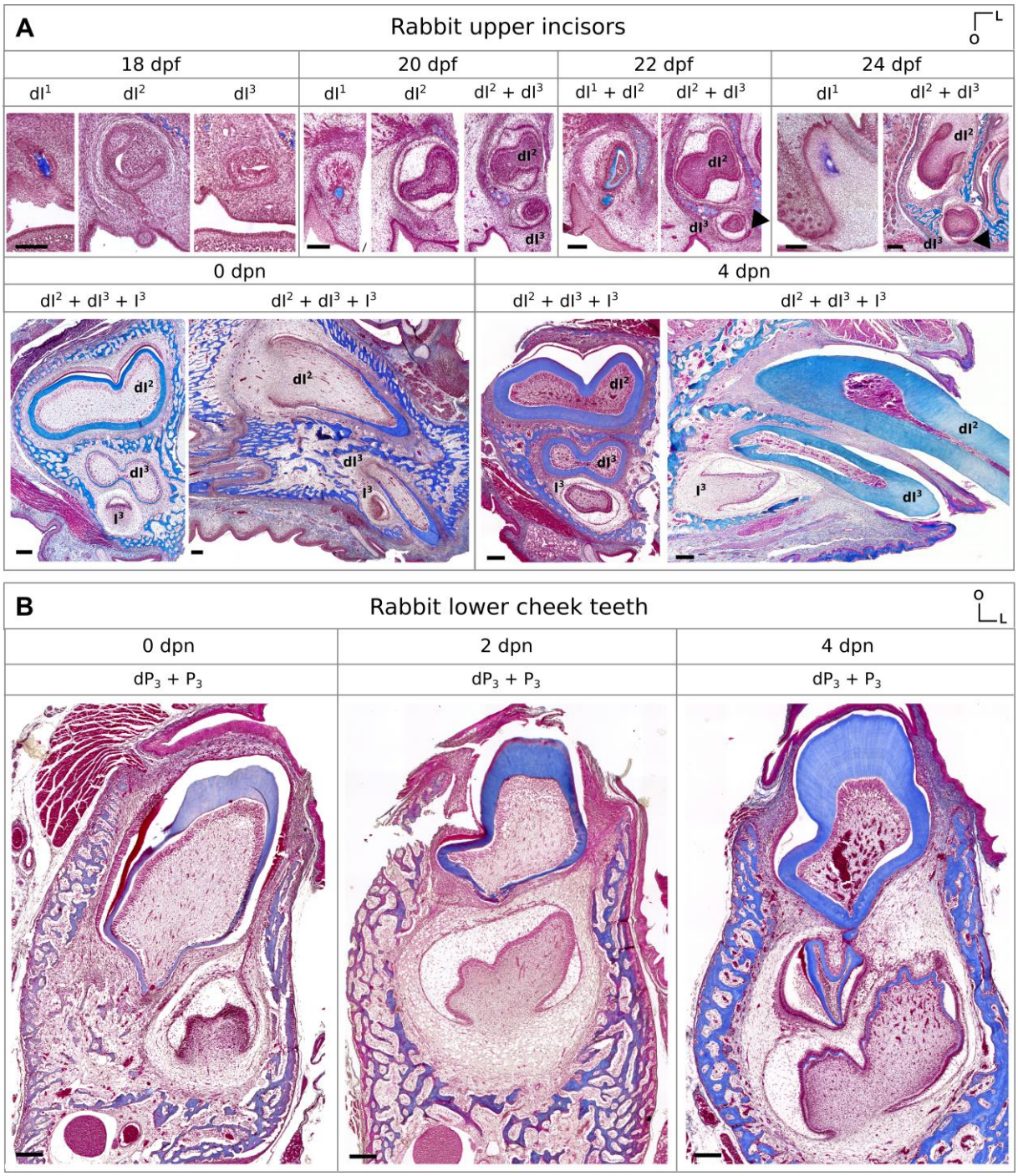

Supplementary 1. 1. Histological sections of the rabbit upper incisors and lower cheek teeth. *(A) Frontal and sagittal sections of the upper incisors from 18 dpf to 4 dpn. Indicated with black arrows, the replacement dental lamina. (B) Frontal sections of the lower third premolar from 0 dpn to 4 dpn. L, lingual; O, occlusal. Scale bar: 200µm.*

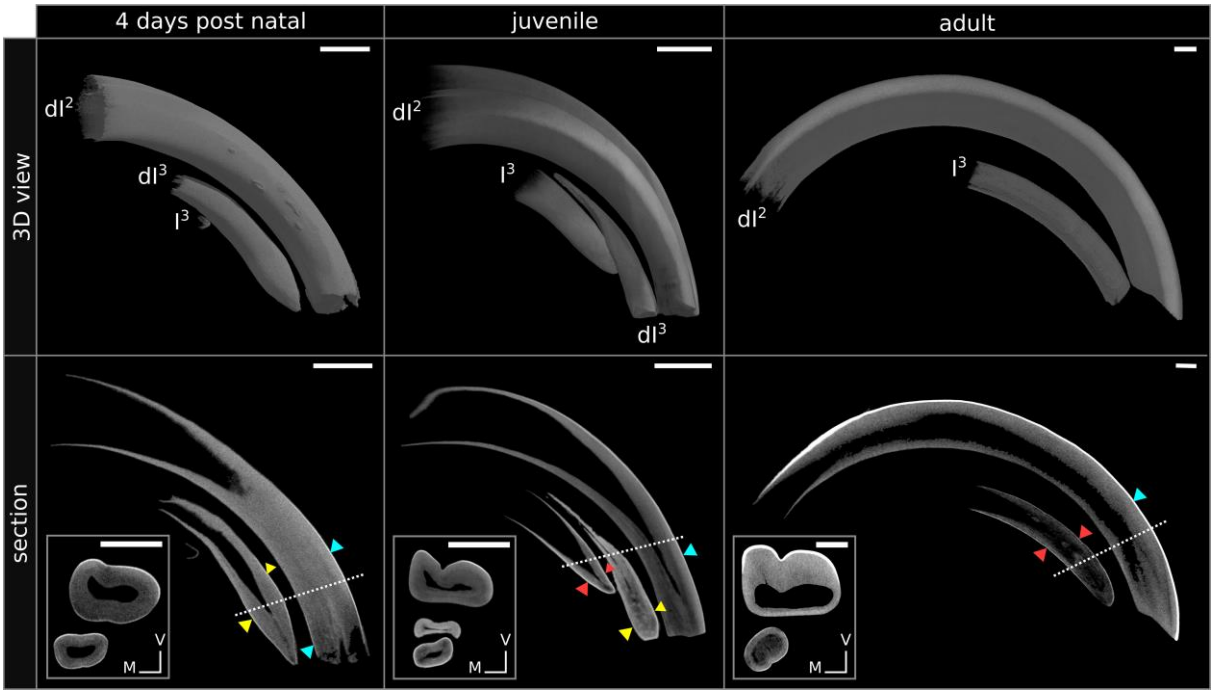

Supplementary 1. 2. Views of the 3D reconstructions of the upper incisors mineralized tissues and virtual sections of the incisors. *In sections, the dentin appears in grey and the enamel in white. Indicated in blue, enamel layer in the dI^2; in yellow, enamel layer in the dI^3; in red, enamel layer in the I^3. The white dotted line indicates the frontal section plane illustrated in the white rectangle. V, vestibular; M, mesial. Scale bar: 1mm.*

Chapter 1.2 – Spatio-temporal regulation of tooth replacement in *Oryctolagus cuniculus*

Even if the majority of mammals are diphyodonts, few is known about mammalian tooth replacement (Jernvall and Thesleff, 2012). Genetic pathways possibly involved in tooth replacement are mainly studied using transgenic mice (Ahn et al., 2010; Popa et al., 2019) or polyphyodont species (Tucker and Fraser, 2014; Whitlock and Richman, 2013). Only few genetic data have been collected in diphyodont mammals such as the ferret or the minipig (Jussila et al., 2014; Wang et al., 2019). So for now, no study follows candidate genes during all the developmental steps of the tooth replacement in a mammal.

In the following paper, we propose to use the rabbit as animal model to study spatio-temporal regulation of mammalian tooth development and replacement. We showed previously that we could study tooth replacement steps in the rabbit using embryos from 14 days post fertilization to newborns. In this study, we followed gene expression or protein localization of five candidate genes supposed to be involved in tooth development and replacement: Shh, Sostdc1, Runx2, Lef1 and Sox2 by immunohistochemistry or *in situ* hybridization at each replacement step. We present the spatio-temporal regulation of tooth replacement in the rabbit lower cheek teeth in order to visualize in the same frontal sections the deciduous and the replacement tooth.

We conclude that expression pattern of Runx2, Sostdc1 and Lef1 in the mesenchyme are correlated with the inhibition of tooth replacement whereas epithelial Lef1 and Sox2 are expressed in tooth replacement structures. Moreover, as in the mouse, Shh and Sostdc1 are expressed in the inner enamel epithelium and may regulate the cusp pattern formation. So, we show in the following paper that rabbits are an useful animal model for molecularly studying mammalian dental replacement.

Article 2: Expression patterns of Runx2, Sox2, Lef1, Shh and Sostdc1 in *Oryctolagus cuniculus* tooth development and replacement

Ludivine Bertonnier-Brouty[1*], Laurent Viriot[1], Thierry Joly[2,3], Cyril Charles[1]

[1] Institut de Génomique Fonctionnelle de Lyon, Université de Lyon, CNRS UMR 5242, Ecole Normale Supérieure de Lyon, Université Claude Bernard Lyon 1, Lyon, France

[2] ISARA-Lyon, F-69007 Lyon, France

[3] VetAgroSup, UPSP ICE, F-69280 Marcy l'Etoile, France

*Corresponding author: ludivine.bertonnierbrouty@ens-lyon.fr

Abstract

Mammalian tooth replacement mechanisms are poorly known due to the absence of an animal model adapted to laboratory animal facilities. The single tooth replacement in mammals differs from the continuous dental replacement of more commonly studied non-mammalian vertebrates. In this study, we use the European rabbit, *Oryctolagus cuniculus*, as a model to study mammalian tooth development and replacement. We describe development and replacement of rabbit premolars and provide data on some key regulators of mammalian dental development and replacement. We show that as in the mouse, rabbit molars develop transiently a rudimentary successional dental lamina, which quickly disappears. We detected the stem cell marker SOX2 in the lingual side of the replacement dental lamina and in the cervical loops of the premolars and molars. We shown that *Shh* expression pattern in the rabbit is the same than in mouse. We also demonstrate that RUNX2 is differentially localized between the deciduous and the permanent premolars as Lef1 and Sostdc1, both involved in the Wnt pathway.

Keywords: deciduous tooth; permanent dentition; Rabbits; Tooth germ; Embryonic development

Introduction

In dental research, and more especially in tooth developmental biology, the mouse is the favorite mammal model. As consequences, the signaling pathways involved in mouse tooth development and the molecular mechanisms responsible of the ever-growing ability of their incisors are well known (i.e Tummers & Thesleff, 2003; Lan et al., 2014; Sharir & Klein, 2016). However, the mouse lost its ability to replace teeth unlike the majority of mammals that replace their teeth once during life (diphyodonty). Thus, tooth replacement is more commonly studied in non-mammalian vertebrates as fish and reptiles (Rasch et al., 2016; Richman and Handrigan, 2011) that have the ability to replace their teeth continuously during all their lifespan (polyphyodonty). So, due to the lack of common diphyodont model, tooth replacement mechanisms are still poorly known in mammals.

In order to better understand morphological and cellular mechanisms involved in mammalian tooth replacement, some non-model mammals as the ferret (Jussila et al., 2014), the elephant shrew (Järvinen et al., 2008), the minipig (Wang et al., 2014a) or the fruit bat (Popa et al., 2016) have been studied. Altogether, these studies have characterized the morphological changes involved in tooth replacement: the initiation of tooth replacement begins by a budding of the replacement dental lamina at the lingual part of the epithelial tooth stalk. Then the replacement dental lamina plunges into the mesenchyme and the tooth morphogenesis begins. Nevertheless, none of these animals is well adapted to laboratory animal facilities due to their gestation time, size or by the presence of seasonal estrus. Due to these constrains, the studies on diphyodont replacement are restricted to morphological description or incomplete gene expression tracking. Indeed, molecular signaling involved in mammalian tooth replacement are still unknown.

By studying the signaling pathways involved in mammalian tooth number regulation in mutant mice (Ahn et al., 2010; Järvinen et al., 2018; Munne et al., 2009) or human pathologies (Juuri and Balic, 2017), some candidate genes as *Runx2*, *Sostdc1*, *Shh* and the Wnt signaling have been identified. These genes also play major roles in tooth development and dental morphogenesis (Seppala et al., 2017; Sun et al., 2016; Kim et al., 2018). RUNX2 is known to regulate tooth number in humans (Cobourne and Sharpe, 2010). A mutation of RUNX2 causes multiple supernumerary teeth (Lo Muzio et al., 2007) whereas a RUNX2 duplication induces a reduction of the tooth number (Merametdjian et al., 2019). In mouse, an over-expression of *Sostdc1* induces a reduction of the tooth number and the loss of *Sostdc1* expression leads to the development of extra-teeth (Ahn et al., 2010; Munne et al., 2009). SOSTDC1 plays also a major role in cusp formation and tooth patterning in mice (Kim et al., 2018). SOSTDC1 is known as an inhibitor of the Wnt/BMP pathway (Itasaki et al., 2003) and Shh pathway is a major target of the Sostdc1-regulated Wnt signaling (Ahn et al., 2010). Moreover, *Shh* has been shown to play numerous roles during vertebrate tooth development, such as tooth development initiation morphogenesis or ameloblasts polarization (Seppala et al., 2017). Järvinen et al. (2018) showed in mouse that the activation of the Wnt signaling in the epithelium leads to tooth induction whereas the activation of Wnt signaling in the mesenchyme inhibits sequential tooth initiation. Moreover, studies in polyphyodont species showed that the Wnt signaling pathway, followed by studying the *Lef1* marker, seems to be a key regulator in ordering tooth replacement and maintaining a regenerative domain at the tip of the replacement dental lamina (Gaete and Tucker, 2013; Handrigan and Richman, 2010a). *Sox2* marker has been studied in the ferret: *Sox2*$^{+}$ cells are localized in the lingual part of the teeth and in the replacement dental lamina, as in numerous polyphyodont reptiles (Juuri et al., 2013). *Sox2* is a marker for the epithelial stem cells in the mouse ever-growing incisors (Juuri et al., 2012) and is also known to interfere with the Wnt signaling by binding to β-catenin and by regulating LEF1 in the adult mouse incisor

(Kormish et al., 2010; Sun et al., 2016). However, none of these candidate genes has been studied during all the steps of the mammalian tooth development and replacement.

In this study, we propose the European rabbit *Oryctolagus cuniculus* as a new model in tooth developmental biology. Rabbits are already used in orthodontic research (Al-Hamdany et al., 2017) and we previously described the histo-morphological chronology of the tooth development and replacement in the rabbit (Bertonnier-Brouty et al., 2019). Tooth development in the rabbit follow the same stages than those defined in the mouse: the placode, the bud, the cap, the bell, and finally the maturation stages. Dental replacement in rabbit begins at the bell stage of the deciduous tooth by a budding of the epithelium in the lingual part of the dental lamina: the replacement dental lamina is formed (**Figure 2. 1**, red). This replacement dental lamina grows and plunges into the surrounding mesenchyme and then begins its morphogenesis and give rise to the replacement tooth (**Figure 2. 1**, pink). As in mice (Dosedělová et al., 2015), we observed a transient rudimentary successional dental lamina in the rabbit molar, morphologically similar to the replacement dental lamina while the molars are not replaced (**Figure 2. 1**, orange). Rabbit appears as a relevant model for its dental features: the incisors and premolars are replaced, the first molars present rudimentary successional dental laminas, and the deciduous teeth have a limited growth whereas the permanent teeth are ever-growing. Here, we studied the spatio-temporal regulation of the mammalian tooth development and replacement by providing data on some key regulators. We described the expression patterns of *Shh*, *Runx2*, *Sostdc1*, *Lef1* and *Sox2* during rabbit lower cheek tooth development and replacement. We compare the expression patterns of these candidate genes during tooth development and replacement of the premolar and in the rudimentary successional lamina transitorily observed in rabbit molars.

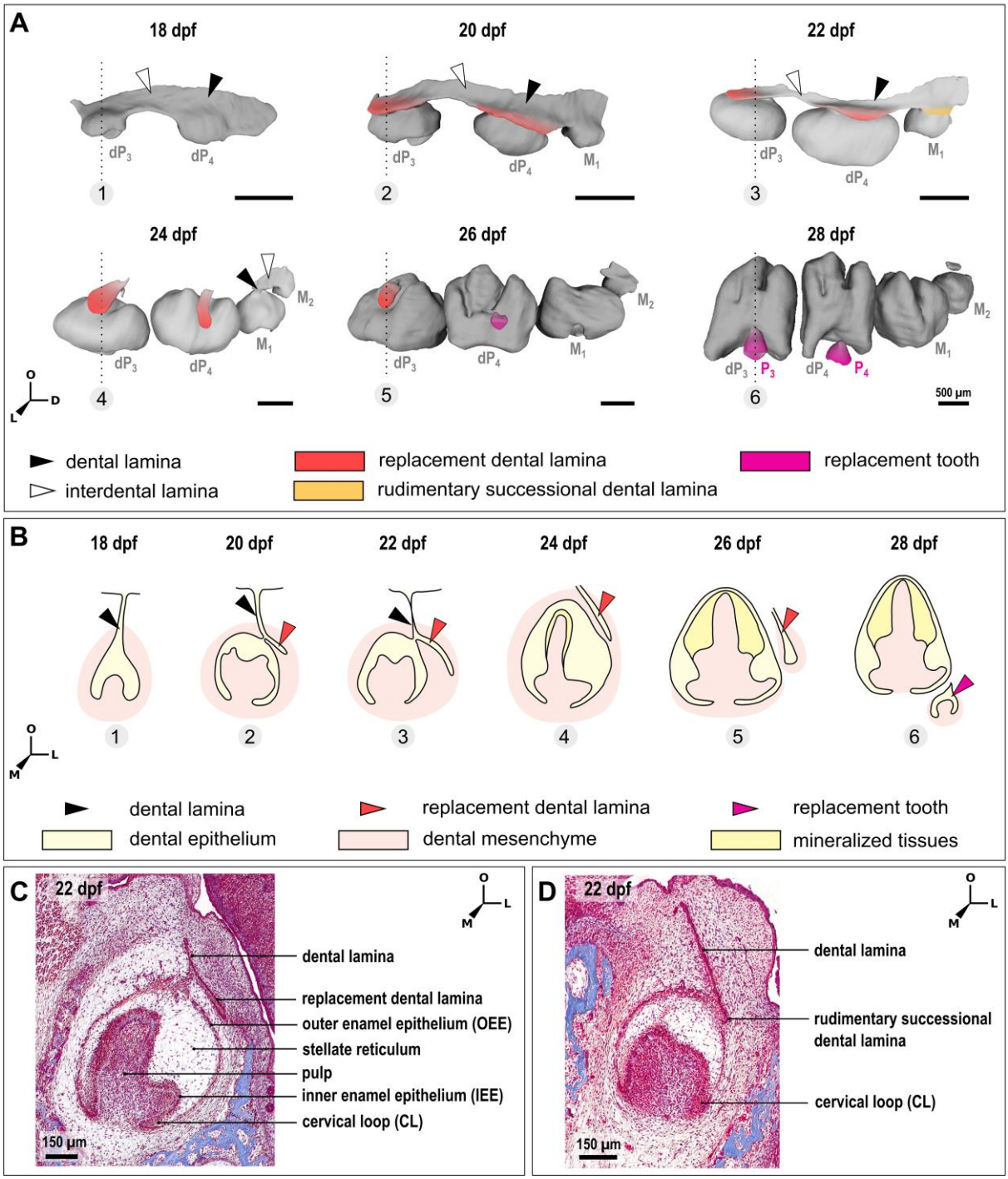

Figure 2. 1 - Morphological features of tooth development and replacement in the rabbit. *(A) Lingual view of the 3D reconstructions from 18 to 28 days post fertilization (dpf) (adapted from Bertonnier-Brouty et al. 2019). Tooth nomenclature: "P" and "M" for premolar and molar; the deciduous teeth are indicated with a "d"; the tooth number is in index for the lower teeth. The dotted line indicates the section plane for each number represented in B. (B) Frontal section illustrations of the third lower premolar from 18 to 28 dpf. (C) Histology of a rabbit third lower premolar at 22 dpf. (D) Histology of a rabbit first lower molar at 22 dpf. L, lingual; O, occlusal; D, distal; M, mesial. Scale bars: 500µm.*

Material & Method

Samples

Embryos and newborn rabbits were obtained through collaboration with a standard production for feeding located at the Biology Departmental livestock establishment (EDE) n°38044102. We collected samples from a common rabbit breeding regularly crossed with wild rabbits to ensure genetic mixing. The gestation period is about 31 days. We collected litters of embryos at 12, 14, 16, 18, 20, 22, 24, 26 and 28 days post fertilization (dpf) and rabbits at 0, 1, 2, 3 and 4 days post-natal (dpn). For each stage, 4 to 21 embryos were collected. Each tooth is specifically named: we use ’P‘ and ’M‘ for premolar and molar respectively; the deciduous teeth are indicated with a ’d‘; the tooth number is in index for the lower teeth.

Histology

After dissection of the lower jaws, samples were fixed overnight in 4% PFA. Samples were then rehydrated and fixed in Holland Bouin solution during 1 day. Jaws were demineralized for 1 to 7 days in Morse’s solution (10% sodium citrate + 22% formic acid) or in RNase-free 12.5% EDTA + 2.5% PFA during 6 weeks, according to the subsequent experiment to be performed. Then, jaws were embedded in paraffin and serially sectioned with a Leica microtome (7 µm thick slices). Sections were carried out in frontal plane.

In situ hybridization

Specific probes for Shh and Sostdc1 have been designed using the rabbit genome available online (OryCun2.0, 2009). Each probe has been sequenced before use, and probes were synthesized with RNA-dig labelling nucleotides. Classical mouse in situ protocol has been optimized to be compatible with paraffin-embedded rabbit tissues. Tissues were treated with HCl 0.2M, with proteinase K 5µg/ml and then incubated with TEA-Acetic anhydride. Hybridization step were done at 62°C. Sections were whashed in a warm washing buffer (1X

SSC and 50% formamide) and in MABT solution. After 2 hours in a blocking solution, slides were covered of anti-Dig-AP-antibody solution at 4°C over night. Sections were washed with MABT and NTMT with teramisol. Sections were stained with BM purple solution and mounted in Aquatex.

Immunohistochemistry

Citrate buffer pH 6 was used for antigen retrieval. Sections were incubated in 3% H_2O_2 to inactivate the endogen peroxidases. Sections were incubated in primary antibody in 1% BSA and 10% goat serum overnight. Primary antibody against SOX2 (1:300, Santa Cruz Biotechnology, sc-365823), RUNX2 (1:300, Santa Cruz Biotechnology, sc-390351), and LEF1 (1:300, Santa Cruz Biotechnology, sc-374412) were used. For immunohistochemistry, signal was amplified using biotinylated secondary antibodies and ABC kit (Santa Cruz Biotechnology, sc-516216). Sections were stained with peroxidase-DAB complex. For immunofluorescence, staining were visualized using Alexa Fluor Plus 647 (1:300) and mounted in fluoroshield with DAPI.

Results

Morphological features of rabbit tooth replacement are presented in **Figure 2. 1**. Although the expression of some genes has been already described during tooth development in other species (Jussila et al., 2014; Juuri et al., 2013), a complete analysis of these genes in a single species is lacking. We decided to describe protein localization of RUNX2, LEF1 and SOX2 and the expression of *Sostdc1* and *Shh* in the rabbit for all the developmental stages during diphyodont tooth development and replacement. We followed these genes during the development and replacement of the lower premolars and in the rudimentary successional dental lamina (RSDL) of the first lower molar. This RSDL in M_1 of 22 dfp rabbits is similar in

shape to the replacement dental lamina but quickly fail to develop. Following its gene expression may be helpful to identify which genes are necessary to maintain tooth replacement establishment.

RUNX2 localization

RUNX2 mutations cause cleidocranial dysplasia in humans, dentally characterized by multiple supernumerary teeth (Cobourne and Sharpe, 2010). We decided to follow Runx2 protein during dP_4 replacement in order to identify how it could modulate tooth number. At 14 dpf, during tooth development initiation, RUNX2 is localized in the mesenchyme surrounding the placode, with more $RUNX2^+$ cells in the vestibular mesenchyme part of the placode (**Figure 2. 2**, A1). At 16 dpf, the mesenchyme surrounding the dental bud is $RUNX2^+$, excepted on the lingual side of the dental lamina (**Figure 2. 2**, A2). Runx2 is also localized in the vestibular part of the dental epithelium. At 18 dpf, RUNX2 is localized in the mesenchyme at the vestibular part of the tooth and around the cervical loops (CL). We also detect RUNX2 in the vestibular part of the outer enamel epithelium (OEE). The lingual part of the dP_4 is free of RUNX2. Between 20 and 24 dpf, Runx2 is localized in the mesenchyme all around the dP_4 but not in the lingual part of the replacement dental lamina (**Figure 2. 2**, A4-6). At 26 dpf, the entire mesenchyme surrounding the P_4 is $RUNX2^+$ and few cells of the vestibular OEE are also $RUNX2^+$. At birth, RUNX2 is localized in the entire mesenchyme around the P_4 (**Figure 2. 2**, A8).

Figure 2. 2. RUNX2 localization during tooth development and replacement. *RUNX2 is localized by immunohistochemistry and immunofluorescence in the fourth lower premolar from 14 days post fertilization to 1 day post-natal (A) and in the first lower molar from 20 to 24 days post fertilization (B). Zoom of the replacement zone is located next to the global view. In blue, DAPI, in Red, RUNX2. Scale bar: 250µm.*

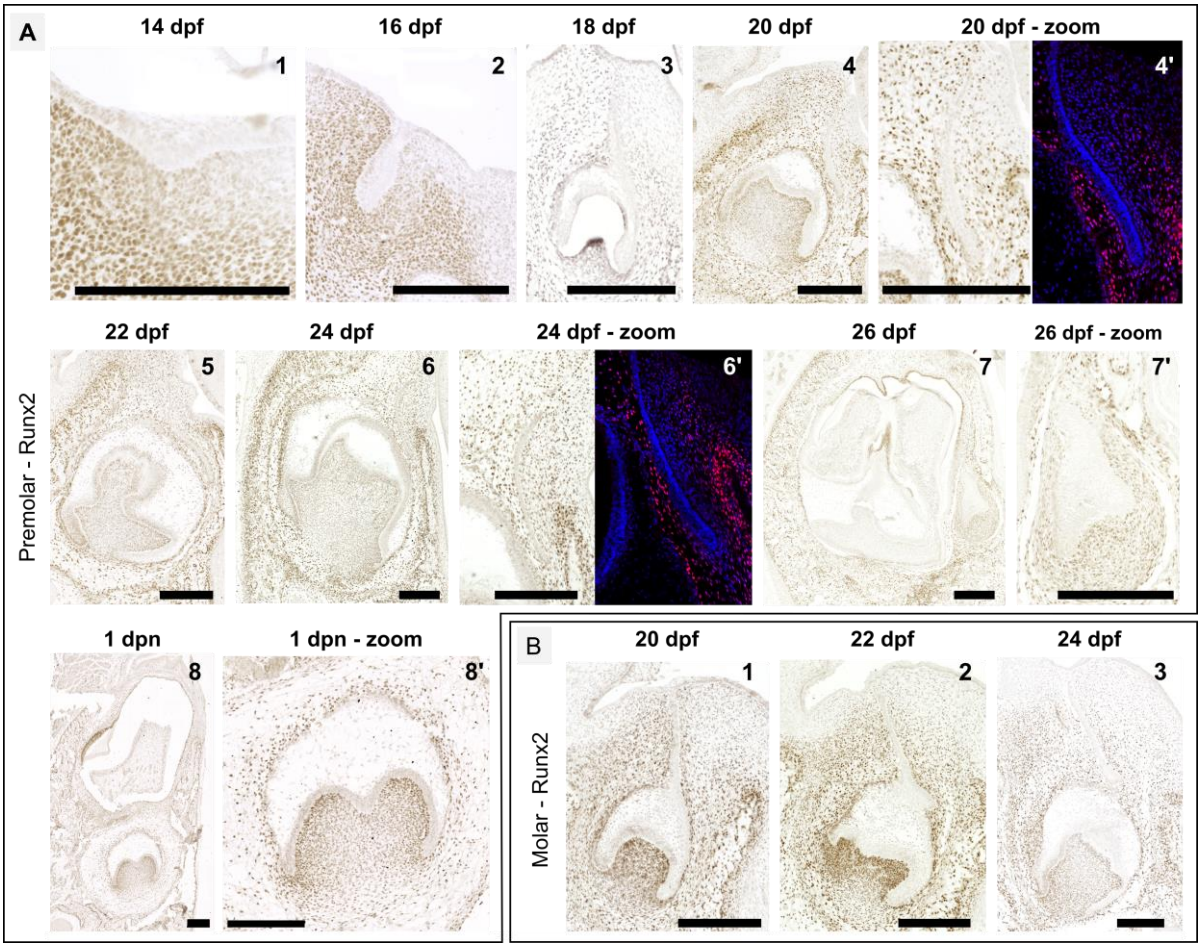

In the M_1, the vestibular OEE is $RUNX2^+$ in the vestibular part of the tooth from 20 to 24 dpf. At 20 dpf, before the morphological appearance of the RSDL, the mesenchyme surrounding the tooth is $RUNX2^+$ (**Figure 2. 2**, B1). At 22 dpf, the RSDL is surrounded by $Runx2^+$ cells. The localization of $RUNX2^+$ cells is not modified when the RSDL and the dental lamina regress at 24 dpf (**Figure 2. 2**, B3).

So, RUNX2 is involved in rabbit tooth development. Moreover, the mesenchymal RUNX2 free area around the lingual part of the dental lamina and the replacement dental lamina in deciduous premolars is correlated with the tooth replacement capacity and is not found in the replacement teeth or molars. Togo et al. (2016) suggested that RUNX2 directly or indirectly limits the number of $SOX2^+$ cells in mutant mice. As RUNX2 seems correlated with tooth replacement ability, we decided to follow SOX2 localization during tooth development and replacement in the rabbit.

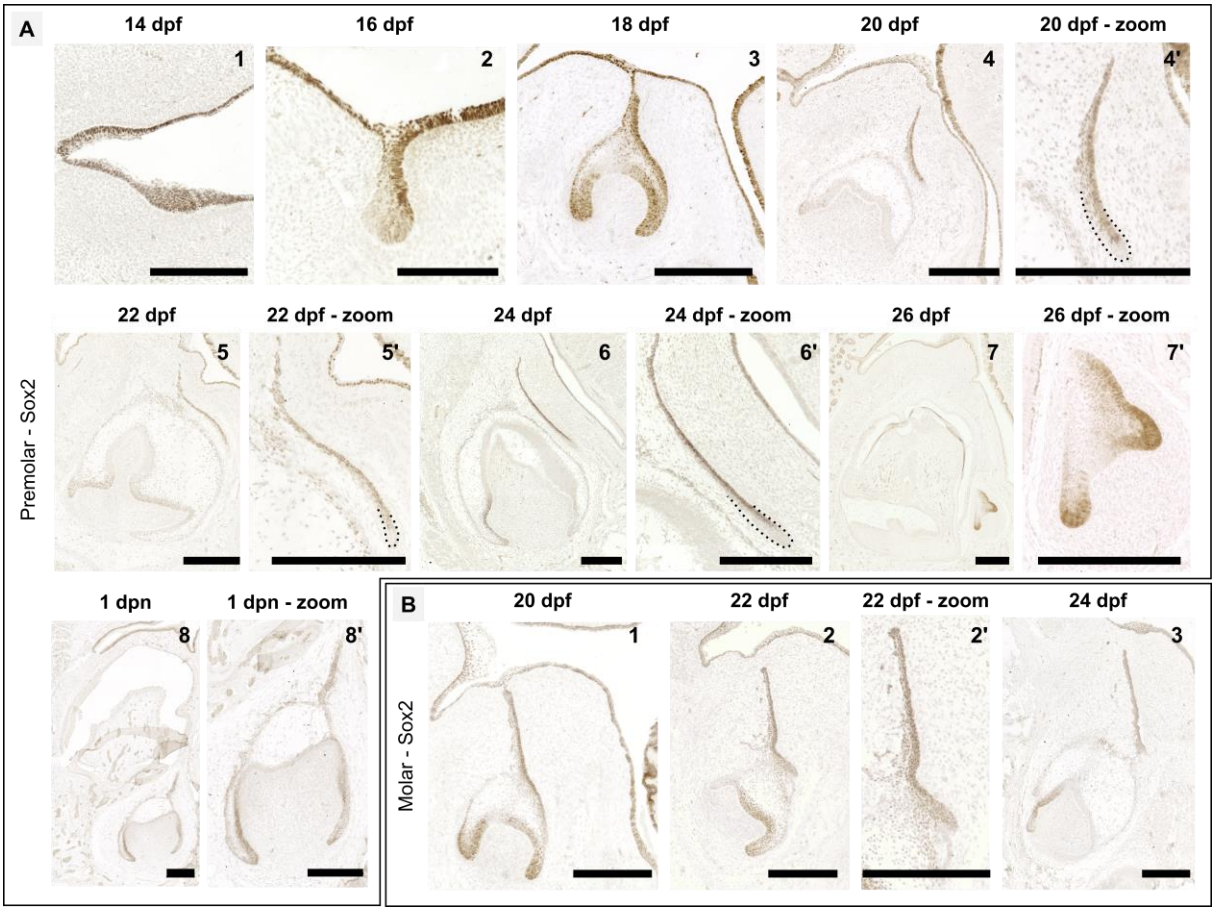

Figure 2. 3. SOX2 localization during tooth development and replacement. *SOX2 is localized by immunohistochemistry in the fourth lower premolar from 14 days post fertilization to 1 day post-natal (A) and in the first lower molar from 20 to 24 days post fertilization (B). Zoom of the replacement zone is located next to the global view. The dental replacement structures are highlighted in black dotted lines. Scale bar: 250µm.*

SOX2 localization

SOX2 is known to be expressed in the tooth during development and maintained during adulthood in ever-growing teeth where it is considered as an epithelial stem cell marker (Juuri et al., 2012). SOX2 pattern has been described in the ferret, the mouse and numerous reptiles (Juuri et al., 2013). In these species, the lingual part of the tooth is $SOX2^+$. We thus decided to follow the localization of the $SOX2^+$ cells during the development and the replacement of the dP_4 in the rabbit (**Figure 2. 3**, A). At 14 dpf, the entire oral and the dental epithelium is $SOX2^+$. At 16 dpf, the staining is more localized in the lingual part of the bud (**Figure 2. 3**, A2). At 18 dpf, SOX2 is localized in the lingual part of the dental lamina, the OEE, in the CL and in some

parts of the inner enamel epithelium (IEE). At 20 and 22 dpf, we detect SOX2 in the CL of the dP_4. The cells of the replacement dental lamina are $SOX2^+$ except at the tip (**Figure 2. 3**, A4-5). At 24 dpf, $SOX2^+$ cells are limited to the lingual part of the replacement dental lamina except at the tip. At 26 dpf, the P_4 has begun its morphogenesis; cells of the CL and the lingual part of the OEE are $SOX2^+$. The $SOX2^+$ pattern of the P_4 at 26 dpf is similar to the pattern of the dP_4 at 18 dpf (**Figure 2. 3**, A7/3). At birth, $SOX2^+$ cells are localized in the CL and in the lingual part of the dental lamina.

In the M_1, the $SOX2^+$ pattern at 20 dpf is the same that the one in dP_4 at 18 dpf, with an expression in the lingual part of the OEE, in the IEE and in the CL ((**Figure 2. 3**, B1/A3). At 22 dpf, the RSDL and the CL are $SOX2^+$ but not the OEE between these two structures. At 24 dpf, the dental lamina is degenerating but still $SOX2^+$. The CL are also $SOX2^+$ (**Figure 2. 3**, B)

So, the SOX2+ pattern does not vary between the deciduous premolar, the replacement premolar and the developing molar. SOX2+ are localized in the lingual part of the developing teeth and in the cervical loops, where the epithelial stem cells are supposed to be, suggesting a probably essential role during tooth development. Tooth replacement begins in the lingual part that is $SOX2^+$, but the presence of SOX2 is not sufficient to initiate tooth replacement. SOX2 is known to interfere with the Wnt signaling by binding to β-catenin and by regulating LEF1 (Kormish et al., 2010; Sun et al., 2016). The Wnt signaling is also inhibited directly or indirectly by RUNX2 (Togo et al., 2016). As RUNX2 seems correlated with tooth replacement and SOX2 is localized in the tooth replacement tissues we decided to follow the localization of LEF1.

LEF1 localization

LEF1 is a transcription factor that mediates the nuclear response to canonical Wnt signals and activates downstream genes by association with β-catenin (Eastman and

Grosschedl, 1999). Moreover, LEF1 has been shown to control stem cell renewal in mouse incisor (Sun et al., 2016). Thus, we decided to follow the localization of LEF1 during rabbit tooth development and replacement. At 14 dpf, LEF1 is localized in the dental epithelium of the dP_4 and only in the vestibular part of the mesenchyme (**Figure 2. 4**, A1). At 16 dpf, LEF1 is localized in the dental bud and in the mesenchyme surrounding the bud, with more cells $LEF1^+$ at the vestibular part. At 18 dpf, we detected $LEF1^+$ cells in the IEE, in the lingual part of the OEE and the dental lamina. LEF1 is also localized in the dental mesenchyme, with more mesenchymal $LEF1^+$ cells in the vestibular part of the dP_4 (**Figure 2. 4**, A3). At 20 dpf, LEF1 is still detected in the IEE, excepted in the CL. $LEF1^+$ cells are detected in the lingual part of the replacement dental lamina and especially in the tip. $LEF1^+$ cells are localized in the dental mesenchyme but we do not detect anymore the asymmetry between the lingual and vestibular mesenchyme. At 22 dpf, the tip of the replacement dental lamina is highly $LEF1^+$. Mesenchymal $LEF1^+$ cells are only seen around the epithelial cells (**Figure 2. 4**, A4). At 24 dpf, the tip of the replacement dental lamina is still highly $LEF1^+$. At 26 dpf, $LEF1^+$ cells are localized in the replacement tooth, with $LEF1^+$ cells in the IEE and in the mesenchyme surrounding the tooth. On contrary to the staining in the dP_4, we do not detect $LEF1^+$ cells in the lingual OEE of the P_4. Then, at birth, $LEF1^+$ cells are found in the IEE of the P_4 and in the mesenchyme around the dental epithelial cells.

Localization of $LEF1^+$ cells in M_1 at 20 dpf is highly similar to the $LEF1^+$ pattern in the dP_4 at 18 dpf (**Figure 2. 4**, B1/A3). At 22 dpf, we detect $LEF1^+$ cells in the lingual part of the dental lamina and in the RSDL. At 24 dpf, the tip of the degraded dental lamina is no more $LEF1^+$.

Figure 2. 4. LEF1 localization during tooth development and replacement. *LEF1 is localized by immunohistochemistry in the fourth lower premolar from 14 days post fertilization to 1 day post-natal (A) and in the first lower molar from 20 to 24 days post fertilization (B). Zoom of the replacement zone is located next to the global view. Scale bar: 250µm.*

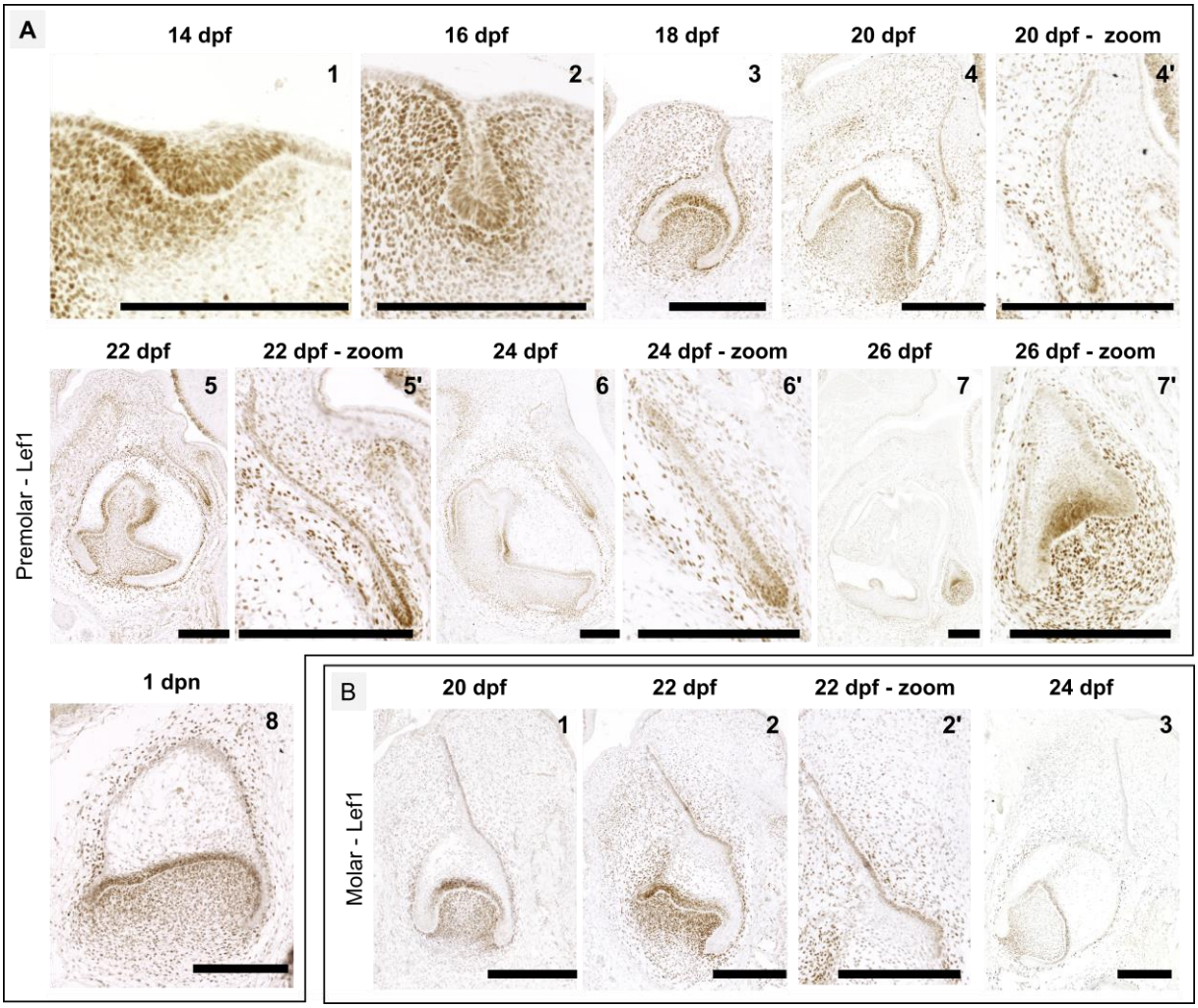

So, LEF1 localization differs between the deciduous and replacement premolars. A high number of LEF1^{+} cells in the lingual part of the dental lamina and the OEE is correlated with the initiation of the tooth replacement. Moreover, LEF1 is also expressed in other structures of the deciduous tooth, indicating a role during tooth development. LEF1 being downstream mediator of the Wnt/β-catenin signaling pathway, we wanted to follow another regulator of this pathway: *Sostdc1*. SOSTDC1 is an inhibitor of the Wnt signaling (Ahn et al., 2010; Itasaki et al., 2003) and is involved in mouse tooth morphogenesis (Cho et al., 2011), so we decided to follow its expression during rabbit tooth development and replacement.

Sostdc1 expression

SOSTDC1 (also named ectodin, Usag-1, and Wise) has been identified as tooth number modulator (Munne et al., 2009). We decided to follow *Sostdc1* expression during the dP_3 development and replacement. At 18 dpf, *Sostdc1* is expressed in the vestibular part of the OEE, in the CL and in the mesenchyme surrounding the CL (**Figure 2. 5**, A1). At the lingual part of the dP_3, we observed that *Sostdc1* is not expressed in the lingual epithelial layers of the dental lamina. At 20 and 22 dpf, *Sostdc1* is expressed in the OEE, in the vestibular layer of the replacement dental lamina and in the mesenchyme around the CL (**Figure 2. 5**, A2-3). Then, at 24 dpf, we detect expression of *Sostdc1* in the IEE and we observe a loss of *Sostdc1* expression in the tip of the replacement dental lamina. At 26 dpf, the P_3 begins its morphogenesis and we do not detect *Sostdc1* expression. At 28 dpf, *Sostdc1* is expressed in the ameloblasts, in the OEE of the P_3 and in the mesenchyme surrounding the CL.

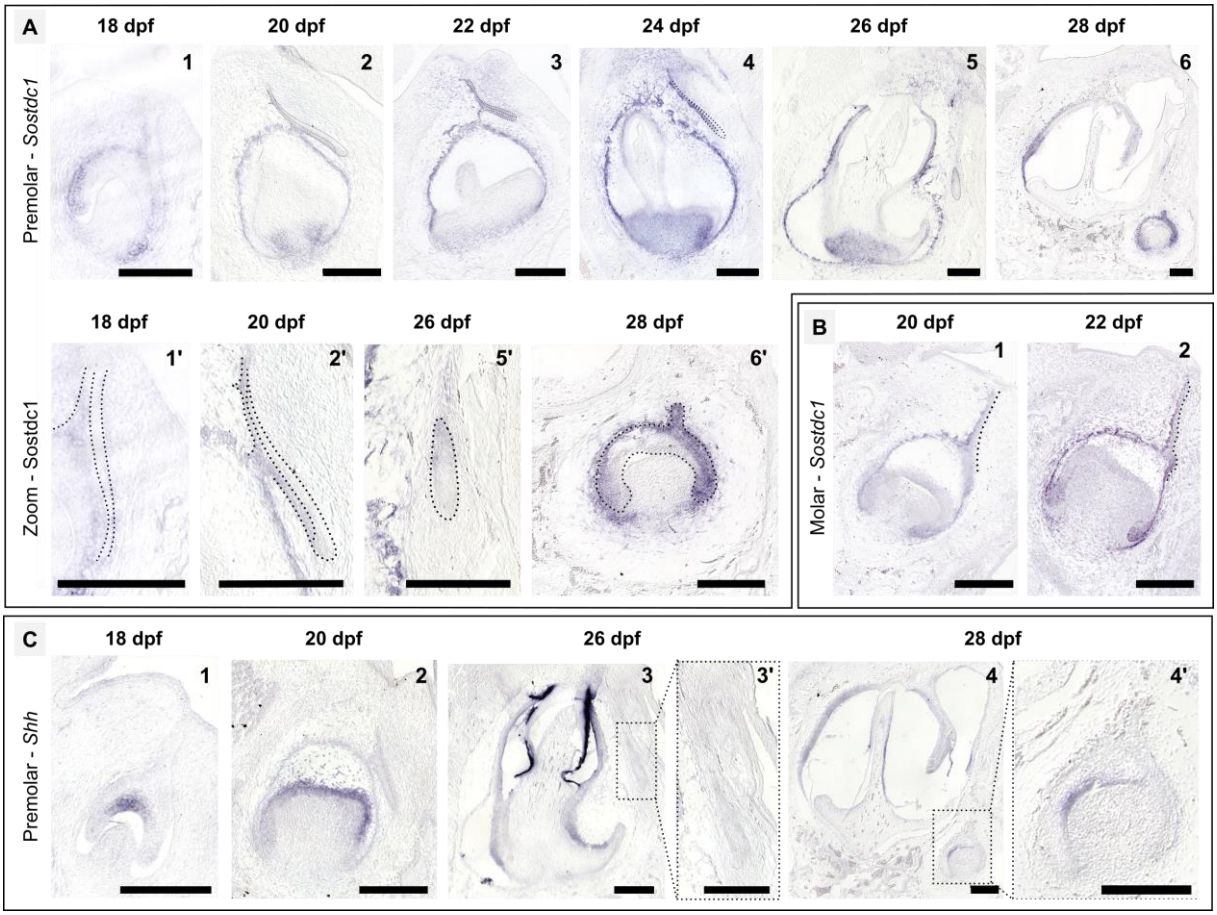

Figure 2. 5. Sostdc1 and Shh expression during tooth development and replacement. *Sostdc1 (A) and Shh (C) expression detected by in situ hybridization in the third lower premolar from 18 to 28 dpf and Sostdc1 expression in the first lower molar (B) at 20 and 22 dpf. In gray, zoom on the dental replacement area. The dental replacement structures and the expression pattern are highlighted in black dotted lines. Scale bar: 250µm.*

In the first lower molar (**Figure 2. 5**, B), we observed that *Sostdc1* is expressed in the vestibular part of the dental lamina, in the OEE and in the CL at 20 dpf. We observed a free area of *Sostdc1* in the lingual part of the dental lamina. At 22 dpf, the RSDL has developed in this *Sostdc1*$^{-}$ area (**Figure 2. 5**, B2). The lingual part of the dental lamina is still *Sostdc1*$^{-}$. However, we detect *Sostdc1* expression in the lingual basis of the RSDL.

Sostdc1 is thus differentially expressed between the deciduous and replacement premolars and between the RSDL and the replacement dental lamina, with *Sostdc1*$^{-}$ area correlated with a tooth replacement initiation. In mice, tooth number defect observed in *Sostdc1-null* mutants have been linked to the Shh signaling pathway (Ahn et al., 2010). Indeed, they showed that Shh signaling might participate in a negative-feedback loop that controls the level of Wnt signaling in order to restore a proper balance between Wnt and Shh signaling. Moreover Kim et al. (2019) suggested that SHH regulates cusp patterning in mouse tooth development by modulating Wnt signaling by SOSTDC1. We thus decided to follow *Shh* expression during rabbit tooth development and replacement.

Shh expression

SHH is essential for tooth development initiation by inducing invagination of the early dental lamina in the mesenchyme, and later during development, SHH is involved in tooth morphogenesis (Seppala et al., 2017). By modeling the Wnt signaling, SHH is involved in tooth number abnormalities in Sostdc1 mutant mice (Ahn et al., 2010). We thus decided to follow *Shh* expression during the dP_3 development and replacement. At 18 dpf, Shh is expressed in the

enamel knot (**Figure 2. 5**, C). At 20 dpf, *Shh* is expressed in the IEE and we do not observed expression in the replacement dental lamina. The expression pattern is similar in 22 and 24 dpf (**Figure 2. 5**, C1-2). At 26 dpf, *Shh* is still expressed in the IEE of the dP_3 and we do not detect *Shh* expression in the P_3. At 28 dpf, the ameloblasts of the dP_3 are Shh^+ as the IEE of the P_3 (**Figure 2. 5**, C4).

Therefore, the dP_3 and the P_3 show same *Shh* expression patterns, in the IEE. *Shh* is never expressed in the dental lamina or the replacement dental lamina during replacement initiation or development. *Shh* expression thus does not seem to directly regulate tooth replacement in the rabbit, but is involved in tooth development.

Discussion

We studied patterns of gene expression and protein localization of five genes supposed to be involved in tooth development and replacement. All of them were expressed in rabbit teeth, confirming their roles during rabbit tooth development. Some of the expression patterns vary between the deciduous premolar, the replacement premolar and the molar, indicating a possible role in the regulation of tooth replacement.

Stem cell maintenance and ever-growing teeth

Permanent premolars and molars are ever-growing in the rabbit, on contrary to the deciduous premolars. We shown that this ever-growing ability seems correlated with the presence of $SOX2^+$ cells in their cervical loops (**Figure 2. 6**) compared to the mouse molars that present a very limited $SOX2^+$ aera (Juuri et al., 2013). It should be interesting to follow $SOX2^+$ cells in adult rabbit teeth in order to compare cheek ever-growing teeth with the well-known mouse ever-growing incisor. Moreover, SOX2 seems to co-localize with RUNX2 in the CL of

the deciduous tooth but not in the CL of the permanent premolar. Togo et al. (2016) showed that these two proteins seem to interact in mutant mice, inducing a reduction of the $SOX2^{+}$ cells. In order to understand how cells may be regulated in the CL, it would be interesting to quantify expression of *Runx2* and *Sox2* in the deciduous and permanent premolars. Studying the differences of gene expressions between the deciduous and the permanent teeth may allow understanding the evergrowing ability of one tooth compared to the other.

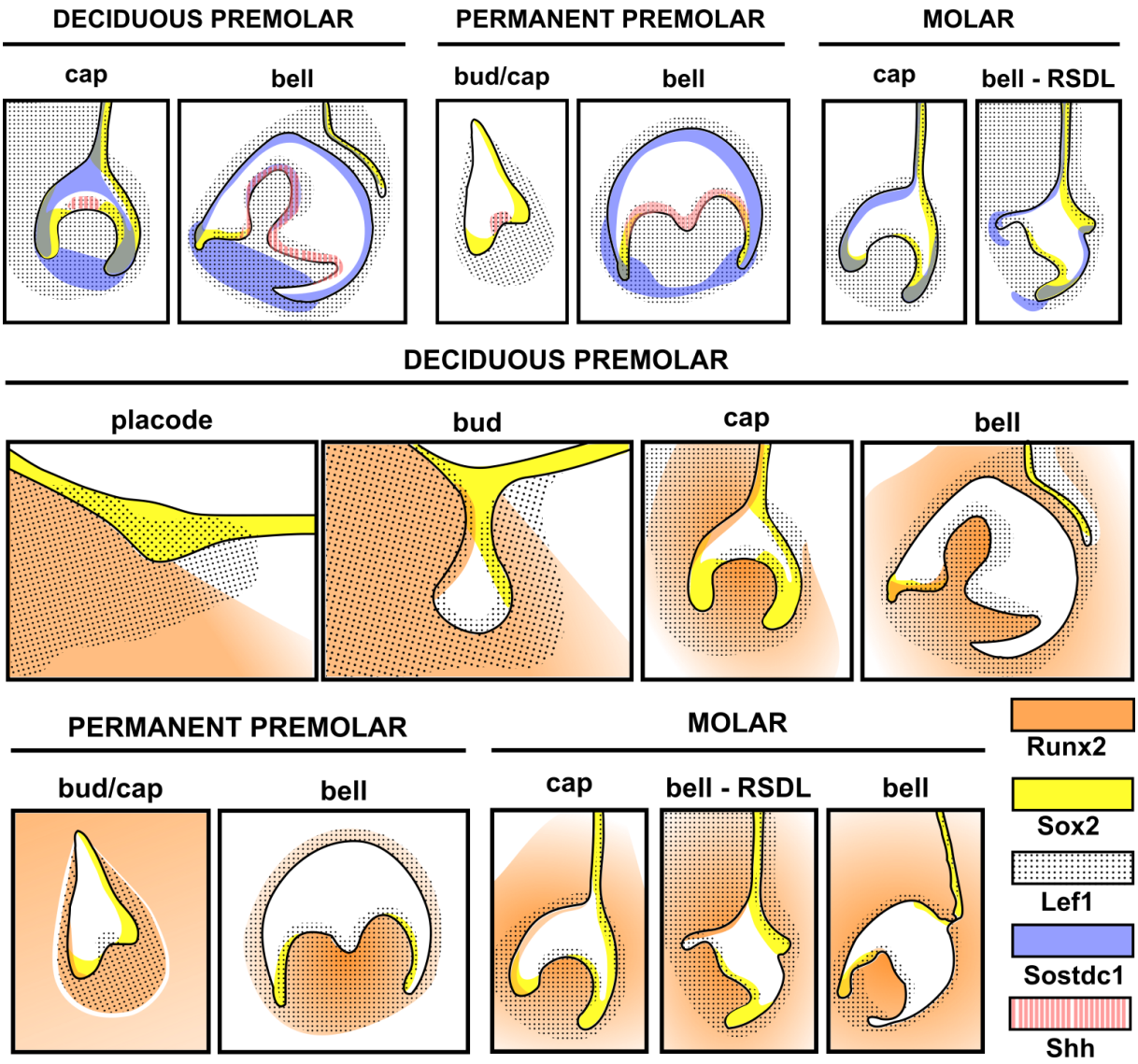

Figure 2. 6. Synthesis of expression patterns. *Synthesis of observed gene expression patterns and protein localizations. On the top, genes expression of Sostdc1, Shh and protein localization of Sox2 and Lef1. Expression patterns of Shh are missing for the molar. Below, protein localization of Runx2, Sox2 and Lef1 during the entire tooth development.*

Tooth morphogenesis

In rabbit, Shh is expressed in the IEE and seems to co-localize with LEF$^+$ and *Sostdc1*$^+$ cells during the bell stage, when the cusps forms (**Figure 2. 6**). Kim et al. (2019) suggested that SHH regulates cusp patterning in mouse by modulating Wnt signaling by SOSTDC1. We shown that these genes involved in mouse cusp patterning are also expressed in rabbit; it will be interesting to follow their expression patterns *in toto* in order to compare it with the cusp appearance and morphogenesis in the rabbit.

Tooth replacement

RUNX2$^+$ cells localization in the lingual part of the tooth correlate with tooth replacement inhibition in the premolars. This observation concords with results obtained in humans: an increase in RUNX2 induces a reduction of the tooth number (Merametdjian et al., 2019). In molars, the RSDL appears when the tooth is surrounded by RUNX2$^+$ cells; however, this RSDL is then unable to develop further. So, free areas of RUNX2 expression may be correlated with the maintenance of the replacement dental lamina. Sostdc1 is also presented as a tooth replacement inhibitor in mice (Munne et al., 2009). In the rabbit, the replacement dental lamina and the RSDL initiate their development in a *Sostdc1*$^-$ area whereas *Sostdc1* is expressed in all the OEE of the replacement tooth and its dental lamina (**Figure 2. 6**). In the molar, *Sostdc1* is expressed in the RSDL, which then disappear. So, *Sostdc1* may be a repressor of tooth replacement. Now that we know that Sostdc1 is differentialy expressed, functional studies with rabbit tooth organe culture could help to define the role of SOSTDC1 during mammalian tooth replacement. Expression pattern of SOX2 in the premolar of the rabbit is similar to the one observed in the canine of the ferret during tooth replacement (Juuri et al., 2013). SOX2$^+$ cells seem not sufficient to initiate tooth replacement due to their expression also in the lingual part of the permanent premolar (**Figure 2. 6**); but these cells are maintained in the lingual tooth part

of so many species that its function seems to have been conserved during evolution. A $SOX2^{+}$ lineage tracing during tooth replacement could help to better understand SOX2 function. LEF1+ cells are localized in the tip of the replacement dental lamina, as in reptiles (Handrigan and Richman, 2010). Then, absence of LEF1 expression in the lingual part of the OEE and its expression in the lingual mesenchyme of the replacement tooth are correlated with the absence of a third dental generation. In mutant mice with a stabilized β-catenin signaling in the RSDL, Popa et al. (2019) were able to obtain a new tooth from the RSDL by isolating it in culture. In rabbit, LEF1 is localized in the RSDL of the molar but is not sufficient to induce a tooth replacement. The Wnt signaling can be regulated in culture using inhibitors; it could be interesting to follow how deciduous premolars, permanents premolars and molars of rabbit are affected by modifying the Wnt signaling in rabbit tooth culture.

Conclusion

We provided here the description of five gene expression patterns during tooth development and replacement in rabbit. These expression patterns provide useful information about the spatio-temporal regulation of the dental development and replacement in a diphyodont species. Our molecular observations in the rabbit is a starting point that will allow further studies of gene functions at specific time windows.

Acknowledgments

We thank Nicolas Goudemand and all the members of his team for their help and support. We thank all the members of the "Evolution of vertebrate dentition" for the helpful advices and comments. We also thank Pierre Godement for giving us the biotinylated secondary antibodies and for his help to improve our protocols. The authors declare no potential conflicts of interest with respect to the authorship and/or publication of this article.

Author contributions

L.B.B: contributed to design, to acquisition, analysis, and interpretation, drafted manuscript. L.V: contributed to conception, to analysis and interpretation, critically revised manuscript. T.J: contributed to interpretation, critically revised manuscript. C.C: contributed to conception and design, to analysis and interpretation, critically revised manuscript

References

Ahn Y, Sanderson BW, Klein OD, et al. (2010) Inhibition of Wnt signaling by Wise (Sostdc1) and negative feedback from Shh controls tooth number and patterning. Development 137, 3221–31.

Al-Hamdany AK, Al-Khatib AR, Al-Sadi HI (2017) Influence of olive oil on alveolar bone response during orthodontic retention period: rabbit model study. Acta Odontol Scand 75, 413–422.

Bertonnier-Brouty L, Viriot L, Joly T, et al. (2019) 3D reconstructions of dental epithelium during Oryctolagus cuniculus embryonic development related to the publication ”Morphological features of tooth development and replacement in the rabbit Oryctolagus cuniculus”. MorphoMuseuM, 5:e90.

Cobourne MT, Sharpe PT (2010) Making up the numbers: The molecular control of mammalian dental formula. Semin Cell Dev Biol 21, 314–324. doi:10.1016/j.semcdb.2010.01.007.

Dosedělová H, Dumková J, Lesot H, et al. (2015) Fate of the molar dental lamina in the monophyodont mouse. PLoS One 10, e0127543.

Eastman Q, Grosschedl R (1999) Regulation of LEF-1/TCF transcription factors by Wnt and other signals. Curr Opin Cell Biol 11, 233–40.

Gaete M, Tucker AS (2013) Organized Emergence of Multiple-Generations of Teeth in Snakes Is Dysregulated by Activation of Wnt/Beta-Catenin Signalling M. Schubert, ed. PLoS One 8, e74484.

Handrigan GR, Richman JM (2010) A network of Wnt, hedgehog and BMP signaling pathways regulates tooth replacement in snakes. Dev Biol 348, 130–141.

Itasaki N, Jones CM, Mercurio S, et al. (2003) Wise, a context-dependent activator and inhibitor of Wnt signalling. Development 121, 3627–3636.

Järvinen E, Shimomura-Kuroki J, Balic A, et al. (2018) Mesenchymal Wnt/β-catenin signaling limits tooth number. Development 145, dev158048.

Järvinen E, Tummers M, Thesleff I. (2009). The role of the dental lamina in mammalian tooth replacement. J Exp Zool Part B Mol Dev Evol. 312B(4):281–291.

Järvinen E, Välimäki K, Pummila M, et al. (2008) The taming of the shrew milk teeth. Evol Dev 10, 477–486.

Jussila M, Crespo Yanez X, Thesleff I (2014) Initiation of teeth from the dental lamina in the ferret. Differentiation 87, 32–43.

Juuri E, Balic A (2017) The Biology Underlying Abnormalities of Tooth Number in Humans. J Dent Res 96, 1248–1256.

Juuri E, Jussila M, Seidel K, et al. (2013) Sox2 marks epithelial competence to generate teeth in mammals and reptiles. Development 140, 1424–32.

Juuri E, Saito K, Ahtiainen L, et al. (2012) Sox2+ Stem Cells Contribute to All Epithelial Lineages of the Tooth via Sfrp5+ Progenitors. Dev Cell 23, 317–328.

Kim J, Ahn , Adasooriya D, Woo EJ, Kim HJ, Hu KS, Krumlauf R CS (2018) Shh Plays an Inhibitory Role in Cusp Patterning by Regulation of Sostdc1. J Dent Res 98, 98–106.

Kormish JD, Sinner D, Zorn AM (2010) Interactions between SOX factors and Wnt/beta-catenin signaling in development and disease. Dev Dyn 239, 56–68.

Lan Y, Jia S, Jiang R (2014) Molecular patterning of the mammalian dentition. Semin Cell Dev Biol 25–26, 61–70.

Lee M-J, Kim E-J, Otsu K, Harada H, Jung H-S. 2016. Sox2 contributes to tooth development via Wnt signaling. Cell Tissue Res. 365(1):77–84.

Merametdjian L, Prud'Homme T, Le Caignec C, et al. (2019) Oro-dental phenotype in patients with RUNX2 duplication. Eur J Med Genet 62, 85–89.

Munne PM, Tummers M, Järvinen E, et al. (2009) Tinkering with the inductive mesenchyme: Sostdc1 uncovers the role of dental mesenchyme in limiting tooth induction. Development 136.

Lo Muzio L, Tetè S, Mastrangelo F, et al. (2007) A novel mutation of gene CBFA1/RUNX2 in cleidocranial dysplasia. Ann Clin Lab Sci 37, 115–20.

Popa, EM., Buchtova, M., and Tucker, AS. (2019). Revitalising the rudimentary replacement dentition in the mouse. Development 146, dev171363.

Popa EM, Anthwal N, Tucker AS (2016) Complex patterns of tooth replacement revealed in the fruit bat (Eidolon helvum). J Anat 229, 847–856.

Rasch LJ, Martin KJ, Cooper RL, et al. (2016) An ancient dental gene set governs development and continuous regeneration of teeth in sharks.

Richman JM, Handrigan GR (2011) Reptilian tooth development. Genesis 49, 247–260.

Seppala M, Fraser GJ, Birjandi AA, et al. (2017) Sonic Hedgehog Signaling and Development of the Dentition. J Dev Biol 5.

Sharir A, Klein OD (2016) Watching a deep dive: Live imaging provides lessons about tooth invagination. J Cell Biol 214, 645–7.

Sun Z, Yu W, Navarro MS, et al. (2016) Sox2 and Lef-1 interact with Pitx2 to regulate incisor development and stem cell renewal. Development, dev.138883.

Togo Y, Takahashi K, Saito K, et al. (2016) Antagonistic Functions of USAG-1 and RUNX2 during Tooth Development P. E. Witten, ed. PLoS One 11, e0161067.

Tummers M, Thesleff I (2003) Root or crown: a developmental choice orchestrated by the differential regulation of the epithelial stem cell niche in the tooth of two rodent species. Development 130, 1049–1057.

Wang F, Xiao J, Cong W, et al. (2014) Morphology and chronology of diphyodont dentition in miniature pigs, Sus Scrofa. Oral Dis 20, 367–379.

PART 2

TOOTH SHAPE MODIFICATIONS DURING LAGOMORPHA EVOLUTION

For centuries, teeth have been studied to understand vertebrate evolution, especially in mammals where morphological variations of the teeth allow reconstructing evolutionary lineages. Nowadays, the field of the evolutionary developmental biology investigates the molecular and developmental mechanisms to better understand evolutionary processes. Developmental heterochrony, the change in the timing or rate of developmental events inducing change in size and or shape of the organs during evolution, can be identified by studying both tooth fossil record and extant morphogenesis. Lagomorpha fossil record is mainly documented by tooth fossils, so we already know that Lagomorpha teeth evolved from moderate hypsodont rooted cheek teeth in late Paleocene to hypselodont teeth, with clear variations of shape (Kraatz et al., 2010). Phylogenetic relationship among Lagomorpha are often based on variation of shape of the P_3 tooth (Čermák et al., 2015a; Hibbard, 1963), but shape modifications of the others teeth are not well documented.

We decided in this second part to study the variation of the first molar morphology during lagomorph evolution and in *Oryctolagus cuniculus* ontogeny. In adult, the rabbit tooth occlusal surface is completely flat. However, we showed that transiently rabbit cheek teeth possess cusps. First, using the 3D-reconstructions of the tooth epitheliums we were able to follow the rabbit cuspidogenesis of the molars during embryogenesis. Then, by studying tooth occlusal shape of many extinct and extant lagomorph (see Annex 3, **p244**), we obtained information about developmental heterochrony during lagomorph evolution. We found out that the evolution of the rabbit cheek teeth can result from developmental heterochronies.

Chapter 2.1 – *Oryctolagus cuniculus* cuspidogenesis

The tooth morphology, in particularity the occlusal surface, is an essential characteristic to study evolutionary history through the study of cusp homology among mammals. Cusp terminology in the rabbit *Oryctolagus cuniculus* or in other extant or extinct lagomorphs is a problematic subject in the literature (Kraatz et al., 2010). Lagomorph ancestors possess a typical tribosphenic cusp pattern, which then changed a lot during lagomorph evolution. Extant species have cusps at birth that are then quickly worn to give flat ever-growing cheek teeth. Studies about cusp homologies are mainly based on extinct stem lagomorph keeping cusps during all their life span, not considering developmental homology. From all the pre-existing studies, Kraatz et al. tried in 2010 to obtain a consensual lagomorph cusp pattern based on topological study of the lagomorph teeth. However, this proposed lagomorph cusp nomenclature is not homologous with other mammals due to the absence of tooth developmental knowledge in Lagomorpha.

In this chapter, we propose a new rabbit cusp identification based on the tribosphenic pattern and cusp homologies. Using 3D-reconstructions of the epithelium tissues during tooth development, we were able to obtain the counterprint of the developing mesenchyme and so study the cusp formation in molariform teeth. By studying the appearance order of the cusps during tooth development, we obtained a chronology of cusps formation and then named these cusps following the terminology of the primary cusps defined by Butler (1956).

We observed that during the 4 days of development necessary for the rabbit cuspidogenesis, we could recognized by homology millions of years of mammal dental evolution. To conclude, during rabbit molar tooth development we identified clear cusp homology with the ancestral tribosphenic pattern.

Article 3: Million years of mammalian tooth evolution revisited in 4 days of development

Ludivine Bertonnier-Brouty[1*], Laurent Viriot[1], Thierry Joly[2,3], Cyril Charles[1]

[1] Institut de Génomique Fonctionnelle de Lyon, Université de Lyon, CNRS UMR 5242, Ecole Normale Supérieure de Lyon, Université Claude Bernard Lyon 1, Lyon, France

[2] ISARA-Lyon, F-69007 Lyon, France

[3] VetAgroSup, UPSP ICE, F-69280 Marcy l'Etoile, France

*Corresponding author: ludivine.bertonnierbrouty@lyon-ens.fr

Abstract

The tooth morphology is a distinctive character to study evolutionary history of mammals through the study of cusp homology. From one haplodont tooth, early mammals acquiered a three cusped shape, called the tribosphenic molar present primitively in all groups of mammals. Cusp homologies are known among most mammals. However, cusp terminology in the European rabbit teeth or in other extant or extinct lagomorphs is a problematic subject due to their highly derived tooth shape. Lagomorph ancestors possessed a typical tribosphenic cusp pattern, which changed a lot during lagomorph evolution. Extant species have cusps at birth that are quickly worn down to flat ever-growing cheek teeth. We propose a new rabbit cusp identification based on the tribosphenic pattern and cusp homologies. Using 3D-reconstructions of the epithelium tissues during tooth development, we were able to study the cusp formation in molariform teeth. By studying the appearance order of the cusps during tooth development, we obtained a chronology of cusps formation. We shown that we could recognized by homology millions of years of mammal dental evolution during the rabbit cuspidogenesis.

Keywords: cusp formation; *Oryctolagus cuniculus*; tribosphenic; odontogenesis; developmental heterochrony

Introduction

Similarity of morphological structure derived from a common ancestral form among species defin the homology. Studying these homologies among species can give evidence for evolution. Embryological development provides one of the best evidence to decipher homologies (Laubichler, 2000). Early stages of development often reveal similarities that are less apparent in final structures. These developmental homologies between species can be compared to the ancestral relationships between them in order to better understand how developmental processes evolved. In paleontology, molar pattern is an essential trait to retrace the evolutionary history of mammals. From one haplodont tooth with a simple crown pattern, early mammalians developed a three cusped shape (paracone, protocone and metacone) called the tribosphenic molar. This tribosphenic molar is present primitively in all groups of mammals and is a main characteristic of the mammalian tooth shape. This ancestral tribosphenic pattern gave rise to the various molar patterns. For instance, the quadritubercular molar appeared first in late Cretaceous by addition of one cusp, the hypocone (Hunter and Jernvall, 1995; Luckett, 1993). Studying the ontogeny of molar pattern in extant species is necessary to better understand the diversity of tooth shapes in extant and extinct mammals. Except few exceptions listed by Butler (1956), the first cusp to develop is the paracone on the upper teeth and the protoconid on the lower teeth; the other cusps arise from a marginal zone around these primary cusps (Butler, 1956). Mammal cusp morphogenesis is mainly studied in mouse due to the large number of embryos needed at different developmental stages (Ahn et al., 2010; Pantalacci et al., 2017; Petit, 2017). So, in numerous species the cusps are only identified by a topological approach of the functional tooth. However, when the teeth are highly derived from the ancestral tribosphenic molar, the topology could not well define cusp homologies. Extant lagomorphs represent such a case, with cheek teeth highly derived and ontogenetic modifications of the crown shape during the animal's life. Therefore, lagomorph cusp pattern is problematic, mostly

due to the central cusp in the unworn upper cheek teeth (Averianov, 1998; Kraatz et al., 2010). The lower cheek tooth cuspidogenesis is better understood, due to a clear tribosphenic organization with the trigonid and the talonid easily identifiable in newborns (Glasstone, 1938; Kraatz et al., 2010). In order to decipher the cusp homologies between the current lagomorphs and their ancestors, we decided to follow the cuspidogenesis in the first upper molar of the European rabbit, *Oryctolagus cuniculus*. Rabbit teeth quickly display a flat occlusal surface due to wear and exhibit a bilophodont morphology. However, rabbit cheek teeth have cusps at birth. To avoid the wear effect, we followed the chronology of the cusp appearance before tooth eruption. Using 3D-reconstructions of dry and soft dental tissues, we here present the developmental and morphological characteristics of the crown surface in *Oryctolagus cuniculus*. We show that millions of years of mammalian tooth evolution are observable within few days of rabbit development.

Materiel & Methods

Samples

Embryos and newborn rabbits studied by X-Ray microtomography were obtained through collaboration with a standard production for feeding located at the Biology Departmental livestock establishment (EDE) n°38044102. The gestation period for a rabbit is about 31 days. We collected embryos at 20, 22, 24, 26 and 28 days post fertilization (dpf) and rabbits at 0, 1, 2, 3 and 4 days post-natal (dpn). We worked on common rabbit breeding regularly crossed with wild rabbits to ensure genetic mixing. Each tooth is specifically named: we use “M” for molar; the tooth number is in exponent for the upper teeth.

X-ray microtomography and 3D reconstruction

Conventional X-ray microtomography allows reconstructing 3D models of mineralized tissues such as bony head and teeth, thus providing a non-invasive access to internal structures. Using phosphotungstic acid (PTA) staining, that binds heavily to various proteins and connective tissue, according to the Metscher method (Metscher, 2009), we were also able to detect soft tissues. After fixation, half-head samples were stained in a solution of 0.3% PTA in 70% ethanol between 1 week to 8 months according to the size of the sample. Oldest specimens were demineralized to better detect the soft tissue staining. Once the PTA contrast staining was complete, samples were embedded in paraffin and radiographed. Specimens were radiographed using a Phoenix Nanotom S (GE Measurement and Control), which was set up with a tungsten source X-ray tube operating at 100 kV and 70 µA for the mineralized tissues and 60kV and 70µA for the soft tissues. The Phoenix datosx2CT software was applied to gather radiographies in a reconstructed 3D volume, in which the voxel size ranged from 1.6 to 7.5 µm depending on the size of the specimen. Post-treatment of 3D volumes, including virtual sectioning as well as sub-volume extraction and surface creation was performed using VG-studio max software. Surface smoothing was done with Meshlab software.

Tooth topography and measures

Colored cusp topography was obtained using CloudCompare software. Mesenchymal surfaces were orientated in an occlusal position and cusp topography was obtained using the Height ramp function. Outlines of the occlusal surface were drawn using GIMP software. The crown area and the crown width were measured using ImageJ software.

Results

Using 3D reconstructions of the dental mesenchyme during tooth development, we followed the cuspidogenesis in the first upper molar of the rabbit before tooth eruption (**Table 3. 1**). We used the 3D-reconstruction of the epithelium-mesenchyme junction as a proxy of the occlusal surface of the tooth. For each stage, we measured the crown width and the crown area.

	paracone	metacone	protocone	main parastyle	hypocone	paraconule	metaconule	mesostyle	Secondary parastyle
22 dpf	X	X							
24 dpf	X	X	X	X					
26 dpf	X	X	X	X	X	X	X		
28 dpf	X	X	X	X	X	X	X	X	
4 dpn	X	X	X	X	X	X	X		X

Table 3. 1. Cusp presence in the M^1 during odontogenesis.

At 20 days post fertilization, the M^1 is still in cap stage, the folding of the inner enamel epithelium has not begun, cusps are not yet present. At 22 dpf, the epithelium start to fold and we can identify the first cusps at the epithelium-mesenchyme junction. At this stage, we observed a big central cusp, and a small developing cusp at its distal side (**Figure 3. 1**A). By following the nomenclature described by Butler (1956) and used during mammalian ontogeny by Luckett (1993), we can consider that the first cusp is the paracone and the smallest one the metacone. A crest links these two cusps. Two days later, at 24 dpf, the crown area has increased by 130% (**Figure 3. 1**B). The crown has expanded mesialy, with a new cusp connected to the two previous one. We homologize this cusp with the parastyle of other mammals due to its localization. However, in rabbits this parastyle is a major cusp of the crown shape, so we will named it the main parastyle. The crown is also wider with an augmentation of the crown width of around 42%. At the lingual part of the crown, we detect appearance of a cusp, considered to be the protocone. At this stage, the three main cusps defining the tribosphenic pattern are set up. From 24 to 26 dpf, the crown increase in width by 48% and in the crown area by 158%.

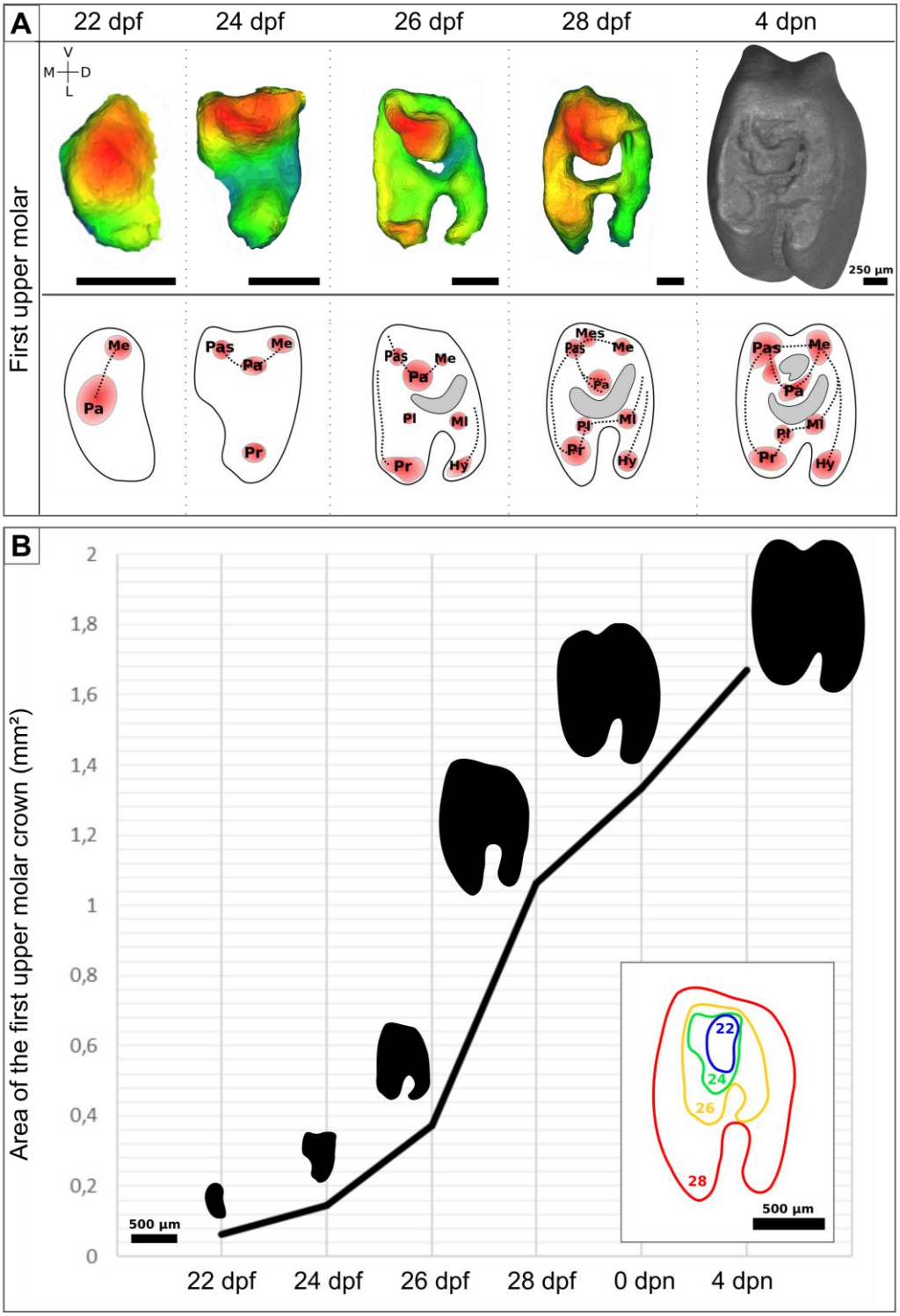

Figure 3. 1. Cusp pattern and area of the crown of the first upper molar during odontogenesis. *(A) At the top, cusp surface of the M^1 from 22 to 28 dpf. Color depends on the height of the cusps, in red the highest, in blue the lowest. 3D reconstruction of the M^1 occlusal surface at 4 days post-natal. At the bottom, diagram representing the cusps in red and the crests in dotted lines. In grey, the valleys. Pa, paracone; Me, metacone; Pas, Parastyle; Pr, protocone; Hy, hypocone; Pl, paraconule; Ml, metaconule; Mes; mesostyle. M, mesial; D, distal; L, lingual; V, vestibular. Scale bar: 250 µm. (B) Area of the crown. In horizontal axis, the stages of development and in vertical axis the area of the crown in mm². In dark, the outlines of the M^1 crown. In color, the relative size of the M^1 occlusal surface according to the different stages of development. Scale bar: 500 µm.*

The main change is the development of the disto-lingual part of the tooth with the appearance of a new cusp, defined as the hypocone (**Figure 3. 1**). We observed the formation of the trigon basin in the middle of the crown. In its lingual side, we detected the appearance of two small cusps: presumably the paraconule (mesial) and the metaconule (distal). A mesial crest is forming, the preprotocrista. At 26 dpf, we detected the first apposition of dentin at the top of the cusps and globally the M^1 has reached its eruption shape. From 26 to 28 dpf, the M^1 undergoes its biggest size variation with an increase in the crown width of 74% and in the crown area of 184% (**Figure 3. 1**B). At this stage, we detected an extra-cusp at the vestibular part of the parastyle, presumably named mesiostyle. The tooth is mineralizing at the top of the crown, so essentially at the mesial part of the tooth. The small extra-cusps are from inter-individual shape variations. In embryos, we followed cusp shape at the epithelium-mesenchyme junction. In new-born rabbits, teeth are too mineralized to reconstruct the soft tissues so we decided to follow the external crown shape, including the layer of enamel compared to previous stages. From 28 dpf to birth, we observed an increase in the crown width of 4%, probably due to the method modification and the inter-individual variations. The crown area continues to grow with a 25% increase detected. The cusp pattern in newborns has been studied in five M^1 in order to identify the cusps always present in the newborn rabbit and detect the small inter-individual variations. We identify eights cusps present in all of the newborns. We detected a cusp between the paracone and the main parastyle, due to its localization we decided to name this new cusp the secondary parastyle. We conclude that the biggest cusp at the center of the tooth is the paracone, and that the four others main cusps detected at each corner are: the metacone (vestibulo-distal), the hypocone (linguo-distal), the protocone (mesio-lingual), and the main parastyle (mesio-vestibular). Secondary cusps, paraconule, metaconule and the secondary parastyle, are located around the two basins, the trigon basin at the center of the tooth and at its vestibular side, the secondary basin (**Table 3. 1**).

Discussion

We decided to follow the usual developmental cusp initiation to identify the cusps in rabbits embryos and thus to analyze cusp homology between rabbits and other mammals (Butler, 1956; Luckett, 1993). So, we named paracone the central main cusp in rabbits, already formed at 22 dpf. Then, at 24 dpf, the crown shape of the rabbit tooth is highly similar to the ancestral tribosphenic (or tritubercular) pattern. Osborn (1907) described that almost all the Mesozoic genera show tribosphenic molars (**Figure 3. 2**) and Van Valen that the tribosphenic pattern was common at the end of the Cretaceous (1994).

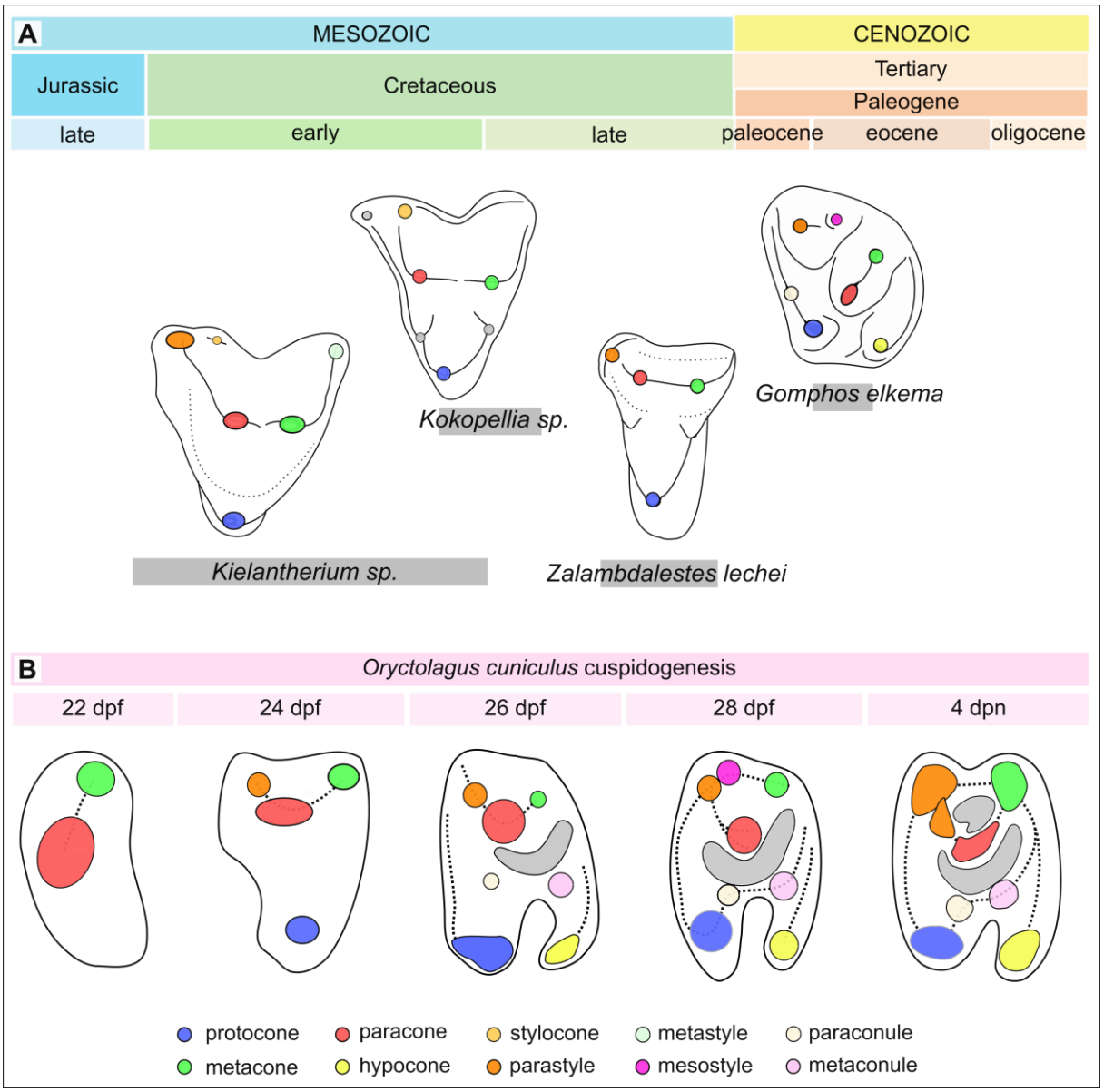

Figure 3. 2. Molar cusp pattern variations during mammalian evolution and rabbit development. *(A) Tribosphenic and quadritubercular molars of various mammalian species from Late Jurassic to the Miocene. Cusps patterns following Davis, 2011; Lopalin & Averianov, 2006; Butler, 1977; Kraatz et al., 2010. In grey, valleys. Not at scale. (B) Cusp pattern during rabbit ontogeny.*

This ancestral pattern is well characterized in fossils, easily recognizable by the presence of three main cusps: the paracone, the metacone and the protocone. The tribosphenic tooth has a triangle shape with the protocone at the apex (Osborn, 1907). Already in 1907, Osborn indicated that the cusps appear in the same order when comparing embryogenesis and evolution. The cusp and crest pattern observed in 24 dpf rabbits is for instance very similar to the cusp pattern observed in Kokopellia fossils, an extinct Marsupialia from Early to Late Cretaceous (Davis 2011, **Figure 3. 2**). We observed the similar "L"-shaped crest containing three cusps from the mesio-vestibular to the distal side of the tooth and the protocone lingualy, positioned at the middle of the tooth length. The general tooth shape is also similar with a triangle form with the protocone in apex and a metaflexus at the vestibular side of the tooth.

At 26 dpf, we detect the appearance of the hypocone, the last main cusp to develop. During mammalian evolution, the hypocone is also the last of four main cusp to appear, convergently many times during mammalian evolution (Hunter and Jernvall, 1995; Luckett, 1993). Appearance of the hypocone, originating from the postprotocingulum in Lagomorpha, induces an increase of the occlusal area (Hunter and Jernvall, 1995). Mimotonids are described as the likely ancestors of Lagomorpha (Kraatz et al. 2009). *Gomphos elkema*, a mimotonid from the Eocene, possesses a clear tribosphenic pattern with a hypocone (**Figure 3. 2**A, Kraatz et al. 2010). The cusp pattern of *Gomphos* is probably closely linked to the cusp pattern observed in young extant Lagomorpha. Stem Lagomorpha from the Eocene already present flat occlusal surface, complicating the study of cusps homologies. From the late Miocene, *Alilepus hibbardi*, a suggested ancestor of the extant genera of leporids, displays an occlusal surface very similar

to current adult leporids (Jin et al. 2010). Indeed, as in extant Lagomorpha, the hypocone and the protocone are separated by a lingual hypoflexus, defining the bilophodont pattern. During development, we observed that the general shape of the crown surface changes with the appearance of the hypocone, the tooth becomes rectangular. At 26 dpf, the mesial crest is well set-up and the protocone is now in the mesio-lingual side of the tooth, similarly to the quadri-tubercular molars (**Figure 3. 2**B). In newborns, we defined two cusps as a parastyle because rabbits possess five main cusps compared to the usual four main cusps of the quadritubercular molars. The so-called main parastyle is probably one cusp novelty in the rabbits, which requires a new name to complete the actual nomenclature. This cusp appear very early in development, disrupting the order of appearance observed during evolution. About 4 days of development elapse between the appearance of the paracone and the hypocone, cusps whose apparition during the evolution is separated by millions of years. Therefore, during development, the evolutionary history of the first upper molar of the rabbit is revisited, dental development extending past the mammalian ancestral ontogeny in older ages. This change of occlusal shape over evolutionary time scales is a developmental heterochrony (Gould, 1977). We observed an over-development of the dental crown pattern in rabbits compared to Cretaceous mammals and ancestor representatives, a peramorphosis. Sadier et al. (2019) showed that in mouse, tooth patterning is far from straight, in link with the mouse evolutionary history. In rabbit molar development, we do not observed tooth fusion as in the mouse, however the new crown shape is also probably obtained by modifying or refining an established developmental pattern during embryogenesis. As showed in the mouse (Sadier et al., 2019), the extant patterning mechanisms involved in the tooth shape are modified versions of the ancestral ones. Variations of tooth shape during development, correlated with the variations during evolution, could be the result of these numerous modifications of patterning mechanisms. Modifications of patterning mechanisms imply modifications of genetic regulation. Cusps are formed during tooth

development in the inner enamel epithelium. At each cusp tips, secondary enamel knots are observed, so each cusp is associated with a signaling center. We can suppose that the genetic cusp regulation network is highly dynamic during rabbit cuspidogenesis, allowing these big variations of shape from one stage to another. Jernvall (1999) showed that morphological variations in size and number of cusps can be explained by only small developmental changes, and a very little increase in developmental complexity can induce a big increase in shape complexity in mammalian cheek teeth. So, we can hypothesize that by studying developmental process responsible of the tooth shape variations during rabbit cuspidogenesis we may identify which are these small changes in the developmental program that induced changes in tooth shape during mammalian evolution. One way to study in more details cusp developmental mechanisms would be a transcriptomic analyze. Pantalacci et al. (2017) showed that transcriptomic approach could be used in evolutionary developmental biology in order to identify transcriptomic signatures and that transcriptomes differ most during crown morphogenesis. So it could be possible to identify the morphogenetic processes involved in tooth crown morphogenesis. To conclude, rabbit odontogenesis and particularly the crown morphogenesis seems closely linked to the evolutionary history of the mammals. By studying transcriptomic variations in link with the morphological changes, we could identify the developmental processes that have been modified during mammalian evolution.

Acknowledgements

We thank Nicolas Goudemand and all the members of his team for their help and support. We thank all the members of the “Evolution of vertebrate dentition” for the helpful advices and comments. We are grateful to Mathilde Bouchet-Combe, from the SFR Biosciences (UMS3444/CNRS, US8/Inserm, ENSL, UCBL1), who helped for X-Ray microtomographic analyses. The authors declare no conflict of interest

Author contributions

L.B.B: contributed to design, to acquisition, analysis, and interpretation, drafted manuscript. L.V: contributed to conception, to analysis and interpretation, critically revised manuscript. T.J: contributed to interpretation, critically revised manuscript. C.C: contributed to conception and design, to analysis and interpretation, critically revised manuscript

References

Ahn, Y., B. W. Sanderson, O. D. Klein, and R. Krumlauf. 2010. Inhibition of Wnt signaling by Wise (Sostdc1) and negative feedback from Shh controls tooth number and patterning. Development 137:3221–31.

Averianov, A. O. 1998. Homology of the cusps in the molars of the lagomorpha (Mammalia) and certain general problems of homology in the morphological structures. Paleontol. J. 32:73–77.

Butler, P. M. 1956. The ontogeny of molar pattern. Biol. Rev. 31:30–69. John Wiley & Sons, Ltd (10.1111).

Davis, B. M. 2011. Evolution of the Tribosphenic Molar Pattern in Early Mammals, with Comments on the "Dual-Origin" Hypothesis. J. Mamm. Evol. 18:227–244..

Glasstone, S. 1938. A Comparative Study of the Development in vivo and in vitro of Rat and Rabbit Molars. Proc. R. Soc. London. Ser. B-Biological Sci. 126:315–330.

Gould, S. J. 1977. Ontogeny and phylogeny. Belknap Press of Harvard University Press.

Hunter, J. P., and J. Jernvall. 1995. The hypocone as a key innovation in mammalian evolution. Proc. Natl. Acad. Sci. U. S. A. 92:10718–22.

Jin et al. 2010 Jin, C. Z., Y. Tomida, Y. Wang, and Y. Q. Zhang. 2010. First discovery of fossil Nesolagus (Leporidae, Lagomorpha) from Southeast Asia. Science China Earth Sciences, 53(8), 1134-1140.

Jernvall, J. 2002. Linking development with generation of novelty in mammalian teeth. Proc. Natl. Acad. Sci. 97:2641–2645.

Kraatz, B. P., Badamgarav, D., & Bibi, F. 2009. Gomphos ellae, a new mimotonid from the middle Eocene of Mongolia and its implications for the origin of Lagomorpha. Journal of Vertebrate Paleontology, 29(2), 576-583.

Kraatz, B. P., J. Meng, M. Weksler, and C. Li. 2010. Evolutionary patterns in the dentition of duplicidentata (Mammalia) and a novel trend in the molarization of premolars. PLoS One 5:1–15.

Laubichler, M. D. 2000. Homology in Development and the Development of the Homology Concept. Am. Zool. 40:777–788.

Luckett, W. P. 1993. An Ontogenetic Assessment of Dental Homologies in Therian Mammals. Pp. 182–204 in Mammal Phylogeny.

Metscher, B. D. 2009. MicroCT for comparative morphology: simple staining methods allow high-contrast 3D imaging of diverse non-mineralized animal tissues. BMC Physiol. 9:11.

Osborn, H. F. 1907. Evolution of Mammalian Molar Teeth: To and from the Triangular Type Including Collected and Revised Researches Trituberculy and New Sections on the Forms and Homologies of the Molar Teeth in the Different Orders of Mammals. Macmillan.

Pantalacci, S., L. Guéguen, C. Petit, A. Lambert, R. Peterkovà, and M. Sémon. 2017. Transcriptomic signatures shaped by cell proportions shed light on comparative developmental biology. Genome Biol. 18:29.

Petit, C. 2017. Évolution et Développement d'un organe sériel Transcriptomique comparée des bourgeons de molaire chez les rongeurs. Thèse Dr. en Sci. la Vie.

Sadier, A., M. Twarogowska, K. Steklikova, L. Hayden, A. Lambert, P. Schneider, V. Laudet, M. Hovorakova, V. Calvez, and S. Pantalacci. 2019. Modeling Edar expression reveals the hidden dynamics of tooth signaling center patterning. PLOS Biol. 17:e3000064.

Van Valen, L. M. 1994. Serial homology: the crests and cusps of mammalian teeth. Acta Palaeontol. Pol. 38:145–158.

Chapter 2.2 – Lagomorpha crown shape variations during development and evolution

Present-days living Lagomorpha are divided into two families that together comprise 12 genera and 91 species spread over almost every continent. The phylogenetic relationships between these species are known (Matthee et al., 2004) as the morphological changes of the P_3 during Lagomorph evolution. However, the first upper molar, the mostly used tooth for comparative anatomy in mammals, has been poorly studied in extant Lagomorpha species. Moreover, even if Major (1899) already identified the morphological changes of the rabbit ever-growing M^1 between newborns and adults more than a century ago, no studies are available in the literature to clearly characterize these morphological changes during rabbit ontogeny.

In this paper, we proposed to investigate the development and the evolution of the Lagomorpha dentition following the first upper molar changes. In order to characterize changes in dental morphology related to age, we studied the morphological variability of cheek teeth in different species of extant and extinct lagomorphs from birth to adulthood. Using X-ray microtomography, we were able to extrapolate the occlusal surface at different wear stages by making virtual sections of 3D tooth reconstructions. We observed modification of the occlusal tooth shape during ontogeny in Lagomorpha.

To conclude, comparison of dental changes during Lagomorph evolution and rabbit odontogenesis allows us to suggest developmental heterochrony modifications of molar development during their evolution. Our results suggest that *Oryctolagus cuniculus* upper molariform teeth evolved by peramorphosis by a retention of ancestral characters at the beginning of the ontogeny as well as by the later occurrence of novel characters, the crenulations.

Article 4: Ontogenetic modifications of tooth crown shape unravel mechanisms of evolution of the dentition in Lagomorpha (Glires, Mammalia)

Ludivine Bertonnier-Brouty [1*], Laurent Viriot [1], Aline Desoutter [2,3], Anne-Gaëlle Chaux-Bodard [2,3]

Thierry Joly[4,5], Cyril Charles [1]

[1] Institut de Génomique Fonctionnelle de Lyon, Université de Lyon, Université Lyon 1, CNRS, Ecole Normale Supérieure de Lyon, 46, allée d'Italie 69364 Lyon Cedex 07, France.

[2] Head and Neck Unit, Surgical Oncology Department, Centre Léon Bérard, 28 rue Laennec, 69008 Lyon, France

[3] Department of Surgical Oncology, Centre Léon Bérard, LabTau, U1032, Inserm, Claude Bernard University, 11 rue Guillaume Paradin, 69008 Lyon, France

[4] ISARA-Lyon, Lyon, France, 69007

[5] VetAgroSup, Marcy l'Etoile, France, 69280

* Corresponding author: Ludivine Bertonnier-Brouty

Abstract

During lagomorph evolution, cheek teeth changed considerably, from rooted to unrooted evergrowing teeth, with modifications of the occlusal morphology. The adult upper cheek teeth of extant lagomorphs are characterized by the presence of two lophs separated by a lingual enamel fold. We observed that juveniles and adults have different morphologies of their occlusal surfaces. To characterize changes in dental morphology related to age, we studied the variability of cheek teeth in 37 different species of lagomorphs. Using microtomography, we were able to extrapolate the occlusal surface at different wear stages by making virtual sections of 3D-reconstitutions. We demonstrate that unworn first upper molars of leporids have a crescent valley structure and those of ochotonids display a vestibular fold. These characters disappear few weeks after birth, when the lingual re-entrant fold invagination increases. This fold is smooth in juveniles and can become increasingly crenulated with age in the majority of

the leporid species. Furthermore, the chronology of the morphological modifications occurring during dental development corresponds step by step to what is observed between basal and derived species of lagomorphs. This observation leads us to hypothesize of a peramorphic dental evolution of lagomorphs that follows the ancestral character states during ontogeny.

Keywords: Evolution, Tooth Development, Lagomorpha, Ontogeny, Peramorphosis, Heterochrony

Introduction

Both the fossil record (Asher et al., 2005; Meng, 2004) and molecular phylogenies (Huchon et al., 2002; Kriegs et al., 2007) support the existence of a Glires grandorder that gathers living Lagomorpha and Rodentia as well as fossil stem groups. Glires are overall characterized by the gnawing function implemented by their two pairs of enlarged and ever-growing incisors. The basal dichotomy of Glires is clearly marked, among many other characters, by the persistence of a second pair of upper incisors in the Duplicidentata like Mimotonida and Lagomorpha whereas these incisors are lost in the Simplicidentata like Mixodontia and Rodentia (Chuan-Kuei et al., 1987). The initial radiation of Glires likely occurred in eastern Asia after the End-Cretaceous Extinction (O'Leary et al., 2013), and circa 5 Ma after this event, a diversity of stem lagomorphs and stem rodents was already present in fossil assemblages from the Middle Paleocene of China (Li et al., 2016; Wang et al., 2007, 2016). However and despite consistent efforts, the evolutionary history of lagomorphs is far from settled. Yet *Litolagus*, which is known from the early Oligocene of North America and China, is considered as the most basal Leporidae (Fostowicz-Frelik, 2013) whereas *Sinolagomys* appears as the most basal Ochotonidae currently known (Erbajeva et al., 2017).

Currently living Lagomorpha are divided into two families that together comprise 12 genera and 91 species (Hoffmann and Smith, 2005). The family Ochotonidae (Pikas) only contains the genus *Ochotona* and its 30 species native to mountainous and rather cold regions of western North America, and Central Asia (Hoffmann and Smith, 2005; Nowak, 1999). The subfamily Leporidae (Hares and Rabbits) is more diverse as it includes 11 living genera and 61 species that have a natural range covering most of the world's major land masses (Hoffmann and Smith, 2005; Nowak, 1999). Importantly, the subfamily Leporidae includes the European rabbit (*Oryctolagus cuniculus*) that is an important model for biomedical research (Bosze and Houdebine, 2006) as it is also a powerful model for the study of genome-based phenotypic variations throughout domestication (Carneiro et al., 2014).

Dentitions of fossil and extant mammals provide pivotal characters that allow reconstructing lineages and tracing their evolutionary history (Osborn, 1907; Rose, 2006). Throughout the evolutionary history of Lagomorpha, incisors remain relatively stable because these teeth are highly constrained functionally. At the opposite, premolar and molar teeth underwent substantial transformations since the Paleocene. Premolars and molars of Lagomorpha notably display a trend in crown heightening over evolution such that extant lagomorphs possess deciduous premolars with high crowns and finite growth (hypsodonty) while permanent premolars and molars have ever-growing crowns without roots (hypselodonty). In modern Leporidae like the European rabbit, the adult cheek dentition comprises five lower and six upper hypselodont teeth per dental quadrant. Most lower and upper cheek teeth exhibit similar crown patterns, thus involving bilophodont molars ($M_{1\text{-}2}$ and $M^{1\text{-}2}$) and molarized bilophodont premolars (P_4 and $P^{3\text{-}4}$) that together make up the core of cheek dental rows. Teeth located at row extremities display either a complex shape (P_3 and P^2) or are highly reduced (M_3 and M^3). The situation is slightly different in Ochotonidae because the M^3 is lost in this family, but the overall arrangement of the cheek dentitions remains similar to this

of Leporidae. Historically, the third lower permanent premolar (P_3) was mainly targeted by paleontologists because this tooth includes many informative characters to investigate phylogenetic relationships among Lagomorpha (Čermák et al., 2015b; Hibbard, 1963). In the present work, we however choose to study the upper first molars (M^1) notably because this tooth shows the typical bilophodont pattern of the jugal dentition of modern lagomorph.

In all vertebrates, the crown of a tooth develops and gradually mineralizes from its occlusal part (cusp tips) to its cervical part (crown base). Many mammals whose diets are highly abrasive develop teeth that grow continuously throughout life (Janis and Fortelius, 1988). In these latter, the dental crown never finishes its development and rhizogenesis is not initiated (Bertin et al., 2018). This is the case of permanent premolars and molars in modern rabbits whereas deciduous premolar teeth have a finite growth. In these continuously growing teeth (or hypselodont teeth), the cervical portion of the crown continues to develop and mineralize while the occlusal part erupts and gradually wears out through functional abrasion. Continuous growth and eruption of the crown are offset by the abrasion resulting from the mastication of ingested food (Müller et al., 2014). The continuous abrasion of the occlusal surface is of great interest because it enables to exhaustively characterize the successive morphologies of the dental crown during the whole life of the animal by using increasing wear stages. Historically, many authors have attempted to simulate crown abrasion of hypsodont toothed mammals in order to reconstruct series of progressive wear stages either by juxtaposing various specimens of ascending age (Madden 2015), or by mechanically abrading teeth (Viriot 1996), or by virtually abrading dental 3D models (Angelone et al., 2014). The basis of the present study consisted in a careful monitoring of the morphogenesis of the M^1 from birth to adulthood in Lagomorpha, with particular attention paid to the European rabbit *Oryctolagus cuniculus*. Three-dimensional models of dental crowns produced by X-ray microtomography and occlusal surface pictures allowed assessing morphological variations of crown pattern in 877 M^{1s} of 37

different species of extant and extinct Lagomorpha. By collecting a whole series of occlusal morphologies between eruptive and advanced wear stages, we were able to characterize the intraspecific variation of the occlusal surface related to dental ontogeny, and to separate it from the inter-individual variation. We observed modification of the occlusal tooth shape during ontogeny in Lagomorpha. In extant leporids, the tooth crenulates and the number of crenulations increased when the individual gets older. Our comparison of dental evolutionary trends and rabbit odontogenesis allows us to suggest modifications in the timing or rate of molar development during their evolution. All of our results suggest that *Oryctolagus cuniculus* upper molariform teeth evolved by peramorphosis by retention of ancestral characters at the beginning ontogeny as well as by the occurrence of novel characters, the crenulations.

Materiel & Method

Sampling

We studied 534 skulls belonging to 36 different extant and 1 extinct species of Lagomorpha. A detailed list of investigated specimens is given in the **Supplementary table 4. 1**. Specimens were studied either *in situ* or borrowed from the collections of the American Museum of Natural History (AMNH, New-York, USA), the Musée National d'Histoire Naturelle (MNHN, Paris, France), and the Musée des Confluences (MCL, Lyon, France). *Oryctolagus cuniculus* (240 specimens, skull size from 36.65 to 108.8mm) and *Lepus capensis* (67 specimens, skull size from 50.5 to 92.5mm) are the two species in our sampling with developmental series from newborns to adults. Three specimens of *Palaeolagus haydeni* coming from the White River Formation (Colorado, USA) were borrowed from the geological collections of the Université de Lyon (UCBL-FSL). Seventy two upper tooth rows belonging to 10 different species were selected for 3D investigations (**Supplementary table 4. 1**). Two newborn rabbits that died during calving have been obtained from the breeding of T. Joly. This

breeding is a standard production for feeding and is located at the Biology Departmental livestock establishment (EDE) n°38044102. Heads were fixed overnight in 4% PFA and conserved in EtOH until 3D investigations.

Irradiated specimens

Four irradiated hemi-mandibles and two control hemi-mandibles were studied. Due to the high proximity between the growth zone of the upper cheek teeth and the eyes in *Oryctolagus cuniculus*, irradiations were not possible in the upper jaw so we studied the effects of the irradiations in the mandible. Two *Oryctolagus cuniculus*, 14 weeks old, have been exposed to irradiations in each hemi-mandible. The irradiation zone was centered in the mental foramen and included the lower cheek teeth. During the radiotherapy experiment, each hemi-mandible has been exposed of a total dose of 42.5 Gy, divided in five doses of 8.5 Gy each week during four weeks and the specimens were sacrificed just after the last radiation session (CEEA n°10). Controls had the same age than irradiated specimens and were raised as the irradiated rabbits. Two other hemi-mandibles where used as control of the intra-species variability. Hemi-mandibles were conserved in EtOH until 3D investigations.

X-Ray microtomography

Conventional X-ray microtomography allows reconstructing 3D models of mineralized tissues such as teeth, thus providing a non-invasive access to internal structures. Specimens were radiographed using a Phoenix Nanotom S (GE Measurement and Control), which was set up with a tungsten source X-ray tube operating at 100 kV and 70 µA. The Phoenix datosx2CT software was applied to gather radiographies in a reconstructed 3D volume, in which the voxel size ranged from 3 to 12 µm depending on the size of the specimen. Post-treatment of 3D volumes, including virtual sectioning as well as sub-volume extraction, was performed using VG-studio max software. Surface smoothing and visualizations has been done with Meshlab software.

Data acquisition

Museum specimens were studied in situ. Pictures of the M^1 occlusal surface were captured using a stereomicroscope Leica EZ4 D equipped with an integrated 3.0 megapixel CMOS camera. Skull length was measured from nasal to external occipital protuberance. The number of crenulations was also counted by differentiating those located on the mesial wall (anteroloph side) from those located on the distal wall (posteroloph side) of the hypoflexus. The HL/CW ratio between the length (vestibulo-lingual dimension) of the hypoflexus and crown width and the ML/CW ratio between the length (vestibulo-lingual dimension) of the metaflexus and crown width were calculated using ImageJ software. Statistics and graphs were done with R and Past 3 software. Hypoflexus crenulation wavelengths were measured from pictures using ImageJ software.

Results

Changes in M^1 occlusal shape through odontogenesis

The adult occlusal surface of a M^1 in modern Lagomorpha displays two lophs, the mesial one being called the anteroloph and the distal one being the posteroloph (**Figure 4. 1**A). The anteroloph and the posteroloph are partly separated by a deep lingual fold called the hypoflexus, as well as by a more modest vestibular fold called the metaflexus (**Figure 4. 1**A). Although they appear to be almost separate, the anteroloph and the posteroloph are always interconnected by a mesio-distal crest that we will call the median mure according to Reig (1977). The mesial and distal enamel layers that neighbors the hypoflexus are respectively called mesial and distal walls (**Figure 4. 1**C1). The mesial and distal walls of the hypoflexus are variably crenulated according to the species and the different stages of tooth wear within the species (**Figure 4. 1**C1-3), and this is one of the issues we will discuss in this article.

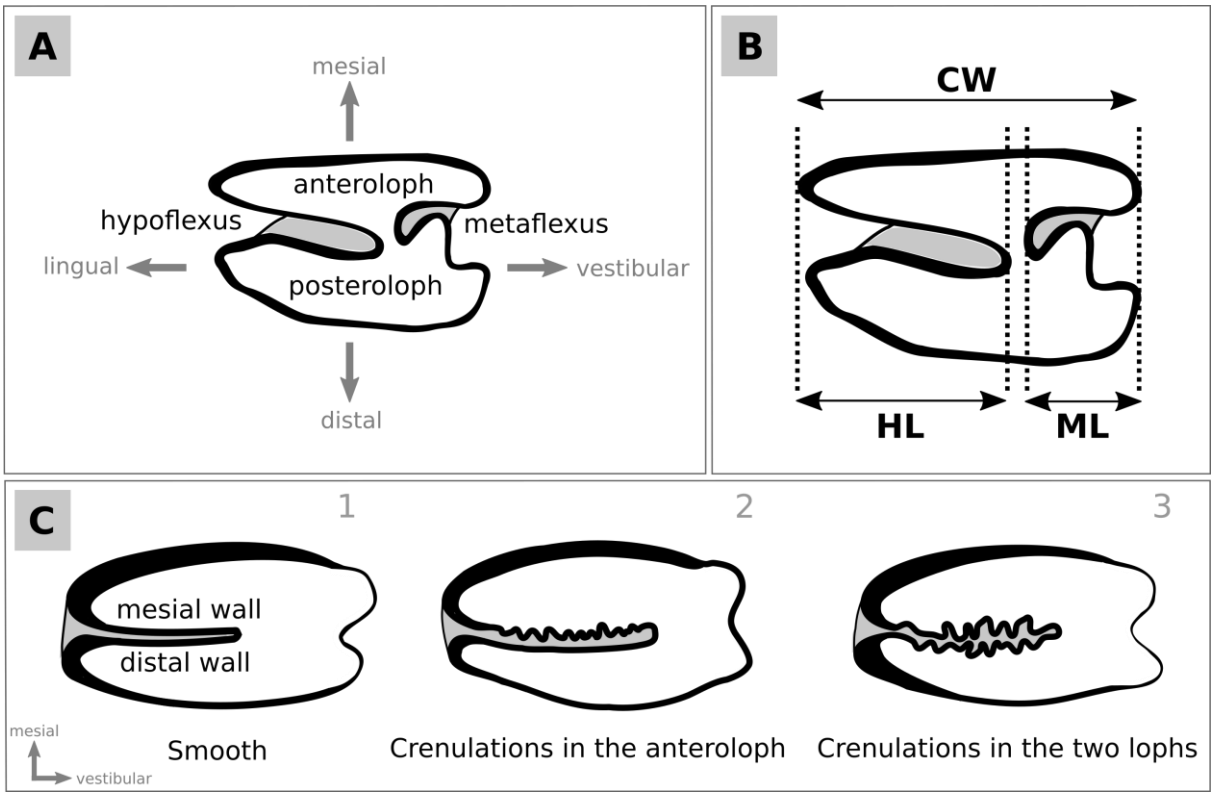

Figure 4. 1. Terminology of the M[1] occlusal surface. *A. the M[1] is characterized by the presence of the anteroloph and the posteroloph that can be separated by a lingual hypoflexus and a metaflexus. B. Representation of the measures and ratios used to define the occlusal surface shape. C. The hypoflexus can present various pattern of crenulations from smooth to highly crenulated in one or the two lophs of the tooth. Cement in grey; enamel in black and dentine in white.*

Ochotona

We studied the morphological changes of the M^1 occlusal surface between two juvenile specimens and two adult specimens of *Ochotona pallasi* and *Ochotona princeps*. Changes in occlusal shape being similar in these two latter species, only the differences observed in *Ochotona princeps* are shown in this article (**Figure 4. 2**A-B). The slightly worn M^1 of a juvenile *Ochotona princeps* already had a bilophodont occlusal pattern, which was however complicated by the presence of a curved metaflexus that meandered relatively deeply on the vestibular side of the crown (**Figure 4. 2**A1-2, **Supplementary figure 4. 1**). The hypoflexus also penetrated deeply the occlusal surface, so that the combined invaginations of the hypoflexus and metaflexus made the two lophs almost independent. The CVA of a juvenile *Ochotona princeps*

M^1, whose crown height was 2.6 mm (Fig. S1), documented the progressive regression of the metaflexus as well as the extension of the hypoflexus (**Figure 4. 2**B1-6). The ML/CW ratio (**Figure 4. 1**B) was 0.24 at the occlusal surface. Then this ratio gradually decreased to 0.19 at 1.8 mm and finally fallen to 0.16 at 2 mm below the occlusal surface. At first, the metaflexus began to close, thus causing the appearance of an enamel islet (**Figure 4. 2**B2-3). Further down, this enamel island wore out (**Figure 4. 2**B4) and the metaflexus gradually regressed to its smallest size (ML/CW: 0.16) at about 2 mm below the occlusal surface (**Figure 4. 2**B5-6). In contrast to the metaflexus, the hypoflexus invaginated progressively, with a HL/CW ratio that went from 0.74 at the occlusal surface to 0.86 at the cervical part of the crown. The bilophodont pattern of adult *Ochotona* M^1 that displayed two almost independent lophs was achieved through regression of the metaflexus (**Figure 4. 2**A3-4, 2B7). At this wear stage, the anteroloph and the posteroloph were separated by a highly invaginated hypoflexus (HL/CW: 0.88), and only a tiny vestibular median mure remained between them. The mesial and distal walls of the hypoflexus both remained completely smooth in adult Ochotonidae whatever the abrasion stage (**Figure 4. 2**A3-4).

Palaeolagus

We studied the maxillary teeth of three specimens belonging to *Palaeolagus haydeni*, an extinct species of stem Leporidae found in the Oligocene Formation of White River, USA (Wood, 1940). Although the M^{1s} of the three specimens already had a worn occlusal surface and no trace of root formation, their occlusal morphologies were not similar (**Figure 4. 2**C1-4). The CVA of the first two M^{1s} (**Figure 4. 2**D1-12) showed a central crescentic valley and a weakly re-entrant hypoflexus (HL/CW: 0.34 and 0.41, respectively). The crescentic valley wore out rapidly (**Figure 4. 2**D3-4, 8-9) while the hypoflexus slightly extended (HL/CW: 0.45) before the central part of the hypoflexus became an enamel islet (**Figure 4. 2**D5-6, 10-11, 13-15). This

enamel islet was called hyposterial lake by Fostowicz-Frelik and Tabrum (2009). The CVA of the third M^1 (**Figure 4. 2**D13-18) showed that both the hyposterial lake and the hypoflexus ended up disappearing, so that the occlusal surface became ovoid in shape, without enamel on the vestibular and disto-vestibular edges (**Figure 4. 2**D12,16-18).

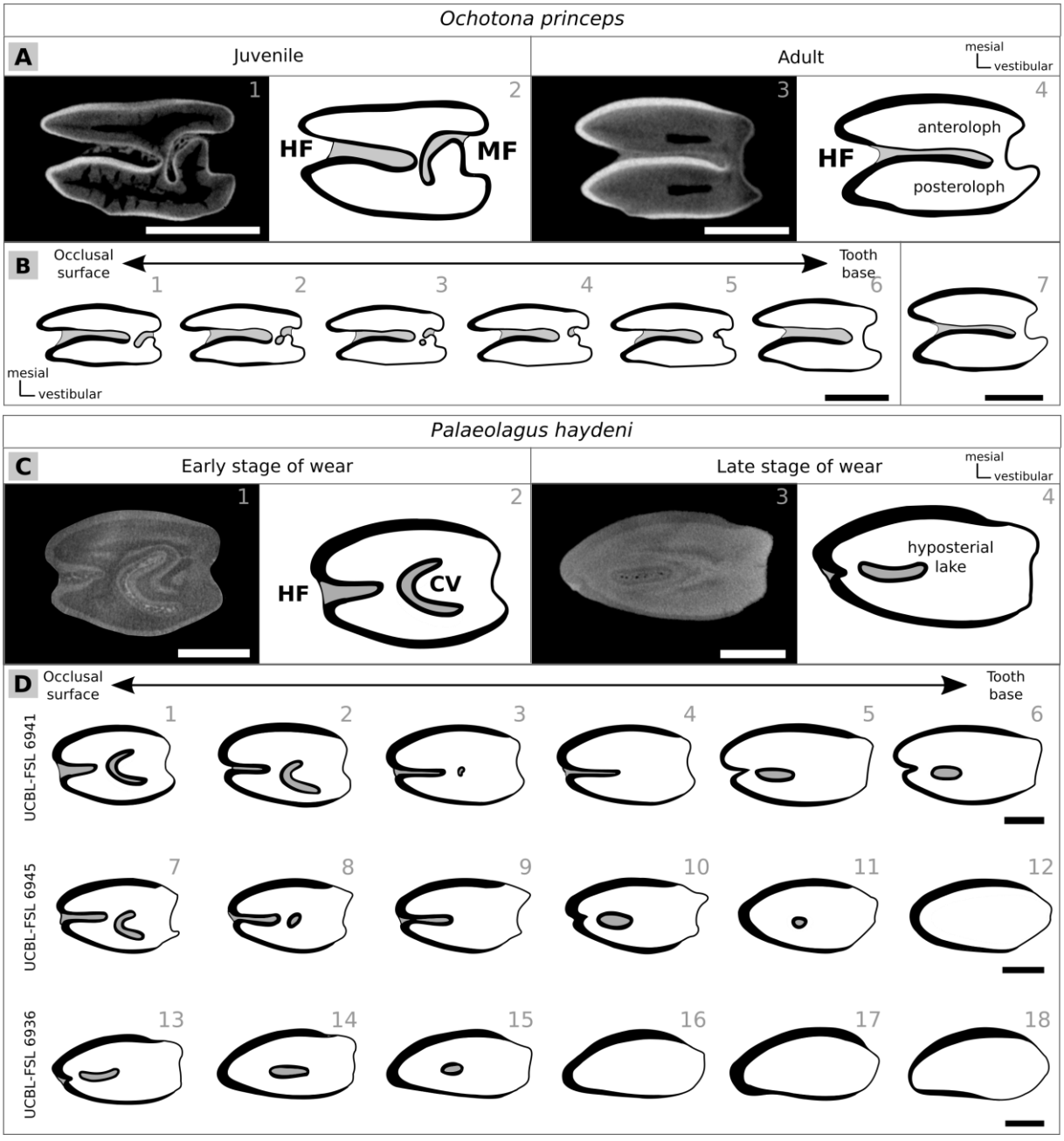

Figure 4. 2. Variation of M^1 occlusal tooth pattern in function of the wear stage in Ochotona princeps and Palaeolagus haydeni. *(A) M^1 of a juvenile and an adult Ochotona princeps. (B) Sections of the M^1 of Ochotona princeps from occlusal to tooth base, virtually imitating different wear stages. (C) M^1 of Palaeolagus haydeni at different wear stages, from an early to a late stage of wear. (D) Sections of three M^1 of Palaeolagus haydeni from occlusal to tooth base, virtually imitating different wear stages. Cement in grey; enamel in black and dentine in white. Scales bar: 1mm.*

Oryctolagus

The unworn M^1 of a neonate *Oryctolagus cuniculus* did not display the typical bilophodont pattern, but an irregular occlusal surface in which five main cusps were recognizable; four of these being interconnected by crests (**Figure 4. 3**A1-3). The mesial part of the crown displayed higher cusps than its distal part (**Figure 4. 3**A1-2). Both the crescentic valley and the hypoflexus already were recognizable and filled with cementum (**Figure 4. 3**A3), and the hypoflexus penetrated up to one-third of the occlusal surface (HL/CW: 0.32). During the juvenile period, the occlusal surface rapidly flattened, thus creating an extension of the occlusal surface in all directions because the early crown of the M^1 had the shape of a top-truncated cone mesio-distally compressed (**Figure 4. 3**A1-3).

The CVA of a juvenile *O. cuniculus* M^1 (**Figure 4. 3**C1-5) rapidly displayed a crescentic valley (**Figure 4. 3**B1-2) and a feebly invaginated hypoflexus (HL/CW: 0.35). At about 1.7 mm below the cusped surface, the crescentic valley was completely worn out (**Figure 4. 3**C3-4) while the hypoflexus continued to extend towards vestibular direction (HL/CW: 0.47). However, the crescentic valley never connected to the hypoflexus and these two structures turned out to be completely distinct. Further down, the hypoflexus continued to invaginate (HL/CW: 0.52), and the first crenulations appeared on hypoflexus mesial wall when HL/CW: 0.52 (**Figure 4. 3**C4). The occlusal surface of an adult *O. cuniculus* M^1 (**Figure 4. 3**B3-4, 3C5) showed two lophs of about the same length, but the width of the anteroloph was one and a half times greater than that the posteroloph. The hypoflexus penetrated up to two-thirds of the occlusal surface (HL/CW: 0.68) while the metaflexus remained tiny (ML/CW: 0.05). The two lophs were firmly linked on their vestibular side for 26% of their length by a mesio-distal connection. The mesial wall of the hypoflexus was strongly crenulated, and more crenulated than the distal wall (**Figure 4. 1**C).

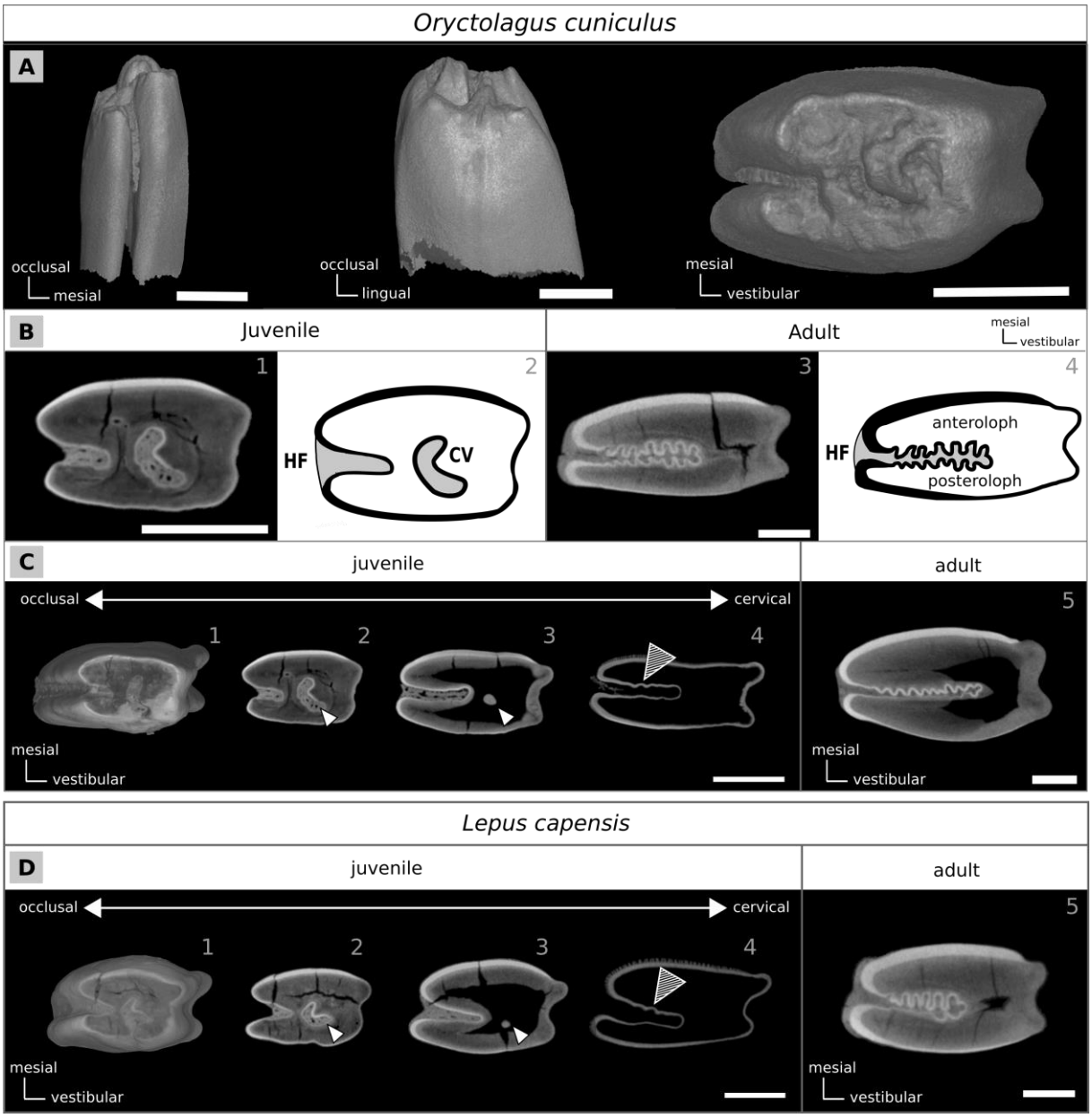

Figure 4. 3. Variation of M^1 occlusal tooth pattern during leporid ontogeny. *(A) Occlusal surfaces of young and adult Oryctolagus cuniculus. Sections from occlusal to growth zone of one single tooth, virtually imitating different wear stages in Oryctolagus cuniculus (B) and Lepus capensis (C). The white arrows show the crescentic valley present only in the juveniles. The arrows with black lines indicate the crenulations in the hypoflexus. Scales bar: 1mm.*

Lepus

The weakly worn occlusal surface of a juvenile *Lepus capensis* M^1 already had a complete anteroloph, but the posteroloph was still not formed at this stage because the future crescentic valley opened towards the back of the crown (**Figure 4. 3**D1). A weakly reentrant hypoflexus was present on the lingual border (HL/CW: 0.33). The CVA of this juvenile

specimen showed that the crescentic valley closed and became insulated in the center of the crown while the posteroloph consequently appeared (**Figure 4. 3**D2-3) at 0.4 mm below the occlusal surface. The crescentic valley in *Lepus* was more curved than in *Oryctolagus* (compare **Figure 4. 3**C2 and 3D2). At 1.29 mm below the occlusal surface (**Figure 4. 3**D4), the crescentic valley completely disappeared while the hypoflexus extended (HL/CW: 0.53). In *Lepus* as in *Oryctolagus*, there was thus no interrelation between the crescentic valley and the hypoflexus and these two structures were unambiguously separated. Further down, the hypoflexus continued to invaginate and its mesial wall became strongly crenulated while the distal wall remained slightly undulated (**Figure 4. 3**D4-5).

Enamel crenulation pattern

Implementation of crenulations throughout odontogenesis

Juvenile rabbits had few and poorly expressed enamel crenulations in the vicinity of the hypoflexus, while adult and old specimens had numerous and more pronounced crenulations. In order to better understand the implementation and morphological variations of crenulations during odontogenesis, we produced M^1 CVA in neonate and juvenile *Oryctolagus cuniculus*, from which we scrutinized the number and shape of crenulations using progressive wear stages. M^1 of neonates and young juveniles had a hypoflexus without any enamel crenulation (**Figure 4. 3**B1-2, C1-2). The first signs of crenulation occurred on the mesial wall of the hypoflexus about 0.75 mm after the disappearance of the crescentic valley (**Figure 4. 3**C4), when the skull reached 50 mm in length. Skull length in *Oryctolagus cuniculus* was found to be correlated not only with the HL/CW ratio (R squared: 0.1405, p-value = 5.17e-12), but also with the number of crenulations on the mesial wall of the hypoflexus (**Supplementary figure 4. 2**, p-value = <2.2e-16), and this was also the case for M^{1s} of *Lepus capensis* (R-square: 0.1324, p-value = 3.39e-4). This indicated that some variations in the shape of M^{1s} were correlated with age in

rabbits and hares. Over the whole sample of *Oryctolagus cuniculus*, the number of crenulations on the M^1 ranged from 0 to 10 on the mesial wall and from 0 to 8 on the distal wall of the hypoflexus (**Supplementary figure 4. 2**A). However, the number of crenulations was always higher on the mesial wall than on the distal wall of the hypoflexus and we never observed crenulations on the distal wall when the mesial wall was not crenulated. M^{1s} of *Oryctolagus cuniculus* did not exhibit distal wall crenulations in 81% of specimens with skull length less than 70 mm. This was also the case for 54% of specimens with skulls between 70 and 80 mm long, and for 14% of specimens with skulls longer than 80 mm. The same results were obtained following a study of *Lepus capensis* M1s, which would tend to prove that the implementation of crenulations would follow similar mechanisms in Leporidae (**Supplementary figure 4. 2**B).

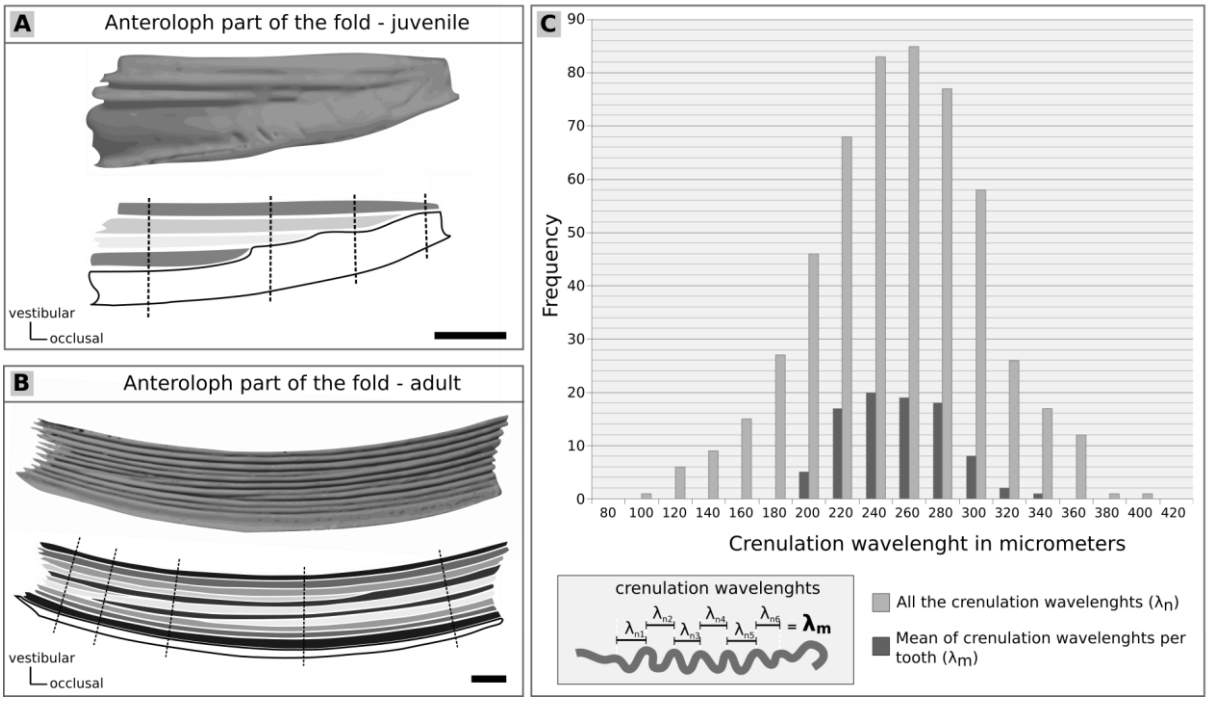

Figure 4. 4. Variation of crenulation pattern in Oryctolagus cuniculus and frequency of the crenulation wavelength in micrometers. *Visualization of the anteroloph part of the hypoflexus from the growth part to the occlusal surface in juvenile (A) and adult O. cuniculus (B). On the top, the 3D surface diagrammed below. Each crenulation is represented by one gray contrast. The black dotted lines indicated the different occlusal crenulation pattern in a same individual. (C) Wavelength is defined by the distance between two maxima of consecutive crenulation (λ_n) and a mean of crenulation wavelength is calculated for each tooth (λ_m). Frequency of crenulation wavelength follows a normal distribution for all the crenulation wavelengths (light grey) and for the mean of crenulation wavelength (dark grey). Scales bar: 1mm.*

We then segmented 3D-reconstructions of *Oryctolagus* M^{1s} in order to observe the hypoflexus mesial wall from inside the anteroloph (**Supplementary figure 4. 1**, **Figure 4. 4**A-B). Therefore, we followed each crenulation longitudinally from its point of appearance until the base of the tooth (**Figure 4. 4**A). The very first crenulation occurred on the vestibular side of the hypoflexus, just next to the folding area. Subsequently, newly formed crenulations progressively appeared on the lingual side of the first crenulation (**Figure 4. 4**A). The formation of new crenulations coincided with a lengthening of the hypoflexus, which doubled in length (HL increased from 0.61 to 1.36 mm) between the appearance of the first and the fourth crenulation (**Supplementary figure 4. 1**, **Figure 4. 4**A). We then studied the fate of crenulations at older ages (**Figure 4. 4**B). Each black dotted line indicated a different crenulation pattern that we determined through a combined study of longitudinal views and successive occlusal views. It therefore emerged that, even at more advanced ontogenetic stages and while the general morphology of the crown underwent very little changes, some crenulations disappeared while new ones appeared. We identified five different crenulation patterns along the illustrated M^1 (**Figure 4. 4**B). In teeth of adult and old specimens, newly formed crenulations no longer appeared on the lingual side of the mesial wall as was the case in teeth of younger individuals, but they arose randomly between two pre-existing crenulations. Thus, both the appearance and disappearance of certain crenulations did not seem to obey a particular rule. In old specimens, the number of crenulations increased together with the variability of the crenulation number between individuals of the same size (**Supplementary figure 4. 2**).

Left-right symmetry of the crenulation pattern

We compared the number and shape of crenulations on right and left M^{1s} of 109 adult specimens to evaluate the left-right symmetry of the crenulation pattern with respect to the sagittal plane. The mesial wall of the hypoflexus was smooth in two specimens (1.8% of the sample) while the distal wall was smooth in 48 specimens (44% of the sample). Regarding

overall symmetry, 21% of the specimens had exactly the same crenulation number on their left and right M^{1s}. A more detailed analysis showed that 33% and 55% of the specimens respectively had a mesial and a distal wall identically crenulated between their left and right M^{1s}. The high percentage of similarities concerning the distal wall is due to the high number of specimens (48 out of 109 specimens) with a smooth enamel band on this wall. Finally, 25% of specimens showed a single difference in the crenulation pattern between left and right M^{1s} and 33% of specimens had two differences. Therefore, the crenulations of the hypoflexus were therefore not strictly symmetrical across the sagittal plane in all specimens, but the number and shape of crenulations of an individual was sufficiently similar between its right and left M^{1s} to allow the identification of a consensual crenulation pattern for an identical wear stage.

Relationships between crenulation number and wavelength

We quantified crenulation wavelengths on occlusal surfaces of 122 M^{1s} belonging to adult *Oryctolagus cuniculus*. The wavelength is defined by the distance between two maximum amplitudes measured on consecutive crenulations. Each crenulation was evaluated independently to calculate the average wavelength on each tooth (**Figure 4. 4**C). Over the entire sample, the molars of 10 specimens showed no crenulation. Over the remainder of the sample, crenulation wavelengths were highly variable, ranging from 100 to 400 µm, with a maximum distribution peak at 260 µm. A Shapiro test was applied to confirm the hypothesis of a normal distribution of crenulation wavelengths. The average crenulation wavelength depended on neither the size of the hypoflexus nor the size of the skull (adjusted R-squared = 0.000 and 0.001, NS). However, the number of crenulations on the mesial wall was correlated with the wavelength average (adjusted R-squared = 0.1597, p-value = 5.647e-05). As a result, crenulation wavelengths were not related to the age of rabbits, but the more the crenulations were abundant the shorter their wavelengths were.

Consequences of irradiation on the crenulation pattern

Like all dental tissues, crenulations form in the tooth growing area that is located beyond the base of each tooth and where dental stem cells proliferate and differentiate. One way to understand how crenulations are formed consists in disrupting their development. In this framework, irradiations are well known for disrupting cell proliferation and enhancing stem cell differentiation (Dare et al., 1997; Mieloch and Suchorska, 2015). Here we benefited from rabbits whose dentary bone was irradiated in order to study the consequences of irradiation on mandibular bone remodeling. In this experiment, the irradiated area of the dentary included the growth zones of lower premolars and molars. We chose to specifically study the P_3 because this tooth is the only lower permanent tooth that has a long reentrant fold with crenulations of surrounding enamel bands. We consider here that developmental mechanisms of crenulations in the P_3 are homologous to those of the M^1 and we will thus be able to widen obtained results with the other permanent crenulated teeth.

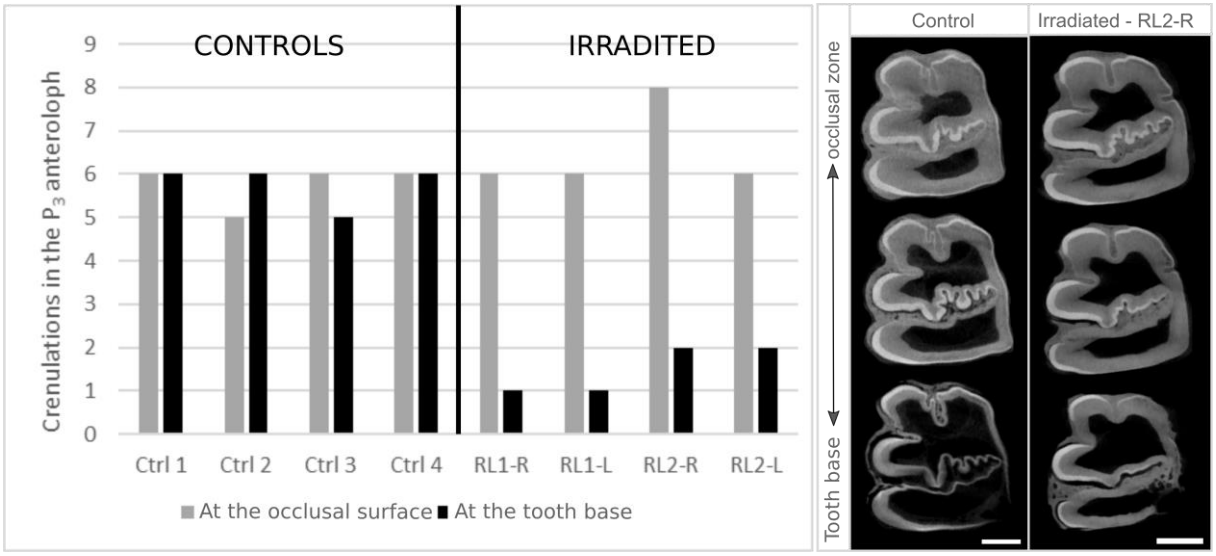

Figure 4. 5. Variation of the number of crenulations between the occlusal and growth zone in controls and irradiated rabbits*. A. In grey the number of crenulation at the occlusal zone, in black at the growth zone. RL sample have been irradiated during 4 weeks, the occlusal surface of these samples was already mineralized before the irradiations. B. Sections from occlusal to growth zone of one single tooth in one control and one irradiated rabbit.*

Rabbit dentaries were irradiated five times over a period of four weeks, allowing the dental crown to grow and mineralize between successive irradiations. We compared the number of crenulations between occlusal surfaces that mineralized before the irradiation experiment and virtual occlusal surfaces corresponding to the growth zone that was irradiated and later mineralized. The number of crenulations between real and virtual occlusal surfaces was relatively stable among control specimens, with a variation of plus or minus one crenulation (**Figure 4. 5**). In contrast, the number of crenulations has decreased significantly, from 66 to 83% depending on the specimens; on P_3 occlusal surfaces whose growth zone was irradiated (**Figure 4. 5**). This implied that the irradiations affected dental cells of the growth zone and resulted in a substantial decrease in the development of crenulations at the base of the tooth

Variations in the crenulation pattern among extant Leporidae

We defined a consensual morphology of the M^1 occlusal surface in adult *Oryctolagus cuniculus*, which included a strongly crenulated mesial wall of the hypoflexus and a relatively less crenulated distal wall. We then collected adult M^1 occlusal morphologies of various extant species of Leporidae by obtaining specimens from museum collections (see list in **Supplementary table 4. 1**) or by repeating illustrations from the literature (Averianov et al., 2000; Major, 1899). We then placed all occlusal morphologies within the most recent phylogeny (Matthee et al., 2004). In this solid framework, we were able to evaluate the diversification of the crenulation pattern during the evolutionary history of Leporidae. We counted the number of crenulations on both sides of the hypoflexus and we evaluated the distribution of the crenulation number using a Krustal-Wallis test. If the result of the test was significant, thus the two walls were not similarly crenulated and inversely if the result was not significant (**Table 4. 1**).

	Mean of crenulations in the		Krustal-wallis		Minimum number of crenulations in		Maximum number of crenulations in		Number
	anteroloph	posteroloph	p-value		anteroloph	posteroloph	anteroloph	posteroloph	of M^1
Brachylagus idehoensis	3.00	0.22	3.046e-02	*	0	0	6	2	9
Bunolagus monticularis	4.00	3.00	1.213e-01	N.S	3	3	5	3	3
Caprolagus hispidus	11.00	10.33	3.458e-01	N.S	10	10	12	11	3
Lepus americanus	4.44	1.78	7.367e-02	N.S	0	0	7	7	9
Lepus californicus	6.89	4.11	6.166e-03	**	0	0	9	7	9
Lepus callotis	7.45	7.27	4.697e-01	N.S	5	6	10	9	12
Lepus capensis	6.09	2.39	3.395e-14	***	1	0	9	8	77
Lepus europaeus	7.58	4.16	8.058e-05	***	1	0	11	8	19
Lepus nigricollis	7.78	7.22	6.223e-01	N.S	5	4	10	10	9
Lepus saxatilis	7.20	4.80	4.230e-02	*	6	1	8	8	10
Lepus starcki	5.93	4.93	3.658e-01	N.S	1	0	11	11	14
Lepus tolai	7.33	3.33	1.789e-02	*	4	2	10	7	6
Lepus townsendi	6.70	4.30	1.989e-03	**	5	3	8	7	10
Lepus victoriae	5.96	2.04	2.452e-10	***	0	0	9	9	50
Nesolagus timminsi	0.00	0.00	N.A	N.A	0	0	0	0	2
Ochotona princeps	0.00	0.00	N.A	N.A	0	0	0	0	4
Oryctolagus cuniculus	5.64	1.21	< 2.2e-16	***	0	0	10	8	292
Poelagus marjorita	6.15	4.55	3.053e-02	*	4	1	10	8	20
Pronolagus rupestris	3.44	0.38	6.115e-05	***	0	0	7	4	16
Romerolagus diazi	3.33	5.11	2.563e-01	N.S	0	4	6	7	9
Sylvilagus audubonii	7.67	5.75	3.685e-02	*	4	2	11	10	14
Sylvilagus brasiliensis	7.11	5.33	5.784e-02	N.S	6	3	9	8	9
Sylvilagus floridanus	6.82	6.09	7.109e-01	N.S	5	0	10	8	11
Sylvilagus nuttallii	7.10	5.00	2.145e-02	*	4	2	10	8	10
Sylvilagus palustris	9.00	7.70	5.746e-02	N.S	7	5	12	12	10

Table 4. 1. Variation of the number of crenulations in function of the species among Lagomorpha.

We labeled six monophyletic groups (**Figure 4. 6**, A to F) within the phylogeny. The Ochotonidae, represented here by *Ochotona princeps* (group A), constituted the most basal lineage of this phylogeny. Ochotonid lagomorphs all had a smooth hypoflexus on their M^{1s}, unlike most leporid lagomorphs (groups B to F). Within each of the groups from B to E, some M^{1s} had a smooth or weakly crenulated hypoflexus (in *Nesolagus*, *Bunolagus*, *Brachylagus*, and *Lepus americanus*) while others had a strongly crenulated hypoflexus (in *Poelagus*, *Caprolagus*, *Sylvilagus*, and *Lepus timidus*). This would indicate that the crenulation of the hypoflexus appeared or regressed several times independently throughout evolution. In more details, the group C presents various crenulation patterns among species (*Oryctolagus cuniculus*, *Caprolagus hispidus*, *Bunolagus monticularis* and *Pentalagus furnessi)*. *Caprolagus* adult specimens are highly crenulated in both the anteroloph and the posteroloph (respectively 11 crenulations in mean in the anteroloph and 10.33 in the posteroloph) whereas *Bunolagus monticularis* has few crenulations homogeneously distributed in the two lophs and *Pentalagus furnessi* has very high amplitude of crenulations compared to the other species

studied. The *Oryctolagus* specimens are mostly crenulated in the anteroloph with a mean of 5.6 crenulations, and less in the posteroloph with 1.2 crenulations in mean, only some of them being crenulated in the posteroloph. *Romerolagus diazi* (group F) is the only species observed that could have more crenulations in the posteroloph than the anteroloph with a mean of 3.33 crenulations in the anteroloph and 5.11 in the posteroloph. The *Lepus* (group E) and *Sylvilagus* (group D) genera are represented by numerous species that are more or less crenulated. Thus, *L. nigricollis*, *L. callotis* and *L. starcki* for the *Lepus* or *S. floridanus* and *S. palustris* for the *Sylvilagus* are similarly crenulated in the anteroloph and posteroloph as *Caprolagus* genus. Other species as *L. victoriae*, *L. capensis* and *L. tolai* or *S. nuttallii* are in mean much more crenulated in the anteroloph than the posteroloph as the *Oryctolagus* genus. However, the intra-specific variability in the crenulation pattern is extremely high. Here, we note only pattern trends that do not allow identifying a species according to its crenulations. Interestingly, the *Nesolagus* genus is the only adult Leporidae with no crenulations (group B). This absence of crenulation is linked with a very short hypoflexus (H/C ratio: 0.35), as previously identified (Koenigswald et al., 2010).

Discussion

Occlusal shape variations

Just erupted M^{1s} in neonate Oryctolagus cuniculus have a cuspidate occlusal surface including a crescentic valley that disappears few weeks after birth associated with an extension of the hypoflexus invagination. We have observed the same transition from a cuspidate to a flattened occlusal surface with disappearance of the crescent valley and extension of the hypoflexus in *Lepus capensis* and we can consider that this process is common at least to all Leporidae. The occlusal pattern tends to become more and more bilophodont with age. In conclusion, the number of crenulations increases with the age and the shape of these

crenulations is correlated with their number. We showed that in *Oryctolagus cuniculus*, the shape of the crenulations is variable at the inter- and intra-individual level. However, the observed intra-individual variability is limited compared to the inter-individual variability. Although the crenulation pattern changes continuously over the life of animals, the size and overall shape of the occlusal surface remain relatively stable in *Oryctolagus cuniculus*, which allows the definition of consensual morphology.

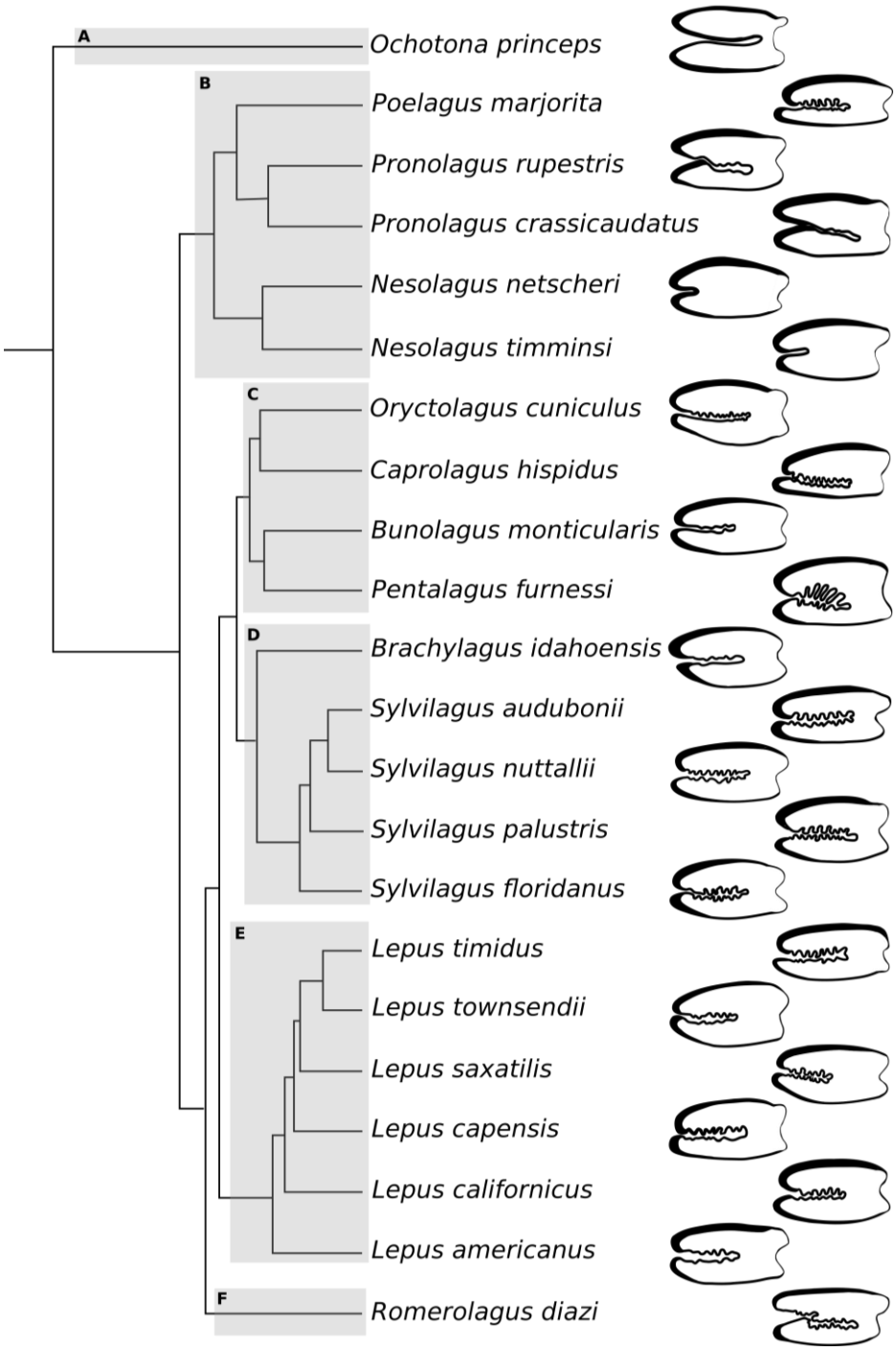

Figure 4. 6. Simplified phylogeny of extant genera and crenulation pattern of the occlusal surface in adult. *Phylogeny adapted from Matthee et al. 2004. Nesolagus netscheri and Pentalagus furnessi adapted from Averianov et al. 2000. Each letter represent one monophyletic group.*

Formation of the crenulations

Among the questions that concern crenulations of the enamel bands bordering the hypoflexus of rabbit teeth, two central issues are how these crenulations are formed and what is their exact function? We found no correlation between diet and crenulation pattern shape. Leporid lagomorphs are not the only mammal group to have crenulated enamel on their cheek tooth crown. Crenulated enamel was reported, for example, on the molars of some Equidae (Forsten, 2002) and some Elephantidae. The crenulation pattern is thus constantly reshaped throughout the life of the animal, which means that the morphogenesis of crenulation varies constantly during odontogenesis. This demonstrates that the continuous growth of a dental crown does not consist of a continuous replication of the same crown shape. The crenulation pattern however is an interesting morphological trait to take into account in taxonomic and evolutionary studies, but it is necessary to use this character with the precautions imposed by the dynamics induced by continuous dental growth. Even if we do not yet understand the function of these crenulations, we now know better their implementation during odontogenesis. The hypoflexus formation begins by an invagination of a monolayer of epithelial cells inside the mesenchyme during tooth morphogenesis, morphologically similar to the sea urchin gastrulation (Davidson et al., 1995) or the ventral furrow invagination in the *Drosophila* (Conte et al., 2008). These epithelial folding and invaginations have been studied to understand their mechanical basis (Odell et al., 1981) and similar mechanisms could play a role in leporid dental morphogenesis. Epithelial folding begins by an apical constriction of the cells that induces the forces driving morphogenesis (Sawyer *et al.* 2010). Some genetic pathways have been identified to regulate this apical constriction by acting on myosin and actin fibers (Sawyer *et al.* 2010). We can hypothesis that similar cell shape changes can take place in the developing

M^1 tooth, inducing epithelial invagination that gives the hypoflexus. Then, in addition to the proliferation in the transit amplifying cells that allows the continuous tooth growth (Tummers and Thesleff, 2003), the hypoflexus may increase in size by cell proliferation in the linguo-vestibular plane in the molar growth zone. This fold then crenulates, and the crenulation pattern can be variable from one individual to another. We can even observe modifications in the crenulation pattern in a single tooth from the occlusal surface to the growing region. The crenulation pattern is highly variable during ontogeny, and these modifications are linked to the continuous growth of the tooth. We can hypothesize that crenulations are the result of mechanical forces induced by differences in the proliferation rates between the epithelium and mesenchyme in the highly invaginated hypoflexus in the molar growing zone. Indeed, as shown for the formation of fingerprint (Kücken and Newell, 2004) and villis (Hannezo et al., 2011), a differential constrained growth on the basal layer of cells can induce compressive stress. If one thin layer has a higher proliferation rate than the layer juxtaposed separated by a basement membrane, it induces modification of shape of the two layers (Ben Amar and Jia, 2013). In the growing zone, the soft tissues containing the thin layers of pre-ameloblasts and pre-odontoblasts separated by the basal lamina may thus crenulate due to compressive stress. Same mechanisms have also been shown in brain convolutional development: with modifications of growth behaviors of the superficial layers, it is possible to predict sinusoidal buckling of the surface (Richman et al., 1975). Thus, we consider that difference of proliferation rate between the epithelial and mesenchymal cells in the growing zone of the tooth may induce hypoflexus invagination and crenulations. If this hypothesis is true, alteration of the epithelial/mesenchymal proliferation rate should greatly affect the crenulation pattern. Irradiations are known to alter the cell proliferation in various proportions depending of the targeted tissue (Dare et al., 1997; Mieloch and Suchorska, 2015). In our experiment, we showed that irradiations induce a high decrease in the number of crenulations. Irradiations at a similar

dose have already been correlated with an inhibition of the cell growth *in vitro* (Dare et al., 1997) and an inhibition of the craniofacial bone growth in rabbits (La Scala et al., 2005). Regarding dental development, Medak *et al.* (1952) studied the effects of irradiation in the ever-growing rat incisors. They show that irradiation induces a decrease in the proliferation rate of the dental mesenchymal cells whereas the epithelial cells continues to grow at a normal rate. In consequence, the irradiated rat incisors have a wavy dentino-enamel junction. We can hypothesize that the irradiations in the ever-growing rabbit teeth similarly affect the cells. By reducing the mesenchymal cell proliferation without affecting the epithelial cells, the irradiations may reduce the difference of proliferation rate between the two cell types and so explain the reduction of the number of crenulations.

Crown heightening

Molar and premolar crown heightening is a common evolutionary pathway among herbivorous mammals and this trend corresponds to a selection of more durable postcanine dentitions in a context of abrasive food intakes (Damuth and Janis, 2011; Janis and Fortelius, 1988). The progressive overgrowth of the crown is counterbalanced by the effects of attrition during the daily feeding process so that the crown occlusal surface rapidly flattens and wears down over the animal's life. Studies conducted in various groups of hypsodont herbivorous mammals showed that the occlusal pattern undergo substantial morphological changes throughout life in African suids (Kullmer 1999), as well as in theridomyid (Schmidt-Kittler, 2002), geomyid (Rensberger, 1975), and cricetid (Viriot *et al.* 1993) rodents. Hypsodonty has been reported to be underlain by heterochronic mechanisms that introduce changes in odontogenetic sequences (Chaline et al., 1999; Koenigswald, 2011; Renvoisé and Michon, 2014). Heterochronies are classically defined as changes in developmental rate and/or timing of an organism in relation to those of its ancestors (Gould, 1977). Resulting morphological

modifications can be substantial over evolution as it has been showed for instance in ammonites (Dommergues et al., 1986), which record ontogeny-related morphological changes all along their mineralized shells (Kennedy, 1989). Hypsodont teeth are mineralized organs with extended to continuous growth, which also record ontogeny-related morphological changes from the tip of the cusps (earliest mineralization stages) until the apex of the roots (latest mineralization stages). However, hypsodont teeth differ from ammonite shells in the sense that wear involve progressive destruction of early stages while later stages mineralize. The ever-growing teeth in rabbits can be useful to detect developmental changes during ontogeny and these results can be compared with the evolutionary history of the Lagomorpha.

Evolutionary developmental biology

Developmental modifications observed during odontogenesis are to be linked with the evolutionary history of the upper molars among Lagomorpha (**Figure 4. 7**). *Dawsonolagus*, a stem Lagomorpha discovered in the late early Eocene deposits of China (Li et al., 2007), had hypsodont yet rooted upper molars that display a cuspidate crown and no hypoflexus (Kraatz et al., 2010). Eocene times mark the split of Lagomorpha into two families, namely the Ochotonidae and the Leporidae. In Ochotonidae, a hypoflexus is present at the end of the Eocene in *Desmatolagus* (Kraatz *et al.* 2010). This fold is never crenulated in Ochotonid (fossil or extant).

Figure 4. 7. Chronology of morphological variations of the M^1 during lagomorph evolution and Oryctolagus cuniculus development. *(A) Occlusal surface of different leporid fossils from Paleocene to Pleistocene adapted from the literature. Tooth drawings and time scales are adapted from Angelone and Rook 2011, Averianov and Tesakov 1997, Čermák 2016, Čermák and Wagner 2013, Erbajeva and Zheng 2005, Erbajeva et al. 2017, Fostowicz-Frelik 2003, Fostowicz-Frelik and Tabrum 2009, Jin et al. 2010, Koenigswald et al. 2010, Kraatz et al. 2010, Li et al. 2007, Lopatin and Averianov 2006, Lopez-Martinez 2008, Sych 1975, White 1991. (B) Oryctolagus cuniculus development from newborn to adult.*

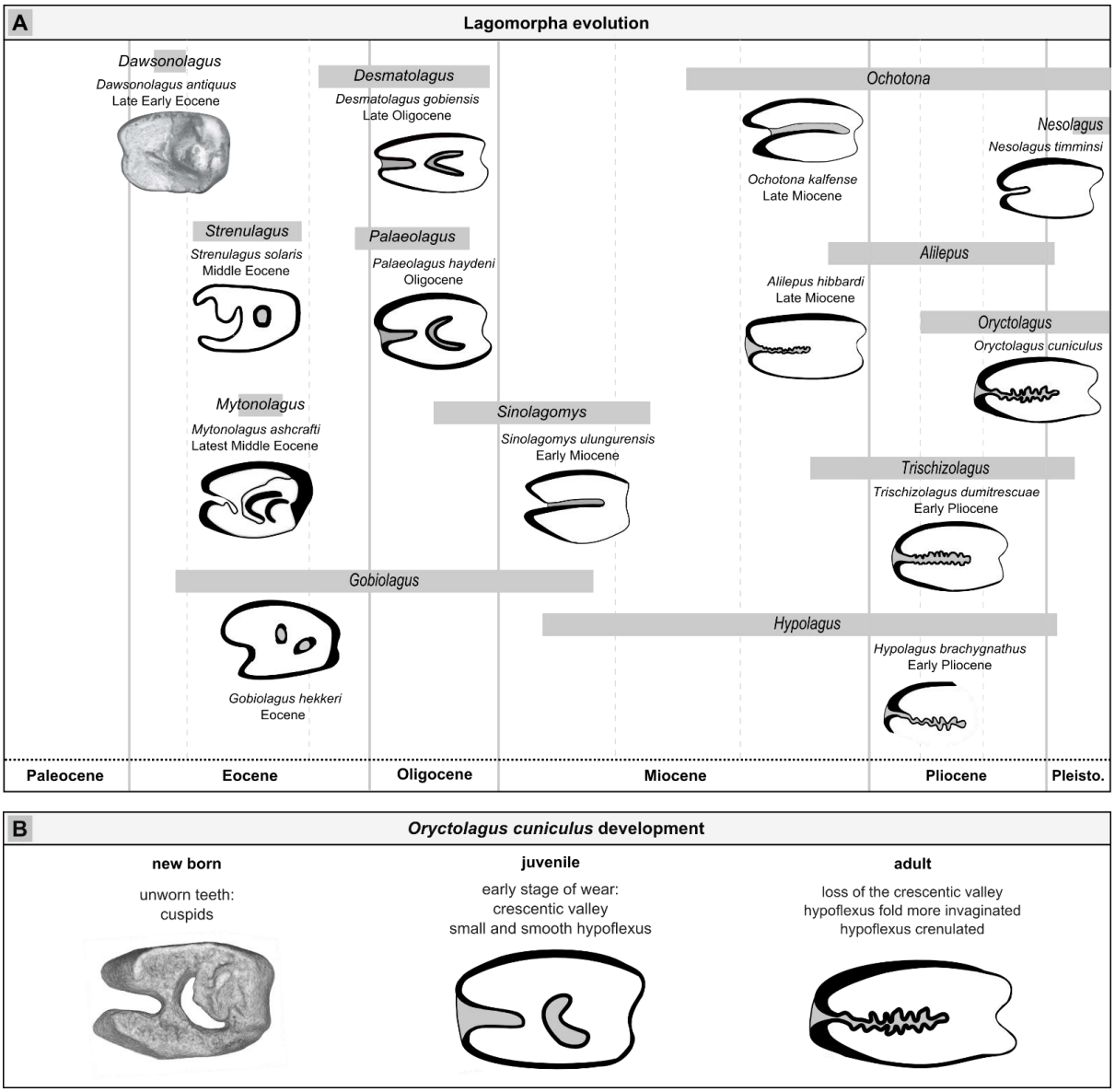

In Leporids from latest middle Eocene, as *Mytonolagus ashcrafti*, Fostowicz-Frelik and Tabrum (2009) illustrate a crescentic valley and a hypoflexus moderately invaginated. The M^1 still has two thin buccal roots and they observed disappearance of the small hypoflexus in moderately worn M^1 and then of the crescentic valley in heavy worn M^1 (Fostowicz-Frelik and Tabrum, 2009). Fostowicz-Frelik (2013) presents ontogenetic development of the upper dentition in *Chadrolagus emryi* from the Late Eocene. He shows that at light wear stage the M^1 have a crescentic valley and a small hypoflexus, the crescentic valley disappears in moderate wear stages and the hypoflexus is absent in the heavily worn stage. Later, in the Oligocene, the

Palaeolagus hemirhizis has a crescentic valley that is already highly reduced in intermediate stage of wear, as observed in the studied *P. haydeni* specimens. The hypoflexus is maintained for a longer time and disappears in late stage of wear, this fold is still completely smooth (Korth and Hageman, 1988). Dawson (1958) describes the tooth morphology of *Litolagus molidens* from Middle Oligocene as more advanced than *Palaeolagus*, the crescentic valley is lost earlier and the hypoflexus is longer. The oldest crenulations in a hypoflexus in fossil Leporidae are observed in the upper molars of the two genera present in the mid-Miocene, *Hypolagus* and *Trischizolagus* that are already crenulated in the two lophs of the hypoflexus (Averianov and Tesakov, 1997; Koenigswald et al., 2010). At the end of the Miocene, the Leporidae are represented by the genera *Alilepus*, and especially *Alilepus hibbardi*, a suggested ancestor of the extant genera of leporids (Jin et al., 2010). *Alilepus* upper molariforms are crenulated in the anteroloph and posteroloph in the majority of species described (Angelone and Rook, 2011). So, crenulations are a character present in the leporid ancestor and the lack of crenulations in *Nesolagus* seems to indicate a secondary loss during evolution. The fossil record of lagomorphs documents a significant increase of cheek teeth crown height (hypsodonty) over evolution. Most basal lagomorphs from Early Eocene had cheek teeth with moderate hypsodonty and a cuspidate occlusal surface. In Ochotonidae evolutionary history, the hypoflexus is more and more invaginated but never crenulated. Most of the more recent species have highly hypsodont cheek teeth with two lophs partly separated by a hypoflexus. Leporidae from the Eocene have higher cheek teeth and most of them present a crescentic valley on their occlusal surface. We thus note a progressive reduction of the crescentic valley to the advantage of an occlusal surface composed of two lophs separated by a fold. The reduction of the crescentic valley seems correlated with the invagination of the hypoflexus and the first proof of crenulations of the hypoflexus appears in leporids from the mid-Miocene. These crenulations are maintained in the majority of the adult extant leporids, and their appearance during tooth development follows

their evolutionary history by the presence of a crescentic valley in the youngest specimens that disappear during ontogeny (**Figure 4. 7**). We thus hypothesize that peramorphic processes might have been involved in the evolution of tooth crown shape in lagomorphs, characterized by a retention of ancestral characters at the very beginning of tooth crown ontogeny (crescentic valley) as well as by the occurrence of novel characters at the end of the crown ontogeny that become increasingly present through evolution (crenulations).

Acknowledgements

We acknowledge the contribution of SFR Biosciences (UMS3444/CNRS, US8/Inserm, ENS de Lyon, UCBL) and the staff of AniRa-ImmOs facilities, especially Mathilde Bouchet, for her help. We thank members of the Evolution of Vertebrate Dentition team and Arezki Boudaoud for fruitful discussions about this work. We acknowledge all the people that allow us to study the Lagomorpha specimens, especially Eileen Westwig (AMNH), Cécile Callou (MNHN), François Vigouroux (Musée des Confluences) and Emmanuel Robert (Geological Collections, UMR CNRS 5276 - CERESE, University Lyon 1 - CNRS - ENS Lyon, University of Lyon) form the museum collections. The irradiation experiments have been funded by Eusapharma, CoE LabTAU (FUSF) and the "Gueules cassées" foundation.

Author contributions

L.B.B: contributed to design, to acquisition, analysis, and interpretation, drafted manuscript. L.V: contributed to conception, to analysis and interpretation, critically revised manuscript. A.D: contributed to acquisition. A.G.C.B: contributed to design. T.J: contributed to interpretation. C.C: contributed to conception and design, to analysis and interpretation, critically revised manuscript

References

Angelone, C., and L. Rook. 2011. Alilepus meini nov. sp. (Leporidae, Lagomorpha) du Messinien inférieur de Toscane (Italie centro-occidentale). Geobios 44:151–156. Elsevier Masson SAS.

Angelone, C., J. A. Schultz, and M. A. Erbajeva. 2014. Determining the ontogenetic variation of lower cheek teeth occlusal surface patterns in lagomorphs using micro-ct technology. Palaeontol. Electron. 17:1–13.

Asher, R. J., J. Meng, J. R. Wible, M. C. McKenna, G. W. Rougier, D. Dashzeveg, and M. J. Novacek. 2005. Stem Lagomorpha and the antiquity of Glires. Science 307:1091–4.

Averianov, A. O., A. V. Abramov, and A. N. Tikhonov. 2000. A new species of. Nesolagus (Lagomorpha, Leporidae) from Vietnam with osteological description. Contrib. from Zool. Inst. 3.

Averianov, A. O., and A. S. Tesakov. 1997. Evolutionary trends in Mio-Pliocene Leporinae, based on Trischizolagus (Mammalia, Lagomorpha). Palaeontol. Zeitschrift 71:145–153. Springer-Verlag.

Ben Amar, M., and F. Jia. 2013. Anisotropic growth shapes intestinal tissues during embryogenesis. Proc. Natl. Acad. Sci. U. S. A. 110:10525–30. National Academy of Sciences.

Bertin, T. J. C., B. Thivichon-Prince, A. R. H. LeBlanc, M. W. Caldwell, and L. Viriot. 2018. Current Perspectives on Tooth Implantation, Attachment, and Replacement in Amniota. Front. Physiol. 9:1630. Frontiers.

Bosze, Z., and L. M. Houdebine. 2006. Application of rabbits in biomedical research: a review. World Rabbit Sci. 14:01-14.

Carneiro, M., C. J. Rubin, F. Di Palma, F. W. Albert, J. Alföldi, A. M. Barrio, G. Pielberg, N. Rafati, S. Sayyab, J. Turner-Maier, S. Younis, S. Afonso, B. Aken, J. M. Alves, D. Barrell, G. Bolet, S. Boucher, H. A. Burbano, R. Campos, J. L. Chang, V. Duranthon, L. Fontanesi, H. Garreau, D. Heiman, J. Johnson, R. G. Mage, Z. Peng, G. Queney, C. Rogel-Gaillard, M. Ruffier, S. Searle, R. Villafuerte, A. Xiong, S. Young, K. Forsberg-Nilsson, J. M. Good, E. S. Lander, N. Ferrand, K. Lindblad-Toh, and L. Andersson. 2014. Rabbit genome analysis reveals a polygenic basis for phenotypic change during domestication. Science (80-.). 345:1074–1079.

Čermák, S., C. Angelone, and M. V Sinitsa. 2015. New late miocene alilepus (Lagomorpha, Mammalia) from Eastern Europe - a new light on the evolution of the earliest old world leporinae. Bull. Geosci. 90:431–451. Czech Geological Survey.

Čermák, S. 2016. The Late Miocene species Ochotona kalfense (Mammalia, Lagomorpha) of Moldova: The oldest European record of the genus in the context of the earliest Ochotoninae. Comptes Rendus Palevol 15:927–940.

Čermák, S. and J. Wagner. 2013. The Pliocene record of Trischizolagus and Pliopentalagus (Leporidae, Lagomorpha, Mammalia) in Central Europe with comments on taxonomy and evolutionary history of Leporinae. Neues Jahrbuch fur Geologie und Paläontologie Abhandlungen 268, 97-111

Chaline, J., P. Brunet-Lecomte, S. Montuire, L. Viriot, and F. Courant. 1999. Anatomy of the arvicoline radiation (Rodentia): palaeogeographical, palaeoecological history and evolutionary data. Finnish Zoological and Botanical Publishing Board.

Chuan-Kuei, L., R. W. Wilson, M. R. Dawson, and L. Krishtalka. 1987. The Origin of Rodents and Lagomorphs. Pp. 97–108 in Current Mammalogy. Springer US, Boston, MA.

Conte, V., J. J. Muñoz, and M. Miodownik. 2008. A 3D finite element model of ventral furrow invagination in the Drosophila melanogaster embryo. J. Mech. Behav. Biomed. Mater. 1:188–198. Elsevier.

Damuth, J., and C. M. Janis. 2011. On the relationship between hypsodonty and feeding ecology in ungulate mammals, and its utility in palaeoecology. Biol. Rev. 86:733–758. Blackwell Publishing Ltd.

Dare, A., R. Hachisu, A. Yamaguchi, S. Yokose, S. Yoshiki, and T. Okano. 1997. Effects of Ionizing Radiation on Proliferation and Differentiation of Osteoblast-like Cells. J. Dent. Res. 76:658–664.

Davidson, L. A., M. A. Koehl, R. Keller, and G. F. Oster. 1995. How do sea urchins invaginate? Using biomechanics to distinguish between mechanisms of primary invagination. Development 121:2005–18.

Dawson, M. R. 1958. Later Tertiary Leporidae of North America. Univ. Kansas Paleontol. Contrib. Vertebrata:1–75.

Dommergues, J.-L., B. David, and D. Marchand. 1986. Les relations ontogenèse-phylogenèse:Applications paléontologiques. Geobios 19:335–356. Elsevier Masson.

Erbajeva, M., B. Baatarjav, G. Daxner-Höck, and L. J. Flynn. 2017. Occurrences of Sinolagomys (Lagomorpha) from the Valley of Lakes (Mongolia). Palaeobiodiversity and palaeoenvironments 97:11–24. Springer.

Erbajeva, M. A., and S. Zheng. 2005. New data on Late Miocene – Pleistocene ochotonids (Ochotonidae, Lagomorpha) from North China. Acta Zool. Cracoviensia 48:93–117.

Forsten, A. 2002. Latest Hipparion Christol, 1832 in Europe. A review of the Pliocene Hipparion crassum Gervais group and other finds (Mammalia, Equidae).

Fostowicz-Frelik, L. 2003. Species distribution and differentiation of Eurasian Hypolagus (Lagomorpha: Leporidae). Deinsea 10:197–211.

Fostowicz-Frelik, Ł. 2013. Reassessment of Chadrolagus and Litolagus (Lagomorpha) and a New Genus of North American Eocene Lagomorph from Wyoming. Am. Museum Novit. 3773:1–76.

Fostowicz-Frelik, Ł., and A. R. Tabrum. 2009. Leporids (Mammalia, Lagomorpha) from the Diamond O Ranch Local Fauna, Latest Middle Eocene of Southwestern Montana. Ann. Carnegie Museum 78:253–271.

Gould, S. J. 1977. Ontogeny and phylogeny. Belknap Press of Harvard University Press.

Hannezo, E., J. Prost, and J. F. Joanny. 2011. Instabilities of monolayered epithelia: Shape and structure of villi and crypts. Phys. Rev. Lett. 107:078104. American Physical Society.

Hibbard, C. W. 1963. The origin of the P3 pattern of Sylvilagus, Caprolagus, Oryctolagus and Lepus. J. Mammal. 14:1–15.

Hoffmann, R. S., and A. Smith. 2005. Order Lagomorpha. Wilson, D.E. Reeder, D.M. Mammal Species World, Third Ed. 185–211.

Huchon, D., O. Madsen, M. J. J. B. Sibbald, K. Ament, M. J. Stanhope, F. Catzeflis, W. W. de Jong, and E. J. P. Douzery. 2002. Rodent Phylogeny and a Timescale for the Evolution of Glires: Evidence\rfrom an Extensive Taxon Sampling Using Three Nuclear Genes. Mol Biol Evol 19:1053–1065.

Janis, C. M., and M. Fortelius. 1988. On the means whereby mammals achieve increased functional durability of their dentitions, with special reference to limiting factors. Biol. Rev. 63:197–230. Blackwell Publishing Ltd.

Jin, C. Z., Y. Tomida, Y. Wang, and Y. Q. Zhang. 2010. First discovery of fossil Nesolagus (Leporidae, Lagomorpha) from Southeast Asia. Sci. China Earth Sci. 53:1134–1140. SP Science China Press.

Kennedy, W. J. 1989. Thoughts on the evolution and extinction of Cretaceous ammonites. Proc. Geol. Assoc. 100:251–279. Elsevier.

Koenigswald, W. Von. 2011. Diversity of hypsodont teeth in mammalian dentitions – construction and classification. Palaeontographica 294:63–94. Schweizerbart'sche Verlagsbuchhandlung.

Koenigswald, W. von, U. Anders, S. Engels, J. A. Schultz, and I. Ruf. 2010. Tooth Morphology in Fossil and Extant Lagomorpha (Mammalia) Reflects Different Mastication Patterns. J. Mamm. Evol. 17:275–299.

Korth, W. W., and J. Hageman. 1988. Lagomorphs (Mammalia) from the Oligocene (Orellan and Whitneyan) Brule Formation, Nebraska. Trans. Nebraska Acad. Sci. Affil. Soc. Pap. Trans. Nebraska Acad. Sci. 182:141–152.

Kraatz, B. P., J. Meng, M. Weksler, and C. Li. 2010. Evolutionary patterns in the dentition of duplicidentata (Mammalia) and a novel trend in the molarization of premolars. PLoS One 5:1–15. Public Library of Science.

Kriegs, J. O., G. Churakov, J. Jurka, J. Brosius, and J. Schmitz. 2007. Evolutionary history of 7SL RNA-derived SINEs in Supraprimates.

Kücken, M., and A. C. Newell. 2004. A model for fingerprint formation. Europhys. Lett. 68:141–146. IOP Publishing.

Kullmer, O. 1999. Evolution of African Plio-Pleistocene suids (Artiodactyla: Suidae) based on tooth pattern analysis. Kaupia Darmstädter Beiträg zur Naturgeschichte, 9, 1-34.

La Scala, G. C., D. A. O'Donovan, I. Yeung, J. Darko, P. D. Addison, P. C. Neligan, C. Y. Pang, and C. R. Forrest. 2005. Radiation-Induced Craniofacial Bone Growth Inhibition: Efficacy of Cytoprotection following a Fractionated Dose Regimen. Plast. Reconstr. Surg. 115:1973–1985.

Li, C.-K., Y.-Q. Wang, Z.-Q. Zhang, F.-Y. Mao, and J. Meng. 2016. A new mimotonidan Mina hui (Mammalia, Glires) from the Middle Paleocene of Qianshan, Anhui, China. Vertebr. Palasiat. 54:121–136.

Li, C., J. Meng, and Y. Wang. 2007. Dawsonolagus antiquus, A Primitive Lagomorph from the Eocene Arshanto Formation, Nei Mongol, China. Bull. Carnegie Museum Nat. Hist. 39:97–110.

Lopatin, A. V., and A. O. Averianov. 2006. Eocene Lagomorpha (Mammalia) of Asia: 2. Strenulagus and Gobiolagus (Strenulagidae). Paleontol. J. 40:198–206.

Lopez-Martinez, N. 2008. The lagomorph fossil record and the origin of the European rabbit. Lagomorph biology, 27-46.

Madden, R. H. 2015. Hypsodonty in Mammals: Evolution, Geomorphology and the Role of Earth Surface Processes. Cambridge University Press, Cambridge

Major, C. I. F. 1899. IX. On Fossil and Recent Lagomorpha. . Transactions of the Linnean Society of London, 7(9), 433-520.

Matthee, C. A., B. J. van Vuuren, D. Bell, and T. J. Robinson. 2004. A molecular supermatrix of the rabbits and hares (Leporidae) allows for the identification of five intercontinental exchanges during the Miocene. Syst. Biol. 53:433–447.

Medak, H., M. Weinreb, H. Sicher, J. P. Weinmann, and I. Schour. 1952. The Effect of Single Doses of Irradiation Upon the Tissues of the Upper Rat Incisor. J. Dent. Res. 31:559–574.

Meng, J. 2004. Chapter 7: Phylogeny and Divergence of Basal Glires. Bull. Am. Museum Nat. Hist. 285:93–109. American Museum of Natural History. 285:93–109.

Mieloch, A. A., and W. M. Suchorska. 2015. The concept of radiation-enhanced stem cell differentiation. Radiol Oncol 49:209–216.

Müller, J., M. Clauss, D. Codron, E. Schulz, J. Hummel, M. Fortelius, P. Kircher, and J.-M. Hatt. 2014. Growth and wear of incisor and cheek teeth in domestic rabbits (Oryctolagus cuniculus) fed diets of different abrasiveness. J. Exp. Zool. Part A Ecol. Genet. Physiol. 321:283–298. John Wiley & Sons, Ltd.

Nowak, R. M. 1999. Walker's mammals of the world. Johns Hopkins University Press.

O'Leary, M. A., J. I. Bloch, J. J. Flynn, T. J. Gaudin, A. Giallombardo, N. P. Giannini, S. L. Goldberg, B. P. Kraatz, Z.-X. Luo, J. Meng, X. Ni, M. J. Novacek, F. A. Perini, Z. S. Randall, G. W. Rougier, E. J. Sargis, M. T. Silcox, N. B. Simmons, M. Spaulding, P. M. Velazco, M. Weksler, J. R. Wible, and A. L. Cirranello. 2013. The Placental Mammal Ancestor and the Post-K-Pg Radiation of Placentals. Science (80-.). 339:662–667.

Odell, G. M., G. Oster, P. Alberch, and B. Burnside. 1981. The mechanical basis of morphogenesis: I. Epithelial folding and invagination. Dev. Biol. 85:446–462.

Osborn, H. F. 1907. Evolution of Mammalian Molar Teeth: To and from the Triangular Type Including Collected and Revised Researches Trituberculy and New Sections on the

Forms and Homologies of the Molar Teeth in the Different Orders of Mammals. Macmillan.

Reig, O. A. 1977. A proposed unified nomenclature for the enamelled components of the molar teeth of the Cricetidae (Rodentia). J. Zool. 181:227–241.

Rensberger, J. M. 1975. Function in the Cheek Tooth Evolution of Some Hypsodont Geomyoid Rodents. J. Paleontol. 49:10–22. SEPM Society for Sedimentary Geology.

Renvoisé, E., and F. Michon. 2014. An Evo-Devo perspective on ever-growing teeth in mammals and dental stem cell maintenance. Front. Physiol. 5:1–12.

Richman, D. P., R. M. Stewart, J. W. Hutchinson, and V. S. Caviness. 1975. Mechanical model of brain convolutional development. Science 189:18–21.

Rose, K. D. 2006. The beginning of the age of mammals. Johns Hopkins University Press.

Sawyer, J. M., Harrell, J. R., Shemer, G., Sullivan-Brown, J., Roh-Johnson, M., & Goldstein, B. 2010. Apical constriction: a cell shape change that can drive morphogenesis. Developmental biology, 341(1), 5-19.

Schmidt-Kittler, N. 2002. Feeding specializations in rodents. Senckenbergiana lethaea 82:141–152. Springer-Verlag.

Sych, L. 1975. Lagomorpha from the Oligocene of Mongolia. Palaeontogica Polonica, 33, 183-200.

Tummers, M., and I. Thesleff. 2003. Root or crown: a developmental choice orchestrated by the differential regulation of the epithelial stem cell niche in the tooth of two rodent species. Development 130:1049–1057.

Viriot, L. 1996. The use of serial sections to estimate age-related occlusal variability in arvicolid molars. Acta Zoologica Cracoviensia, 39(1).

Viriot, L., Chaline, J., Schaaf, A., & Le Boulengé, E. 1993. Ontogenetic change of Ondatra zibethicus (Arvicolidae, Rodentia) cheek teeth analyzed by digital image processing. Morphological change in Quaternary mammals of North America, 373-391.

Wang, Y.-Q., C.-K. Li, Q. Li, and D.-S. Li. 2016. A synopsis of Paleocene stratigraphy and vertebrate paleontology in the Qianshan Basin , Anhui , China. 54.

Wang, Y., J. Meng, N. Xijun, and L. Chuankui. 2007. Major events of Paleogene mammal radiation in China. Geol. J. 42:415–430. John Wiley & Sons, Ltd.

White, J. A. 1991. North American Leporinae (Mammalia: Lagomorpha) from late Miocene (Clarendonian) to latest Pliocene (Blancan). Journal of Vertebrate Paleontology, 11(1), 67-89.

Wood, A. E. 1940. The Mammalian Fauna of the White River Oligocene: Part III. Lagomorpha**.** Trans. Am. Philos. Soc. 28:271.

Supplementary files

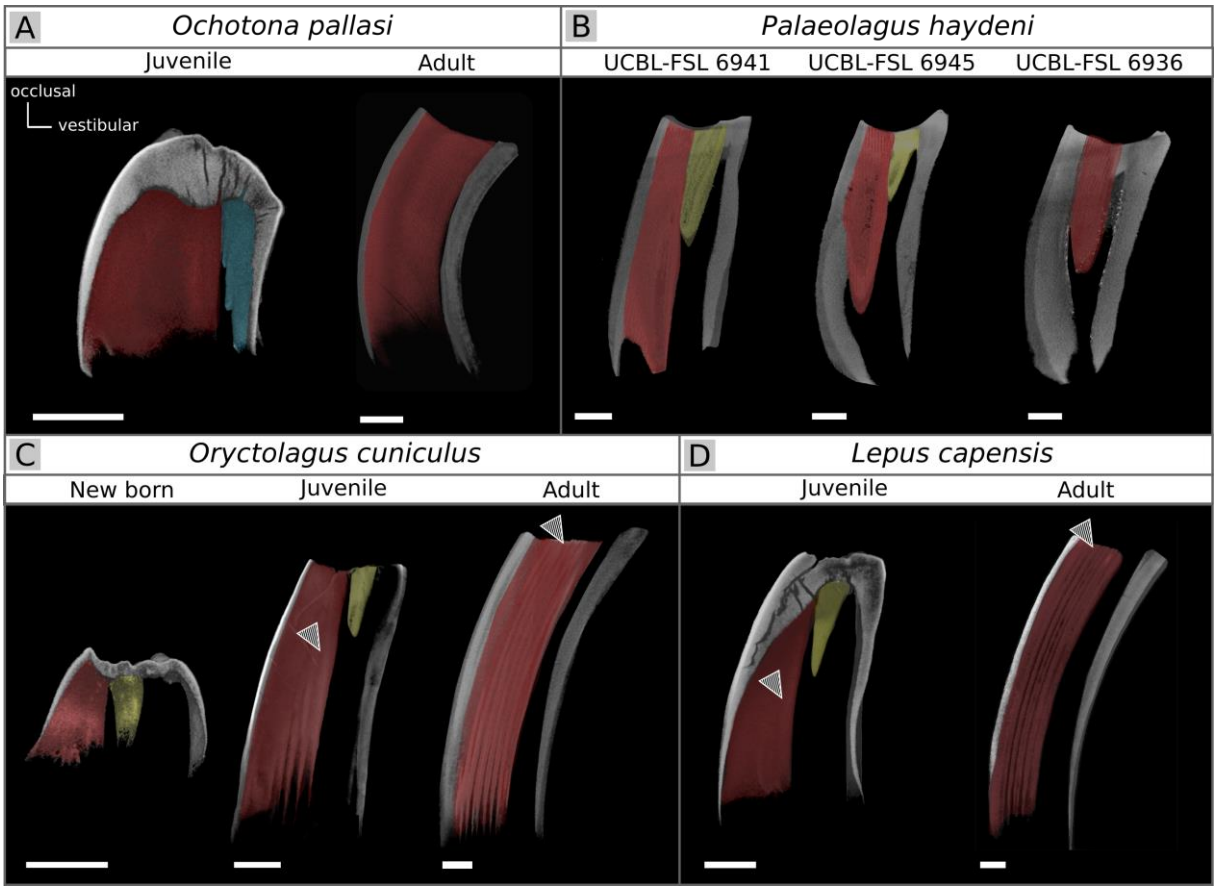

Supplementary figure 4. 1. Variation of the M^1 from the occlusal to the growth part in Ochotona pallasi, Palaeolagus haydeni, Oryctolagus cuniculus and Lepus capensis. *Section of the M^1 to visualize internal structures of the tooth. In red, the re-entrant fold named hypoflexus. In blue, the metaflexus present in the juvenile ochotonids. In yellow, the crescentic valley present only in the juvenile leporids. The black and white arrow shows crenulations. Scales bar: 1mm*

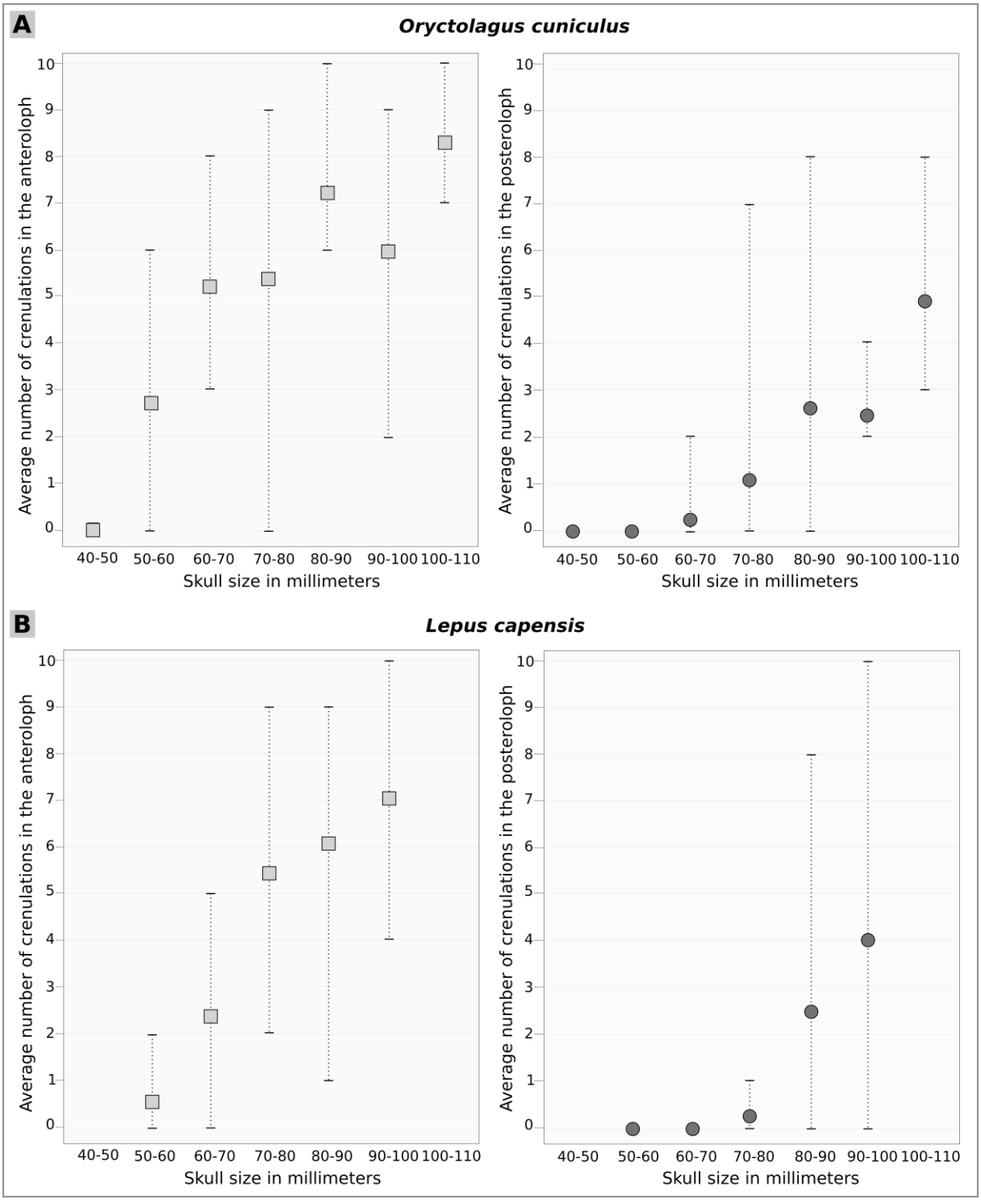

Supplementary figure 4. 2. Variations of the crenulation number in function of the skull size in Oryctolagus cuniculus and Lepus capensis. *Distribution of the average number of crenulations in the anteroloph and posteroloph in function of the size of the skull in Oryctolagus cuniculus (A) and Lepus capensis (B). Squares and circles are the average and horizontal black lines show minimum and maximum number of crenulations for each skull size categories.*

		Skulls from museums				M^1
Species	**M^1**	AMNH	MNHN	UCBL-FSL	Confluences	**X-ray**
Brachylagus idehoensis	14	6	1			2
Bunolagus monticularis	3	2				
Caprolagus hispidus	2 + 1 (Major, 1899)	1				
Lepus americanus	12	2	5			4
Lepus arcticus	2		1			
Lepus californicus	13	5	4			
Lepus callotis	12	5	2			
Lepus capensis	105		66		1	14
Lepus europaeus	36		21			2
Lepus granatensis	2		1			
Lepus insularis	2		1			
Lepus mandshuricus	1		1			
Lepus nigricollis	12	2	6			
Lepus peguensis	2		1			
Lepus saxatilis megalotis	10	5				
Lepus sinensis	2		1			
Lepus starcki	16		11			
Lepus timidus	7		4		1	4
Lepus tolai	9		6			
Lepus townsendi	10	6				
Lepus victoriae	73		44			
Lepus yarkandensis	2		1			
Nesolagus timminsi	2	1				
Ochotona pallasi	4	2				4
Ochotona principes	5	2	1			5
Oryctolagus cuniculus	386		230		10	30
Palaeolagus haydeni †	3			3		3
Poelagus marjorita	29	20				
Pronolagus crassicaudatus	1	1				
Pronolagus rupestris	16	8				
Romerolagus diazi	13	5	1			
Sylvilagus audubonii	12	5	1			
Sylvilagus bachmani	4		2			
Sylvilagus brasiliensis	17	4	5			
Sylvilagus floridanus	16		9			4
Sylvilagus nuttallii	10	5				
Sylvilagus palustris	11	6				
Nesolagus netscheri	1 (Averianov, 2000)					
Pentalagus furnessi	1 (Averianov, 2000)					
	877 M^1	93 skulls	426 skulls	3 maxillary	12 skulls	72 M^1

Supplementary table 4. 1. List of the species studied. *In black, M^1 studied from museum specimens; in red, M^1 studied from the bibliography. Four controls and four irradiated mandibles have been added to these upper molars.*

GENERAL CONCLUSION & PERSPECTIVES

In this PhD work, I addressed some aspects of the morphological and molecular mechanisms underlying dental development, replacement and evolution in Lagomorpha, and especially in *Oryctolagus cuniculus*. The primary goal of this thesis was to characterize the morphological and molecular dynamics underlying the tooth development and replacement in mammals using a new animal model in the dental development field, the rabbit. Then, we placed these results in a broad evolutionary context via the study of intra- and inter- specific variations within Lagomorpha.

Morphological features of tooth development in *Oryctolagus cuniculus*

Before focusing on dental replacement molecular mechanisms, it was crucial to understand the initial development of the deciduous dentition. It has been performed by studying early dental development in rabbit embryos. We followed dental development histo-morphologically at different embryonic stages, from the initiation of the deciduous dental placode to the mineralization of the replacement teeth. We characterized the implementation of all the rabbit teeth. Using 3D-reconstructions of the epithelial dental tissues, we expected to clearly understand the relationship between the vestigial and the ever-growing incisors during development. However, this point already discussed in previous studies (Hirschfeld et al., 1973; Ooë, 1980) is still problematic. In two days of development, a quick transition from the bud stage to an already mineralized vestigial tooth is observed. More data on the precise dynamics of the incisor development between 16 and 18 dpf are still needed to fully understand the nature of the so-called dI^2. A supplementary study of the concerned structures during the transition from bud to separated teeth is necessary to conclude on the links between these incisors. 3D-reconstructions from the placode stage head to the conclusion that the canine and first premolars dP^1 and dP_{1-2} are never detected in rabbit embryos. These results suggest a complete loss of

these teeth on contrary to vestigial tooth rudiments in mice that could be homologous to the dP_3 and dP_4, detected in early tooth development (Sadier et al., 2019; Viriot et al., 2002).

Dentin holes in the upper ever-growing incisor

By studying the rabbit tooth development, we also find one specificity of the rabbit incisor: the presence of holes, opening the pulp cavity at birth. These holes are quickly repaired by apposition of dentin from the pre-existing odontoblasts, without involving reparative dentin mechanisms. However, the causes of hole formations are still unknown. These tooth defects have been observed in all our samples, indicating a common phenomenon. We did not find in literature any description of systematic presence of tooth defects at one specific age in rabbits or other species. In this study, we worked on common rabbit breeding regularly crossed with wild rabbits to ensure genetic mixing, limiting the possibility that these dental abnormalities are specific to one genetic selection in a closed breeding. It could be interesting to identify which mechanical forces at birth are responsible for tooth fractures without morphologically affecting the other tissues. These causes could be purely mechanical (development of the bones or the other upper incisors) or molecularly facilitated (involvement of signaling pathways involved in root resorption for example).

Genetic basis involved in rabbit tooth replacement

One of the major points of this thesis is a better understanding of the genetic basis of the mammalian tooth replacement. We identified that the canonical Wnt pathway is expressed throughout the dental replacement in the rabbit, suggesting that this signaling pathway plays a major role in this process. Wnt signaling pathway has already been suggested as a key regulator of tooth replacement in mutant mice and polyphyodont species (Handrigan and Richman,

2010a; Jarvinen et al., 2006; Popa et al., 2019). The only way to properly understand the role of this pathway in diphyodont species would be to perform functional studies of the canonical Wnt pathway and regulators. In culture, the Wnt/ β-catenin signaling could be enhanced using GSK3 inhibitor in order to better understand its function as already used in snakes teeth (Gaete and Tucker, 2013). From fresh samples, dental organs could be cultured and modifications of specific signaling pathways identified in our study could be done to better understand the mammalian tooth replacement.

Rudimentary successional dental lamina in the molars

Molars are considered as deciduous teeth that are never replaced (Luckett, 1993). However, we observed a budding of the dental lamina at the lingual part of the first molars as observed in many monophyodont species. It should be interesting to genetically compare this budding with the replacement dental lamina of the premolars and follow how it disappears in molars. Popa et al. (2019) showed in mouse that by stabilizing the β-catenin signaling in the epithelium of the rudimentary successional dental lamina, they were able to give an odontogenic capacity to this structure. In rabbit, on contrary to the mouse, $Lef1^{+}$ cells are already localized in the RSDL of the molar. It could be interesting to identify which signals are involved in the inhibition of the molar tooth replacement and if they vary between monophyodont and diphyodont species.

Transcriptomic study of the tooth replacement

In this thesis, we identify candidate genes possibly involved in tooth replacement by studying the bibliography and following the expression pattern at various stages. The most efficient but more expensive way to identify various genes involved would be a transcriptomic study. Indeed, a transcriptomic study could answer different questions:

(1) What are the molecular differences between the lingual and vestibular parts of the dental lamina inducing lingual initiation of the tooth replacement?

(2) What are the molecular differences between the deciduous and the permanent premolars involved in the end of the tooth replacement process in mammals?

(3) What are the molecular differences between the replacement dental lamina and the rudimentary successional dental lamina?

Using 3D-reconstructions, we showed that rabbit embryos at 20 days post fertilization could be a good time point for transcriptomic analyses: the dP^2 do not show morphological sign of tooth replacement, the replacement dental lamina begins to bud from the dental lamina of the dP^3 and is already present in the dP^4. We studied 3D-reconstructions of 12 embryos at 20 dpf from two litters, each of them were exactly at the same dental development stages. Absence of developmental variations between litters facilitates the use of the rabbit as model. However, transcriptomic study to identify signaling involved in tooth replacement needs to be attentive to several factors. First, the ratios between mesenchyme and epithelium cells need to be the same in each sample or the two tissues need to be separated; then, the enamel knot signaling center could disrupt the analysis so it seems necessary to avoid it (Petit, 2017). A laser dissection of frontal sections of the specific tissues at different developmental steps could allow identifying genes involved in the initiation of the tooth replacement and the maintenance.

The rabbit as model for human pathologies linked to radiation therapies

During this thesis, I also studied dental morphological variations during rabbit lifespan. We observed that even in adults, the tooth shape is variable from the growth zone to the occlusal

surface. Thanks to a collaboration with Dr. Dessouter and Dr. Chaux-Bodard we obtained irradiated mandibles of rabbits. We studied the mineralized structures of these samples. We observed that irradiations of the mandible bone in the rabbit induce modifications of the tooth shape (Article 4, **p132**). After few weeks of recovery post-irradiations, a global modification of the tooth shape takes place. Indeed, we observed a complete mineralization of the pulp cavity.

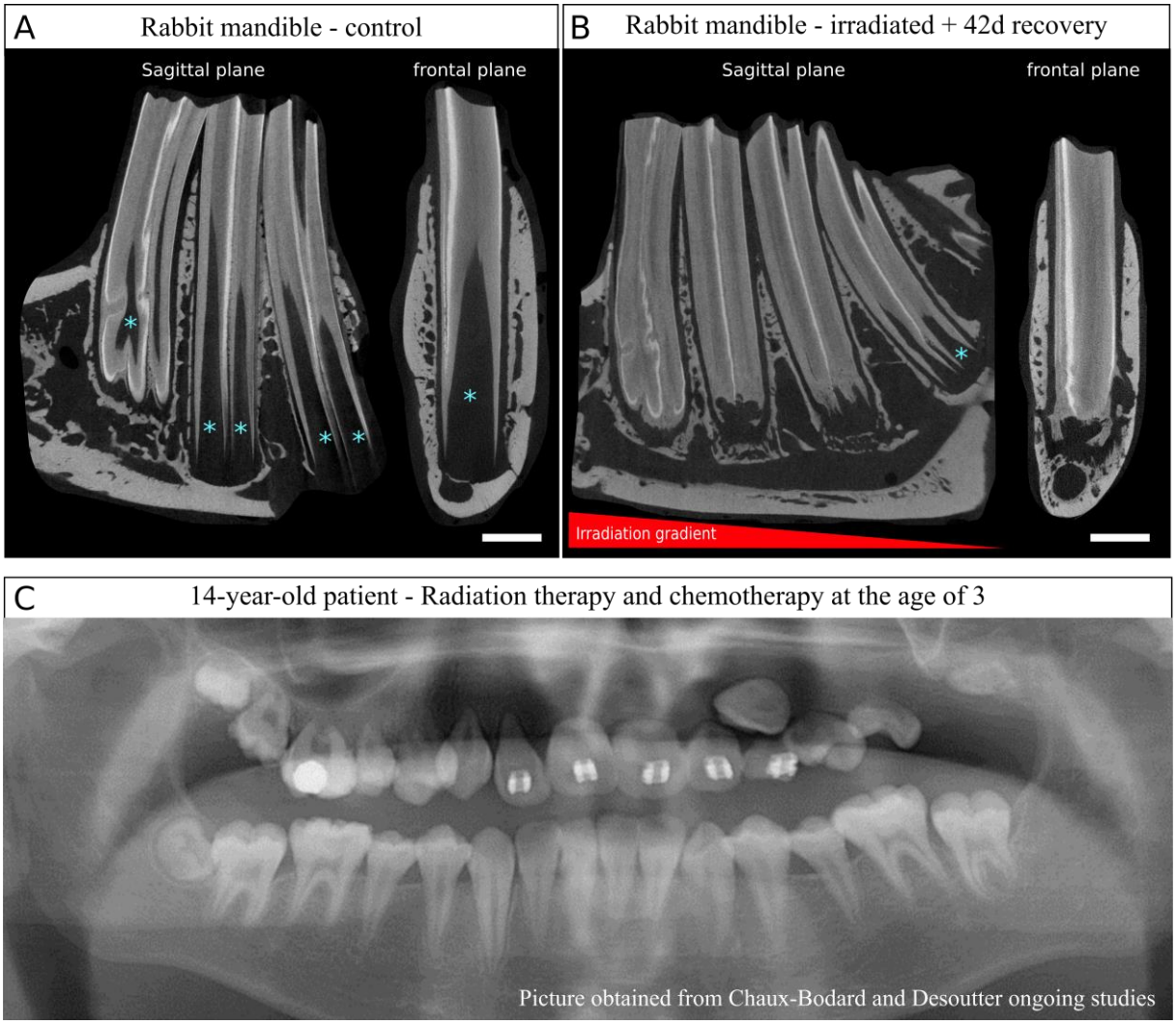

Figure C. 1. Effects of radiation therapy on dental development in rabbits and humans. *(A) Normal lower cheek tooth morphology in adult rabbits, in sagittal and frontal planes. In sagittal plane, P_3, P_4 and M_1. The pulp cavity is illustrated by the blue asterisks. (B) Consequences of a radiation exposition (42.5 Gy) in the mandible after 42 days of recovery, in sagittal and frontal planes. In sagittal plane, P_3, P_4, M_1 and M_2. Pulp cavity is detected only in the M_2 (blue asterisk). (C) Long-term sequelae of radiotherapy and chemotherapy in a 14-year-old patient treated for an orofacial tumor at 3. Maxillary teeth have atypical root morphology, with highly reduced roots. (Picture obtained from Chaux-Bodard and Desoutter, ongoing study, unpublished). Scale bar: 3mm.*

In rabbit ever-growing teeth, the dental pulp contains stem cells at the basis of the tooth that give rise in a layer of pre-odontoblasts and then mature secretory odontoblasts (**Figure C. 1**A, Ali and Mubarak, 2012). Rabbit premolars have a growth rate between 0.93 and 2.14 mm per week in function of their diet compensated by dental wear at the occlusal surface (Wyss et al. 2016). Excess of mineralization in the pulp cavity probably disrupt the organization of the secreting cells and so, the growth of the tooth. Surprisingly, while no more dental pulp cavity is detected at 28 days of recovery post irradiations, rabbits continue to eat normally even after 42 days of recovery. In 42 days, a rabbit tooth is supposed to grow and wear out by around 6mm. It seems necessary to check the cell state of the tooth growth zone in order to see if the tooth is still able to grow and how the cells have been affected by radiations. Irradiation zone was centered in the mental foramen, so mesialy compared to the cheek teeth. In these specimens, we observed a gradient of phenotypes linked to the irradiation zone diffusion, with the pulpal cavity completely mineralized in the $P_{2\text{-}3}$ and the M_1, but with a less severe phenotype in the M_2 (**Figure C. 1**B, blue asterisks). In humans, irradiation treatment against oro-facial tumor in children, especially younger than 6 year old, can induce a limitation of the jawbone or tooth germs growth and mineralization problems (Chaux-Bodard and Desoutter *unpublished*, King 2019). Dental development can be delayed or arrested, inducing atypical root morphology (**Figure C. 1**C). Due to the ever-growing ability of the rabbit cheek teeth, we could mimics developmental disorders observed in children in adult rabbits and test various treatments against radiation-therapy induced dental disorders. All the dental responses to small doses of radiations or treatments will be preserved in the dental tissues of the ever-growing teeth. In rabbit mandible bones, low intensity pulsed ultrasound (LIPUS) therapy is proposed to limit the damage and accelerated new bone formation (Xie et al., 2011). Therefore, LIPUS therapy could be useful to limit irradiation defects on healthy tissues. In order to test this hypothesis, we will study dental morphology of irradiated rabbits then treated by LIPUS therapy.

Developmental heterochronies in rabbit ondontogenesis

Study of the occlusal tooth shape in Lagomorpha allowed determining inter-species homologies. We identified a developmental heterochrony process during their evolutionary history. First, during rabbit embryogenesis, the cuspidogenesis follows the phylogenetic appearance of cusps during mammalian evolution. Luckett (1993) already described this phenomenon through the comparison of the cusp mineralization instead of cusp formation. With soft tissues, we have access to information less apparent after mineralization. The paracone is the first cusp to appear and the hypocone the last main cusp to differentiate. Most cusp morphology studies are completed by a functional study of the molar occlusion. However, in extant Lagomorpha, all the cusps are completely worn early in ontogeny and teeth are functional when the occlusal surface is flat. The cusps in the rabbit are transient, but their shape is closely related to the mammalian evolutionary history. It also means that at eruption, rabbit teeth do not have their final shape.

During ontogeny and by wear, the occlusal surface changes, and these changes mimics the lagomorph evolution. Then, even when the general occlusal shape of the tooth has an adult morphology, we detected intra-individual variations of the hypoflexus structure. The ever-growing ability of the cheek teeth induces permanent changes of this fold. We showed that these variations of shape are probably dependent of the cell proliferation in the developing part of the tooth. These variations of shape during ontogeny has to be known, especially for paleontologists, in order to carefully identify species according to the tooth shape.

Conclusion

To conclude, rabbit seem to be a good model in dental research. Rabbits are already used in odontological studies but we showed here that they are also useful for studying tooth morphogenesis. Studies of tooth development and replacement in rabbits could allow understanding the mechanisms of mammalian tooth replacement. We showed in this thesis that common molecular experiments can be done in rabbit tissues and rabbits can also be a relevant model to use more advanced techniques as CRISPR/Cas9 technology (Yan et al., 2014). Rabbit dentition, with its ever-growing ability, could also be used to better understand human dental pathologies. We show that pathologies due to irradiations of the developing teeth in humans are also observed in rabbits with more cellular plasticity. So, rabbits could be used as model in order find how to preserve dental stem cells in children. Finally, rabbit dentition development seems to highly follow the mammalian tooth evolution, making rabbit teeth are a very good model for dental Evo-Devo thematics.

REFERENCES

Abtahi, S., Poosti, M., and Saghravanian, N. (2018). Histological evaluation of orthodontic tooth movement following low level laser irradiation in rabbits. Med. Oral Patol. Oral y Cir. Bucal, S228–. doi:10.4317/medoral.17643728.

Ahn, Y., Sanderson, B. W., Klein, O. D., and Krumlauf, R. (2010). Inhibition of Wnt signaling by Wise (Sostdc1) and negative feedback from Shh controls tooth number and patterning. Development 137, 3221–31. doi:10.1242/dev.054668.

Al-Hamdany, A. K., Al-Khatib, A. R., and Al-Sadi, H. I. (2017). Influence of olive oil on alveolar bone response during orthodontic retention period: rabbit model study. Acta Odontol. Scand. 75, 413–422. doi:10.1080/00016357.2017.1328613.

Ali, Z. H., and Mubarak, R. (2012). Histomorphological study of dentine pulp complex of continuously growing teeth in the rabbits. Life Sci. J. 9, 1554–1564.

Angelone, C., and Rook, L. (2011). Alilepus meini nov. sp. (Leporidae, Lagomorpha) du Messinien inférieur de Toscane (Italie centro-occidentale). Geobios 44, 151–156. doi:10.1016/j.geobios.2010.11.003.

Angelone, C., Schultz, J. A., and Erbajeva, M. a. (2014). Determining the ontogenetic variation of lower cheek teeth occlusal surface patterns in lagomorphs using micro-ct technology. Palaeontol. Electron. 17, 1–13.

Asher, R. J., Meng, J., Wible, J. R., McKenna, M. C., Rougier, G. W., Dashzeveg, D., et al. (2005). Stem Lagomorpha and the antiquity of Glires. Science 307, 1091–4. doi:10.1126/science.1107808.

Averianov, A. O. (1998). Homology of the cusps in the molars of the lagomorpha (Mammalia) and certain general problems of homology in the morphological structures. Paleontol. J. 32, 73–77.

Averianov, A. O., Abramov, A. V., and Tikhonov, A. N. (2000). A new species of. Nesolagus (Lagomorpha, Leporidae) from Vietnam with osteological description. Contrib. from Zool. Inst. 3.

Averianov, A. O., and Tesakov, A. S. (1997). Evolutionary trends in Mio-Pliocene Leporinae, based on Trischizolagus (Mammalia, Lagomorpha). Palaeontol. Zeitschrift 71, 145–153. doi:10.1007/BF03022556.

Balic, A., and Thesleff, I. (2015). Tissue Interactions Regulating Tooth Development and Renewal. Curr. Top. Dev. Biol. 115, 157–186. doi:10.1016/BS.CTDB.2015.07.006.

Ball, R. S. (2006). Issues to Consider for Preparing Ferrets as Research Subjects in the Laboratory. ILAR J. 47, 348–357. doi:10.1093/ilar.47.4.348.

Ben Amar, M., and Jia, F. (2013). Anisotropic growth shapes intestinal tissues during embryogenesis. Proc. Natl. Acad. Sci. U. S. A. 110, 10525–30. doi:10.1073/pnas.1217391110.

Bertin, T. J. C., Thivichon-Prince, B., LeBlanc, A. R. H., Caldwell, M. W., and Viriot, L. (2018). Current Perspectives on Tooth Implantation, Attachment, and Replacement in Amniota. Front. Physiol. 9, 1630. doi:10.3389/fphys.2018.01630.

Bertonnier-Brouty, L., Viriot, L., Joly, T., and Charles, C. (2019). 3D reconstructions of dental epithelium during Oryctolagus cuniculus embryonic development related to the publication ”Morphological features of tooth development and replacement in the rabbit Oryctolagus cuniculus”. MorphoMuseuM, 5:e90. doi:10.18563/journal.m3.90.

Biehs, B., Hu, J. K.-H., Strauli, N. B., Sangiorgi, E., Jung, H., Heber, R.-P., et al. (2013). BMI1 represses Ink4a/Arf and Hox genes to regulate stem cells in the rodent incisor. Nat. Cell Biol. 15, 846–852. doi:10.1038/ncb2766.

Bosze, Z., and Houdebine, L. M. (2006). Application of rabbits in biomedical research: a review. World Rabbit Sci. 14, 01-14. doi:10.4995/wrs.2006.712.

Butler, P. M. (1956). The ontogeny of molar pattern. Biol. Rev. 31, 30–69. doi:10.1111/j.1469-185X.1956.tb01551.x.

Carneiro, M., Rubin, C. J., Palma, F. Di, Albert, F. W., Alföldi, J., Barrio, A. M., et al. (2014). Rabbit genome analysis reveals a polygenic basis for phenotypic change during domestication. Science (80-.). 345, 1074–1079. doi:10.1126/science.1253714.

Čermák, S., Angelone, C., and Sinitsa, M. V. (2015). New late miocene alilepus (Lagomorpha, Mammalia) from Eastern Europe - a new light on the evolution of the earliest old world leporinae. Bull. Geosci. 90, 431–451. doi:10.3140/bull.geosci.1523.

Chaline, J., Brunet-Lecomte, P., Montuire, S., Viriot, L., and Courant, F. (1999). Anatomy of the arvicoline radiation (Rodentia): palaeogeographical, palaeoecological history and evolutionary data. Ann. Zool. Fennici 36, 239–267. doi:10.2307/23735732.

Chavez, M. G., Yu, W., Biehs, B., Harada, H., Snead, M. L., Lee, J. S., et al. (2012). Characterization of Dental Epithelial Stem Cells from the Mouse Incisor with Two-Dimensional and Three-Dimensional Platforms. Tissue Eng. Part C Methods 19, 120816080322006. doi:10.1089/ten.tec.2012.0232.

Chuan-Kuei, L., Wilson, R. W., Dawson, M. R., and Krishtalka, L. (1987). "The Origin of Rodents and Lagomorphs," in Current Mammalogy (Boston, MA: Springer US), 97–108. doi:10.1007/978-1-4757-9909-5_3.

Cobourne, M. T., and Sharpe, P. T. (2010). Making up the numbers: The molecular control of mammalian dental formula. Semin. Cell Dev. Biol. 21, 314–324. doi:10.1016/j.semcdb.2010.01.007.

Conte, V., Muñoz, J. J., and Miodownik, M. (2008). A 3D finite element model of ventral furrow invagination in the Drosophila melanogaster embryo. J. Mech. Behav. Biomed. Mater. 1, 188–198. doi:10.1016/J.JMBBM.2007.10.002.

Damuth, J., and Janis, C. M. (2011). On the relationship between hypsodonty and feeding ecology in ungulate mammals, and its utility in palaeoecology. Biol. Rev. 86, 733–758. doi:10.1111/j.1469-185X.2011.00176.x.

Dare, A., Hachisu, R., Yamaguchi, A., Yokose, S., Yoshiki, S., and Okano, T. (1997). Effects of Ionizing Radiation on Proliferation and Differentiation of Osteoblast-like Cells. J. Dent. Res. 76, 658–664. doi:10.1177/00220345970760020601.

Davidson, L. A., Koehl, M. A., Keller, R., and Oster, G. F. (1995). How do sea urchins invaginate? Using biomechanics to distinguish between mechanisms of primary invagination. Development 121, 2005–18.

Davis, B. M. (2011). Evolution of the Tribosphenic Molar Pattern in Early Mammals, with Comments on the "Dual-Origin" Hypothesis. J. Mamm. Evol. 18, 227–244. doi:10.1007/s10914-011-9168-8.

Dommergues, J.-L., David, B., and Marchand, D. (1986). Les relations ontogenèse-phylogenèse:Applications paléontologiques. Geobios 19, 335–356. doi:10.1016/S0016-6995(86)80022-5.

Dosedělová, H., Dumková, J., Lesot, H., Glocová, K., Kunová, M., Tucker, A. S., et al. (2015). Fate of the molar dental lamina in the monophyodont mouse. PLoS One 10, e0127543.

doi:10.1371/journal.pone.0127543.

Eastman, Q., and Grosschedl, R. (1999). Regulation of LEF-1/TCF transcription factors by Wnt and other signals. Curr. Opin. Cell Biol. 11, 233–40.

Erbajeva, M., Baatarjav, B., Daxner-Höck, G., and Flynn, L. J. (2017). Occurrences of Sinolagomys (Lagomorpha) from the Valley of Lakes (Mongolia). Palaeobiodiversity and palaeoenvironments 97, 11–24. doi:10.1007/s12549-016-0262-z.

Forsten, A. (2002). Latest Hipparion Christol, 1832 in Europe. A review of the Pliocene Hipparion crassum Gervais group and other finds (Mammalia, Equidae). Geodiversitas 24, 465–486.

Fostowicz-Frelik, Ł. (2013). Reassessment of Chadrolagus and Litolagus (Lagomorpha) and a New Genus of North American Eocene Lagomorph from Wyoming. Am. Museum Novit. 3773, 1–76. doi:10.1206/3773.2.

Fostowicz-Frelik, Ł., and Tabrum, A. R. (2009). Leporids (Mammalia, Lagomorpha) from the Diamond O Ranch Local Fauna, Latest Middle Eocene of Southwestern Montana. Ann. Carnegie Museum 78, 253–271. doi:10.2992/007.078.0303.

Gaete, M., and Tucker, A. S. (2013). Organized Emergence of Multiple-Generations of Teeth in Snakes Is Dysregulated by Activation of Wnt/Beta-Catenin Signalling. PLoS One 8, e74484. doi:10.1371/journal.pone.0074484.

Glasstone, S. (1938). A Comparative Study of the Development in vivo and in vitro of Rat and Rabbit Molars. Proc. R. Soc. London. Ser. B-Biological Sci. 126, 315–330.

Gould, S. J. (1977). Ontogeny and phylogeny. Belknap Press of Harvard University Press.

Handrigan, G. R., Leung, K. J., Richman, J. M., Barker, N., Es, J. H. van, Kuipers, J., et al. (2010). Identification of putative dental epithelial stem cells in a lizard with life-long tooth replacement. Development 137, 3545–9. doi:10.1242/dev.052415.

Handrigan, G. R., and Richman, J. M. (2010a). A network of Wnt, hedgehog and BMP signaling pathways regulates tooth replacement in snakes. Dev. Biol. 348, 130–141. doi:10.1016/J.YDBIO.2010.09.003.

Handrigan, G. R., and Richman, J. M. (2010b). Autocrine and paracrine Shh signaling are necessary for tooth morphogenesis, but not tooth replacement in snakes and lizards

(Squamata). Dev. Biol. 337, 171–186. doi:10.1016/j.ydbio.2009.10.020.

Hannezo, E., Prost, J., and Joanny, J. F. (2011). Instabilities of monolayered epithelia: Shape and structure of villi and crypts. Phys. Rev. Lett. 107, 078104. doi:10.1103/PhysRevLett.107.078104.

Hibbard, C. W. (1963). The origin of the P3 pattern of Sylvilagus, Caprolagus, Oryctolagus and Lepus. J. Mammal. 14, 1–15. doi:10.2307/1377162.

Hirschfeld, Z., Weinreb, M. M., and Michaeli, Y. (1973). Incisors of the Rabbit: Morphology, Histology, and Development. J. Dent. Res. 52, 377–384. doi:10.1177/00220345730520023201.

Hoffmann, R. S., and Smith, A. . (2005). Order Lagomorpha. Wilson, D.E. Reeder, D.M. Mammal Species World, Third Ed., 185–211.

Horowitz, S. L., Weisbroth, S. H., and Scher, S. (1973). Deciduous dentition in the rabbit (Oryctolagus cuniculus). A roentgenographic study. Arch. Oral Biol. 18, 517–23.

Huchon, D., Madsen, O., Sibbald, M. J. J. B., Ament, K., Stanhope, M. J., Catzeflis, F., et al. (2002). Rodent Phylogeny and a Timescale for the Evolution of Glires: Evidence\rfrom an Extensive Taxon Sampling Using Three Nuclear Genes. Mol Biol Evol 19, 1053–1065. doi:https://doi.org/10.1093/oxfordjournals.molbev.a004164.

Hunter, J. P., and Jernvall, J. (1995). The hypocone as a key innovation in mammalian evolution. Proc. Natl. Acad. Sci. U. S. A. 92, 10718–22.

Itasaki, N., Jones, C. M., Mercurio, S., Rowe, A., Domingos, P. M., Smith, J. C., et al. (2003). Wise, a context-dependent activator and inhibitor of Wnt signalling. Development 121, 3627–3636. doi:10.1242/dev.00674.

Jaks, V., Barker, N., Kasper, M., van Es, J. H., Snippert, H. J., Clevers, H., et al. (2008). Lgr5 marks cycling, yet long-lived, hair follicle stem cells. Nat. Genet. 40, 1291–1299. doi:10.1038/ng.239.

Janis, C. M., and Fortelius, M. (1988). On the means whereby mammals achieve increased functional durability of their dentitions, with special reference to limiting factors. Biol. Rev. 63, 197–230. doi:10.1111/j.1469-185X.1988.tb00630.x.

Jarvinen, E., Salazar-Ciudad, I., Birchmeier, W., Taketo, M. M., Jernvall, J., and Thesleff, I.

(2006). Continuous tooth generation in mouse is induced by activated epithelial Wnt/beta-catenin signaling. Proc. Natl. Acad. Sci. 103, 18627–18632. doi:10.1073/pnas.0607289103.

Järvinen, E., Shimomura-Kuroki, J., Balic, A., Jussila, M., and Thesleff, I. (2018). Mesenchymal Wnt/β-catenin signaling limits tooth number. Development 145, dev158048. doi:10.1242/dev.158048.

Järvinen, E., Tummers, M., and Thesleff, I. (2009). The role of the dental lamina in mammalian tooth replacement. J. Exp. Zool. Part B Mol. Dev. Evol. 312B, 281–291. doi:10.1002/jez.b.21275.

Järvinen, E., Välimäki, K., Pummila, M., Thesleff, I., and Jernvall, J. (2008). The taming of the shrew milk teeth. Evol. Dev. 10, 477–486. doi:10.1111/j.1525-142X.2008.00258.x.

Jernvall, J. (2002). Linking development with generation of novelty in mammalian teeth. Proc. Natl. Acad. Sci. 97, 2641–2645. doi:10.1073/pnas.050586297.

Jernvall, J., and Thesleff, I. (2012). Tooth shape formation and tooth renewal: evolving with the same signals. Development 139, 3487–3497. doi:10.1242/dev.085084.

Jin, C. Z., Tomida, Y., Wang, Y., and Zhang, Y. Q. (2010). First discovery of fossil Nesolagus (Leporidae, Lagomorpha) from Southeast Asia. Sci. China Earth Sci. 53, 1134–1140. doi:10.1007/s11430-010-4010-3.

Jussila, M., Crespo Yanez, X., and Thesleff, I. (2014). Initiation of teeth from the dental lamina in the ferret. Differentiation 87, 32–43. doi:10.1016/j.diff.2013.11.004.

Juuri, E., and Balic, A. (2017). The Biology Underlying Abnormalities of Tooth Number in Humans. J. Dent. Res. 96, 1248–1256. doi:10.1177/0022034517720158.

Juuri, E., Jussila, M., Seidel, K., Holmes, S., Wu, P., Richman, J., et al. (2013). Sox2 marks epithelial competence to generate teeth in mammals and reptiles. Development 140, 1424–32. doi:10.1242/dev.089599.

Juuri, E., Saito, K., Ahtiainen, L., Seidel, K., Tummers, M., Hochedlinger, K., et al. (2012). Sox2+ Stem Cells Contribute to All Epithelial Lineages of the Tooth via Sfrp5+ Progenitors. Dev. Cell 23, 317–328. doi:10.1016/j.devcel.2012.05.012.

Kennedy, W. J. (1989). Thoughts on the evolution and extinction of Cretaceous ammonites.

Proc. Geol. Assoc. 100, 251–279. doi:10.1016/S0016-7878(89)80047-1.

Kim J, Ahn , Adasooriya D, Woo EJ, Kim HJ, Hu KS, Krumlauf R, C. S. (2018). Shh Plays an Inhibitory Role in Cusp Patterning by Regulation of Sostdc1. J. Dent. Res. 98, 98–106. doi:10.1177/0022034518803095.

King, E. (2019). Oral sequelae and rehabilitation considerations for survivors of childhood cancer. Br. Dent. J. 226, 323–329. doi:10.1038/s41415-019-0043-y.

Klein, O. D., Minowada, G., Peterkova, R., Kangas, A., Yu, B. D., Lesot, H., et al. (2006). Sprouty Genes Control Diastema Tooth Development via Bidirectional Antagonism of Epithelial-Mesenchymal FGF Signaling. Dev. Cell 11, 181–190. doi:10.1016/J.DEVCEL.2006.05.014.

Koenigswald, W. Von (2011). Diversity of hypsodont teeth in mammalian dentitions – construction and classification. Palaeontographica 294, 63–94. doi:10.1127/pala/294/2011/63.

Koenigswald, W. von, Anders, U., Engels, S., Schultz, J. A., and Ruf, I. (2010). Tooth Morphology in Fossil and Extant Lagomorpha (Mammalia) Reflects Different Mastication Patterns. J. Mamm. Evol. 17, 275–299. doi:10.1007/s10914-010-9140-z.

Kormish, J. D., Sinner, D., and Zorn, A. M. (2010). Interactions between SOX factors and Wnt/beta-catenin signaling in development and disease. Dev. Dyn. 239, 56–68. doi:10.1002/dvdy.22046.

Korth, W. W., and Hageman, J. (1988). Lagomorphs (Mammalia) from the Oligocene (Orellan and Whitneyan) Brule Formation, Nebraska. Trans. Nebraska Acad. Sci. Affil. Soc. Pap. Trans. Nebraska Acad. Sci. 182, 141–152.

Kraatz, B. P., Meng, J., Weksler, M., and Li, C. (2010). Evolutionary patterns in the dentition of duplicidentata (Mammalia) and a novel trend in the molarization of premolars. PLoS One 5, 1–15. doi:10.1371/journal.pone.0012838.

Kriegs, J. O., Churakov, G., Jurka, J., Brosius, J., and Schmitz, J. (2007). Evolutionary history of 7SL RNA-derived SINEs in Supraprimates. Trends Genet. 23, 158–161. doi:10.1016/j.tig.2007.02.002.

Kücken, M., and Newell, A. C. (2004). A model for fingerprint formation. Europhys. Lett. 68, 141–146. doi:10.1209/epl/i2004-10161-2.

Kumar, G. S. (2014). Orban’s Oral Histology & Embryology. Elsevier Health Sciences APAC.

La Scala, G. C., ODonovan, D. A., Yeung, I., Darko, J., Addison, P. D., Neligan, P. C., et al. (2005). Radiation-Induced Craniofacial Bone Growth Inhibition: Efficacy of Cytoprotection following a Fractionated Dose Regimen. Plast. Reconstr. Surg. 115, 1973–1985. doi:10.1097/01.PRS.0000163322.22436.3B.

Lan, Y., Jia, S., and Jiang, R. (2014). Molecular patterning of the mammalian dentition. Semin. Cell Dev. Biol. 25–26, 61–70. doi:10.1016/j.semcdb.2013.12.003.

Laubichler, M. D. (2000). Homology in Development and the Development of the Homology Concept. Am. Zool. 40, 777–788. doi:10.1093/icb/40.5.777.

Li, C.-K., Wang, Y.-Q., Zhang, Z.-Q., Mao, F.-Y., and Meng, J. (2016). A new mimotonidan Mina hui (Mammalia, Glires) from the Middle Paleocene of Qianshan, Anhui, China. Vertebr. Palasiat. 54, 121–136.

Li, C., Meng, J., and Wang, Y. (2007). Dawsonolagus antiquus, A Primitive Lagomorph from the Eocene Arshanto Formation, Nei Mongol, China. Bull. Carnegie Museum Nat. Hist. 39, 97–110. doi:10.2992/0145-9058(2007)39[97:DAAPLF]2.0.CO;2.

Lo Muzio, L., Tetè, S., Mastrangelo, F., Cazzolla, A. P., Lacaita, M. G., Margaglione, M., et al. (2007). A novel mutation of gene CBFA1/RUNX2 in cleidocranial dysplasia. Ann. Clin. Lab. Sci. 37, 115–20.

Luckett, W. P. (1993). “An Ontogenetic Assessment of Dental Homologies in Therian Mammals,” in Mammal Phylogeny (New York, NY), 182–204. doi:10.1007/978-1-4615-7381-4_13.

Luo, Z.-X., Kielan-Jaworowska, Z., and Cifelli, R. L. (2008). Evolution of dental replacement in mammals. Bull. Carnegie Museum Nat. Hist. 36, 159–175. doi:10.2992/0145-9058(2004)36[159:eodrim]2.0.co;2.

Major, C. I. F. (1899). IX. On Fossil and Recent Lagomorpha. doi:10.1111/j.1096-3642.1899.tb002021.x.

Matthee, C. A., van Vuuren, B. J., Bell, D., and Robinson, T. J. (2004). A molecular supermatrix of the rabbits and hares (Leporidae) allows for the identification of five intercontinental exchanges during the Miocene. Syst. Biol. 53, 433–447.

doi:10.1080/10635150490445715.

Medak, H., Weinreb, M., Sicher, H., Weinmann, J. P., and Schour, I. (1952). The Effect of Single Doses of Irradiation Upon the Tissues of the Upper Rat Incisor. J. Dent. Res. 31, 559–574. doi:10.1177/00220345520310040601.

Meng, J. (2004). Chapter 7: Phylogeny and Divergence of Basal Glires. Bull. Am. Museum Nat. Hist. 285, 93–109. doi:10.1206/0003-0090(2004)285<0093:C>2.0.CO;2.

Merametdjian, L., Prud'Homme, T., Le Caignec, C., Isidor, B., and Lopez-Cazaux, S. (2019). Oro-dental phenotype in patients with RUNX2 duplication. Eur. J. Med. Genet. 62, 85–89. doi:10.1016/j.ejmg.2018.05.019.

Meredith, A. (2007). "Rabbit dentistry," in (European Journal of Companion Animal Practice), 55–62.

Metscher, B. D. (2009). MicroCT for comparative morphology: simple staining methods allow high-contrast 3D imaging of diverse non-mineralized animal tissues. BMC Physiol. 9, 11. doi:10.1186/1472-6793-9-11.

Michaeli, Y., Hirschfeld, Z., and Weinreb, M. M. (1980). The cheek teeth of the rabbit: morphology, histology and development. Cells Tissues Organs 106, 223–239. doi:10.1159/000145185.

Mieloch, A. A., and Suchorska, W. M. (2015). The concept of radiation-enhanced stem cell differentiation. Radiol Oncol 49, 209–216. doi:10.1515/raon-2015-0022.

Moses, K. D., Butler, W. T., and Qin, C. (2006). Immunohistochemical study of small integrin-binding ligand, N-linked glycoproteins in reactionary dentin of rat molars at different ages. Eur. J. Oral Sci. 114, 216–22. doi:10.1111/j.1600-0722.2006.00353.x.

Mucchielli, M. L., and Mitsiadis, T. A. (2000). Correlation of asymmetric Notch2 expression and mouse incisor rotation. Mech. Dev. 91, 379–382. doi:10.1016/S0925-4773(99)00293-2.

Müller, J., Clauss, M., Codron, D., Schulz, E., Hummel, J., Fortelius, M., et al. (2014). Growth and wear of incisor and cheek teeth in domestic rabbits (Oryctolagus cuniculus) fed diets of different abrasiveness. J. Exp. Zool. Part A Ecol. Genet. Physiol. 321, 283–298. doi:10.1002/jez.1864.

Munne, P. M., Tummers, M., Järvinen, E., Thesleff, I., and Jernvall, J. (2009). Tinkering with the inductive mesenchyme: Sostdc1 uncovers the role of dental mesenchyme in limiting tooth induction. Development 136, 393–402. doi:10.1242/dev.025064.

Navarro, J. A. C., Sottovia-Filho, D., Leite-Ribeiro, M. C., and Taga, R. (1975). Histological Study on the Postnatal Development and Sequence of Eruption of the Maxillary Cheek-Teeth of Rabbits (Oryctolagus cuniculus). Arch. Histol. Jpn. 38, 17–30. doi:10.1679/aohc1950.38.17.

Navarro, J. A. C., Sottovia-Filho, D., Leite-Ribeiro, M. C., and Taga, R. (1976). Histological study on the postnatal development and sequence of eruption of the mandibular cheek-teeth of rabbits (Oryctolagus cuniculus). Arch. Histol. Jpn. Nippon soshikigaku kiroku 39, 23–32. doi:10.1679/aohc1950.39.23.

Nowak, R. M. (1999). Walker's mammals of the world. Johns Hopkins University Press

O'Leary, M. A., Bloch, J. I., Flynn, J. J., Gaudin, T. J., Giallombardo, A., Giannini, N. P., et al. (2013). The Placental Mammal Ancestor and the Post-K-Pg Radiation of Placentals. Science (80-.). 339, 662–667. doi:10.1126/science.1229237.

Odell, G. M., Oster, G., Alberch, P., and Burnside, B. (1981). The mechanical basis of morphogenesis: I. Epithelial folding and invagination. Dev. Biol. 85, 446–462. doi:10.1016/0012-1606(81)90276-1.

Ooë, T. (1980). Développement embryonnaire des incisives chez le lapin (Oryctolagus cuniculus L.). Interpretation de la formule dentaire. Mammalia 44, 259–270. doi:10.1515/mamm.1980.44.2.259.

Osborn, H. F. (1907). Evolution of Mammalian Molar Teeth: To and from the Triangular Type Including Collected and Revised Researches Trituberculy and New Sections on the Forms and Homologies of the Molar Teeth in the Different Orders of Mammals. Macmillan.

Pantalacci, S., Guéguen, L., Petit, C., Lambert, A., Peterkovà, R., and Sémon, M. (2017). Transcriptomic signatures shaped by cell proportions shed light on comparative developmental biology. Genome Biol. 18, 29. doi:10.1186/s13059-017-1157-7.

Petit, C. (2017). Évolution et Développement d'un organe sériel Transcriptomique comparée des bourgeons de molaire chez les rongeurs. Thèse Dr. en Sci. la Vie. Available at:

http://www.theses.fr/2017LYSEN009.

Pillet, S., Svitek, N., and von Messling, V. (2009). “Ferrets as a Model for Morbillivirus Pathogenesis, Complications, and Vaccines,” in (Springer, Berlin, Heidelberg), 73–87. doi:10.1007/978-3-540-70617-5_4.

Pispa, J., and Thesleff, I. (2003). Mechanisms of ectodermal organogenesis. Dev. Biol. 262, 195–205. doi:10.1016/S0012-1606(03)00325-7.

Popa, E. M., Anthwal, N., and Tucker, A. S. (2016). Complex patterns of tooth replacement revealed in the fruit bat (Eidolon helvum). J. Anat. 229, 847–856. doi:10.1111/joa.12522.

Popa, E. M., Buchtova, M., and Tucker, A. S. (2019). Revitalising the rudimentary replacement dentition in the mouse. Development 146, dev171363. doi:10.1242/dev.171363.

Rasch, L. J., Martin, K. J., Cooper, R. L., Metscher, B. D., Underwood, C. J., and Fraser, G. J. (2016). An ancient dental gene set governs development and continuous regeneration of teeth in sharks. doi:10.1016/j.ydbio.2016.01.038.

Reig, O. A. (1977). A proposed unified nomenclature for the enamelled components of the molar teeth of the Cricetidae (Rodentia). J. Zool. 181, 227–241. doi:10.1111/j.1469-7998.1977.tb03238.x.

Rensberger, J. M. (1975). Function in the Cheek Tooth Evolution of Some Hypsodont Geomyoid Rodents. J. Paleontol. 49, 10–22. doi:10.2307/1303314.

Renvoisé, E., and Michon, F. (2014). An Evo-Devo perspective on ever-growing teeth in mammals and dental stem cell maintenance. Front. Physiol. 5, 1–12. doi:10.3389/fphys.2014.00324.

Richman, D. P., Stewart, R. M., Hutchinson, J. W., and Caviness, V. S. (1975). Mechanical model of brain convolutional development. Science 189, 18–21.

Richman, J. M., and Handrigan, G. R. (2011). Reptilian tooth development. Genesis 49, 247–260. doi:10.1002/dvg.20721.

Rose, K. D. (2006). The beginning of the age of mammals. Johns Hopkins University Press

Sadier, A., Twarogowska, M., Steklikova, K., Hayden, L., Lambert, A., Schneider, P., et al. (2019). Modeling Edar expression reveals the hidden dynamics of tooth signaling center

patterning. PLOS Biol. 17, e3000064. doi:10.1371/journal.pbio.3000064.

Sanz-Navarro, M., Seidel, K., Sun, Z., Bertonnier-Brouty, L., Amendt, B. A., Klein, O. D., et al. (2018). Plasticity within the niche ensures the maintenance of a Sox2+ stem cell population in the mouse incisor. Development 145, dev155929. doi:10.1242/dev.155929.

Schmidt-Kittler, N. (2002). Feeding specializations in rodents. Senckenbergiana lethaea 82, 141–152. doi:10.1007/BF03043780.

Seppala, M., Fraser, G. J., Birjandi, A. A., Xavier, G. M., Cobourne, M. T., Roelink, H., et al. (2017). Sonic Hedgehog Signaling and Development of the Dentition. J. Dev. Biol. 5. doi:10.3390/jdb5020006.

Sharir, A., and Klein, O. D. (2016). Watching a deep dive: Live imaging provides lessons about tooth invagination. J. Cell Biol. 214, 645–7. doi:10.1083/jcb.201608088.

Sun, Z., Yu, W., Navarro, M. S., Sweat, M., Eliason, S., Sharp, T., et al. (2016). Sox2 and Lef-1 interact with Pitx2 to regulate incisor development and stem cell renewal. Development, dev.138883. doi:10.1242/dev.138883.

Sych, L. S., and Reade, P. C. (1987). Heterochrony in the development of vestigial and functional deciduous incisors in rabbits (Oryctolagus cuniculus L.). J. Craniofac. Genet. Dev. Biol. 7, 81–94.

Thesleff, I. (2004). How to build a tooth? Developmental biology is revealing the instructions. Nor Tann. Tid, 327.

Togo, Y., Takahashi, K., Saito, K., Kiso, H., Tsukamoto, H., Huang, B., et al. (2016). Antagonistic Functions of USAG-1 and RUNX2 during Tooth Development. PLoS One 11, e0161067. doi:10.1371/journal.pone.0161067.

Tucker, A. S., and Fraser, G. J. (2014). Evolution and developmental diversity of tooth regeneration. Semin. Cell Dev. Biol. 25–26, 71–80. doi:10.1016/j.semcdb.2013.12.013.

Tumbar, T., Guasch, G., Greco, V., Blanpain, C., Lowry, W. E., Rendl, M., et al. (2004). Defining the Epithelial Stem Cell Niche in Skin. Science (80-.). 303, 359–363. doi:10.1126/SCIENCE.1092436.

Tummers, M., and Thesleff, I. (2003). Root or crown: a developmental choice orchestrated by

the differential regulation of the epithelial stem cell niche in the tooth of two rodent species. Development 130, 1049–1057. doi:10.1242/dev.00332.

Vaahtokari, A., Aberg, T., Jernvall, J., Keränen, S., and Thesleff, I. (1996). The enamel knot as a signaling center in the developing mouse tooth. Mech. Dev. 54, 39–43.

Van Valen, L. M. (1994). Serial homology: the crests and cusps of mammalian teeth. Acta Palaeontol. Pol. 38, 145–158.

Viriot, L., Peterková, R., Peterka, M., and Lesot, H. (2002). Evolutionary Implications of the Occurrence of Two Vestigial Tooth Germs During Early Odontogenesis in the Mouse Lower Jaw. Connect. Tissue Res. 43, 129–133. doi:10.1080/03008200290001168.

Wang, F., Li, G., Wu, Z., Fan, Z., Yang, M., Wu, T., et al. (2019). Tracking diphyodont development in miniature pig in vitro and in vivo. Biol. Open, bio.037036. doi:10.1242/bio.037036.

Wang, F., Xiao, J., Cong, W., Li, A., Song, T., Wei, F., et al. (2014a). Morphology and chronology of diphyodont dentition in miniature pigs, Sus Scrofa. Oral Dis. 20, 367–379. doi:10.1111/odi.12126.

Wang, F., Xiao, J., Cong, W., Li, A., Wei, F., Xu, J., et al. (2014b). Stage-specific differential gene expression profiling and functional network analysis during morphogenesis of diphyodont dentition in miniature pigs, Sus Scrofa. BMC Genomics 15, 103. doi:10.1186/1471-2164-15-103.

Wang, X.-P., Aberg, T., James, M. J., Levanon, D., Groner, Y., and Thesleff, I. (2005). Runx2 (Cbfa1) Inhibits Shh Signaling in the Lower but not Upper Molars of Mouse Embryos and Prevents the Budding of Putative Successional Teeth. J. Dent. Res. 84, 138–143. doi:10.1177/154405910508400206.

Wang, Y.-Q., Li, C.-K., Li, Q., and Li, D.-S. (2016). A synopsis of Paleocene stratigraphy and vertebrate paleontology in the Qianshan Basin , Anhui , China. 54.

Wang, Y., Meng, J., Xijun, N., and Chuankui, L. (2007). Major events of Paleogene mammal radiation in China. Geol. J. 42, 415–430. doi:10.1002/gj.1083.

Whitlock, J. A., and Richman, J. M. (2013). Biology of tooth replacement in amniotes. Int. J. Oral Sci. 5, 66–70. doi:10.1038/ijos.2013.36.

Wood, A. E. (1940). The Mammalian Fauna of the White River Oligocene: Part III. Lagomorpha. Trans. Am. Philos. Soc. 28, 271. doi:10.2307/1005524.

Xie, L. K., Wangrangsimakul, K., Suttapreyasri, S., Cheung, L. K., and Nuntanaranont, T. (2011). A preliminary study of the effect of low intensity pulsed ultrasound on new bone formation during mandibular distraction osteogenesis in rabbits. Int. J. Oral Maxillofac. Surg. 40, 730–736. doi:10.1016/j.ijom.2011.03.016.

Yan, Q., Zhang, Q., Yang, H., Zou, Q., Tang, C., Fan, N., et al. (2014). Generation of multi-gene knockout rabbits using the Cas9/gRNA system. Cell Regen. 3, 3:12. doi:10.1186/2045-9769-3-12.

Yardin, M. (1968). Evolution des dents du jeune lapin. Mammalia 32, 677–689. doi:10.1515/mamm.1968.32.4.677.

Zeichner-David, M., Oishi, K., Su, Z., Zakartchenko, V., Chen, L.-S., Arzate, H., et al. (2003). Role of Hertwig's epithelial root sheath cells in tooth root development. Dev. Dyn. 228, 651–663. doi:10.1002/dvdy.10404.

ANNEXES

Annex 1: Plasticity within the niche ensures the maintenance of a Sox2$^+$ stem cell population in the mouse incisor

Maria Sanz-Navarro[1,2], Kerstin Seidel[3], Zhao Sun[4], Ludivine Bertonnier-Brouty[1,5], Brad A. Amendt[4,6], Ophir D. Klein[3,7] and Frederic Michon[1,8,*]

[1] Helsinki Institute of Life Sciences, Institute of Biotechnology, University of Helsinki, 00014 Helsinki, Finland.

[2] Orthodontics, Department of Oral and Maxillofacial Diseases, University of Helsinki, 00290 Helsinki, Finland.

[3] Department of Orofacial Sciences and Program in Craniofacial Biology, UCSF, San Francisco, CA 94143, USA.

[4] Department of Anatomy and Cell Biology, and the Craniofacial Anomalies Research Center, The University of Iowa, Iowa City, IA 52242, USA.

[5] Département de Biologie, École Normale Supérieure de Lyon, Universitéde Lyon, 69007 Lyon, France.

[6] College of Dentistry, The University of Iowa, Iowa City, IA 52242, USA.

[7] Department of Pediatrics and Institute for Human Genetics, University of California San Francisco, San Francisco, CA 94143, USA.

[8] Keele Medical School and Institute for Science and Technology in Medicine, Keele University, Keele ST5 5BG, UK.

*Author for correspondence (frederic.michon@helsinki.fi)

Abstract

In mice, the incisors grow throughout the animal's life, and this continuous renewal is driven by dental epithelial and mesenchymal stem cells. Sox2 is a principal marker of the epithelial stem cells that reside in the mouse incisor stem cell niche, called the labial cervical loop, but relatively little is known about the role of the Sox2$^+$ stem cell population. In this study, we show that conditional deletion of Sox2 in the embryonic incisor epithelium leads to growth defects and impairment of ameloblast lineage commitment. Deletion of Sox2 specifically in Sox2$^+$ cells during incisor renewal revealed cellular plasticity that leads to the relatively rapid restoration of a Sox2-expressing cell population. Furthermore, we show that Lgr5-expressing cells are a subpopulation of dental Sox2$^+$ cells that also arise from Sox2$^+$ cells during tooth formation. Finally, we show that the embryonic and adult Sox2$^+$ populations are regulated by distinct signalling pathways, which is reflected in their distinct transcriptomic signatures. Together, our findings demonstrate that a Sox2$^+$ stem cell population can be regenerated from Sox2$^-$ cells, reinforcing its importance for incisor homeostasis.

© 2018. Published by The Company of Biologists Ltd | Development (2018) 145, dev155929. doi:10.1242/dev.155929

STEM CELLS AND REGENERATION

RESEARCH ARTICLE

Plasticity within the niche ensures the maintenance of a *Sox2*$^+$ stem cell population in the mouse incisor

Maria Sanz-Navarro[1,2], Kerstin Seidel[3], Zhao Sun[4], Ludivine Bertonnier-Brouty[1,5], Brad A. Amendt[4,6], Ophir D. Klein[3,7] and Frederic Michon[1,8,*]

ABSTRACT

In mice, the incisors grow throughout the animal's life, and this continuous renewal is driven by dental epithelial and mesenchymal stem cells. *Sox2* is a principal marker of the epithelial stem cells that reside in the mouse incisor stem cell niche, called the labial cervical loop, but relatively little is known about the role of the *Sox2*$^+$ stem cell population. In this study, we show that conditional deletion of *Sox2* in the embryonic incisor epithelium leads to growth defects and impairment of ameloblast lineage commitment. Deletion of *Sox2* specifically in *Sox2*$^+$ cells during incisor renewal revealed cellular plasticity that leads to the relatively rapid restoration of a *Sox2*-expressing cell population. Furthermore, we show that *Lgr5*-expressing cells are a subpopulation of dental *Sox2*$^+$ cells that also arise from *Sox2*$^+$ cells during tooth formation. Finally, we show that the embryonic and adult *Sox2*$^+$ populations are regulated by distinct signalling pathways, which is reflected in their distinct transcriptomic signatures. Together, our findings demonstrate that a *Sox2*$^+$ stem cell population can be regenerated from *Sox2*$^-$ cells, reinforcing its importance for incisor homeostasis.

KEY WORDS: Incisor, Stem cells, *Sox2*, *Lgr5*, Hierarchy, Morphogenesis, Renewal

INTRODUCTION

Renewing organs, such as hair, intestine and certain types of teeth, rely on the ability of stem cells (SCs) to self-renew and differentiate. To ensure tissue homeostasis, the number of SCs in a niche must be kept stable, and conditions such as tissue damage can trigger an SC population increase (Fuchs and Chen, 2012). When the damage is too great or when it affects SCs themselves, the early SC progeny or the niche cells can exhibit plasticity and de-differentiate in order to replenish the SC compartment (Rompolas et al., 2013; Tian et al., 2011). These capacities reflect the potential of the SC niche to control cell fate (Lane et al., 2014).

To compensate for its constant wear, the mouse incisor grows continuously. This life-long growth is fuelled by dental epithelial SCs located at the proximal end of the incisor, in a structure called the labial cervical loop (laCL). The laCL arises from the dental epithelium around embryonic day (E) 14, and its various cell types are well defined prior to birth (E19) (Fig. 1A). The stellate reticulum (SR) is a pool of epithelial cells located at the core of the laCL. It is surrounded posteriorly and labially by the columnar outer enamel epithelium (OEE), and anteriorly and lingually by the columnar inner enamel epithelium (IEE). The IEE houses the early SC progeny, namely the transient-amplifying (TA) cells and the stratum intermedium (SI) cells (Harada et al., 2006). The TA cells generate pre-ameloblasts, which then differentiate into enamel-secreting ameloblasts (Fig. 1A) (Thesleff and Tummers, 2008). Initial reports suggesting that dental epithelial SCs are present in the SR (Harada et al., 1999) were followed by *in vivo* genetic fate mapping experiments demonstrating that *Gli1* (Seidel et al., 2010), *Sox2* (Juuri et al., 2012), *Bmi1* (Biehs et al., 2013), *Lrig1* and *Igfbp5* (Seidel et al., 2017) mark SCs in the laCL; a number of potential dental SC markers that have not yet been tested through lineage tracing were recently identified using gene co-expression analysis (Seidel et al., 2017). Moreover, the expression of some genes that mark SCs in other organs, such as *Lgr5* (Suomalainen and Thesleff, 2009), *Abcg2*, *Oct3/4* (*Pou5f1*), *Tbx1*, *Pitx2* and *Yap* (*Yap1*) (Cao et al., 2013; Gao et al., 2015; Hu et al., 2017; Li et al., 2011), has also been detected in the incisor SC niche.

SOX2, the focus of this study, is an important transcription factor in the maintenance of pluripotency (Takahashi et al., 2006), formation of endodermal organs (Que et al., 2007; Xie et al., 2014) and development of ectodermal tissues (Arnold et al., 2011; Clavel et al., 2012). We previously reported that SOX2 is a marker for dental epithelial SCs in the mouse incisor and that it is not expressed in the mesenchyme (Juuri et al., 2012). Recently, we showed that deletion of *Sox2* in the dental epithelium at E10.5 ($Pitx2^{Cre/+};Sox2^{fl/fl}$) drastically impairs incisor formation and leads to disappearance of the organ by E18. We also showed that *Sox2* deletion using a ubiquitous promoter during incisor renewal ($Rosa26^{CreER/+};Sox2^{fl/fl}$) slowed down incisor growth (Sun et al., 2016).

Here, we deleted *Sox2* in the epithelium at E11 using $Shh^{GFP\text{-}Cre/+}$ (Dassule and McMahon, 1998) to analyse the effects on cell differentiation. We found that SOX2 is necessary for ameloblast lineage commitment. Also, we specifically deleted *Sox2* expression from *Sox2*$^+$ cells ($Sox2^{CreER/fl}$) and assessed the consequences of short- and long-term deletion on the laCL. We analysed the effect on laCL shape and on the expression pattern of *Sox2* as well as *Lgr5*, a marker that has been suggested to be expressed by SCs in the laCL (Chang et al., 2013; Suomalainen and Thesleff, 2009). We found that loss of *Sox2* led to a change in laCL morphology and to the disappearance of *Lgr5* expression. Moreover, our data suggest that SR cells are capable of re-establishing a cell population expressing *Sox2* and *Lgr5*. Together, these data indicated the importance of maintaining a *Sox2*$^+$ SC population within the adult laCL. Moreover,

[1]Helsinki Institute of Life Sciences, Institute of Biotechnology, University of Helsinki, 00014 Helsinki, Finland. [2]Orthodontics, Department of Oral and Maxillofacial Diseases, University of Helsinki, 00290 Helsinki, Finland. [3]Department of Orofacial Sciences and Program in Craniofacial Biology, UCSF, San Francisco, CA 94143, USA. [4]Department of Anatomy and Cell Biology, and the Craniofacial Anomalies Research Center, The University of Iowa, Iowa City, IA 52242, USA. [5]Département de Biologie, École Normale Supérieure de Lyon, Université de Lyon, 69007 Lyon, France. [6]College of Dentistry, The University of Iowa, Iowa City, IA 52242, USA. [7]Department of Pediatrics and Institute for Human Genetics, University of California San Francisco, San Francisco, CA 94143, USA. [8]Keele Medical School and Institute for Science and Technology in Medicine, Keele University, Keele ST5 5BG, UK.

*Author for correspondence (frederic.michon@helsinki.fi)

F.M., 0000-0003-4305-305X

Received 11 June 2017; Accepted 15 November 2017

Development (2018) 145, dev155929. doi:10.1242/dev.155929

we have observed that the transcriptomic signature of the *Sox2*$^{+}$ cells varies between embryonic and adult stages, reflecting their distinct potential. Our data reveal a complex hierarchy in the laCL, and a degree of cellular plasticity not previously identified in the incisor SC niche.

RESULTS

Sox2 expression pattern changes during the transition from embryonic to adult incisor

Our previous use of a reporter mouse strain (*Sox2*^{GFP}), immunohistochemistry, and RNA *in situ* hybridisation pointed to distinct *Sox2*-expressing populations (Juuri et al., 2012), and thus the *Sox2*$^{+}$ cell population in the mouse incisor had not yet been definitively identified. Therefore, we used the highly sensitive RNAscope single mRNA *in situ* hybridisation method (Wang et al., 2012) to investigate the expression pattern of *Sox2* during tooth morphogenesis (Fig. 1). Consistent with previous reports (Juuri et al., 2012; Sun et al., 2016; Zhang et al., 2012), *Sox2* was expressed throughout the dental epithelium at E13.5 (Fig. 1B) and became gradually restricted to the laCL perinatally (Fig. 1C). At postnatal day (P) 60, the *Sox2* transcripts appeared more scattered than at P3, when most cells within the laCL are *Sox2*$^{+}$ (Juuri et al., 2012). The use of this more sensitive method allowed the detection of *Sox2* transcripts in several epithelial lineages of the P60 incisor (Fig. 1D). Although most of the *Sox2*$^{+}$ cells were found in the SR and enamel epithelium (EE) of the laCL, we detected transcripts in the TA cells, pre-ameloblasts, ameloblasts, and the SI (Fig. 1D′). We have previously shown that *Sox2* and its upstream regulator *Fgf8* are regulated by miRNAs in the laCL (Juuri et al., 2012; Michon et al., 2010), and this miRNA regulation could be the cause of the more restricted SOX2 protein domain.

Deletion of *Sox2* leads to incisor defects during morphogenesis

To decipher the function of SOX2 during incisor morphogenesis, we conditionally deleted the gene in the dental epithelium. We have previously demonstrated that the timing of Cre-driven recombination can dramatically impact the dental phenotype (Cao et al., 2010; Michon et al., 2010; Seidel et al., 2010). As the *Pitx2*-driven *Sox2*^{cKO} led to the absence of incisors at late stages of morphogenesis (Sun et al., 2016), we decided to use *Shh*$^{Cre\text{-}GFP/+}$ to delete *Sox2*. *Shh* is expressed later than *Pitx2*, and almost all dental epithelial cells derive from early *Shh*$^{+}$ cells (Juuri et al., 2013b). The *Shh*-driven *Sox2*^{cKO} mice have a hyperplastic dental epithelium in the second and third molars (Juuri et al., 2013a), but no incisor phenotype has been described. As the incisors of the *Shh-Cre; Sox2*$^{fl/fl}$ mice had a different phenotype to that previously reported in *Pitx2-Cre;Sox2*$^{fl/fl}$ mice (Sun et al., 2016), and the incisor was present until the end of embryogenesis, this gave us the opportunity to analyse the dental phenotype at later developmental stages.

We used RNAscope to determine the efficiency of *Sox2* ablation in *Shh-Cre;Sox2*$^{fl/fl}$ mice. By E13.5, essentially no *Sox2* transcripts were detected in the incisor epithelium (Fig. S1A,B). Moreover, the incisor shape was drastically affected in the mutants. At this stage, the control incisor had invaginated into the dental mesenchyme, and the forming laCL contained a large *Sox2*$^{+}$ cell population (Fig. S1A).

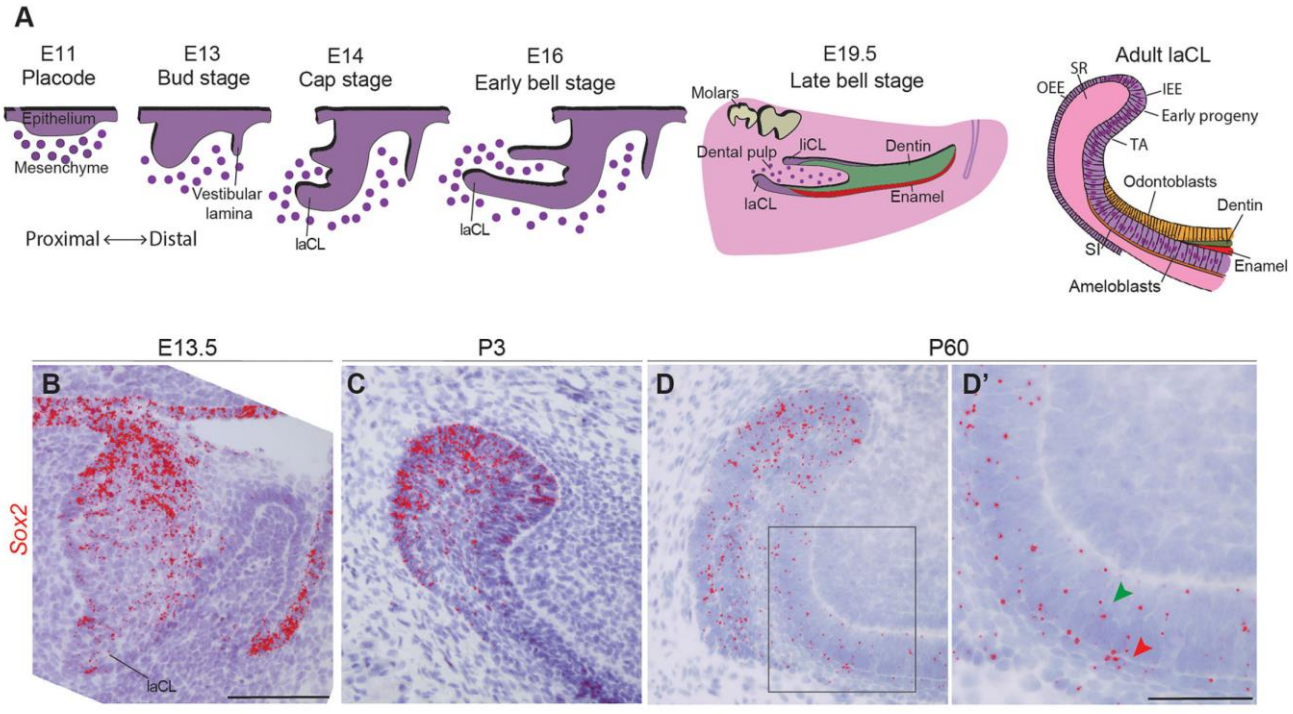

Fig. 1. *Sox2* expression during incisor morphogenesis. (A) Illustration of mouse incisor development, representing the morphological steps from placode stage to adult. At E14, the dental lingual epithelium gives rise to the lingual cervical loop (liCL), while the labial side originates a larger structure: the labial cervical loop (laCL). The adult laCL is composed of the stellate reticulum (SR), the outer enamel epithelium (OEE) and inner enamel epithelium (IEE). The latter gives rise to the stem cell early progeny, namely the transient-amplifying cells (TA), the stratum intermedium (SI) and the ameloblasts. (B) *Sox2* expression (red) is present throughout the entire dental epithelium at E13.5, at highest levels in the lingual side. (C) At P3, *Sox2* expression is more sparse, and restricted to the laCL. (D,D′) In adult mice (P60), *Sox2* is expressed in the laCL (SR, IEE, OEE and TA cells), as well as in the pre-ameloblasts, ameloblasts (green arrowhead) and SI (red arrowhead). The boxed region in D is magnified in D′. Scale bars: B-D, 100 µm; D′, 50 µm.

Development (2018) 145, dev155929. doi:10.1242/dev.155929

The incisor of the *Sox2*^{cKO} littermates displayed a shallow laCL and a wider dental lamina (Fig. S1B). As previously reported (Sun et al., 2016), this phenotype was accompanied by an enlargement of the *Shh*$^{+}$ population (Fig. S1C,D). At E13.5, both the basal (high P-cadherin) and suprabasal (low P-cadherin) (Jussila et al., 2015) cell compartments were present in the mutant incisors (Fig. S1E,F).

To determine the consequences of this early phenotype for subsequent dental morphogenesis, we reconstructed the dental epithelium from micro-computed tomography (micro-CT) scans of *Sox2*^{cKO} embryos and their control littermates from E13.5 to E18.5. The three-dimensional (3D) renderings showed that the morphology of the *Sox2*^{cKO} incisor differed from that of control littermates at all developmental stages (Fig. 2Aa-h), and the shape and length of the incisors varied both among and within individual embryos (Fig. 2Ae-h; data not shown). A recurrent trait in the *Sox2*^{cKO} incisors was the presence of clefts in the labial epithelium (Fig. 2Af-h). These defects were visualised in histological sections as discontinuities in the epithelial tissue (Fig. 2B, red arrowhead). Histological sections also evidenced defective cell differentiation at E18.5, with ameloblast-like cells present in the lingual region (Fig. 2B, green arrowhead).

We observed no significant differences in incisor length at E15.5 (Fig. 2C). However, *Sox2*^{cKO} lower incisors were significantly shorter than those of control littermates at E17.5, and they did not grow further after this stage. The tooth size defect was not attributable to decreased cell proliferation, as we did not detect any significant difference in the density of phospho-histone H3 (pH-H3)$^{+}$ cells in the dental epithelium at E13.5, nor in the laCL at E18.5 (Fig. 3A). These results are in line with the report on the molars of *Shh*$^{Cre\text{-}GFP/+}$;*Sox2*$^{fl/fl}$ embryos (Juuri et al., 2013a). Moreover, we did not observe any obvious increase in apoptotic cells by TUNEL assay in the *Sox2*^{cKO} (Fig. S2), indicating that *Sox2* loss does not affect cell death rate, in agreement with other *Sox2* loss-of-function models (Sun et al., 2016). Taken together, our data indicated a role for SOX2 in incisor morphogenesis and dental epithelium cell differentiation.

The laCL and its cell populations are established in *Shh-Cre; Sox2*$^{fl/fl}$ mice

Next, we investigated the structure of the laCL upon *Sox2* deletion in *Shh-Cre;Sox2*$^{fl/fl}$ embryos. As expected from the epithelial reconstructions (Fig. 2A), laCL volume was drastically reduced in the *Sox2*^{cKO} (Fig. 3B), but the structure was not completely absent. Hence, in addition to *Sox2* we assessed via RT-qPCR the expression of *Sfrp5*, which is a marker of early *Sox2*$^{+}$ cell progeny (Juuri et al., 2012), *Shh*, which is expressed in TA cells, pre-ameloblasts and immature ameloblasts (Seidel et al., 2010), and *Lgr5*, which is expressed by a minor cell population in the laCL and marks SCs in several adult organs (Chang et al., 2013; Suomalainen and Thesleff, 2009; Yang et al., 2015) (Fig. 3C). *Sox2* expression was drastically reduced in the mutant incisors. *Sfrp5* and *Shh* expression levels were also decreased, indicating defects in cell differentiation. Surprisingly, reduced SHH expression was found only in the lingual side of the incisor (Fig. S3). We did not detect an impact on *Lgr5*

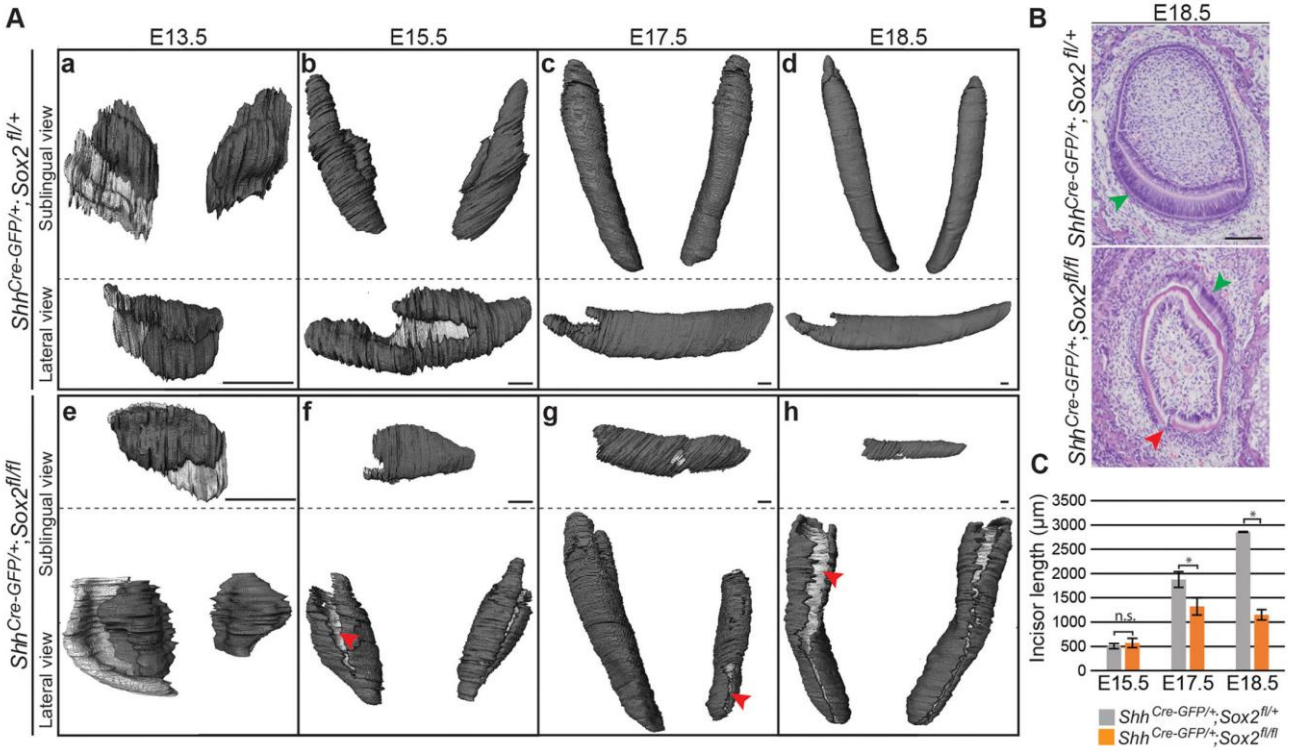

Fig. 2. Mouse lower incisor shape and length are regulated by *Sox2*. (A) 3D reconstructions from micro-CT scans showing the dental epithelium in dark grey. The internal layer of the dental epithelium (b-d,f-h) or vestibular lamina (a,e) appears in light grey. *Sox2*^{cKO} incisors exhibit an aberrant morphology at all embryonic stages. At E13.5, the tooth domain is broader, and at E15.5 clefts (red arrowhead) appear. The defects can vary within the same individual (g). (B) Histological staining of frontal sections shows that the well-organised ameloblast layer seen in control incisor (green arrowhead) is not visible in *Sox2*^{cKO} individuals. A cleft is visible on the labial side of the mutant incisor (red arrowhead). (C) The length of the epithelial compartment is similar in the control and *Sox2*^{cKO} at E15.5. The incisor length increases over 2 mm from E15.5 to E18.5 in controls, but only 0.6 mm in mutants. E17.5, **P*=0.016; E18.5, **P*=1×10^{-5}; n.s., not significant. *n*=3. Scale bars: A, 50 µm; B, 100 µm.

Development (2018) 145, dev155929. doi:10.1242/dev.155929

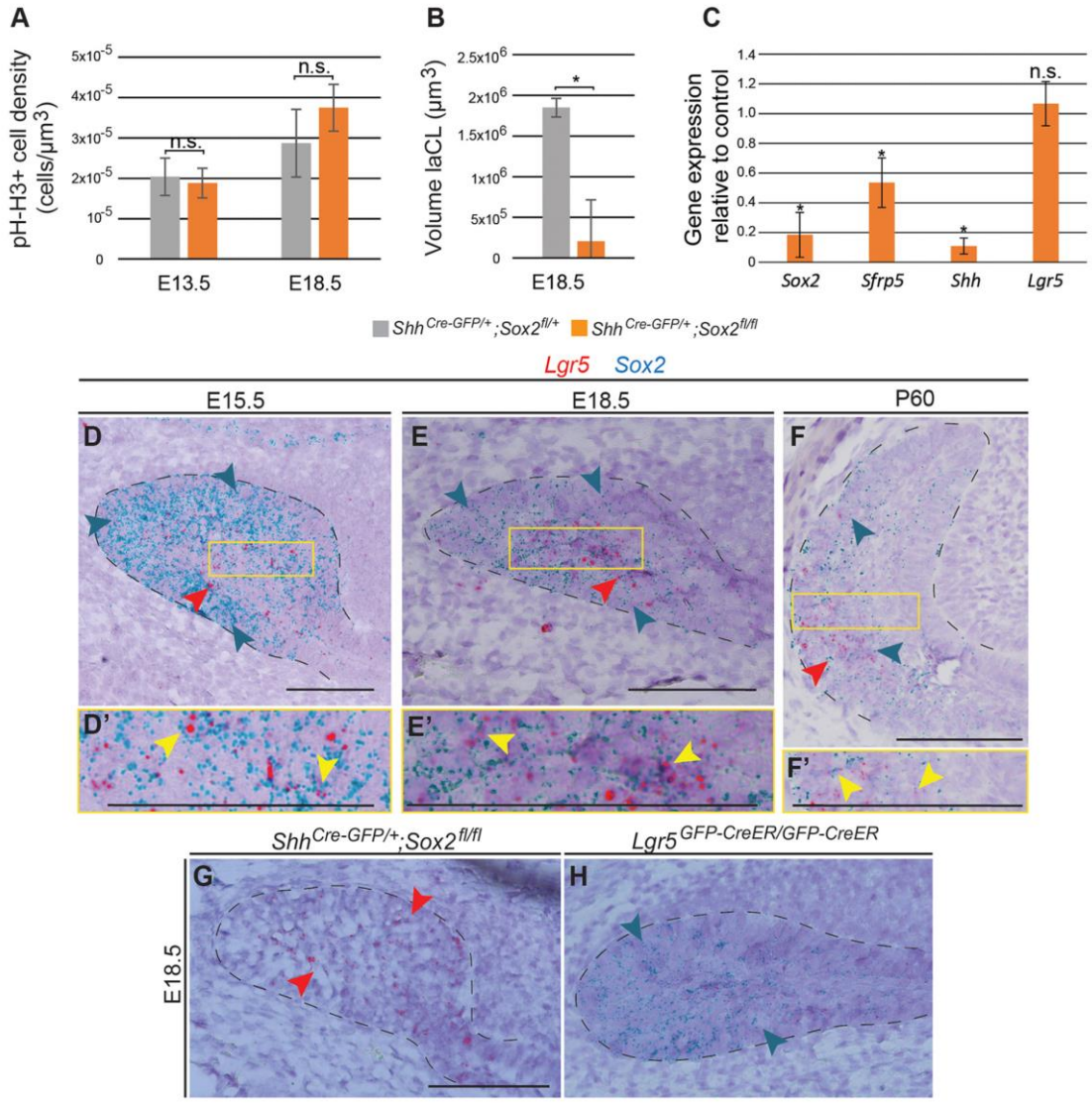

Fig. 3. *Sox2*^{cKO} impacts laCL volume and the expression of different differentiation markers. (A) Quantification of phospho-histone H3 (pH-H3)$^{+}$ cell density in the dental epithelium reveals no significant defect in cell proliferation in *Sox2*^{cKO}. (B) The volume of the E18.5 laCL is drastically decreased in *Sox2*^{cKO}. **P*=0.026. (C) qPCR analysis demonstrates that *Sox2*^{cKO} induces a decrease in *Sfrp5* and *Shh* expression. *Lgr5* expression remains unaffected. **P*<0.05. (A-C) *n*=3. (D) *Sox2* transcripts (blue arrowheads in all images) at E15.5 are detected in all cells of the laCL (outlined). *Lgr5* transcripts (red arrowheads in all images) mark a subset of the *Sox2*$^{+}$ population in the SR. (E) At E18.5 the *Sox2* expression domain is smaller than at previous stages. *Lgr5* expression is localised to the SR. The laCL houses the expression of both *Sox2* (EE and SR) and *Lgr5* (SR). (F) In the adult incisor, *Sox2* transcripts are localised in different areas of the laCL, while *Lgr5* expression is confined to the most proximal part. (D′,E′,F′) Magnifications of the boxed regions in D,E,F. Yellow arrowheads indicate cells expressing both *Lgr5* and *Sox2* transcripts. (G,H) *Sox2*^{cKO} shows no changes in *Lgr5* expression, as *Lgr5*^{KO} displays a normal *Sox2* expression pattern. Scale bars: 100 µm. qPCR.

expression, which has been reported at E14.5 in the molar bud (Kawasaki et al., 2014) but in the laCL incisor only after E16.5 (Suomalainen and Thesleff, 2009). However, the sensitivity of the RNAscope assay enabled the detection of *Lgr5* transcripts already at E15.5 in the incisor laCL (Fig. 3D-F) and, interestingly, the expression patterns of *Sox2* and *Lgr5* overlap (Fig. 3D-F′, Fig. S4).

To further study the connection between *Sox2* and *Lgr5* expression, we analysed their expression patterns upon deletion of either gene (Fig. 3E,G,H). *Lgr5* null mice (*Lgr5*^{KO}) die neonatally due to gastrointestinal problems and ankyloglossia (Morita et al., 2004). These mice also exhibit cleft palate, but we did not identify morphological abnormalities in the laCL. In the control embryos, *Sox2* transcripts were found in the EE and SR, and *Lgr5* transcripts were mainly restricted to the SR. Interestingly, in the *Sox2*^{cKO} laCL, *Lgr5* expression was maintained, and the *Sox2* expression pattern did not change in the *Lgr5*^{KO} incisor (Fig. 3G,H). These observations highlighted the importance of *Sox2* for ameloblast lineage commitment, but not for establishment of the laCL.

Sox2 expression is quick to recover after transient *Sox2* deletion in the adult incisor

Having identified the importance of *Sox2* for dental epithelial cell differentiation during embryogenesis, we next analysed the effects of *Sox2* absence in the renewing incisor. As *Sox2*^{cKO} mice die perinatally, we used *K14-CreER* mice (Huelsken et al., 2001; Järvinen et al., 2006; Vasioukhin et al., 1999) to delete *Sox2* in the

Development (2018) 145, dev155929. doi:10.1242/dev.155929

laCL. We investigated the morphology and *Sox2* expression pattern at 2 days, 11 days and 1 month after Cre activation. No obvious differences were observed in histological sections (Fig. S5A) nor in the SOX2 pattern (by immunofluorescence staining; data not shown). We also analysed the expression levels of *Sox2*, *Sfrp5*, *Lrg5* and *Bmi1* 24 h after induction via qPCR and found no statistically significant differences from controls (data not shown). This suggested a lack of recombination in the laCL, and our examination of *Sox2* and keratin 14 (*K14*) expression in the adult laCL at the protein and transcript levels (Fig. S5B,C) showed minimal overlap. *K14* was expressed in the SR region, but not in the most lingual part of the SR, nor in the IEE, where many of the $Sox2^{+}$ cells reside; this is in line with the low recombination levels reported in the OEE with this Cre line (Hu et al., 2017).

Therefore, we generated $Sox2^{CreER/fl}$ mice to specifically delete *Sox2* in the $Sox2^{+}$ cells upon Tamoxifen administration. Two-month-old $Sox2^{CreER/fl}$ mice were administered Tamoxifen for three consecutive days. We then examined the laCL at 3 days, 1 week and 4 weeks chase (Fig. 4A), and $Sox2^{fl/+}$ littermates were used as controls. We also injected adult $Sox2^{CreER/fl}$ mice with corn oil and observed no aberrant phenotype (Fig. S6). After 3 days of chase, we observed a large decrease in the number of *Sox2* transcripts (Fig. 4B,C). Moreover, the spherical shape of the laCL was lost in the mutants, which instead exhibited an elongated SC niche (Fig. 4D,E). However, the transient loss of *Sox2* expression did not lead to cell death (Fig. S7), and after 5 days without Cre activation some *Sox2* transcripts were detected, although the expression was fainter than in the control laCL (Fig. 4F,G). Interestingly, by this time point, laCL shape was restored (Fig. 4H,I). At 1 month chase, we did not detect any differences in laCL morphology or *Sox2* expression pattern between control and mutant (Fig. 4J,K).

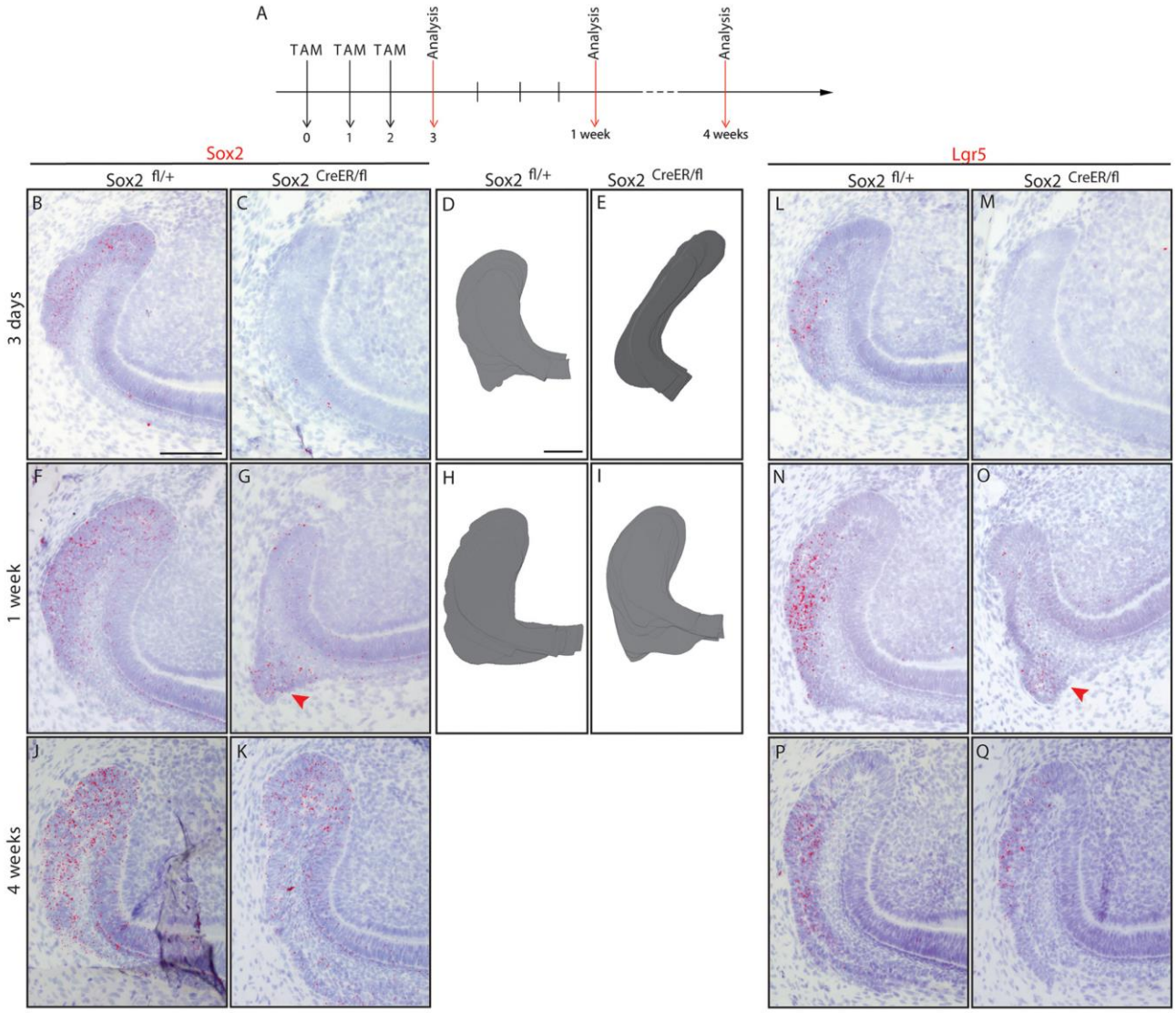

Fig. 4. *Sox2* and *Lgr5* expression are lost then restored in $Sox2^{CreER/fl}$ laCL. (A) The experimental setup. (B,C) *Sox2* and (L,M) *Lgr5* expression are almost abolished after three Tamoxifen injections in $Sox2^{CreER/fl}$ mice. (D,E) The $Sox2^{CreER/fl}$ laCL is narrower than that of controls. One week after the first Tamoxifen administration, a faint *Sox2* signal is detected in the laCL (F,G, arrowhead), while the *Lgr5* expression pattern appears to be normal in the mutant (N,O, arrowhead). (H,I) At this stage, the morphology of the laCL appears to be normal. (J,K,P,Q) One month after Cre recombinase activation, the mouse incisor SC niche of $Sox2^{CreER/fl}$ mice is indistinguishable from that of control littermates. Scale bars: 100 µm.

Development (2018) 145, dev155929. doi:10.1242/dev.155929

Lgr5 marks a small cell population in the laCL (Suomalainen and Thesleff, 2009; Yang et al., 2015), and its expression pattern overlaps with that of *Sox2* (Fig. 3D-F, Fig. S3). Therefore, we investigated the effect of *Sox2* loss on *Lgr5* expression. After 3 days of Tamoxifen administration, *Lgr5* transcripts were greatly decreased (Fig. 4L,M), similarly to *Sox2*. Four days later, *Lgr5* expression levels were similar to those of the control (Fig. 4N,O) and returned to normal after 1 month of chase (Fig. 4P,Q).

To evaluate the effect of long-term *Sox2* loss, we administered Tamoxifen to $Sox2^{CreER/fl}$ mice seven times over 11 days. Incisors were collected 1 day after the last injection (Fig. 5A). As expected, very few *Sox2* transcripts were detected in the laCL, whereas controls exhibited expression of *Sox2* as previously reported (Fig. 5B-C′). *Lgr5* expression was faint as well (Fig. 5D-E′). Very few *Sox2* transcripts were detected in the area where *Lgr5* expression was localised. Moreover, the morphology of the laCL was not affected, similar to results obtained with another $Sox2^{cKO}$

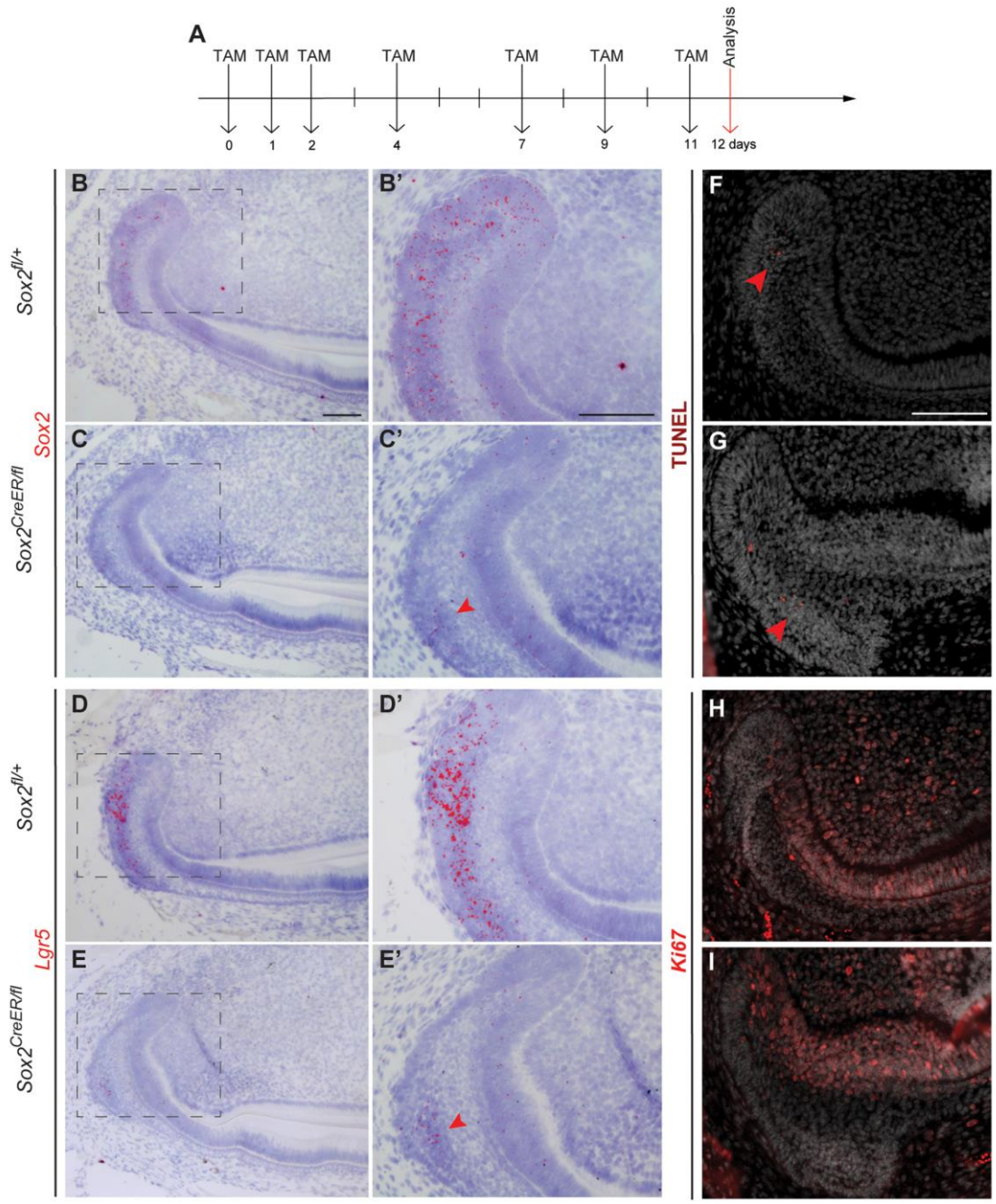

Fig. 5. A day after an 11-day *Sox2* ablation, the *Sox2* expression pattern, proliferation and cell differentiation appear disturbed. (A) The experimental setup. (B-E′) A small amount of *Sox2* transcripts is detected in the proximal area of the SR (arrowhead), where faint expression of *Lgr5* is seen (arrowhead). (F,G) TUNEL assay confirms that there is no increase in apoptosis in the laCL, where only a few positive cells were found (arrowheads). (H,I) The domain of proliferating cells, visualised with Ki67 staining, appears similar to the control. Scale bars: 100 µm.

Development (2018) 145, dev155929. doi:10.1242/dev.155929

model *Rosa26*$^{CreER/+}$;*Sox2*$^{fl/fl}$ (Sun et al., 2016). We further examined the cellular response to the deletion of *Sox2* in the *Sox2*$^+$ SCs and did not observe any obvious increase in cell death or aberrant cell proliferation (Fig. 5F-I).

The *Sox2*$^+$ population is regenerated from the SR

The restoration of a *Sox2*$^+$ cell population days after deleting *Sox2* suggested a high degree of plasticity within the laCL. To understand the origin of the newly generated *Sox2*$^+$ population, we studied the dividing cells during laCL restoration using EdU incorporation. Under normal renewal conditions, dividing cells are localised to the lingual and distal part of the laCL, the IEE, the TA cells, and the distalmost SR cells (Hu et al., 2017) (Fig. 6A). In comparing this pattern with *Sox2* expression, it is apparent that most of the proliferating cells in the laCL do not strongly express *Sox2* (Fig. 6B). In addition, the cells in the proximal region of the laCL are quiescent (Seidel et al., 2010). We marked the proliferative cells 3 days after the first Tamoxifen administration and analysed their position and quantity 4 days later (Fig. 6C). In the control, the EdU$^+$ cells were located in the central and proximal sections of the SR, where *Sox2* is faintly expressed (Fig. 6D-E′). By contrast, in the *Sox2*$^{CreER/fl}$ mice, these cells were displaced to the proximalmost part, close to the *Lgr5*$^+$ cell area (Fig. 6F-G′). Furthermore, the percentage of EdU$^+$ cells was significantly increased in the mutant SR compared with the control (Fig. 6H). This reflected an increase in proliferation in the SR at the beginning of the rescue period.

Modulation of the *Sox2*$^+$ cell signature in embryonic versus adult incisors

The observation that almost all laCL cells are *Sox2*$^+$ at E15.5 (Fig. S3), when *Lgr5* expression appears, suggested that embryonic *Sox2*$^+$ cells might give rise to the *Lgr5*$^+$ subpopulation during incisor formation. However, during laCL regeneration after *Sox2* ablation, the *Sox2*$^+$ cells seemed to partially arise from the subpopulation expressing both *Sox2* and *Lgr5* (Fig. 4F,G,N,O). This observation raised the question: how similar are the *Sox2*$^+$ populations in the forming and renewing incisor? We therefore compared the transcriptome of the *Sox2*$^+$ cells in the early incisor (E14.5) with that of the *Sox2*$^+$ cells in the renewing incisor (P30) using gene expression microarrays. We first extracted the transcripts that were similarly expressed in embryonic and adult *Sox2*$^+$ cells ($-2<$fold change<2) and compared them with the transcriptome of mouse embryonic stem cells (mESCs) as a naïve cell reference (Fig. 7A). Then, we compared the transcriptomes of the embryonic and adult *Sox2*$^+$ cells (Fig. 7B). We selected the transcripts that were statistically significant ($P<0.05$, ANOVA) and exhibited a consequential fold change (fold change>2) (Table S1).

For the first analysis (*Sox2*$^+$ versus mESCs), we observed that 927 transcripts (2.34% of the signature) were enriched in *Sox2*$^+$ cells, independent of their stage, and 1583 transcripts (4% of the signature) were downregulated. This observation reflected that ~6.34% of the signature was differentially regulated in *Sox2*$^+$ cells compared with mESCs (Fig. 7A, Table S2). We compared the gene ontology processes (GOPs) between these samples and found that 187 were activated in *Sox2*$^+$ cells, including those specific to ectodermal organ formation and regulation, and odontogenesis (Table S3). Also, both canonical and non-canonical Wnt signalling were activated. Among the enriched genes, we examined *Vangl2* as a test case because it is a member of the planar cell polarity signalling pathway (non-canonical Wnt). Moreover, its expression has previously been reported in the ameloblasts and odontoblasts of embryonic molars, where it regulates cell alignment (Obara et al., 2017; Wu et al., 2016). We found *Vangl2* transcripts in the incisor at E14.5 and in the adult laCL. However, in the adult stage, most of the transcripts were found in TA cells and ameloblasts, where there are fewer *Sox2*$^+$ cells (Fig. 7C-D′).

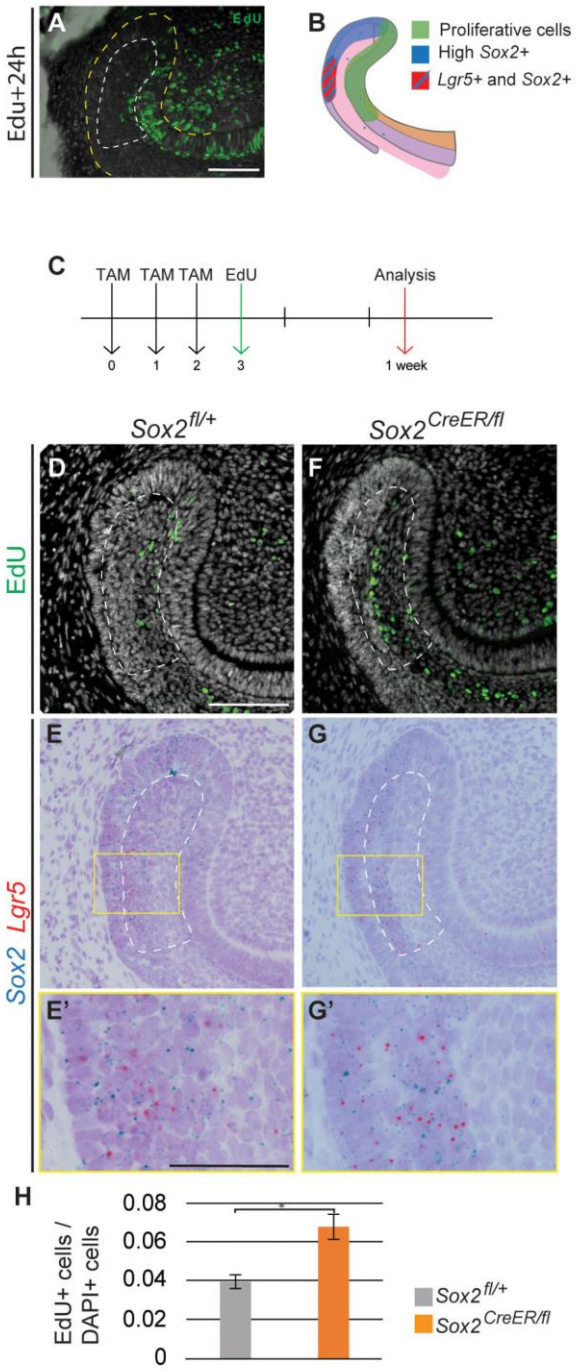

Fig. 6. Expression of *Sox2* and *Lgr5* is rescued from the SR. (A) Pattern of proliferative cells (EdU$^+$) 24 h after being administered to the mouse. (B) Schematic representation of the proliferative region and the *Sox2*$^+$ and *Lgr5*$^+$ domains. (C) The experimental setup. EdU$^+$ cells (D,F) and *Sox2* and *Lgr5* mRNA detection (E,G) performed in identical sections. (E′,G′) Higher magnifications of the boxed regions in E,G. (H) Quantification of EdU$^+$ cells in the SR of control and *Sox2*$^{CreER/fl}$ mice. The area quantified is delineated by the dashed line in D-G. Results are expressed as the fraction of EdU$^+$ cells among total cells (number of nuclei, DAPI) compared with the control. *P=0.007. Scale bars: D-G, 100 µm; E′,G′, 50 µm.

Development (2018) 145, dev155929. doi:10.1242/dev.155929

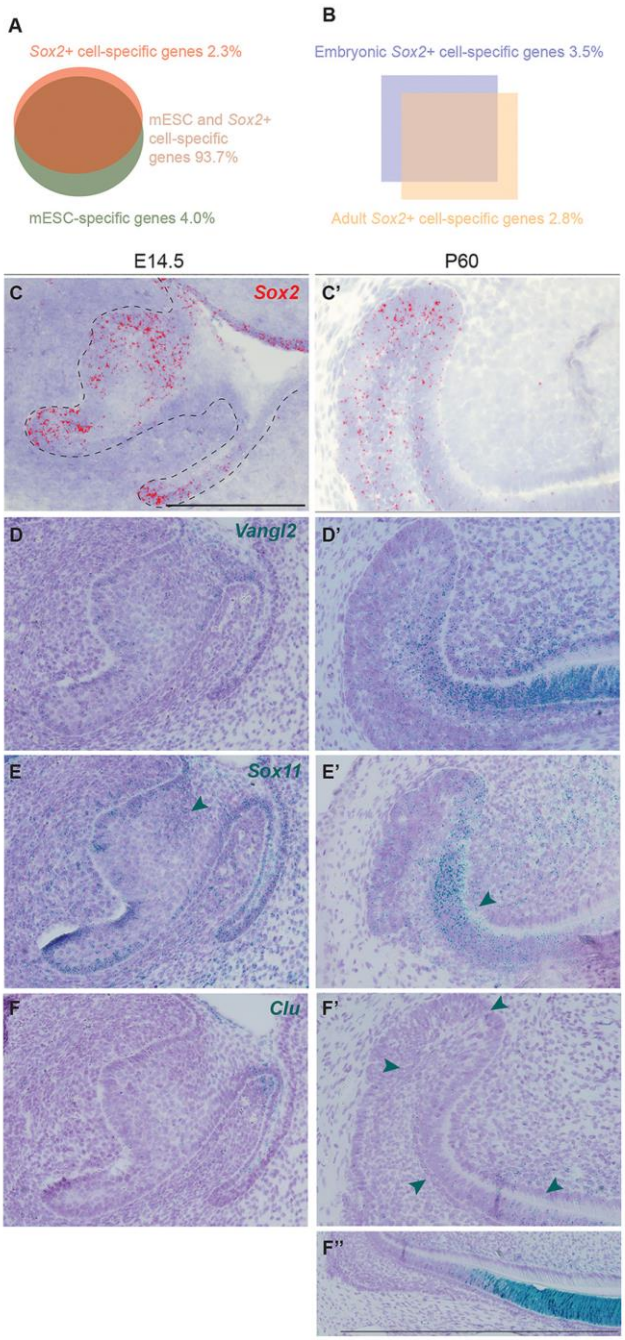

Fig. 7. Transcriptomic changes between *Sox2*$^+$ embryonic progenitors and *Sox2*$^+$ dental SC. (A) Signatures of *Sox2*$^+$ cells and mESCs overlap by 93.7%. (B) Comparison of embryonic and adult *Sox2*$^+$ cells: 3.5% of genes are specific to embryonic *Sox2*$^+$ cells, and 2.8% specific to the renewing incisor *Sox2*$^+$ SCs. (C,C′) *Sox2* expression pattern at E14.5 and adult stage. (D,D′) *Vangl2* is enriched in *Sox2*$^+$ cells compared with mESCs. It is expressed in the embryonic incisor and in the adult tooth. (E,E′) *Sox11* is highly expressed in the embryonic incisor (arrowhead) and in the surrounding mesenchyme. In the adult, expression is mostly localised to the TA cells (arrowhead). (F,F′) *Clu* expression is seen in the adult incisor (arrowheads), with the majority of transcripts found in the differentiated epithelial cells (F″). Scale bars: 100 µm.

When comparing embryonic and adult *Sox2*$^+$ cells, we observed that 3.54% of the signature (1400 hits) was enriched in embryonic cells (Fig. 7B, Table S1). Among these, 143 GOPs were enriched over 2.5 fold, including cell division regulation processes (e.g. mitotic DNA replication, DNA replication initiation) (Table S4). We also found a number of genes important for the mineralisation of forming teeth, such as embigin (Xie et al., 2015), *Six4* (Nonomura et al., 2010) and *Cxcr4* (Juuri et al., 2013b), the last of which is thought to be important for the migration of epithelial progenitors in adult laCL (Yokohama-Tamaki et al., 2015). Also, *Sox11*, which is involved in palate development (Sock et al., 2004; Watanabe et al., 2016) and expressed in the mouse embryonic molar (Dy et al., 2008; Hargrave et al., 1997), was enriched by 4.40 fold. *Sox11* transcripts were abundant in the mouse incisor epithelium at E14.5, with fewer transcripts in the adult laCL. In adults, we found *Sox11* expression also in pre-ameloblasts and in the mesenchymal compartment (Fig. 7E,E′).

Similarly, 2.75% (1089 transcripts) of the signature was enriched in the adult *Sox2*$^+$ population (Fig. 7B); 153 GOPs were enriched in adult *Sox2*$^+$ cells, with those specific for the immune response well represented (e.g. antigen processing, macrophage activation, Toll-like receptor signalling) (Table S5). The adult *Sox2*$^+$ population signature contained mineralisation markers (e.g. *Dspp*, enamelin, amelogenin, ameloblastin) and metalloproteinases (e.g. *Mmp13*, *Mmp14*, *Mmp20*) (Table S1). We also detected expression of *Barx2*, a gene involved in cell migration and differentiation (Juuri et al., 2013b). Moreover, clusterin (Clu), a stress-activated and apoptosis-associated chaperone, which has been found in embryonic and postnatal mouse molars (Chou et al., 2009; Khan et al., 2013; Shiota et al., 2012), was enriched in adult *Sox2*$^+$ cells by a fold change of 187.08. In the embryonic (E14.5) incisor we found almost negligible amounts of *Clu* expression, and few transcripts were found in the vestibular lamina at this stage. In the adult, low *Clu* expression levels were found in the laCL; higher expression levels were evident in the pre-ameloblasts and ameloblasts (Fig. 7F-F″), where *Sox2* transcripts were also found (Fig. 7C,C′).

DISCUSSION

We have previously demonstrated the role of *Sox2*$^+$ SCs in incisor renewal (Juuri et al., 2012) and in successional tooth formation in the mouse (Juuri et al., 2013a). More recently, we showed that early deletion of *Sox2* in the dental epithelium led to the absence of the incisor at E18 (Sun et al., 2016). As this prevented analysis during late time points of embryonic development, here we used the *Shh*$^{GFPCre/+}$ allele to delete *Sox2* at the dental placode stage. *Sox2* deletion using this driver resulted in growth and shape irregularities, including a curved incisor phenotype, which, together with the drastic decrease of *Shh* and *Sfrp5* expression, pointed to improper differentiation of cell lineages. Interestingly, SHH expression (Fig. S6) and ameloblast-like cells (Fig. 2B) were found on the lingual side of the incisor. SHH expression adjacent to the lingual cervical loop (liCL) has previously been linked to an expanded liCL and to ectopic lingual ameloblasts (Klein et al., 2008). However, the laCL structure was preserved, but its morphology and the cell arrangement were affected. These observations suggest an essential role for *Sox2* in lineage commitment and early differentiation towards the enamel-secreting ameloblast fate. We have previously reported that the number of proliferative cells is reduced after early *Sox2* deletion (Sun et al., 2016). However, we did not detect a significant reduction in proliferation in the *Sox2*^{cKO} model used here; instead, we propose that slower renewal is caused by defects in cell differentiation. We conclude that *Sox2* plays a key role in the maintenance of enamel organ morphology and proper cell differentiation during incisor morphogenesis.

Lgr5 marks intestinal and skin SCs (Barker et al., 2007; Haegebarth and Clevers, 2009; Jaks et al., 2008), and it also

Development (2018) 145, dev155929. doi:10.1242/dev.155929

marks a small epithelial cell population in the mouse incisor laCL (Chang et al., 2013; Suomalainen and Thesleff, 2009; Yang et al., 2015). Our identification of *Lgr5*$^{+}$ cells within the *Sox2*^{cKO} laCL indicates that other potential laCL SC populations can be present in the absence of *Sox2*. Therefore, we propose that *Sox2* expression is of importance for initiating differentiation towards ameloblast fate, but not for establishing the SC niche.

In the adult incisor, *Sox2* deletion in the *Sox2*$^{+}$ cells (*Sox2*$^{CreER/fl}$) caused a drastic, but temporary change in laCL shape, and the loss of *Lgr5* expression. We showed that *Lgr5* and *Sox2* expression overlap during embryonic and postnatal stages. Therefore, we conclude that *Lgr5*$^{+}$ cells represent a subpopulation of *Sox2*$^{+}$ cells in the developing and renewing laCL. This situation differs from other SC niches, such as the stomach, where *Lgr5* and *Sox2* mark distinct cell populations (Arnold et al., 2011).

To ensure tissue homeostasis, the number of SCs in a niche is kept stable, but tissue damage can trigger an SC increase (Fuchs and Chen, 2012). If the damage is too great, the niche cells can display signs of transient plasticity in order to replenish the SC compartment, as shown in skin (Rompolas et al., 2013) and intestine (Tian et al., 2011). Such intra-organ plasticity (Blanpain and Fuchs, 2014) requires cell de-differentiation or transdifferentiation to ensure the maintenance of organ integrity. While this mechanism is well studied in other SC niches, it has not yet been documented in the dental context. The loss of *Sox2* expression in *Sox2*$^{CreER/fl}$ mice led to a morphologically thinner laCL depleted of *Sox2*$^{+}$ and *Lgr5*$^{+}$ cells. This phenotype was rapidly rescued, and the *Lgr5*$^{+}$ subpopulation was the first to emerge, from the distal section of the laCL. Moreover, our EdU incorporation experiment demonstrated that some SR cells were plastic enough to regenerate the lost cell populations within the laCL.

Taken together, our data suggest that after damage the SR cells regenerate first a *Sox2*$^{+}$ *Lgr5*$^{+}$ double-positive cell population, and then a *Sox2*$^{+}$ *Lgr5*$^{-}$ population (Fig. 8A-D). Also, these results suggest that *Sox2* marks a heterogeneous population, where different lineage specificities exist. However, long-term ablation of *Sox2* did not lead to laCL shape malformation, and the laCL maintained a very small *Sox2*$^{+}$ *Lgr5*$^{+}$ cell population (Fig. 8E).

We have previously reported that the global deletion of *Sox2* (*Rosa26*$^{CreER/+}$;*Sox2*$^{fl/fl}$) in adult mice leads to a reduction in incisor renewal rate (Sun et al., 2016). In the *Sox2*$^{Cre/fl}$ mice, the proliferation pattern in the laCL is maintained after prolonged *Sox2* ablation. Therefore, we hypothesize that the incisor growth defect reported earlier (Sun et al., 2016) is caused by defective cell differentiation, similar to the embryonic scenario.

Finally, an important question that remains largely unanswered in the stem cell field is that of the origin of adult SCs. We found that the transcriptomic signatures of embryonic and adult *Sox2*$^{+}$ cells are very similar. Moreover, they express a number of genes differently compared with naïve mESCs. From this observation, we propose that dental SC identity is represented either in the embryonic and adult *Sox2*$^{+}$ cell overlapping transcriptomes or in the genes enriched in adult *Sox2*$^{+}$ cells. Although our results alone are not enough to distinguish between these possibilities, an early generation of the dental SC signature would require the formation of the niche microenvironment early on. Interestingly, *Notch1*, a marker of the dental epithelial SC niche, is expressed in the mouse incisor at E14.5 (Felszeghy et al., 2010; Mucchielli and Mitsiadis, 2000). Therefore, we postulate that SC niche and *Sox2*$^{+}$ cell dental fate are already established by E14.5 in the mouse incisor. The corollary of such a conclusion would be that the genes enriched in embryonic or adult *Sox2*$^{+}$ cells should be related to the role of cells within the organ at this stage. For instance, *Sox11*, a transcription factor involved in epithelial-mesenchymal interactions (Hargrave et al., 1997), was enriched in the forming incisor. On the other hand, we found an enrichment of *Clu* in adult *Sox2*$^{+}$ cells. This chaperone has been reported to play a role in secretory odontogenesis, an important function in the adult incisor (Khan et al., 2013), and was highly enriched in the incisor ameloblasts. These observations strengthen our hypothesis that the differences between embryonic and adult *Sox2*$^{+}$ transcriptomes are inherent to the temporal role of the cell population (morphogenesis versus ameloblast lineage renewal). From these data, we conclude that the differences in gene expression that we observed reflect cues from the microenvironment and minor changes in the role of the *Sox2*$^{+}$ cells.

Collectively, our data demonstrate the importance of a *Sox2*$^{+}$ cell population for incisor renewal and cell differentiation. We also observed an impressive cellular plasticity in the laCL that acts to maintain the *Sox2*$^{+}$ population. We propose that *Lgr5*$^{+}$ cells are a subpopulation of the *Sox2*$^{+}$ cells, and are the first cells to reappear in the event of transient *Sox2* loss. This indicates the existence of a complex relationship between the *Lgr5*-expressing and *Sox2*-expressing cells.

MATERIALS AND METHODS

Mouse lines

The stage of the embryos was determined according to morphological criteria and noon of plug day was counted as E0.5. All animals are available from The

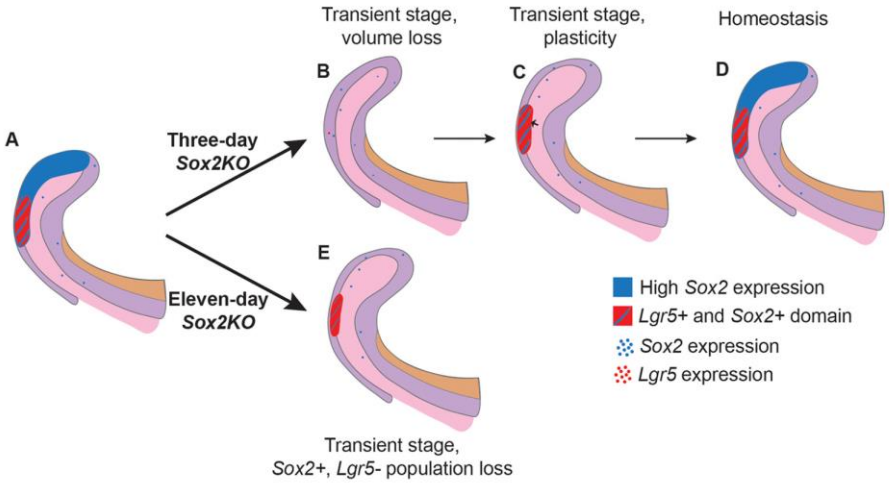

Fig. 8. Model for the effects of short- and long-term *Sox2* ablation. (A) Summary of *Sox2* and *Lgr5* expression domains in normal conditions within the laCL. (B) Upon conditional deletion of *Sox2* in *Sox2*-expressing cells for 3 days, the laCL becomes narrower, and almost all *Sox2* and *Lgr5* transcripts are lost. (C) Shortly after, the volume of the laCL is back to normal due to an increase in cell proliferation in the SR (small arrow). Overlapping expression of *Sox2* and *Lgr5* is found in the distal side of the laCL. (D) Eventually, the laCL reaches homeostasis and returns to its original state. (E) In the event of *Sox2* ablation for 11 days, the laCL maintains a small *Lgr5*$^{+}$ *Sox2*$^{+}$ cell population.

Development (2018) 145, dev155929. doi:10.1242/dev.155929

Jackson Laboratory. *Shh*$^{GFP\text{-}Cre/+}$;*Sox2*$^{fl/fl}$ were used as *Sox2*^{cKO} (Juuri et al., 2013a). *K14-CreER* males [Tg(KRT14-cre/ERT)20Efu/J, stock 005107] were crossed with *Sox2*$^{fl/fl}$ females (*Sox2*$^{tm1.1Lan}$/J, stock 013093) to generate *K14-CreER;Sox2*$^{fl/fl}$ mice. To generate the *Sox2*$^{CreER/fl}$ mice (inducible *Sox2* cKO), *Sox2*$^{fl/fl}$ females were crossed with *Sox2*$^{CreER/+}$ males [*Sox2*$^{tm1(cre/ERT2)Hoch}$/J, stock 017593]. *Lgr5*$^{GFP\text{-}CreER/+}$ [B6.129P2-*Lgr5*$^{tm1(cre/ERT2)Cle}$/J, stock 008875] animals were crossed to generate *Lgr5*$^{GFP\text{-}CreER/GFP\text{-}CreER}$ embryos (*Lgr5*^{KO}) embryos. *Sox2*^{GFP} males (B6;129S-*Sox2*^{tm2Hoch}/J, stock 017592) were crossed with NMRI females to produce *Sox2*^{GFP} embryos. Mice were genotyped using the primers listed in Table S6. All aspects of mouse care and experimental protocols were approved by the Finnish National Board of Animal Experimentation.

Tamoxifen administration

A working solution of Tamoxifen (Sigma-Aldrich, T5648) in corn oil (Sigma-Aldrich, 47112-U) was prepared at 50 mg/ml. Tamoxifen solution was sonicated for 15 min and kept at −20°C. Mice were administered 10 mg Tamoxifen solution via oral gavage.

Tissue processing, histology, immunofluorescence, RNAscope, and TUNEL assay

For histology, tissues were fixed in 4% paraformaldehyde (PFA) at 4°C overnight, dehydrated, and embedded in paraffin. Adult samples were decalcified for 2 weeks in 0.5 M EDTA pH 7.5 after fixation. Samples were processed into 5 µm-thick sagittal sections. Hematoxylin-Eosin (H&E) staining was performed as previously described (Juuri et al., 2012).

For RNAscope *in situ* hybridisation (Advanced Cell Diagnostics, ACDbio), we used both the red channel and duplex kits. Mouse tissues were processed into 5 µm sections as described above. Sections were processed using an optimised protocol (as detailed in the supplementary Materials and Methods). Probes were purchased from ACDbio.

TUNEL assay was performed using the *In Situ* Cell Death Detection Kit, Fluorescein (Roche, 11684795910) according to the manufacturer's protocol.

We used the following antibodies in immunofluorescence assays: SOX2 (goat, Santa Cruz, SC-17320; 1:200), keratin 14 (rabbit, NeoMarkers, RB-9020-P; 1:200), P-cadherin (cadherin 3) (goat, R&D Systems, AF761; 1:500), phospho-histone H3 (rabbit, Abcam, ab5176; 1:200), Ki67 (rabbit, Abcam, ab16667; 1:200) and GFP (chicken, Abcam, ab13970; 1:200). As secondary antibodies, we used Alexa 488 goat anti-rabbit (Life Technologies, A11057; 1:500) and Alexa 568 donkey anti-goat (Life Technologies, A11008; 1:500). Nuclei were stained with Hoechst 33342 (Thermo Fisher Scientific, H3570). For DAB immunostaining we used SHH primary antibody (mouse, R&D Systems, AF464) with HRP anti-goat secondary antibody (rabbit, Jackson ImmunoResearch, 305-035-003). Detailed protocols are provided in the supplementary Materials and Methods.

EdU labelling assay

Mice were intraperitoneally injected with EdU (25 µg/g body weight; Thermo Fisher Scientific, A10044) 3 days after the first Tamoxifen administration. Samples were collected 4 days later and processed into 5 µm paraffin sections. Detection was performed using the Click-iT EdU Alexa Fluor 488 Imaging Kit (Thermo Fisher Scientific, C10337) according to the manufacturer's instructions.

Data acquisition and processing

Samples were imaged with a Zeiss Axio Imager M2 microscope and further processed with Adobe Photoshop. RNAscope signal was enhanced by selecting the red or blue-green pixels of the image using the 'select color range tool'. The selected areas were false-coloured using the 'brush tool'.

pH-H3$^+$ cell, EdU$^+$ cell and laCL volume quantifications

Samples were imaged with a Zeiss Axio Imager M2 microscope and processed with Adobe Photoshop. For embryonic stages, pH-H3$^+$ cells were quantified for every second 5 µm-thick section, and the incisor area was drawn by hand using Zen 2011 software (Zeiss). For adult stages, EdU$^+$ cells and laCL area were quantified from every second 5 µm-thick section from the central region of the incisor (a total of 70 µm). Volumes were calculated by taking into account the thickness of the sections.

Multiplex quantitative real-time (qRT) PCR

The proximal end of the incisor was dissected out from E18 embryos (approximately one-third of the total length) and stored at −80°C. RNA was extracted using the RNeasy Micro kit (Qiagen, 74004) and reverse transcribed using the QuantiTect Reverse Transcription Kit (Qiagen, 205310).

Multiplex qRT-PCR (CFX96 Touch Real-Time PCR Detection System, Bio-Rad) was performed using iTaq Universal Probe Super Mix (Bio-Rad, 1725130) and 10 ng cDNA per reaction. Probe combinations (PrimePCR Probe Assay, Bio-Rad) are provided in the supplementary Materials and Methods.

Micro-CT and 3D reconstructions

Samples were fixed in 4% PFA, rinsed with PBS, dehydrated in an ethanol series, and stained for 2 weeks in 0.1% phosphotungstic acid (PTA) in 70% ethanol. Samples were scanned with a micro-CT scanner (Phoenix Nanotom). Three mutant and two control lower jaws were scanned for each stage. 3D reconstructions were prepared with Avizo software (Thermo Fisher Scientific) from micro-CT scans (embryonic stages) and from H&E-stained sagittal sections (adult stages).

Microarray

Incisor buds and laCL were microdissected from *Sox2*^{GFP} animals and then incubated with 0.2 U/ml dispase for 10 min at room temperature and the mesenchymal tissue removed. The epithelial explants were incubated with StemPro accutase (Thermo Fisher Scientific, A1110501) for 45 min at 37°C. Samples were passed through a cell strainer (pore size 35 µm) and 7AAD (Thermo Fisher Scientific, A1310) was added to mark dead cells. 7AAD-negative and GFP-positive cells were collected by fluorescence-activated cell sorting (FACS). RNA was extracted using the RNeasy Micro Kit (Qiagen, 74004). Total RNAs were provided to the Functional Genomics Unit, University of Helsinki, Finland, for hybridisation on MTA Affymetrix Arrays. Samples were amplified and labelled using the Affymetrix WT Pico Reagent Kit (Thermo Fisher Scientific, 902622) (see the supplementary Materials and Methods). Three replicates were prepared for each sample, and mESCs were used as a non-dental cell reference. For further analysis, we discarded the non-significant hits (P>0.05, ANOVA).

Statistical analysis

For each experiment n=3, except for gene expression analysis in *K14-CreER;Sox2*$^{fl/fl}$ mice where n=6 (data not shown). Each incisor is considered one biological replicate (only one incisor was analysed per animal), except for gene expression in *Sox2*^{cKO}, where one litter was considered as a biological replicate (n=3). Data are shown as mean±s.d. (equal variances not assumed). Unpaired, two-tailed t-test was used to test statistical significance. P<0.05 was used as significance threshold.

Acknowledgements

We thank Kaisa Ikkala, Solja Kalha, Raija Savolainen, Jhon Alves and Merja Mäkinen for excellent technical help, and Irma Thesleff and Anamaria Balic for critical reading of the manuscript.

Competing interests

The authors declare no competing or financial interests.

Author contributions

Conceptualization: M.S.-N., Z.S., B.A.A., O.D.K., F.M.; Methodology: M.S.-N., K.S., O.D.K., F.M.; Validation: M.S.-N., K.S., F.M.; Formal analysis: M.S.-N., O.D.K., F.M.; Investigation: M.S.-N., K.S., L.B.-B.; Resources: M.S.-N., O.D.K., F.M.; Data curation: M.S.-N., F.M.; Writing - original draft: M.S.-N., O.D.K., F.M.; Writing - review & editing: M.S.-N., K.S., Z.S., L.B.-B., B.A.A., O.D.K., F.M.; Visualization: M.S.-N., F.M.; Supervision: F.M.; Project administration: F.M.; Funding acquisition: M.S.-N., O.D.K., F.M.

Funding

This work was supported by the Finnish Doctoral Program in Oral Sciences (M.S.-N.), the Academy of Finland (Suomen Akatemia) (F.M.), and by National Institutes of Health grant R35-DE026602 (O.D.K). Deposited in PMC for release after 12 months.

Data availability

The microarray data have been deposited at Gene Expression Omnibus under accession number GSE104808.

Supplementary information

Supplementary information available online at
http://dev.biologists.org/lookup/doi/10.1242/dev.155929.supplemental

References

Arnold, K., Sarkar, A., Yram, M. A., Polo, J. M., Bronson, R., Sengupta, S., Seandel, M., Geijsen, N. and Hochedlinger, K. (2011). Sox2+ adult stem and progenitor cells are important for tissue regeneration and survival of mice. *Cell Stem Cell* **9**, 317-329.

Barker, N., van Es, J. H., Kuipers, J., Kujala, P., van den Born, M., Cozijnsen, M., Haegebarth, A., Korving, J., Begthel, H., Peters, P. J. et al. (2007). Identification of stem cells in small intestine and colon by marker gene Lgr5. *Nature* **449**, 1003-1007.

Biehs, B., Hu, J. K.-H., Strauli, N. B., Sangiorgi, E., Jung, H., Heber, R.-P., Ho, S., Goodwin, A. F., Dasen, J. S., Capecchi, M. R. et al. (2013). BMI1 represses Ink4a/Arf and Hox genes to regulate stem cells in the rodent incisor. *Nat. Cell Biol.* **15**, 846-852.

Blanpain, C. and Fuchs, E. (2014). Plasticity of epithelial stem cells in tissue regeneration. *Science* **344**, 1242281-1242281.

Cao, H., Wang, J., Li, X., Florez, S., Huang, Z., Venugopalan, S. R., Elangovan, S., Skobe, Z., Margolis, H. C., Martin, J. F. et al. (2010). MicroRNAs play a critical role in tooth development. *J. Dent. Res.* **89**, 779-784.

Cao, H., Jheon, A., Li, X., Sun, Z., Wang, J., Florez, S., Zhang, Z., McManus, M. T., Klein, O. D. and Amendt, B. A. (2013). The Pitx2:miR-200c/141:noggin pathway regulates Bmp signaling and ameloblast differentiation. *Development* **140**, 3348-3359.

Chang, J. Y. F., Wang, C., Jin, C., Yang, C., Huang, Y., Liu, J., McKeehan, W. L., D'Souza, R. N. and Wang, F. (2013). Self-renewal and multilineage differentiation of mouse dental epithelial stem cells. *Stem Cell Res.* **11**, 990-1002.

Chou, T.-Y., Chen, W.-C., Lee, A.-C., Hung, S.-M., Shih, N.-Y. and Chen, M.-Y. (2009). Clusterin silencing in human lung adenocarcinoma cells induces a mesenchymal-to-epithelial transition through modulating the ERK/Slug pathway. *Cell Signal.* **21**, 704-711.

Clavel, C., Grisanti, L., Zemla, R., Rezza, A., Barros, R., Sennett, R., Mazloom, A. R., Chung, C.-Y., Cai, X., Cai, C.-L. et al. (2012). Sox2 in the dermal papilla niche controls hair growth by fine-tuning BMP signaling in differentiating hair shaft progenitors. *Dev. Cell* **23**, 981-994.

Dassule, H. R. and McMahon, A. P. (1998). Analysis of epithelial–mesenchymal interactions in the initial morphogenesis of the mammalian tooth. *Dev. Biol.* **202**, 215-227.

Dy, P., Penzo-Méndez, A., Wang, H., Pedraza, C. E., Macklin, W. B. and Lefebvre, V. (2008). The three SoxC proteins – Sox4, Sox11 and Sox12 – exhibit overlapping expression patterns and molecular properties. *Nucleic Acids Res.* **36**, 3101-3117.

Felszeghy, S., Suomalainen, M. and Thesleff, I. (2010). Notch signalling is required for the survival of epithelial stem cells in the continuously growing mouse incisor. *Differentiation* **80**, 241-248.

Fuchs, E. and Chen, T. (2012). A matter of life and death: self-renewal in stem cells. *EMBO Rep.* **14**, 39-48.

Gao, S., Moreno, M., Eliason, S., Cao, H., Li, X., Yu, W., Bidlack, F. B., Margolis, H. C., Baldini, A. and Amendt, B. A. (2015). TBX1 protein interactions and microRNA-96-5p regulation controls cell proliferation during craniofacial and dental development: implications for 22q11.2 deletion syndrome. *Hum. Mol. Genet.* **24**, 2330-2348.

Haegebarth, A. and Clevers, H. (2009). Wnt signaling, lgr5, and stem cells in the intestine and skin. *Am. J. Pathol.* **174**, 715-721.

Harada, H., Kettunen, P., Jung, H.-S., Mustonen, T., Wang, Y. A. and Thesleff, I. (1999). Localization of putative stem cells in dental epithelium and their association with Notch and FGF signaling. *J. Cell Biol.* **147**, 105-120.

Harada, H., Ichimori, Y., Yokohama-Tamaki, T., Ohshima, H., Kawano, S., Katsube, K.-I. and Wakisaka, S. (2006). Stratum intermedium lineage diverges from ameloblast lineage via Notch signaling. *Biochem. Biophys. Res. Commun.* **340**, 611-616.

Hargrave, M., Wright, E., Kun, J., Emery, J., Cooper, L. and Koopman, P. (1997). Expression of theSox11 gene in mouse embryos suggests roles in neuronal maturation and epithelio-mesenchymal induction. *Dev. Dyn.* **210**, 79-86.

Hu, J. K.-H., Du, W., Shelton, S. J., Oldham, M. C., DiPersio, C. M. and Klein, O. D. (2017). An FAK-YAP-mTOR signaling axis regulates stem cell-based tissue renewal in mice. *Cell Stem Cell* **21**, 91-106.

Huelsken, J., Vogel, R., Erdmann, B., Cotsarelis, G. and Birchmeier, W. (2001). beta-Catenin controls hair follicle morphogenesis and stem cell differentiation in the skin. *Cell* **105**, 533-545.

Jaks, V., Barker, N., Kasper, M., van Es, J. H., Snippert, H. J., Clevers, H. and Toftgård, R. (2008). Lgr5 marks cycling, yet long-lived, hair follicle stem cells. *Nat. Genet.* **40**, 1291-1299.

Järvinen, E., Salazar-Ciudad, I., Birchmeier, W., Taketo, M. M., Jernvall, J. and Thesleff, I. (2006). Continuous tooth generation in mouse is induced by activated epithelial Wnt/beta-catenin signaling. *Proc. Natl. Acad. Sci. USA* **103**, 18627-18632.

Jussila, M., Aalto, A. J., Sanz Navarro, M., Shirokova, V., Balic, A., Kallonen, A., Ohyama, T., Groves, A. K., Mikkola, M. L. and Thesleff, I. (2015). Suppression of epithelial differentiation by Foxi3 is essential for molar crown patterning. *Development* **142**, 3954-3963.

Juuri, E., Saito, K., Ahtiainen, L., Seidel, K., Tummers, M., Hochedlinger, K., Klein, O. D., Thesleff, I. and Michon, F. (2012). Sox2+ stem cells contribute to all epithelial lineages of the tooth via Sfrp5+ progenitors. *Dev. Cell* **23**, 317-328.

Juuri, E., Jussila, M., Seidel, K., Holmes, S., Wu, P., Richman, J., Heikinheimo, K., Chuong, C.-M., Arnold, K., Hochedlinger, K. et al. (2013a). Sox2 marks epithelial competence to generate teeth in mammals and reptiles. *Development* **140**, 1424-1432.

Juuri, E., Saito, K., Lefebvre, S. and Michon, F. (2013b). Establishment of crown–root domain borders in mouse incisor. *Gene Expr. Patterns* **13**, 255-264.

Kawasaki, M., Porntaveetus, T., Kawasaki, K., Oommen, S., Otsuka-Tanaka, Y., Hishinuma, M., Nomoto, T., Maeda, T., Takubo, K., Suda, T. et al. (2014). R-spondins/Lgrs expression in tooth development. *Dev. Dyn.* **243**, 844-851.

Khan, Q.-E.-S., Sehic, A., Khuu, C., Risnes, S. and Osmundsen, H. (2013). Expression of *Clu* and *Tgfb1* during murine tooth development: effects of *in-vivo* transfection with anti-miR-214. *Eur. J. Oral Sci.* **121**, 303-312.

Klein, O. D., Lyons, D. B., Balooch, G., Marshall, G. W., Basson, M. A., Peterka, M., Boran, T., Peterkova, R. and Martin, G. R. (2008). An FGF signaling loop sustains the generation of differentiated progeny from stem cells in mouse incisors. *Development* **135**, 377-385.

Lane, S. W., Williams, D. A. and Watt, F. M. (2014). Modulating the stem cell niche for tissue regeneration. *Nat. Biotechnol.* **32**, 795-803.

Li, L., Kwon, H.-J., Harada, H., Ohshima, H., Cho, S.-W. and Jung, H.-S. (2011). Expression patterns of ABCG2, Bmi-1, Oct-3/4, and Yap in the developing mouse incisor. *Gene Expr. Patterns* **11**, 163-170.

Michon, F., Tummers, M., Kyyrönen, M., Frilander, M. J. and Thesleff, I. (2010). Tooth morphogenesis and ameloblast differentiation are regulated by micro-RNAs. *Dev. Biol.* **340**, 355-368.

Morita, H., Mazerbourg, S., Bouley, D. M., Luo, C.-W., Kawamura, K., Kuwabara, Y., Baribault, H., Tian, H. and Hsueh, A. J. W. (2004). Neonatal lethality of LGR5 null mice is associated with ankyloglossia and gastrointestinal distension. *Mol. Cell. Biol.* **24**, 9736-9743.

Mucchielli, M.-L. and Mitsiadis, T. A. (2000). Correlation of asymmetric Notch2 expression and mouse incisor rotation. *Mech. Dev.* **91**, 379-382.

Nonomura, K., Takahashi, M., Wakamatsu, Y., Takano-Yamamoto, T. and Osumi, N. (2010). Dynamic expression of *Six* family genes in the dental mesenchyme and the epithelial ameloblast stem/progenitor cells during murine tooth development. *J. Anat.* **216**, 80-91.

Obara, N., Suzuki, Y., Irie, K. and Shibata, S. (2017). Expression of planar cell polarity genes during mouse tooth development. *Arch. Oral Biol.* **83**, 85-91.

Que, J., Okubo, T., Goldenring, J. R., Nam, K.-T., Kurotani, R., Morrisey, E. E., Taranova, O., Pevny, L. H. and Hogan, B. L. M. (2007). Multiple dose-dependent roles for Sox2 in the patterning and differentiation of anterior foregut endoderm. *Development* **134**, 2521-2531.

Rompolas, P., Mesa, K. R. and Greco, V. (2013). Spatial organization within a niche as a determinant of stem-cell fate. *Nature* **502**, 513-518.

Seidel, K., Ahn, C. P., Lyons, D., Nee, A., Ting, K., Brownell, I., Cao, T., Carano, R. A. D., Curran, T., Schober, M. et al. (2010). Hedgehog signaling regulates the generation of ameloblast progenitors in the continuously growing mouse incisor. *Development* **137**, 3753-3761.

Seidel, K., Marangoni, P., Tang, C., Houshmand, B., Du, W., Maas, R. L., Murray, S., Oldham, M. C. and Klein, O. D. (2017). Resolving stem and progenitor cells in the adult mouse incisor through gene co-expression analysis. *Elife* **6**, e24712.

Shiota, M., Zardan, A., Takeuchi, A., Kumano, M., Beraldi, E., Naito, S., Zoubeidi, A. and Gleave, M. E. (2012). Clusterin mediates TGF-β-induced epithelial-mesenchymal transition and metastasis via twist1 in prostate cancer cells. *Cancer Res.* **72**, 5261-5272.

Sock, E., Rettig, S. D., Enderich, J., Bosl, M. R., Tamm, E. R. and Wegner, M. (2004). Gene targeting reveals a widespread role for the high-mobility-group transcription factor Sox11 in tissue remodeling. *Mol. Cell. Biol.* **24**, 6635-6644.

Sun, Z., Yu, W., Sanz Navarro, M., Sweat, M., Eliason, S., Sharp, T., Liu, H., Seidel, K., Zhang, L., Moreno, M. et al. (2016). Sox2 and Lef-1 interact with Pitx2 to regulate incisor development and stem cell renewal. *Development* **143**, 4115-4126.

Suomalainen, M. and Thesleff, I. (2009). Patterns of Wnt pathway activity in the mouse incisor indicate absence of Wnt/β-catenin signaling in the epithelial stem cells. *Dev. Dyn.* **239**, 364-372.

Takahashi, K., Yamanaka, S., Randle, D. H., Kamijo, T., Cleveland, J. L., Sherr, C. J., Roussel, M. F., Kraft, A. S., Yang, V. W., Farese, R. V. et al. (2006). Induction of pluripotent stem cells from mouse embryonic and adult fibroblast cultures by defined factors. *Cell* **126**, 663-676.

Thesleff, I. and Tummers, M. (2008). *Tooth Organogenesis and Regeneration*. *StemBook* (ed. The Stem Cell Research Community), doi/10.3824/stembook.1.37.1.

Tian, H., Biehs, B., Warming, S., Leong, K. G., Rangell, L., Klein, O. D. and de Sauvage, F. J. (2011). A reserve stem cell population in small intestine renders Lgr5-positive cells dispensable. *Nature* **478**, 255-259.

Vasioukhin, V., Degenstein, L., Wise, B. and Fuchs, E. (1999). The magical touch: genome targeting in epidermal stem cells induced by tamoxifen application to mouse skin. *Proc. Natl. Acad. Sci. USA* **96**, 8551-8556.

Wang, F., Flanagan, J., Su, N., Wang, L.-C., Bui, S., Nielson, A., Wu, X., Vo, H.-T., Ma, X.-J. and Luo, Y. (2012). RNAscope. *J. Mol. Diagnostics* **14**, 22-29.

Watanabe, M., Kawasaki, K., Kawasaki, M., Portaveetus, T., Oommen, S., Blackburn, J., Nagai, T., Kitamura, A., Nishikawa, A., Kodama, Y. et al. (2016). Spatio-temporal expression of Sox genes in murine palatogenesis. *Gene Expr. Patterns* **21**, 111-118.

Wu, Z., Epasinghe, D. J., He, J., Li, L., Green, D. W., Lee, M.-J. and Jung, H.-S. (2016). Altered tooth morphogenesis after silencing the planar cell polarity core component, Vangl2. *Cell Tissue Res.* **366**, 617-621.

Xie, W., Lynch, T. J., Liu, X., Tyler, S. R., Yu, S., Zhou, X., Luo, M., Kusner, D. M., Sun, X., Yi, Y. et al. (2014). Sox2 modulates Lef-1 expression during airway submucosal gland development. *AJP Lung Cell. Mol. Physiol.* **306**, L645-L660.

Xie, M., Xing, G., Hou, L., Bao, J., Chen, Y., Jiao, T. and Zhang, F. (2015). Functional role of EMMPRIN in the formation and mineralisation of dental matrix in mouse molars. *J. Mol. Histol.* **46**, 21-32.

Yang, Z., Balic, A., Michon, F., Juuri, E. and Thesleff, I. (2015). Mesenchymal Wnt/β-catenin signaling controls epithelial stem cell homeostasis in teeth by inhibiting the antiapoptotic effect of Fgf10. *Stem Cells* **33**, 1670-1681.

Yokohama-Tamaki, T., Otsu, K., Harada, H., Shibata, S., Obara, N., Irie, K., Taniguchi, A., Nagasawa, T., Aoki, K., Caliari, S. R. et al. (2015). CXCR4/CXCL12 signaling impacts enamel progenitor cell proliferation and motility in the dental stem cell niche. *Cell Tissue Res.* **362**, 633-642.

Zhang, L., Yuan, G., Liu, H., Lin, H., Wan, C. and Chen, Z. (2012). Expression pattern of Sox2 during mouse tooth development. *Gene Expr. Patterns* **12**, 273-281.

Supplemental Information

Figures

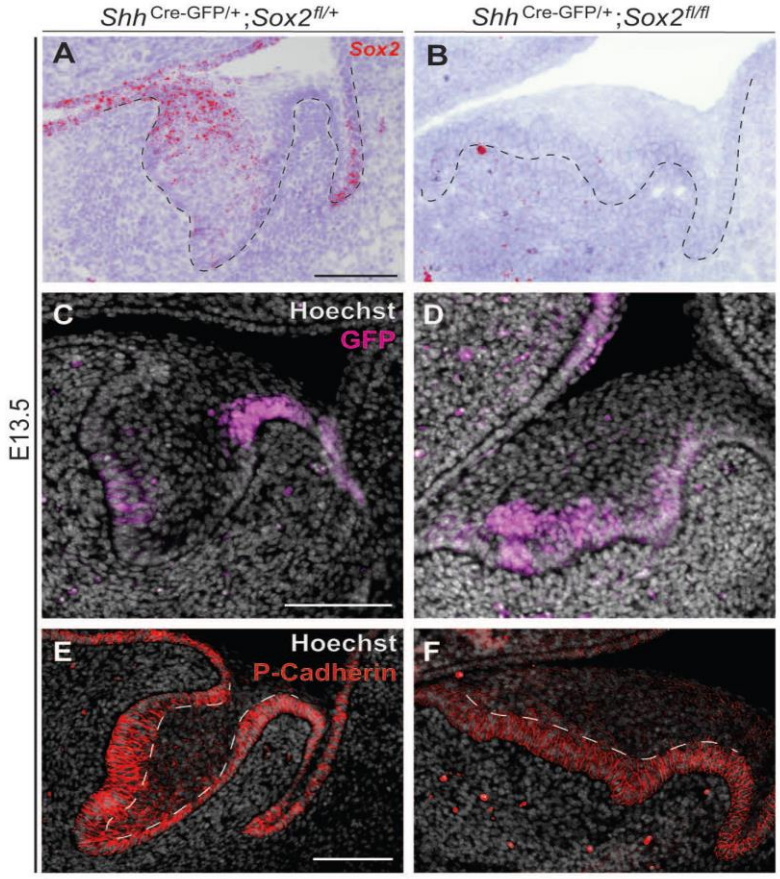

Figure S1. *Sox2* expression is efficiently knocked out from the dental epithelium of *Sox2*^{cKO} embryos. Expansion of the *Shh* domain in *Sox2*^{cKO}, but similar patterns of P-Cadherin in *Sox2*^{cKO} and control incisors.

(A) *Sox2* transcripts (red) are present in the dental epithelium at E13.5 (lingual CL, laCL, enamel knot, oral epithelium and vestibular lamina). **(B)** *Sox2* expression is not detected in the *Sox2*^{cKO}. The mutant incisor cap exhibits a wider dental lamina than the control littermates. **(C, D)** *Shh* expression pattern is expanded in the *Sox2*^{cKO} incisor buds at E13.5. **(E, F)** Sagittal sections of *Sox2*^{cKO} and control incisors at E13.5 show similar patterns of P-Cadherin.

Scale bars: 100μm.

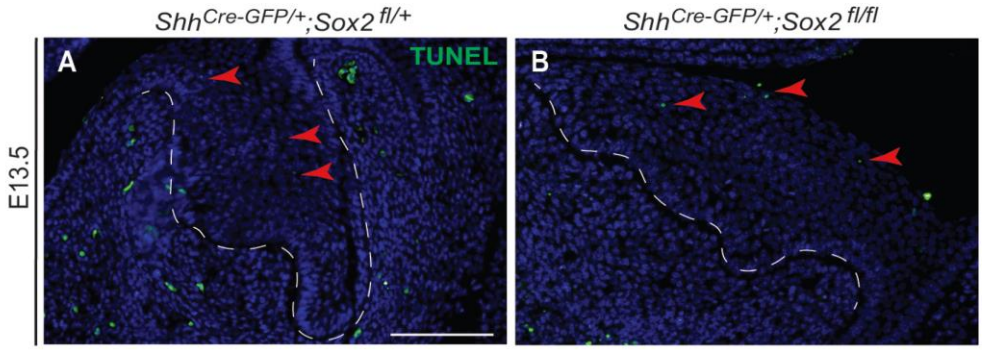

Figure S2. Cell death is unchanged in *Sox2*^{cKO} incisors at E13.5.

Cell death detection via TUNEL assay reveals that a similarly small number of apoptotic cells in both control **(A)** and *Sox2*^{cKO} **(B)** incisor. Red arrowheads point at TUNEL+ staining.

Scale bar: 100μm.

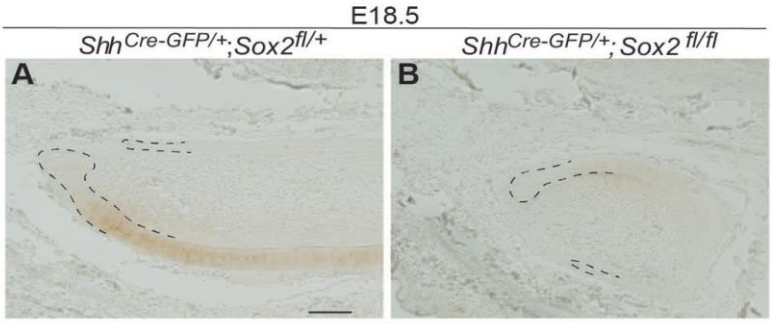

Figure S3. SHH expression pattern in *Sox2*^{cKO} incisors.

Immunodetection of SHH in E18.5 incisor in control **(A)** and *Sox2*^{cKO} **(B).** liCL and laCL are contoured with a dotted black line.

Scale bar: 100µm.

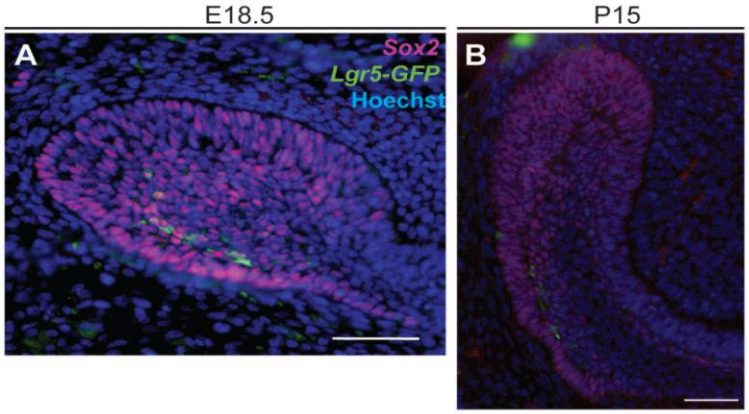

Figure S4. *Lgr5*+ cells are a subpopulation of *Sox2*+ cells.

(A) Immunodetection of Sox2 and Lgr5-GFP proteins at E18.5 shows overlap of both expression patterns. **(B)** Most of the cells in the postnatal laCL express Sox2 protein, while Lgr5-GFP appears in the distal SR and OEE.

Scale bars: 100µm.

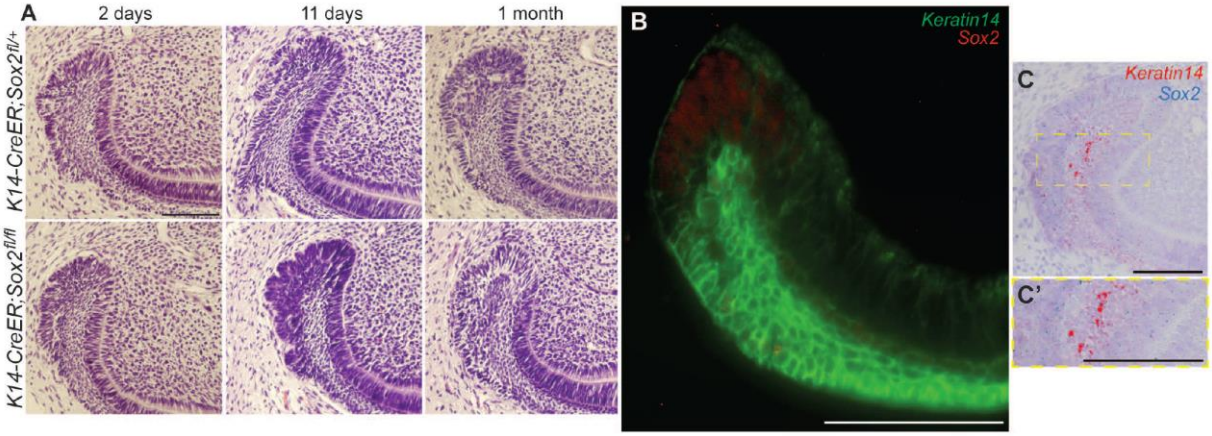

Figure S5. *K14-CreER* is not suitable for Sox2 deletion, due to partial overlap of *K14* and *Sox2* expression patterns.

(A) No abnormal phenotype is observed in the laCL of *K14-CreER;Sox2*$^{fl/fl}$ mice at two days, 11 days or one month after Tamoxifen administration. **(B, C, C')** *Sox2* and *K14* patterns overlap only partially, both at the transcriptomic and protein levels. Majority of *Sox2* and SOX2 expression is found in the enamel epithelium, where low levels of K14 are found. Majority of *K14* expression is localised to the SR.

Scale bars: 100μm.

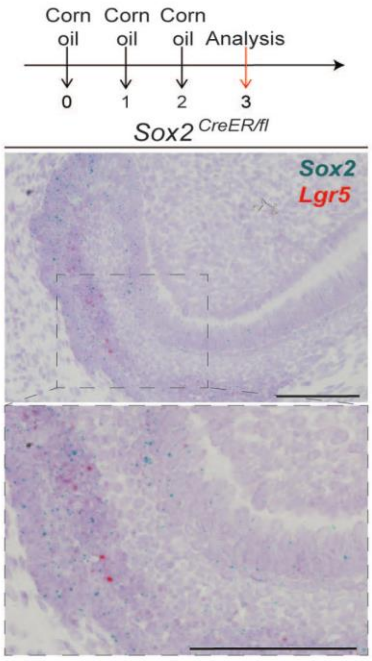

Figure S6. *Sox2*$^{CreER/fl}$ mice injected with Corn oil (Tamoxifen vehicle) as negative controls.

Sox2 and *Lgr5* mRNA detection for *Sox2*$^{CreER/fl}$ laCL 3 dies after the first corn oil injection.

Scale bars: 100μm.

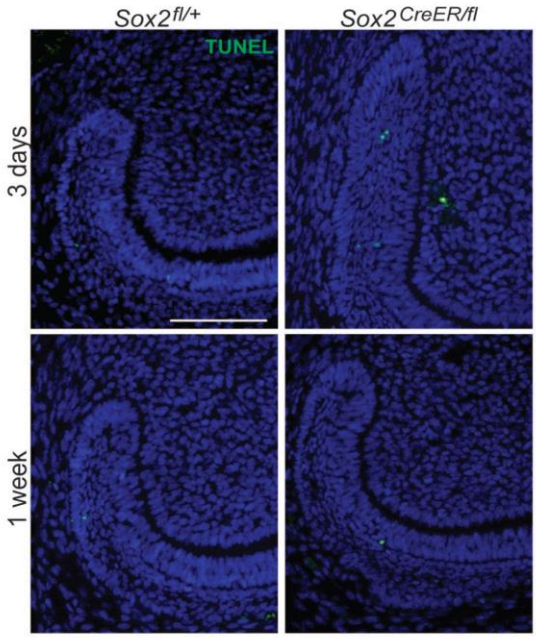

Figure S7. Apoptosis is not the driving force causing the narrowing of the laCL in the *Sox2*$^{CreER/fl}$ mice.

TUNEL assay on *Sox2*$^{CreER/fl}$ incisors, three days and one week after Tamoxifen administration shows low levels of cell death.

Scale bars: 100μm.

Table S1. List of transcripts obtained from the microarray.

All transcripts with the fold change of the following conditions: mESCs vs. Embryonic *Sox2*+ cells, mESCs vs. Adult *Sox2*+ cells, and Embryonic *Sox2*+ cells vs. Adult *Sox2*+ cells.

Click here to Download Table S1

Table S2. List of transcripts differentially expressed between *Sox2*+ cells and mESCs.

WE observed that 2.34% of the signature was enriched in Sox2+ cells and 4% of the signature was downregulated. This list does not contain the fold of change.

Click here to Download Table S2

Table S3. Gene ontology processes (GOP) activated in *Sox2*+ cells compared to mESCs.

From the genes enriched in Sox2 positive cells, listed in table S2, we found that 187 processes were activated over 2.5 fold.

Click here to Download Table S3

Table S4. GOP enriched in Embryonic compared to Adult *Sox2*+ cells.

We observed that 3.54% of the signature was enriched in embryonic cells. Among these, 143 GOP were enriched over 2.5 fold.

Click here to Download Table S4

Table S5. GOP enriched in Adult compared to Embryonic *Sox2*+ cells.

We observed that 2.75% of the signature was enriched in adult cells. Amongst these, 153 GOP were enriched over 2.5 fold.

Click here to Download Table S5

Table S6. List of genotyping primers.

Click here to Download Table S6

Supplemental Material and Methods

RNAscope protocol

Single channel RNAscope, red kit

Slides containing 5-µm sections were preheated for 1h in +60^{0}C and deparafinized for ten minutes in a series of three xylenes, two minutes in a series of two 94% ethanol with agitation and dried for 30 minutes on a hotplate at 60°C. Samples were incubated with hydrogen peroxide (included in the kit) for 10 minutes. Slides were incubated for 30 minutes in the target retrieval reagent at 85°C, rinsed with distilled water and dried on a hot plate at 60°C for 30 minutes.

A barrier around the sections was drawn with Immedge pen, and were incubated with protease (included in the kit) during 15 minutes. Hybridization of the probe, amplification and detection of the signal steps were done according to the manufacturer's protocol.

Samples were counterstained by incubating for two minutes in 50 % hematoxylin and rinsed with ammonia water. Sections were dehydrated by incubating them at 60°C during 45 minutes and mounted using VectaMount.

Duplex RNAscope, red and blue-green kit

Pretreatment of the samples was done as described for the single channel RNAscope, hybridization of the probe, amplification and detection of the signal steps were done according to the manufacturer's protocol.

Samples were counterstained by incubating for 30 seconds in 50 % hematoxylin and rinsed with water. Sections were dehydrated by incubating them at 60° during 45 minutes and mounted using VectaMount.

Immunofluorescence Protocol

Tissue sections were deparafinized and rehydrated five minutes in a series of four xylenes, two minutes in a series of three absolute ethanol, two minutes in a series of two 94% ethanol, two minutes in 70% ethanol, two minutes in 50% ethanol and two minutes in distilled water. Slides were washed for 10 minutes in 1x PBS-0.3% triton and incubate for two hours in 10mM sodium citrate, inside a pressurized device (2100 retriever; APTUM), for antigen retrieval. Slides were washed for 10 minutes in 1x PBS-0.3% triton. Blocking was performed for one hour in 1x PBS-0.3% Triton, 1% BSA, 10% serum (depending on the secondary antibody). The slides were incubated with the primary antibody in blocking solution overnight.

The following day, slides were washed thrice for five minutes in 1x PBS-0.3% triton. Incubation with the secondary antibody 1:400 and Hoechst 1:2000 in 5% BSA in PBS-0.3% triton was held for two hours at room temperature. Slides were washed for ten minutes in 1x PBS-0.3% Triton, ten minutes in 1x PBS-0.1% Triton and ten minutes in 1xPBS to reduce the background staining. Sections were mounted using Vectashield (Vector).

DAB Immunohistochemistry Protocol

Samples were deparaffinised using the same protocol as for immunofluorescence. Samples were washed three times with 1x PBS-0.3% triton for ten minutes and incubated for two hours in blocking solution (1x PBS-0.3% triton with 2% Skimmed milk powder). Primary antibody was incubated overnight at +4^{0}C. Samples were washed thrice in blocking solution for 10 minutes. Secondary antibody was incubated in blocking solution overnight at +4^{0}C. Samples were washed in blocking solution three times for 10 minutes. DAB colour development was done using the Mouse on Mouse Elite Peroxidase Kit (Vector, PK-2200), following the manufacturer's protocol. Samples were mounted with Immu-Mount (ThermoFisher Scientific, 9990402).

Sample amplification and preparation for microarray

RNA samples from embryonic (E14.5) and adult (P60) *Sox2*+ cells were prepared for whole transcriptome expression analysis (Affymetrix MTA) using the Affymetrix's WT Pico Reagent kit. First, in the reverse transcription, RNA is primed with primers containing a T7 promoter sequence, and a single-stranded cDNA is synthesized. Using this cDNA as a template, a second-strand cDNA is synthesized. Next, the complimentary RNA (cRNA) is synthesized and amplified by *in vitro* transcription of the second-stranded cDNA using T7 RNA polymerase. Unincorporated nucleotides and other debri are removed at this point. Sense-strand cDNA is synthesized by reverse transcription of cRNA using second-cycle primers. The sense-strand cDNA contains dUTP at a fixed ratio relative to dTTP. The secnd-cycle single-stranded cDNA is purified. Next, the sense-strand cDNA is fragmented by uracil-DNA glycosylase (UDG) andapurinic/apyrimidinic endonuclease 1 (APE 1) at the unnatural dUTP residues. The fragmented cDNA is labeled by terminal deoxynucleotidyl transferase (TdT) using the Affymetrix proprietary DNA Labeling Reagent, covalently linked to biotin. A hybridization cocktail containing the target and hybridization controls is prepared. The target is hybridized to the GeneChip array in cartridge format during 17-hour incubation at 45 °C. After hybridization, the array is washed and stained with streptavidin phycoerythrin conjugate using an automated protocol on the GeneChip® Fluidics Station 450, followed by scanning on a GeneChip® Scanner.

Probe combinations for multiplex qPCR

For *K14-CreER;Sox2*$^{fl/fl}$ we used the following combination: Lgr5-TEX (qMmuCEP0053421), Sox2-FAM (qMmuCEP0060283), Sfrp5-HEX (qMmuCEP0053072), Bmi1-Cy5.5 (qMmuCEP0043063) and GAPDH-Cy5 (qMmuCEP0039581).

For *Sox2*^{cKO} gene analysis two combinations of PrimePCR Probe Assay (Bio-Rad) were used: Lgr5-TEX (qMmuCEP0053421), Sox2-FAM (qMmuCEP0060283), Hprt-

HEX (qMmuCEP0054164) and Shh-FAM (qMmuCIP0028772), Sfrp5-HEX (qMmuCEP0053072), GAPDH-Cy5 (qMmuCEP0039581).

Annex 2: A giant step backward, molar replacement in mutant mice

Cyril Charles[1], Kerstin Seidel[2], Pauline Marangoni[1], Ludivine Bertonnier-Brouty[1], Mathilde Bouchet[1], Laurent Viriot[1*], Ophir Klein[2,4*]

[1]: Institute of Functional Genomics of Lyon, ENS de Lyon, CNRS UMR 5242, University of Lyon 1, 46 allée d'Italie, 69364 Lyon cedex 07, France

[2]: Department of Orofacial Sciences and Program in Craniofacial and Mesenchymal Biology, University of California San Francisco, San Francisco, CA 94143, USA

[3]: Department of Pediatrics and Institute for Human Genetics, University of California San Francisco, San Francisco, CA 94143, USA

[*]Contributed equally to the work.

The following paper is a draft from an ongoing study about dental morphology of Sprouty mutants. Molar development and adult morphology of *Spry1*$^{-/-}$; *Spry2*$^{-/-}$ and *Spry2*$^{+/-}$; *Spry4*$^{-/-}$ KO-mice were studied. In these mutant mice, evidences of molar replacement induced by the *Spry* loss of function were provide. By surveyed wild populations of mice, we found out a striking specimen that phenocopies the *Spry2*$^{+/-}$; *Spry4*$^{-/-}$ dentition. We detect presence of a supernumerary tooth at the lingual part of the first molar.

In this project, I worked on the wild mouse specimen exhibiting a supernumerary tooth. I participated in the acquisition of data for the sequencing as well as the study of the sequences obtained. We identified sequences modifications in the wild mouse exhibiting a supernumerary tooth that may affect the Spry1 protein and induce the abnormal development of a supernumerary tooth among the normal molars.

A giant step backward, molar replacement in mutant mice

Cyril Charles[1], Kerstin Seidel[2], Pauline Marangoni[1], Ludivine Bertonnier-Brouty[1], Mathilde Bouchet[1], Laurent Viriot[1*], Ophir Klein[2,4*]

[1]: Institute of Functional Genomics of Lyon, ENS de Lyon, CNRS UMR 5242, University of Lyon 1, 46 allée d'Italie, 69364 Lyon cedex 07, France

[2]: Department of Orofacial Sciences and Program in Craniofacial and Mesenchymal Biology, University of California San Francisco, San Francisco, CA 94143, USA

[3]: Department of Pediatrics and Institute for Human Genetics, University of California San Francisco, San Francisco, CA 94143, USA

[*]Contributed equally to the work.

Introduction

Tooth replacement is a common process among vertebrates. Many non-mammal vertebrates have a highly dynamic dentition in which teeth are constantly replaced throughout the animal's lifetime (polyphyodonty). In contrast, most mammals develop a maximum of two dental generations (diphyodonty), at the exception of three genera that replace their cheek teeth all along their life [1]. In the diphyodont system, the incisors, canines, and premolars may still be replaced but placental mammals lost their ability to replace molars around 205 million years ago [2]. The mouse, which is commonly used as a model to study mammalian development, has only one evergrowing incisor and three molar in each dental quadrant, none of these teeth being replaced. Among the various genes involved in dental development, the FGF (Fibroblast Growth Factors) pathway can have an impact on the odontogenesis either through the level of expression of Fgf genes or by their modulation through mutations in Sprouty genes, antagonists of the FGF pathway. Modulation of the FGF pathway is sufficient to modify molar morphology [3], crown to root transition [4], number of incisors [5] and number of cheek teeth [6]. In the present work, we studied molar development and adult morphology of *Spry1*$^{-/-}$; *Spry2*$^{-/-}$, and *Spry2*$^{+/-}$; *Spry4*$^{-/-}$ KO-mice and we provide evidences of molar replacement induced by these loss of functions. We also surveyed wild populations of mice and found out a striking specimen that phenocopies the *Spry2*$^{+/-}$; *Spry4*$^{-/-}$ dentition. We thus tested if this phenotype occurring in natural condition shared similar genetic bases with our laboratory model and found genetic modifications that correlate with the developmental anomalies.

Results

Development of a lingual tooth bud in Spry1$^{-/-}$; Spry2$^{-/-}$ embryonic mutant mice

Our study of the *Sprouty1$^{-/-}$; Sprouty2$^{-/-}$* (*Spry1$^{-/-}$; Spry2$^{-/-}$*) mice revealed no anatomical modifications during the early molar development. The first histological difference we observed in the *Spry1$^{-/-}$; Spry2$^{-/-}$* mutants was the occurrence from E13.5 on of lingual tooth buds connected to the normal first molar buds in the gubernaculum area (Figure 1). This supernumerary bud is present in all studied upper and lower tooth rows, always protruding in the lingual side of first molar germs. The replacement buds are then observed at all stages following E13.5 and is still visible as a deep folding of the epithelium on the lingual side of the first molar shortly before birth (Figure 1). This location matches the minute rudimental successional dental lamina (RDSL) already described during the mouse first molar development [7]. This RDSL has been interpreted as a rudiment of the replacement tooth though analogy with diphyodont species. Considering the timing and location of the supernumerary dental buds, we thus consider the observed dental buds as replacement teeth of the first molars. Markers of the dental epithelium are expressed in the supernumerary tooth buds as in the normal molar underlining the dental identity of this structure (e.g. *Pitx2*, Figure 1), however, *Msx1*, normally expressed in the dental mesenchyme is not expressed around the supernumerary bud (Figure 1). *Msx1* is necessary to achieve the bud to cap transition during mouse dental development [8], the absence of expression around the supernumerary bud at E13.5 despite its expression around the normal bud might explain why the supernumerary bud stay at the same developmental stage for the remaining embryonic development.

Supernumerary teeth along the molar tooth row in Sprouty mutants

Because the *Spry1$^{-/-}$; Spry2$^{-/-}$* mutant mice die at birth, we decided to culture molar rows under kidney capsule to test the potential for the supernumerary buds to form mineralized

teeth. Results show that small extra teeth are formed in the double knock-out mutants and not in our control experiments (Figure 2). The morphology of molars are highly disturbed compared to the wild-type morphology in both experiments and control cultures, however, all teeth are made of cusps, crests and contain enamel and dentin. We hypothesize that the disturbed morphologies are due to the development context in the kidney that differs from the normal mechanical conditions in the odontogenic alverolar bones. The extra teeth found in *Spry1*$^{-/-}$;*Spry2*$^{-/-}$ mutants are monocuspidate and mineralized with enamel and dentine. We hypothesize that at least some of the small teeth observed in the mutant grafts originated from the supernumerary buds observed in *Spry1*$^{-/-}$; *Spry2*$^{-/-}$ embryos, showing that these buds are capable to develop further and to give rise to a functional tooth. In addition to this kidney capsule culture of the replacement tooth bud, we scrutinized the dentition of other *Sprouty* mutants (compound and single knock-out mice) using a X-ray microtomographic study of tooth rows to check for the presence of traces of replacement teeth. Out of 20 *Spry2*$^{+/-}$; *Spry4*$^{-/-}$ mice, we found out 2 specimens with a small supernumerary mineralized molar along the normal molar row (Figure 2). We hypothesize that these supernumerary teeth and buds observed in a few proportion of *Spry2*$^{+/-}$; *Spry4*$^{-/-}$ mice (5% of tooth rows) have the same developmental origin than the *Spry1*$^{-/-}$; *Spry2*$^{-/-}$supernumerary buds. In a study of effects of *Shh* downregulation during development using 5E1 anti-Shh antibody, Cho *et al.* [9] found four tooth rows out of 78 with a supernumerary tooth beside the normal first molar. This phenotype is very close to the observed *Spry2*$^{+/-}$; *Spry4*$^{-/-}$ mouse tooth row developing the replacement tooth. In a previous study, we already showed that *Spry2*$^{+/-}$; *Spry4*$^{-/-}$ mutants express a higher level of *Shh* during dental development [5]. We could thus hypothesize that the development a modification of *Shh* expressions during dental development can lead to the development of this putatively replacement tooth. This observation indicates, similarly to our

kidney capsule experiments, that the presumptive tooth replacement germ can indeed develop past the bud stage and undergo a complete development to give raise to a functional tooth.

Phenocopy of the Sprouty compound mutant in a wild mouse

We examined wild mice populations, including one sampling of 10 mice from Gétigné (West of France) encompassing one specimen exhibiting a supernumerary tooth located on the vestibular side of the left first upper molar. The supernumerary tooth is located in the same position than the supernumerary teeth observed in the Sprouty mutants, along the normal first molar. As in the mutant, the supernumerary tooth is a simple (conical) one. The specimen displayed no other visible defects on teeth or on other examined organs (hair, tail, skull, digits, limbs). The development of the supernumerary tooth did not impact the adjacent molars (Figure 3). To check if a mutation could be responsible for this striking phenocopy, we decided to sequence coding sequences of Sprouty genes and other genes considered from the literature as potential candidates for abnormal tooth development (*Sox2*, *Bmp4*). We sequenced these genes in the abnormal wild mouse as well as in other mice from the same population and to compare these results with reference sequences. Several Single Nucleotide Polymorphisms with a version for various mice of the natural population that differs from the published sequences have been detected for the studies genes (6 for *Bmp4*, 1 for *Sox2*, 4 for *Spry1*, 1 for *Spry2* and 2 for *Spry4*). The *Spry1* gene sequenced in the wild population also has 5 synonym point-mutations (transitions only) seen only in the abnormal specimen and more interestingly an insertion of 20 nucleotides near the 3' end of Sprouty1 coding sequence (for normal and abnormal specimens). We hypothesize that this frame-shift insertion might impair some functions of the protein and play a role in the abnormal development of a

supernumerary tooth along the normal molars. However the exact impact of this insertion on the protein functions still needs to be investigated.

Discussion / Conclusion

The FGF pathway plays a major role in dental development. Various genes of this pathway have been recently highlighted as involved in the distribution of mineralized dental tissues [10], in the setting up tooth shape, number, and arrangement [3,5,6,11], as well as in evolutionary mechanisms of the dentition in mammals [3,11]. We show here that knocking out both *Spry1* and *Spry2* genes controls the replacement of molar teeth in mouse whereas mammals are characterized by their incapacity to replace their molars. It is widely accepted that the mammalian diphyodonty was derived from an ancestrally polyphyodont replacement that was the rule in pre-mammalian synapsids [12]. In this context, what generation do belong molar teeth? Are they non-replaced deciduous teeth or are they permanent teeth without deciduous precursors?

Within the fossil record of synapsids, *Morganucodon* is considered to be the earliest true mammal because it did not replace its molar teeth whereas some contemporaneous stem mammals such as *Sinoconodon* still replaced their molar teeth [2]. The transition from plophyodonty to diphyodonty corresponds to a slowing down of tooth replacement frequency likely linked to the parallel acquisition of lactation and determinate growth of the skull [13]. The end of skull growth (determinate pattern) usually coincides with eruptions of the last molars (wisdom teeth in humans). Because it is impossible to detect lactation from a fossil skeleton, dentition is hence used by paleontologists as a proxy to trace crucial changes in synapsid physiology over evolution. Using the fossil record, we can date the onset of molar non-replacement at about 205 milion years ago, just at the end of the Triassic period [2].

The dental phenotype displayed by *Spry1*$^{-/-}$; *Spry2*$^{-/-}$ mutants is thus a giant step backward in evolutionary terms and *Spry1*$^{-/-}$; *Spry2*$^{-/-}$ mutant mice are a great model to study the loss of molar replacement in mammalian evolution. Yet the fact that *Spry1*$^{-/-}$; *Spry2*$^{-/-}$ mutants generate a second generation of molar teeth strongly suggests that the regular molars of mammals are deciduous (milk) teeth that never become replaced.

Finally, the phenotype observed in adult *Spry2*$^{+/-}$; *Spry4*$^{-/-}$ mice and in the wild-type abnormal specimen could be compared to the rare reported cases of paramolar in human patients [14]. The He-Zhao deficiency is also interesting as the non-replacement of teeth is the only developmental defect [15]. *Spry1*$^{-/-}$; *Spry2*$^{-/-}$ mutant mice are a good model to study the mechanisms of molar replacement in mammals as well as the loss of this capacity over mammalian evolution.

Figures

Figure 1: Supernumerary tooth buds attached to the first molars of *Sprouty1*$^{-/-}$;*Sprouty2*$^{-/-}$ mutants. A. General view of first molars in a mutant embryo, teeth are located by the black squares, note the presence of supernumerary buds in all four rows. B. Tooth bud of a WT first molar at E13.5 (histological staining). C. in situ hybridization showing *Msx1* expression in E13.5 WT first molar bud. D. in situ hybridization showing *Pitx2* expression in E13.5 WT first molar bud. E. Tooth bud of a *Sprouty1*$^{-/-}$;*Sprouty2*$^{-/-}$ first molar at E13.5 (histological staining). F. in situ hybridization showing *Msx1* expression in E13.5 *Sprouty1*$^{-/-}$;*Sprouty2*$^{-/-}$ first molar bud G. in situ hybridization showing *Pitx2* expression in E13.5 *Sprouty1*$^{-/-}$;*Sprouty2*$^{-/-}$ first molar bud. Scale bar : 100µm.

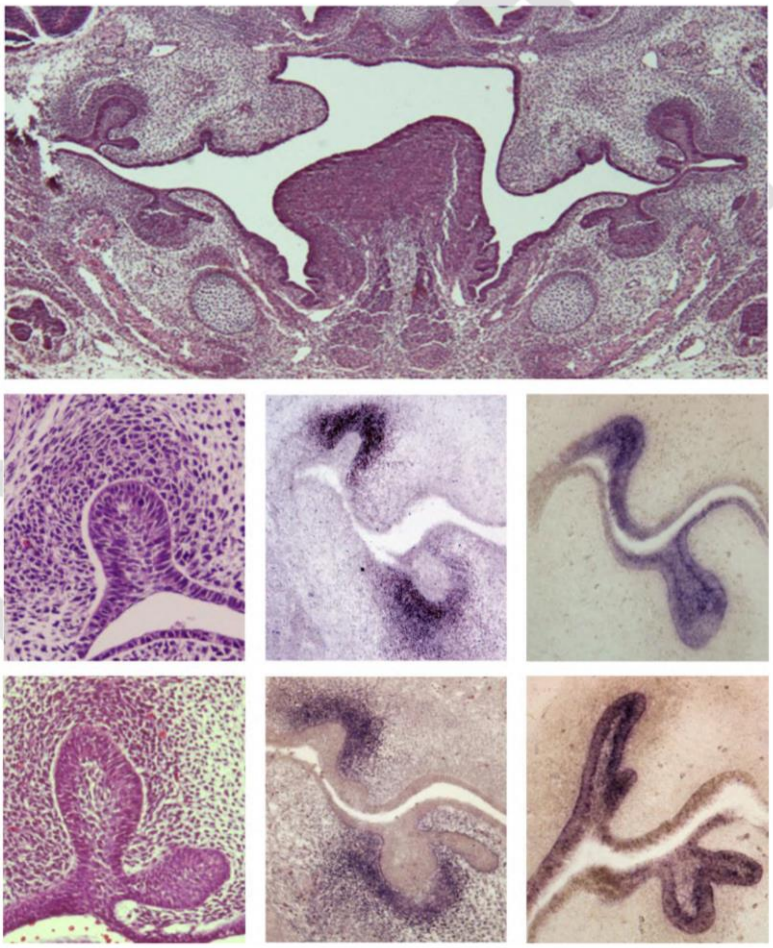

Figure 2: Result of a kidney capsule culture of *Sprouty1*$^{+/-}$;*Sprouty2*$^{+/-}$ (A) and *Sprouty1*$^{-/-}$;*Sprouty2*$^{-/-}$ molar rows, showing development and mineralization of four teeth in the mutant (B) ; Wild-type (C) and (D) *Sprouty2*$^{+/}$;*Sprouty4*$^{-/-}$ mutant molar rows showing an erupted paramolar beside the normal first molar in the mutant. Scale bar : 500µm

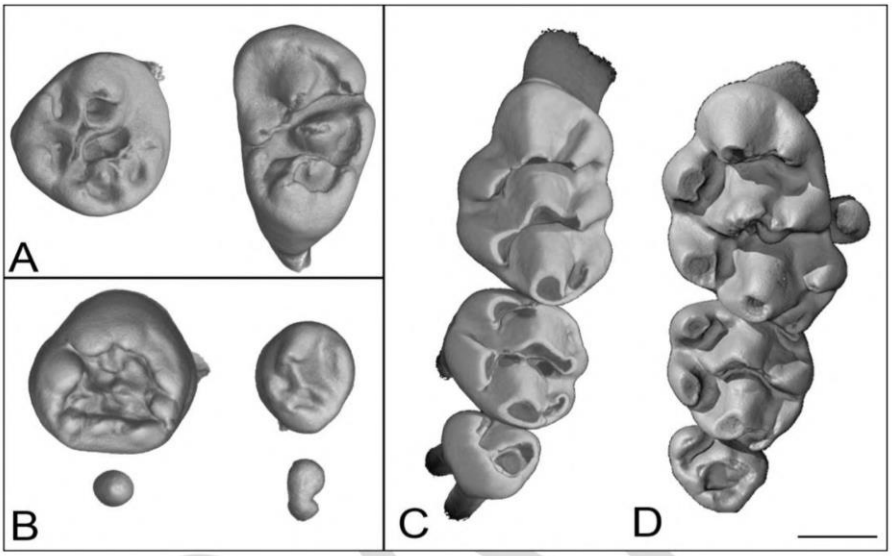

Figure 3: Wild mouse phenocopying the *Sprouty1*$^{-/-}$;*Sprouty2*$^{-/-}$ mutant. In the right panel, ellipses indicate the root positions of the first molar (in blue), second molar (in green), the third molar (in yellow) and the supernumerary tooth (in red). Scale bar: 500µm.

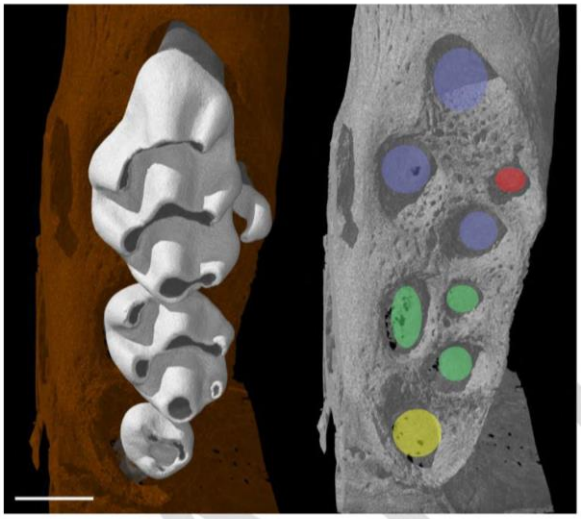

Figure 4: Schematic molar developments in mice, mutant Sprouty1-/-;Sprouty2-/- mice and mammalian ancestors representatives *Sinoconodon* and *Morganucodon*.

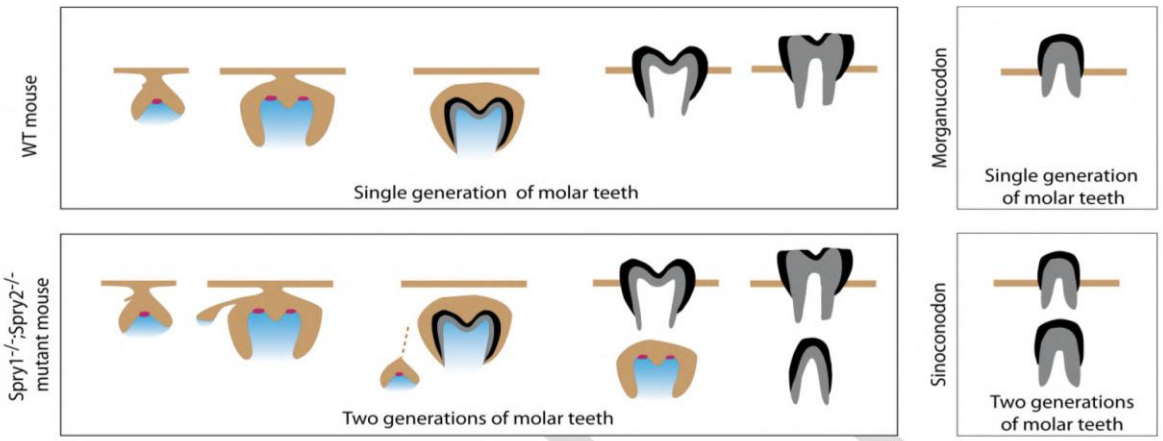

Material and Methods

Mice

Mouse lines carrying mutant alleles of *Spry1* [16], *Spry2* [17], and *Spry4* [10] were maintained on a mixed genetic background, crossed to obtain the studied mutation combinations and genotyped as reported. Noon of the day when a vaginal plug was detected was considered as embryonic day (E) 0.5. The pregnant mice were killed by *carbon dioxide* exposure followed by cervical dislocation. Wet body weight of the fetuses was determined immediately after their removal from the uterus to be able to correctly compare age- and weight-matched embryos. A population of 10 wild mice has been trapped during nights at Gétigné (West of France) in mouse traps designed to kill the specimens by cervical dislocation, these samples have been collected in the morning and stored in Ethanol for further DNA studies.

In situ hybridization

After harvesting, embryos were fixed overnight in 4% paraformaldehyde. RNA *in situ* hybridizations were performed paraffin sections using digoxigenin-labeled probes according to classic protocols.

Histology of dental tissues

Embryos were collected in 1X PBS and fixed overnight in 4% PFA. After dehydration in graded ethanol, embryos were processed in paraffin and serially sectioned (7 µm thick) using a Leica Autocut 2055 microtome. Masson's trichrome was used to conduct the

histological analyses of the sectioned dental germs (hemalum, 8 min; fushine, 2 min; aniline blue,1 min). Pictures were taken with an Olympus microscope equipped with a CCD camera and Cell F™.

Dental germ culture under kidney capsule

Because Sprouty1$^{-/-}$;Sprouty2$^{-/-}$ embryos are not viable, we cultures explants of dental germs under kidney capsules. Dental germs have been dissected on mutant and wild-type littermates embryos at E14.5 and grafted into a renal capsule of a recipient adult nude mice. The recipient mice have been sacrificed four weeks later to collect the kidney and study the grafted teeth.

3D data acquisition

Samples were scanned using a microfocused X-ray tomographic system (MicroXCT-200, Xradia, Pleasanton, CA), at 55 kV and 144 mA. 2000 projection images at an exposure time of 13 s with a linear magnification of 2X were taken. The volume was reconstructed using a back projection filtered algorithm (XRadia). Following reconstruction, 3D image processing has been performed with VGStudioMax (Version 2.2) software and enamel thickness analyses were carried out using Amira (Version 5.3) software.

References

1. Gomes Rodrigues H, Marangoni P, Sumbera R, Tafforeau P, Wendelen W, et al. (2011) Continuous dental replacement in a hyper-chisel tooth digging rodent. Proc Natl Acad Sci U S A 108: 17355-17359.

2. Luo Z-X, Kielan-Jaworowska Z, Cifelli RL (2004) Evolution of dental replacement in Mammals. Bulletin of Carnegie Museum of Natural History 36: 159-175.

3. Charles C, Lazzari V, Tafforeau P, Schimmang T, Tekin M, et al. (2009) Modulation of Fgf3 dosage in mouse and men mirrors evolution of mammalian dentition. Proceedings of the National Academy of Sciences of the United States of America 106: 22364-22368.

4. Yokohama-Tamaki T, Ohshima H, Fujiwara N, Takada Y, Ichimori Y, et al. (2006) Cessation of Fgf10 signaling, resulting in a defective dental epithelial stem cell compartment, leads to the transition from crown to root formation. Development 133: 1359-1366.

5. Charles C, Hovorakova M, Ahn Y, Lyons DB, Marangoni P, et al. (2011) Regulation of tooth number by fine-tuning levels of receptor-tyrosine kinase signaling. Development 138: 4063-4073.

6. Klein OD, Minowada G, Peterková R, Kangas A, Yu BD, et al. (2006) Sprouty Genes Control Diastema Tooth Development via Bidirectional Antagonism of Epithelial-Mesenchymal FGF Signaling. Developmental Cell 11: 181-190.

7. Dosedelova H, Dumkova J, Lesot H, Glocova K, Kunova M, et al. (2015) Fate of the molar dental lamina in the monophyodont mouse. PLoS One 10: e0127543.

8. Chen Y, Bei M, Woo I, Satokata I, Maas R (1996) Msx1 controls inductive signaling in mammalian tooth morphogenesis. Development 122: 3035-3044.

9. Cho SW, Kwak S, Woolley TE, Lee MJ, Kim EJ, et al. (2011) Interactions between Shh, Sostdc1 and Wnt signaling and a new feedback loop for spatial patterning of the teeth. Development 138: 1807-1816.

10. Klein O, Lyons D, Balooch G, Marshall G, Basson M, et al. (2008) An FGF signaling loop sustains the generation of differentiated progeny from stem cells in mouse incisors. Development 135: 377-385.

11. Marangoni P, Charles C, Tafforeau P, Laugel-Haushalter V, Joo A, et al. (2015) Phenotypic and evolutionary implications of modulating the ERK-MAPK cascade using the dentition as a model. Scientific Reports 5: 11658.

12. Ziegler AC (1971) Theory of Evolution of Therian Dental Formulas and Replacement Patterns. Quarterly Review of Biology 46: 226-&.

13. Pond CM (1977) Significance of Lactation in Evolution of Mammals. Evolution 31: 177-199.

14. Nagaveni N, Umashankara K, Radhika N, Praveen Reddy B, Manjunath S (2010) Maxillary paramolar: report of a case and literature review. Arch Orofac Sci 5: 24-28.

15. Wang H, Zhao S, Zhao W, Feng G, Jiang S, et al. (2000) Congenital absence of permanent teeth in a six-generation Chinese kindred. Am J Med Genet 90: 193-198.

16. Basson MA, Akbulut S, Watson-Johnson J, Simon R, Carroll TJ, et al. (2005) Sprouty1 is a critical regulator of GDNF/RET-mediated kidney induction. Dev Cell 8: 229-239.

17. Shim K, Minowada G, Coling DE, Martin GR (2005) Sprouty2, a mouse deafness gene, regulates cell fate decisions in the auditory sensory epithelium by antagonizing FGF signaling. Dev Cell 8: 553-564.

Annex 3: Collection numbers of the lagomorph specimens coming from natural history museums

Species	Source	Collection number
Brachylagus idahoensis	MNHN	1939.1087
Brachylagus idehoensis	AMNH	140866
Brachylagus idehoensis	AMNH	140865
Brachylagus idehoensis	AMNH	92869
Brachylagus idehoensis	AMNH	33616
Brachylagus idehoensis	AMNH	33615
Brachylagus idehoensis	AMNH	33609
Bunolagus monticularis	AMNH	146662
Bunolagus monticularis	AMNH	146663
Caprolagus hispidus	AMNH	54852
Lepus saxatilis megalotis	AMNH	168904
Lepus saxatilis megalotis	AMNH	168905
Lepus saxatilis megalotis	AMNH	168906
Lepus saxatilis megalotis	AMNH	168909
Lepus saxatilis megalotis	AMNH	168908
Lepus americanus	MNHN	1987.419
Lepus americanus	MNHN	1962.955
Lepus americanus	MNHN	2009.269
Lepus americanus bairdii	AMNH	41961
Lepus americanus bairdii	AMNH	124433
Lepus americanus bishopi	MNHN	2009.267
Lepus americanus pallidus	MNHN	2009.266
Lepus arcticus	MNHN	1962.2558
Lepus californicus	MNHN	1898.1108
Lepus californicus	MNHN	1862.2543
Lepus californicus	MNHN	1898.1107
Lepus californicus	MNHN	1879.2488
Lepus californicus wallawalla	AMNH	38223
Lepus californicus wallawalla	AMNH	38220
Lepus californicus wallawalla	AMNH	38228
Lepus californicus wallawalla	AMNH	38227
Lepus californicus wallawalla	AMNH	40882
Lepus callotis	MNHN	1896.2457
Lepus callotis	MNHN	1896.2459
Lepus callotis	AMNH	35158
Lepus callotis	AMNH	26143
Lepus callotis	AMNH	25997
Lepus callotis	AMNH	26144
Lepus capensis	MNHN	2009.274
Lepus capensis	MNHN	2014.1062
Lepus capensis	MNHN	2009.275

Lepus capensis	MNHN	2009.276
Lepus capensis	MNHN	1915.47
Lepus capensis	MNHN	1995.1279
Lepus capensis	MNHN	1995.1278
Lepus capensis	MNHN	1961.1070
Lepus capensis	MNHN	1961.1072
Lepus capensis	MNHN	1961.136
Lepus capensis	MNHN	1961.139
Lepus capensis	MNHN	1971.379
Lepus capensis	MNHN	1971.370
Lepus capensis	MNHN	1971.395
Lepus capensis	MNHN	1971.391
Lepus capensis	MNHN	1971.398
Lepus capensis	MNHN	1971.377
Lepus capensis	MNHN	1971.386
Lepus capensis	MNHN	1971.373
Lepus capensis	MNHN	1971.401
Lepus capensis	MNHN	1971.385
Lepus capensis	MNHN	1971.371
Lepus capensis	MNHN	1971.378
Lepus capensis	MNHN	1951.390
Lepus capensis	MNHN	1943.77
Lepus capensis	MNHN	1980.409
Lepus capensis	MNHN	1911.805
Lepus capensis	MNHN	1973.239
Lepus capensis	MNHN	1973.211
Lepus capensis	MNHN	1973.241
Lepus capensis	MNHN	1973.265
Lepus capensis	MNHN	1973.210
Lepus capensis	MNHN	1973.249
Lepus capensis	MNHN	1973.247
Lepus capensis	MNHN	1973.262
Lepus capensis	MNHN	1973.248
Lepus capensis	MNHN	1912.550
Lepus capensis	MNHN	1903.153
Lepus capensis	MNHN	1898.1646
Lepus capensis	MNHN	1973.303
Lepus capensis	MNHN	1973.301
Lepus capensis	MNHN	1973.300
Lepus capensis	MNHN	1973.302
Lepus capensis	MNHN	2004.398
Lepus capensis	MNHN	1978.150
Lepus capensis	MNHN	1978.148
Lepus capensis	MNHN	1978.151
Lepus capensis	MNHN	1983.687
Lepus capensis	MNHN	1980.262

Lepus capensis	MNHN	1991.32
Lepus capensis	MNHN	1995.1277
Lepus capensis	MNHN	1961.960
Lepus capensis	MNHN	2001.800
Lepus capensis	MNHN	2001.801
Lepus capensis	MNHN	1983.438
Lepus capensis	MNHN	2004.309
Lepus capensis	MNHN	2004.388
Lepus capensis	MNHN	2004.387
Lepus capensis	MNHN	1981.296
Lepus capensis	MNHN	1955.86
Lepus capensis	MNHN	1952.667
Lepus capensis	MNHN	1995.1566
Lepus capensis	MNHN	1951.297
Lepus capensis	MNHN	1971.269
Lepus capensis	Confluences	50.000835
Lepus capensis arabicus	MNHN	2006.472
Lepus capensis arabicus	MNHN	2006.471
Lepus europaeus	MNHN	1962.2261
Lepus europaeus	MNHN	1992.1480
Lepus europaeus	MNHN	2006.448
Lepus europaeus	MNHN	2006.447
Lepus europaeus	MNHN	1962.1980
Lepus europaeus	MNHN	1962.1979
Lepus europaeus	MNHN	1962.1978
Lepus europaeus	MNHN	1961.161
Lepus europaeus	MNHN	1966.232
Lepus europaeus	MNHN	1966.229
Lepus europaeus	MNHN	1961.166
Lepus europaeus	MNHN	1961.162
Lepus europaeus	MNHN	1961.167
Lepus europaeus	MNHN	2006.450
Lepus europaeus	MNHN	1962.2546
Lepus europaeus	MNHN	2009.256
Lepus europaeus	MNHN	1985.2012
Lepus europaeus	MNHN	1985.222
Lepus europaeus	MNHN	1963.1410
Lepus europaeus	MNHN	1958.211
Lepus europaeus	MNHN	1966.152
Lepus granatensis	MNHN	1985.39
Lepus insularis	MNHN	1898.1109
Lepus isabellinus	MNHN	2004.399
Lepus mandshuricus	MNHN	1966.151
Lepus nigricollis	MNHN	1961.944
Lepus nigricollis	MNHN	1981.338
Lepus nigricollis	MNHN	1981.339

Lepus nigricollis	MNHN	1961.1012
Lepus nigricollis	MNHN	1961.158
Lepus nigricollis	AMNH	163105
Lepus nigricollis	AMNH	163103
Lepus nigricollis vassali	MNHN	1961.947
Lepus peguensis	MNHN	1877.1831
Lepus sinensis	MNHN	1874.678
Lepus sp.	Confluences	50.000841
Lepus sp.	Confluences	50.003353
Lepus sp.	Confluences	50.000836
Lepus sp.	Confluences	50.000851
Lepus sp.	Confluences	50.000854
Lepus sp.	Confluences	50.00086
Lepus sp.	Confluences	50.000857
Lepus sp.	Confluences	50.000856
Lepus starcki	MNHN	1970.253
Lepus starcki	MNHN	1984.1173
Lepus starcki	MNHN	1970.254
Lepus starcki	MNHN	1973.226
Lepus starcki	MNHN	1973.230
Lepus starcki	MNHN	1973.275
Lepus starcki	MNHN	1973.259
Lepus starcki	MNHN	1973.270
Lepus starcki	MNHN	1973.212
Lepus starcki	MNHN	1973.218
Lepus starcki	MNHN	1973.205
Lepus timidus	MNHN	2009.263
Lepus timidus	MNHN	1971.1115
Lepus timidus	MNHN	1933.2150
Lepus timidus	MNHN	1954.67
Lepus timidus	Confluences	50.000834
Lepus tolai	MNHN	1980.422
Lepus tolai	MNHN	1970.78
Lepus tolai	MNHN	1980.76
Lepus tolai	MNHN	1980.73
Lepus tolai	MNHN	1980.77
Lepus tolai	MNHN	1980.72
Lepus townsendi	AMNH	40312
Lepus townsendi	AMNH	40881
Lepus townsendi	AMNH	40311
Lepus townsendi	AMNH	40883
Lepus townsendi	AMNH	93232
Lepus townsendi	AMNH	120787
Lepus variabilis	Confluences	50.00084
Lepus victoriae	MNHN	2001.1598
Lepus victoriae	MNHN	1961.762

Lepus victoriae	MNHN	1958.782
Lepus victoriae	MNHN	1995.474
Lepus victoriae	MNHN	1995.481
Lepus victoriae	MNHN	1995.480
Lepus victoriae	MNHN	1995.475
Lepus victoriae	MNHN	1995.477
Lepus victoriae	MNHN	1995.476
Lepus victoriae	MNHN	1971.713
Lepus victoriae	MNHN	1971.715
Lepus victoriae	MNHN	1971.714
Lepus victoriae	MNHN	1971.712
Lepus victoriae	MNHN	1971.711
Lepus victoriae	MNHN	1969.290
Lepus victoriae	MNHN	1969.287
Lepus victoriae	MNHN	1971.696
Lepus victoriae	MNHN	1971.703
Lepus victoriae	MNHN	1971.699
Lepus victoriae	MNHN	1971.704
Lepus victoriae	MNHN	1966.149
Lepus victoriae	MNHN	1961.1014
Lepus victoriae	MNHN	1966.227
Lepus victoriae	MNHN	1961.643
Lepus victoriae	MNHN	1961.642
Lepus victoriae	MNHN	1958.787
Lepus victoriae	MNHN	1970.252
Lepus victoriae	MNHN	1960.556
Lepus victoriae	MNHN	1960.553
Lepus victoriae	MNHN	1960.554
Lepus victoriae	MNHN	1960.552
Lepus victoriae	MNHN	1958.789
Lepus victoriae	MNHN	1911.826
Lepus victoriae	MNHN	1951.590
Lepus victoriae	MNHN	1973.234
Lepus victoriae	MNHN	1973.233
Lepus victoriae	MNHN	1973.277
Lepus victoriae	MNHN	1973.278
Lepus victoriae	MNHN	1973.217
Lepus victoriae	MNHN	1988.54
Lepus victoriae	MNHN	1990.628
Lepus victoriae	MNHN	1989.42
Lepus victoriae	MNHN	1989.39
Lepus victoriae	MNHN	1989.38
Lepus yarkandensis	MNHN	1911.759
Nesolagus timminsi	AMNH	276142
Ochotona principes	AMNH	149467
Oryctolagus cuniculus	MNHN	1991.13

Oryctolagus cuniculus	MNHN	1991.05
Oryctolagus cuniculus	MNHN	1991.19
Oryctolagus cuniculus	MNHN	2001.224
Oryctolagus cuniculus	MNHN	1991.3
Oryctolagus cuniculus	MNHN	1911.25
Oryctolagus cuniculus	MNHN	2001.225
Oryctolagus cuniculus	MNHN	2001.214
Oryctolagus cuniculus	MNHN	2001.230
Oryctolagus cuniculus	MNHN	2001.237
Oryctolagus cuniculus	MNHN	2001.236
Oryctolagus cuniculus	MNHN	1991.28
Oryctolagus cuniculus	MNHN	2001.241
Oryctolagus cuniculus	MNHN	2001.246
Oryctolagus cuniculus	MNHN	2001.245
Oryctolagus cuniculus	MNHN	1991.02
Oryctolagus cuniculus	MNHN	1991.29
Oryctolagus cuniculus	MNHN	1991.30
Oryctolagus cuniculus	MNHN	1991.24
Oryctolagus cuniculus	MNHN	1983.106
Oryctolagus cuniculus	MNHN	1983.100
Oryctolagus cuniculus	MNHN	1991.10
Oryctolagus cuniculus	MNHN	2010.644
Oryctolagus cuniculus	MNHN	1991.58
Oryctolagus cuniculus	MNHN	2001.185
Oryctolagus cuniculus	MNHN	2001.152
Oryctolagus cuniculus	MNHN	2001.186
Oryctolagus cuniculus	MNHN	2001.187
Oryctolagus cuniculus	MNHN	2001.184
Oryctolagus cuniculus	MNHN	2001.24
Oryctolagus cuniculus	MNHN	2001.04
Oryctolagus cuniculus	MNHN	2001.05
Oryctolagus cuniculus	MNHN	2001.198
Oryctolagus cuniculus	MNHN	2001.292
Oryctolagus cuniculus	MNHN	2009.282
Oryctolagus cuniculus	MNHN	2009.281
Oryctolagus cuniculus	MNHN	1995.1276
Oryctolagus cuniculus	MNHN	1991.72
Oryctolagus cuniculus	MNHN	1995.32
Oryctolagus cuniculus	MNHN	1995.64
Oryctolagus cuniculus	MNHN	1995.142
Oryctolagus cuniculus	MNHN	2005.819
Oryctolagus cuniculus	MNHN	1980.25
Oryctolagus cuniculus	MNHN	1980.26
Oryctolagus cuniculus	MNHN	1980.29
Oryctolagus cuniculus	MNHN	1980.28
Oryctolagus cuniculus	MNHN	1980.27

Oryctolagus cuniculus	MNHN	1980.23
Oryctolagus cuniculus	MNHN	1945.112
Oryctolagus cuniculus	MNHN	1945.113
Oryctolagus cuniculus	MNHN	2001.1150
Oryctolagus cuniculus	MNHN	2001.1147
Oryctolagus cuniculus	MNHN	2001.1148
Oryctolagus cuniculus	MNHN	2001.1149
Oryctolagus cuniculus	MNHN	2001.1146
Oryctolagus cuniculus	MNHN	1974.330
Oryctolagus cuniculus	MNHN	1985.1837
Oryctolagus cuniculus	MNHN	1962.1982
Oryctolagus cuniculus	MNHN	1962.1964
Oryctolagus cuniculus	MNHN	1962.1969
Oryctolagus cuniculus	MNHN	1962.1965
Oryctolagus cuniculus	MNHN	1962.1966
Oryctolagus cuniculus	MNHN	1962.1968
Oryctolagus cuniculus	MNHN	2004.88
Oryctolagus cuniculus	MNHN	1962.1014
Oryctolagus cuniculus	MNHN	1962.1972
Oryctolagus cuniculus	MNHN	1974.329
Oryctolagus cuniculus	MNHN	2009.252
Oryctolagus cuniculus	MNHN	2001.1154
Oryctolagus cuniculus	MNHN	2001.1153
Oryctolagus cuniculus	MNHN	1983.103
Oryctolagus cuniculus	MNHN	1983.105
Oryctolagus cuniculus	MNHN	1985.2011
Oryctolagus cuniculus	MNHN	1985.1838
Oryctolagus cuniculus	MNHN	1947.239
Oryctolagus cuniculus	MNHN	1971.364
Oryctolagus cuniculus	MNHN	1971.364B
Oryctolagus cuniculus	MNHN	1971.367
Oryctolagus cuniculus	MNHN	1971.368
Oryctolagus cuniculus	MNHN	1954.308
Oryctolagus cuniculus	MNHN	1912.668
Oryctolagus cuniculus	MNHN	1914.329
Oryctolagus cuniculus	MNHN	1983.97
Oryctolagus cuniculus	MNHN	1960.3810
Oryctolagus cuniculus	MNHN	1961.947
Oryctolagus cuniculus	MNHN	1983.439
Oryctolagus cuniculus	MNHN	1962.4207
Oryctolagus cuniculus	MNHN	1995.2692
Oryctolagus cuniculus	MNHN	1963.1409
Oryctolagus cuniculus	MNHN	1963.1408
Oryctolagus cuniculus	MNHN	2001.1048
Oryctolagus cuniculus	MNHN	2001.1049
Oryctolagus cuniculus	MNHN	2001.1046

Oryctolagus cuniculus	MNHN	2001.1136
Oryctolagus cuniculus	MNHN	2001.1138
Oryctolagus cuniculus	MNHN	2001.1137
Oryctolagus cuniculus	MNHN	2001.1135
Oryctolagus cuniculus	MNHN	2001.1134
Oryctolagus cuniculus	MNHN	2001.1132
Oryctolagus cuniculus	MNHN	2001.1140
Oryctolagus cuniculus	MNHN	2001.1139
Oryctolagus cuniculus	MNHN	2001.1145
Oryctolagus cuniculus	MNHN	2001.1144
Oryctolagus cuniculus	MNHN	2001.1142
Oryctolagus cuniculus	MNHN	2001.1122
Oryctolagus cuniculus	MNHN	2001.1130
Oryctolagus cuniculus	MNHN	2001.1118
Oryctolagus cuniculus	MNHN	2001.1107
Oryctolagus cuniculus	MNHN	2001.1116
Oryctolagus cuniculus	MNHN	2001.1131
Oryctolagus cuniculus	MNHN	2001.1106
Oryctolagus cuniculus	MNHN	2001.1983
Oryctolagus cuniculus	MNHN	2001.1109
Oryctolagus cuniculus	MNHN	2001.1129
Oryctolagus cuniculus	MNHN	2001.1121
Oryctolagus cuniculus	MNHN	2001.1113
Oryctolagus cuniculus	MNHN	2001.1117
Oryctolagus cuniculus	MNHN	2001.1126
Oryctolagus cuniculus	MNHN	2001.1123
Oryctolagus cuniculus	MNHN	2001.1125
Oryctolagus cuniculus	MNHN	2001.1115
Oryctolagus cuniculus	MNHN	2001.1127
Oryctolagus cuniculus	MNHN	2001.1077
Oryctolagus cuniculus	MNHN	2001.1055
Oryctolagus cuniculus	MNHN	2001.1076
Oryctolagus cuniculus	MNHN	2001.1061
Oryctolagus cuniculus	MNHN	2001.1064
Oryctolagus cuniculus	MNHN	2001.1067
Oryctolagus cuniculus	MNHN	2001.1078
Oryctolagus cuniculus	MNHN	2001.1058
Oryctolagus cuniculus	MNHN	2001.1079
Oryctolagus cuniculus	MNHN	2001.1072
Oryctolagus cuniculus	MNHN	2001.1070
Oryctolagus cuniculus	MNHN	2001.1075
Oryctolagus cuniculus	MNHN	2001.1104
Oryctolagus cuniculus	MNHN	2001.1084
Oryctolagus cuniculus	MNHN	2001.1081
Oryctolagus cuniculus	MNHN	2001.1101
Oryctolagus cuniculus	MNHN	2001.1097

Oryctolagus cuniculus	MNHN	2001.1096
Oryctolagus cuniculus	MNHN	2001.1102
Oryctolagus cuniculus	MNHN	2001.1087
Oryctolagus cuniculus	MNHN	2001.1100
Oryctolagus cuniculus	MNHN	2001.1098
Oryctolagus cuniculus	MNHN	2001.1105
Oryctolagus cuniculus	MNHN	2001.1085
Oryctolagus cuniculus	MNHN	2001.1027
Oryctolagus cuniculus	MNHN	2001.1028
Oryctolagus cuniculus	MNHN	2001.1038
Oryctolagus cuniculus	MNHN	2001.1035
Oryctolagus cuniculus	MNHN	2001.1040
Oryctolagus cuniculus	MNHN	2001.1037
Oryctolagus cuniculus	MNHN	2001.1034
Oryctolagus cuniculus	MNHN	2001.1030
Oryctolagus cuniculus	MNHN	2001.1031
Oryctolagus cuniculus	MNHN	1980.3
Oryctolagus cuniculus	MNHN	1980.6
Oryctolagus cuniculus	MNHN	1980.16
Oryctolagus cuniculus	MNHN	1980.7
Oryctolagus cuniculus	MNHN	1980.2
Oryctolagus cuniculus	MNHN	1980.10
Oryctolagus cuniculus	MNHN	1980.11
Oryctolagus cuniculus	MNHN	1980.8
Oryctolagus cuniculus	MNHN	1980.20
Oryctolagus cuniculus	MNHN	1980.19
Oryctolagus cuniculus	MNHN	1980.17
Oryctolagus cuniculus	MNHN	1980.4
Oryctolagus cuniculus	MNHN	1980.15
Oryctolagus cuniculus	MNHN	1980.14
Oryctolagus cuniculus	MNHN	180.12
Oryctolagus cuniculus	MNHN	1980.22
Oryctolagus cuniculus	MNHN	1980.21
Oryctolagus cuniculus	MNHN	1980.9
Oryctolagus cuniculus	MNHN	1980.1
Oryctolagus cuniculus	MNHN	1980.18
Oryctolagus cuniculus	MNHN	1980.13
Oryctolagus cuniculus	MNHN	1914.72
Oryctolagus cuniculus	MNHN	1914.72b
Oryctolagus cuniculus	MNHN	A7714
Oryctolagus cuniculus	MNHN	1899.74
Oryctolagus cuniculus	MNHN	1908.194
Oryctolagus cuniculus	MNHN	2001.1008
Oryctolagus cuniculus	MNHN	2001.1001
Oryctolagus cuniculus	MNHN	2001.993
Oryctolagus cuniculus	MNHN	2001.1010

Oryctolagus cuniculus	MNHN	2001.1007
Oryctolagus cuniculus	MNHN	2001.1005
Oryctolagus cuniculus	MNHN	2001.1002
Oryctolagus cuniculus	MNHN	2001.998
Oryctolagus cuniculus	MNHN	2001.999
Oryctolagus cuniculus	MNHN	2001.1009
Oryctolagus cuniculus	MNHN	2001.1863
Oryctolagus cuniculus	MNHN	2001.875
Oryctolagus cuniculus	MNHN	2001.881
Oryctolagus cuniculus	MNHN	2001.866
Oryctolagus cuniculus	MNHN	2001.871
Oryctolagus cuniculus	MNHN	2001.874
Oryctolagus cuniculus	MNHN	2001.870
Oryctolagus cuniculus	MNHN	2001.879
Oryctolagus cuniculus	MNHN	2001.867
Oryctolagus cuniculus	MNHN	2001.876
Oryctolagus cuniculus	MNHN	2001.872
Oryctolagus cuniculus	MNHN	2001.865
Oryctolagus cuniculus	MNHN	2001.899
Oryctolagus cuniculus	MNHN	2001.887
Oryctolagus cuniculus	MNHN	2001.890
Oryctolagus cuniculus	MNHN	2001.893
Oryctolagus cuniculus	MNHN	2001.891
Oryctolagus cuniculus	MNHN	2001.894
Oryctolagus cuniculus	MNHN	2001.971
Oryctolagus cuniculus	MNHN	2001.910
Oryctolagus cuniculus	MNHN	2001.915
Oryctolagus cuniculus	MNHN	2001.918
Oryctolagus cuniculus	MNHN	2001.923
Oryctolagus cuniculus	MNHN	2001.922
Oryctolagus cuniculus	MNHN	1924.1033
Oryctolagus cuniculus	MNHN	2003.139
Oryctolagus cuniculus	MNHN	2001.1020
Oryctolagus cuniculus	MNHN	2001.1018
Oryctolagus cuniculus	MNHN	2001.1021
Oryctolagus cuniculus	MNHN	2001.1017
Oryctolagus cuniculus	MNHN	2001.1014
Oryctolagus cuniculus	MNHN	2001.1016
Oryctolagus cuniculus	MNHN	2001.980
Oryctolagus cuniculus	MNHN	2001.979
Oryctolagus cuniculus	MNHN	2001.974
Oryctolagus cuniculus	Confluences	50.000833
Oryctolagus cuniculus	Confluences	50.00087
Oryctolagus cuniculus	Confluences	50.000846
Oryctolagus cuniculus	Confluences	50.000848
Oryctolagus cuniculus	Confluences	50.000855

Oryctolagus cuniculus	Confluences	50.003357
Oryctolagus cuniculus	Confluences	50.000839
Oryctolagus cuniculus	Confluences	50.000838
Oryctolagus cuniculus	Confluences	50.000845
Oryctolagus cuniculus	Confluences	50.000847
Oryctolagus cuniculus	MNHN	1971.210
Oryctolagus cuniculus	MNHN	1909.137
Paleolagus haydeni	UCBL-FSL	6945
Paleolagus haydeni	UCBL-FSL	6941
Paleolagus haydeni	UCBL-FSL	6933
Paleolagus haydeni	UCBL-FSL	6934
Paleolagus haydeni	UCBL-FSL	6937
Paleolagus haydeni	UCBL-FSL	6939
Paleolagus haydeni	UCBL-FSL	6940
Paleolagus haydeni	UCBL-FSL	6942
Paleolagus haydeni	UCBL-FSL	6946
Paleolagus haydeni	UCBL-FSL	6935
Paleolagus haydeni	UCBL-FSL	6936
Poelagus marjorita	AMNH	118666
Poelagus marjorita	AMNH	118667
Poelagus marjorita	AMNH	51396
Poelagus marjorita	AMNH	118856
Poelagus marjorita	AMNH	118864
Poelagus marjorita	AMNH	118869
Poelagus marjorita	AMNH	118865
Poelagus marjorita	AMNH	51052
Poelagus marjorita	AMNH	51049
Poelagus marjorita	AMNH	51048
Poelagus marjorita	AMNH	51055
Poelagus marjorita	AMNH	51054
Poelagus marjorita	AMNH	51056
Poelagus marjorita	AMNH	51035
Poelagus marjorita	AMNH	51044
Poelagus marjorita	AMNH	51045
Poelagus marjorita	AMNH	51042
Poelagus marjorita	AMNH	51039
Poelagus marjorita	AMNH	51037
Poelagus marjorita	AMNH	51031
Prolagus sardus	MNHN	1987.27
Pronolagus Crassicaudatus	AMNH	89033
Pronolagus rupestris	AMNH	168888
Pronolagus rupestris	AMNH	168891
Pronolagus rupestris	AMNH	168890
Pronolagus sp.	AMNH	168899
Pronolagus sp.	AMNH	168903
Pronolagus sp.	AMNH	168901

Pronolagus sp.	AMNH	168939
Romerolagus diazi	MNHN	1960.3808
Romerolagus diazi	AMNH	148173
Romerolagus diazi	AMNH	148172
Romerolagus diazi	AMNH	148181
Romerolagus diazi	AMNH	148171
Romerolagus diazi	AMNH	148178
Sylvilagus brasiliensis	AMNH	66659
Sylvilagus brasiliensis	AMNH	66661
Sylvilagus brasiliensis	AMNH	66662
Sylvilagus brasiliensis	AMNH	66663
Sylvilagus audubonii	AMNH	132542
Sylvilagus audubonii	AMNH	125924
Sylvilagus audubonii	AMNH	125925
Sylvilagus audubonii	AMNH	132538
Sylvilagus audubonii	AMNH	132543
Sylvilagus audubonii vallicola	MNHN	1939.1086
Sylvilagus bachmani exigus	MNHN	1927.1830
Sylvilagus bachmani macrorhinus	MNHN	1939.1085
Sylvilagus brasiliensis	MNHN	1962.2555
Sylvilagus brasiliensis	MNHN	1933.2335
Sylvilagus brasiliensis	MNHN	1848.246
Sylvilagus brasiliensis	MNHN	1910.240
Sylvilagus brasiliensis	MNHN	1896.2455
Sylvilagus floridanus	MNHN	1934.1205
Sylvilagus floridanus	MNHN	2009.277
Sylvilagus floridanus	MNHN	1921.58
Sylvilagus floridanus	MNHN	1980.505
Sylvilagus floridanus	MNHN	1929.676
Sylvilagus floridanus	MNHN	1929.677
Sylvilagus floridanus	MNHN	1929.678
Sylvilagus floridanus	MNHN	1929.680
Sylvilagus floridanus chapmani	MNHN	1962.954
Sylvilagus nuttallii	AMNH	92858
Sylvilagus nuttallii	AMNH	92857
Sylvilagus nuttallii	AMNH	92856
Sylvilagus nuttallii	AMNH	4336
Sylvilagus nuttallii	AMNH	7381
Sylvilagus palustris	AMNH	163975
Sylvilagus palustris	AMNH	93231
Sylvilagus palustris	AMNH	91136
Sylvilagus palustris	AMNH	25707
Sylvilagus palustris	AMNH	147446
Sylvilagus palustris	AMNH	147447
Sylvilagus sp.	MNHN	1903.85

Annex 4: Denture of *Oryctolagus cuniculus*

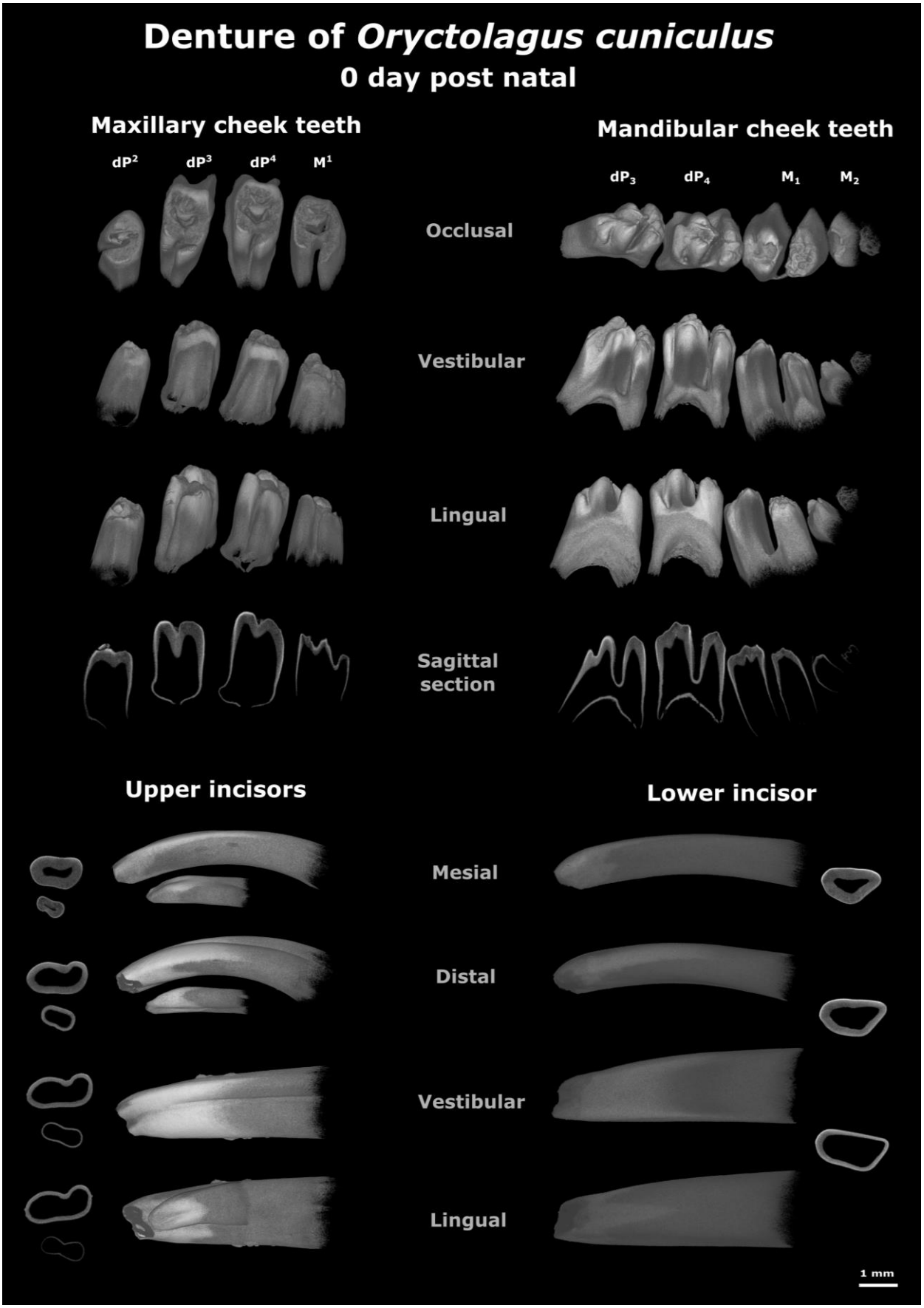

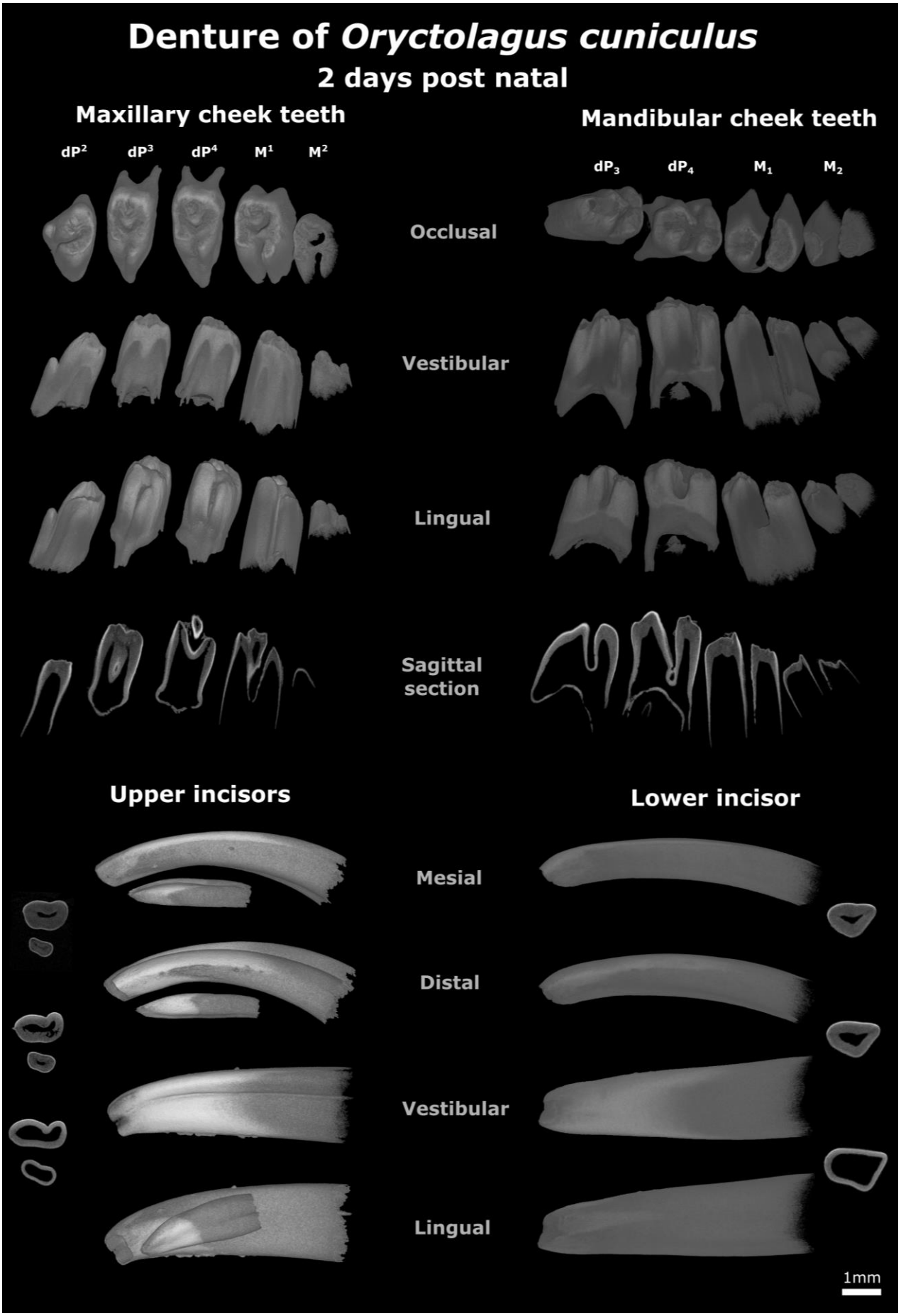
Denture of Oryctolagus cuniculus
2 days post natal
Maxillary cheek teeth
Mandibular cheek teeth
dP2 dP3 dP4 M1 M2
dP3 dP4 M1 M2
Occlusal
Vestibular
Lingual
Sagittal section
Upper incisors
Lower incisor
Mesial
Distal
Vestibular
Lingual
1mm

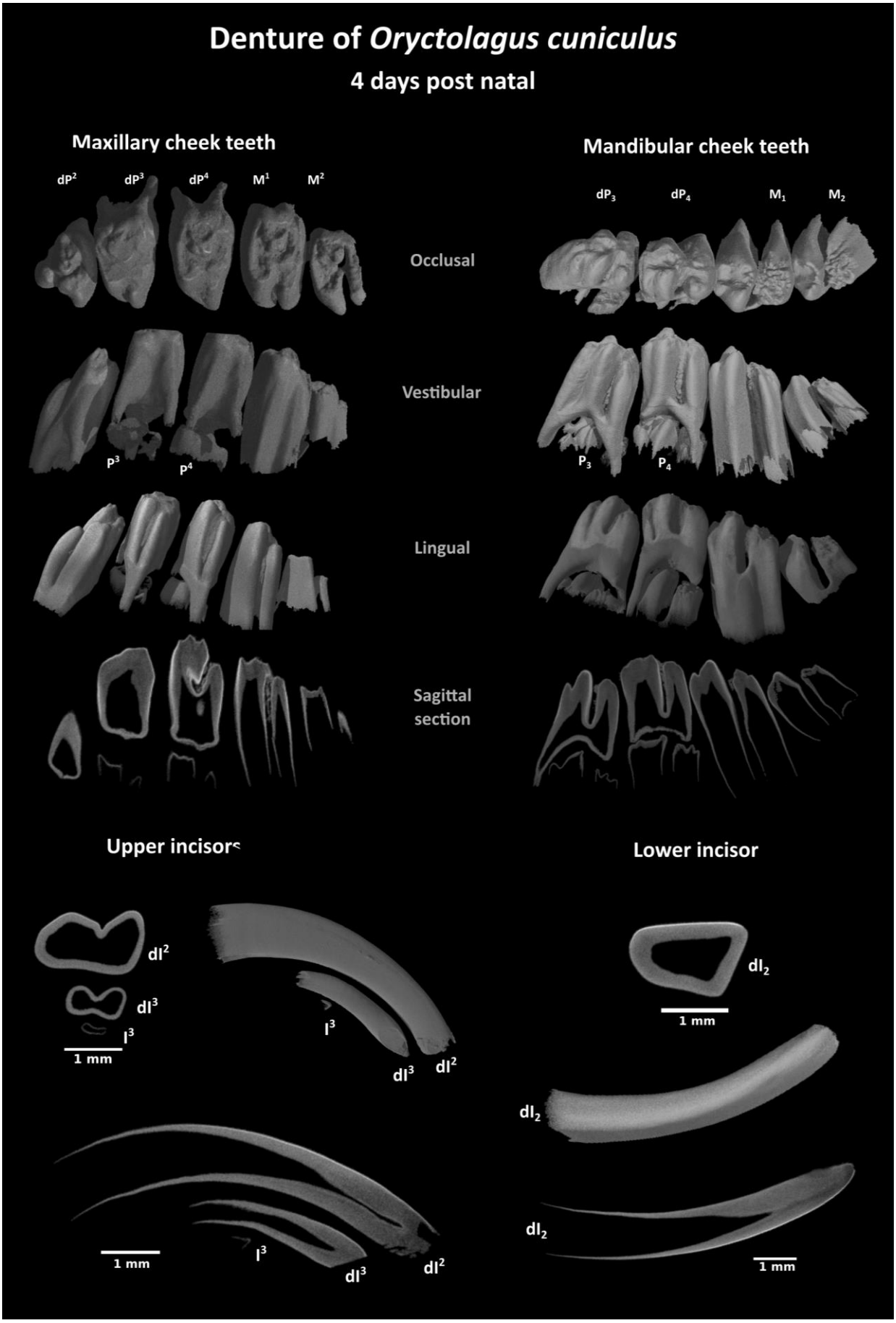
Denture of *Oryctolagus cuniculus*
4 days post natal
Maxillary cheek teeth
Mandibular cheek teeth
dP2
dP3
dP4
M1
M2
dP3
dP4
M1
M2
Occlusal
Vestibular
Lingual
Sagittal section
P3
P4
P3
P4
Upper incisors
Lower incisor
dI2
dI3
I3
1 mm
I3
dI3
dI2
dI2
1 mm
dI2
dI2
1 mm
I3
dI3
dI2
1 mm

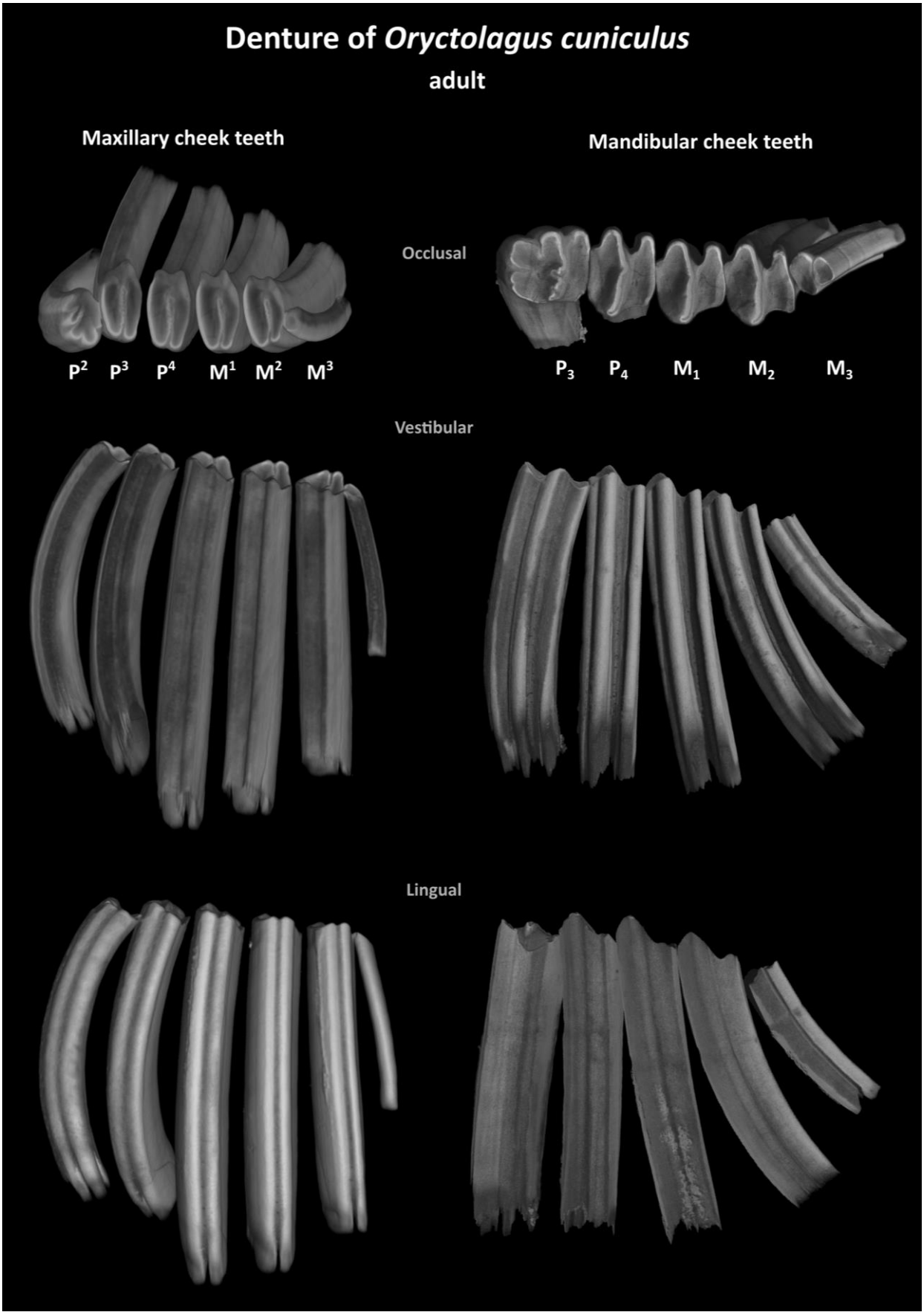
Denture of *Oryctolagus cuniculus*
adult
Maxillary cheek teeth
Mandibular cheek teeth
Occlusal
P2 P3 P4 M1 M2 M3
P3 P4 M1 M2 M3
Vestibular
Lingual

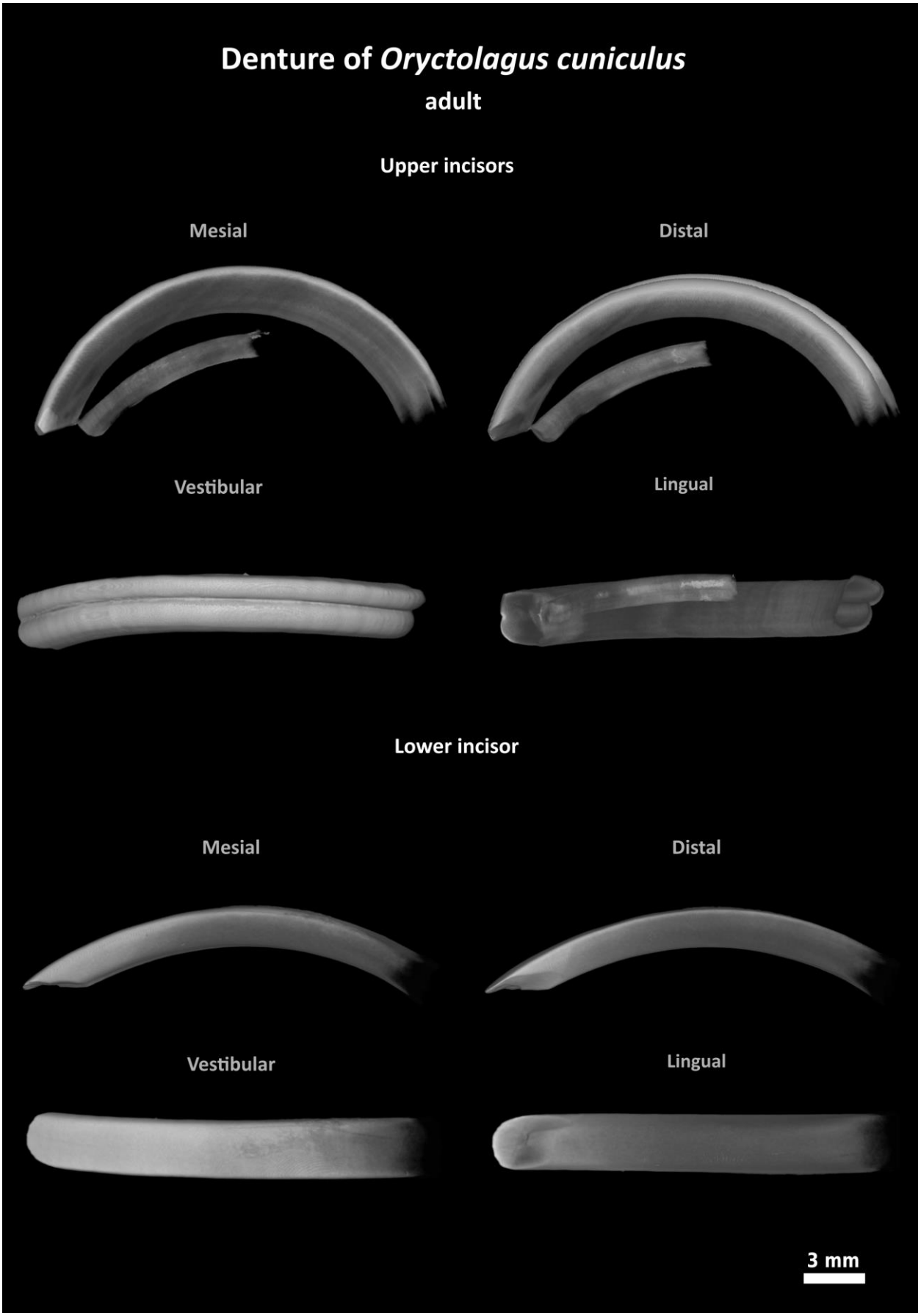
Denture of *Oryctolagus cuniculus*
adult
Upper incisors
Mesial
Distal
Vestibular
Lingual
Lower incisor
Mesial
Distal
Vestibular
Lingual
3 mm

Annex 5: 3D reconstructions of dental epithelium during *Oryctolagus cuniculus* embryonic development.

Bertonnier-Brouty Ludivine[1*], Viriot Laurent[1], Joly Thierry[2,3], Charles Cyril[1]

[1] Institut de Génomique Fonctionnelle de Lyon, Université de Lyon, CNRS UMR 5242, Ecole Normale Supérieure de Lyon, Université Claude Bernard, Lyon 1, 69007, Lyon, France

[2] ISARA-Lyon, 69007, Lyon, France

[3] VetAgroSup, 69280, Marcy l'Etoile, France

[*] Corresponding author: ludivine.bertonnierbrouty@ens-lyon.fr

MorphoMuseum has accepted the 3D reconstructions listed below. These 3D reconstructions are linked to the article 1 (p **52**) and will be locked until publication of the main article.

zip	ID	Teeth	Age	Left/Right	Voxel size (mm)
E14	E14-right	E14-CheekTeeth	14 dpf	RIGHT	0.00328003
		E14-LowerIncisors	14 dpf	LEFT+RIGHT	0.00328003
		E14-UpperIncisors	14 dpf	LEFT+RIGHT	0.00328003
E16	E16-left	E16-CheekTeeth	16 dpf	LEFT	0.00161137
		E16-LowerIncisors	16 dpf	LEFT+RIGHT	0.00161137
		E16-UpperIncisors	16 dpf	LEFT+RIGHT	0.00161137
E18	E18-right	E18-LowerCheekTeeth	18 dpf	LEFT	0.00299989
		E18-LowerIncisors	18 dpf	LEFT	0.00299989
		E18-UpperCheekTeeth	18 dpf	LEFT	0.00299989
		E18-UpperIncisors	18 dpf	LEFT	0.00299989
E20	E20-left	E20-LowerCheekTeeth	20 dpf	LEFT	0.00324637
		E20-LowerIncisors	20 dpf	LEFT	0.00324637
		E20-UpperCheekTeeth	20 dpf	LEFT	0.00324637
		E20-UpperIncisors	20 dpf	LEFT	0.00324637
E22	E22-lower-left	E22-LowerCheekTeeth	22 dpf	LEFT	0.00399988
		E22-LowerIncisors	22 dpf	LEFT	0.00399988
	E22-UpperCheekTeeth	E22-UpperCheekTeeth	22 dpf	RIGHT	0.00348826
	E22-UpperIncisors	E22-UpperIncisors	22 dpf	RIGHT	0.00348826
E24	E24-left	E24-LowerCheekTeeth	24 dpf	LEFT	0.00499989
		E24-LowerIncisors	24 dpf	LEFT	0.00499989
		E24-UpperCheekTeeth	24 dpf	RIGHT	0.00499989
	E24-UpperCheekTeeth	E24-UpperIncisors	24 dpf	LEFT	0.00499989
E26	E26-right	E26-LowerCheekTeeth	26 dpf	RIGHT	0.00474982
		E26-LowerIncisors	26 dpf	RIGHT	0.00474982
		E26-UpperCheekTeeth	26 dpf	RIGHT	0.00474982
	E26-UpperIncisors	E26-UpperIncisors	26 dpf	RIGHT	0.00474982
E28	E28-right	E28-LowerCheekTeeth	28 dpf	RIGHT	0.00749989
		E28-LowerIncisors	28 dpf	RIGHT	0.00749989
		E28-UpperCheekTeeth	28 dpf	RIGHT	0.00749989
		E28-UpperIncisors	28 dpf	RIGHT	0.00749989

Dataset

3D reconstructions of dental epithelium during *Oryctolagus cuniculus* embryonic development related to the publication "Morphological features of tooth development and replacement in the rabbit *Oryctolagus cuniculus*"

Bertonnier-Brouty Ludivine[1]*, Viriot Laurent[1], Joly Thierry[2,3], Charles Cyril[1]

[1] *Institut de Génomique Fonctionnelle de Lyon, Université de Lyon, CNRS UMR 5242, Ecole Normale Supérieure de Lyon, Université Claude Bernard Lyon 1, 69007, Lyon, France*
[2] *ISARA-Lyon, 69007, Lyon, France*
[3] *VetAgroSup, 69280, Marcy l'Etoile, France*
***Corresponding author**: ludivine.bertonnierbrouty@ens-lyon.fr

Abstract
The present 3D Dataset contains the 3D models analyzed in "Morphological features of tooth development and replacement in the rabbit *Oryctolagus cuniculus*", Journal of Anatomy, doi: XXXXXXXXXX

Keywords: dental development, *Oryctolagus cuniculus*, rabbit teeth, tooth replacement

Submitted:2019-04-03, published online:2019-26-04. https://doi.org/10.18563/journal.m3.90

Inv. nr	Description
E14	Right cheek teeth, Left and right incisors at 14 dpf
E16	Left cheek teeth, Left and right incisors at 16 dpf
E18	Left cheek teeth and incisors at 18 dpf
E20	Left cheek teeth and incisors at 20 dpf
E22	Left lower cheek teeth and incisors, right upper cheek teeth and incisors at 22 dpf
E24	Left cheek teeth and incisors at 24 dpf
E26	Right cheek teeth and incisors at 26 dpf
E28	Right cheek teeth and incisors at 28 dpf

Table 1. List of the dental epitheliums 3D reconstructions *in Oryctolagus cuniculus* from 14 to 28 dpf included in this study.

INTRODUCTION

The present 3D dataset contains reconstructions of dental epithelium tissues of eight rabbit embryos (*Oryctolagus cuniculus*) from 14 to 28 days post fertilization, see table 1 and figure 1. In the referred original publication, we described the chronology of rabbit tooth development of incisors and cheek teeth from the initiation of the deciduous teeth to the morphogenesis of the replacement teeth using 3D reconstruction of soft tissues.

METHODS

Embryo heads were stained with phosphotungstic acid (PTA) and radiographed using a Phoenix Nanotom S (GE Measurement and Control). The 3D surfaces of the dental epithelium were extracted manually within VG-studio max software. Right and left teeth were segmented in embryos from 14 to 18 dpf and half-heads were segmented in embryos from 20 to 28 dpf. Surface smoothing was done with Meshlab software. The 3D surface models are provided in .ply format, and can therefore be opened with a wide range of freeware.

ACKNOWLEDGEMENTS

We acknowledge the contribution of SFR Biosciences (UMS 3444/CNRS, US8/Inserm, ENS de Lyon, UCBL) facilities: We are grateful to Mathilde Bouchet-Combe from AniRa-ImmOs plateform, who helped for X-Ray microtomographic analyses.

BIBLIOGRAPHY

Bertonnier Brouty L., Viriot L., Joly T., Charles C. 20XX, 3D reconstructions of dental epithelium during *Oryctolagus cuniculus* embryonic development. Journal of Anatomy. doi: XXXXXXX

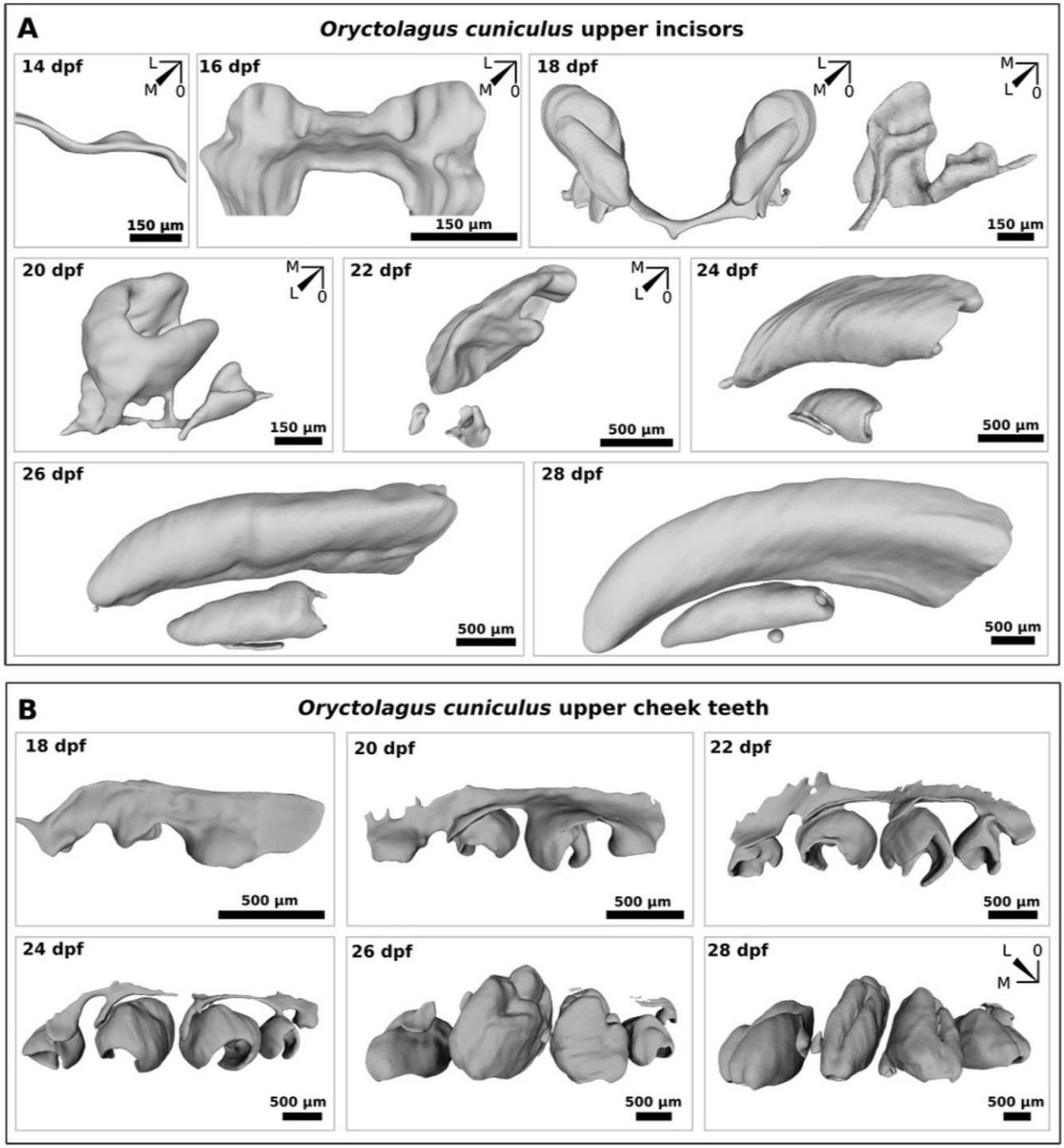

Figure 1. 3D reconstructions of *Oryctolagus cuniculus* upper dental epitheliums from 14 to 28 days post fertilization (dpf). A, Dental epitheliums of upper incisors. B, Dental epitheliums of upper cheek teeth. M, mesial; L, lingual and O, occlusal.